Analysis of the cell cycle regulatory system MASTL-ENSA/ARPP19-PP2A in human platelets

Dissertation

zur Erlangung des Grades

"Doktor der Naturwissenschaften"

im Promotionsfach Chemie

am Fachbereich Chemie, Pharmazie und Geowissenschaften

der Johannes-Gutenberg-Universität Mainz

Elena Johanna Kumm (geb. Walter)

M.Sc. Chemie

geboren in Darmstadt

Mainz, 2018

Centrum für Thrombose und Hämostase (CTH)

der Universitätsmedizin Mainz

und

Institut für Pharmazie und Biochemie

der Johannes Gutenberg-Universität Mainz

Tag der mündlichen Prüfung: 18.02.2019

Table of contents

Abstract

Small non-nucleated platelets, circulating in the blood, are activated upon vessel injury, to immediately stop the blood loss via thrombus formation. Under resting conditions, circulating platelets are inhibited through nitric oxide (NO, activating protein kinase G (PKG)) or prostacyclin (PGI_2, activating protein kinase A (PKA)). These inhibitors induce phosphorylation of multiple proteins inside the platelet to inhibit platelet activation and signaling pathways. Platelet signal transduction upon activation or inhibition is regulated through protein kinases and phosphatases.

A full phosphoproteomic study headed by PD Dr. K. Jurk and Dr. R. Zahedi with inhibited human platelets (data unpublished), revealed a high number of proteins regulated upon PKA and PKG activation. Two proteins, α-endosulfine (ENSA or ARPP19e) and cAMP-regulated phosphoprotein 19 (ARPP19), were strongly phosphorylated at S109/S104 (ENSA/ARPP19) in response to PKA and PKG activation (PKG effect was unknown before). The functional role of the PKA phosphorylation of ENSA and ARPP19 (identified years ago in different cell systems) is still unknown. The phosphorylation of ENSA/ARPP19 at S67/S62 via the Greatwall kinase in *Drosophila, Xenopus* and yeast and in mammalian cells by its homolog, the microtubule-associated serine/threonine kinase-like (MASTL), converts ENSA and ARPP19 to strong inhibitors of the protein phosphatase PP2A resembling the pharmacological inhibitor okadaic acid (OA). In dividing cells, this PP2A regulation is important for the cell cycle control; it is not reported for platelets so far.

The overall aim of this thesis was to elucidate the regulation and function of ENSA S67/S109 and ARPP19 S62/S104 phosphorylation in human platelets and the relation to the MASTL-ENSA/ARPP19-PP2A regulatory mechanism. As experimental approaches, ENSA and ARPP19 phosphorylation was analyzed by recombinant MASTL, recombinant PKG and purified PKA, as well as ENSA and ARPP19 phosphorylation at S67/S62 in intact human platelets and platelet lysates. The influence of recombinant pS67 ENSA/pS62 ARPP19 on platelet PP2A activity and the functional relevance of PP2A inhibition for platelet activation was investigated.

ENSA, ARPP19 and PP2A, but not MASTL, were detected in human platelets at significant protein levels. ENSA, cloned from human platelets, was expressed in HEK293 cells and *E.coli* BL21, on top, recombinant HisENSA was purified from BL21. ENSA and ARPP19 phosphorylation was studied with intact human platelets, platelet lysates and recombinant proteins as well as with ENSA phosphosite-mutants. ENSA S67/ARPP19 S62 phosphorylation was elevated upon phosphatase PP1/PP2A inhibition with OA for endogenous ENSA, recombinant ARPP19 and wild type ENSA in human platelet lysates, and in intact platelets. These data clearly demonstrated the presence of a MASTL-like kinase activity in human platelets. A broad spectrum of PP2A holoenzymes was shown to be present in human platelets. pS67 HisENSA and pS62 GST-ARPP19 reduced platelet PP2A activity of about 20% (compared to unphosphorylated control) in platelet lysates, using a PP2A specific non-radioactive serine/threonine phosphatase activity assay. With 1 nM of OA, platelet PP2A activity was completely inhibited. The phosphorylation of PP2A substrates (vasodilator-stimulated phosphoprotein, VASP, and mitogen-activated protein kinase (MAPK), p38) was increased in low dose OA treated isolated human platelets. The same concentration of OA decreased platelet activation/aggregation upon thrombin stimulation, revealing a regulatory role of PP2A upon platelet activation mechanisms in human platelets.

Based on these results, it can be concluded that human platelets contain all components of the [MASTL-like]–ENSA/ARPP19–PP2A (B55/B56) pathway, which is essential for the cell cycle control but must have other function(s) in non-dividing platelets. In the future it will be important to elucidate the molecular and functional targets of the [MASTL-like]-ENSA/ARPP19-PP2A pathway in human platelets.

Zusammenfassung

Zellkernlose Thrombozyten, die kleinsten Zellen des Blutes, zirkulieren im Blutkreislauf. Wird eine Gefäßwand verletzt, werden Thrombozyten aktiviert, um die Blutung schnellstmöglich durch die Bildung eines Thrombus zu stillen. Um eine ungewollte Aktivierung der Thrombozyten zu verhindern, werden sie durch Endothelzellen, die Stickstoffmonoxid (NO) (Aktivierung von Protein Kinase G (PKG)), oder Prostacyclin (PGI_2) (Aktivierung von Protein Kinase A (PKA)) freisetzen, negativ reguliert. PKA und PKG inhibieren Thrombozyten-Aktivierungssignalwege durch die Phosphorylierung diverser Proteine. Signalübertragungen werden generell durch Proteinkinasen und Proteinphosphatasen innerhalb einer Zelle reguliert.

Eine umfangreiche Phosphoproteom-Studie von inhibierten humanen Thrombozyten (Daten noch nicht publiziert) unter der Leitung von Frau PD Dr. K. Jurk und Herrn Dr. R. Zahedi identifizierte diverse Proteine, die durch PKA und PKG phosphoryliert und somit reguliert werden. Zwei Proteine, α-Endosulfin (ENSA bzw. ARPP19e) und cAMP-reguliertes Phosphoprotein 19 (ARPP19), werden an S109/S104 durch PKA und PKG stark phosphoryliert (dass PKG die beiden Proteine ebenfalls phosphoryliert, war vorher nicht bekannt). Die PKA Phosphorylierung von ENSA und ARPP19 ist in mehreren Zellsystemen seit Jahren bekannt, aber die Funktion ist bis heute nicht geklärt. Eine Phosphorylierung von ENSA/ARPP19 an S67/S62 durch die „Greatwall Kinase“ (in *Drosophila*, *Xenopus* und Hefen) bzw. ihr Homolog in Säugetierzellen, die „microtubule-associated serine/threonine kinase-like“ MASTL Kinase, macht aus ENSA und ARPP19 extrem starke Inhibitoren der Protein Phosphatase PP2A, ähnlich zu dem pharmakologischen Inhibitor Okadasäure (OA). Diese PP2A Regulierung ist in sich teilenden Zellen sehr wichtig für die Kontrolle des Zellzyklus, sie wurde in Thrombozyten bis jetzt noch nicht beobachtet.

Das primäre Ziel dieser Arbeit war die Aufklärung der Regulierung und Funktion der ENSA S67/S109 und der ARPP19 S62/S104 Phosphorylierung in humanen Thrombozyten und die Verbindung zu dem MASTL-ENSA/ARPP19-PP2A Regulierungsmechanismus zu identifizieren. Dafür wurde die ENSA und ARPP19 Phosphorylierung durch rekombinante MASTL, rekombinante PKG und gereinigte PKA analysiert. Zusätzlich wurde die ENSA und ARPP19 Phosphorylierung an S67/S62 in intakten humanen Thrombozyten und Thrombozytenlysaten untersucht. Der Einfluss von pS67 ENSA/pS62 ARPP19 auf die Aktivität von PP2A in Thrombozyten sowie die funktionelle Relevanz der PP2A Hemmung auf die Thrombozyten-Aktivierung wurde überprüft.

Die Proteine ENSA, ARPP19 und PP2A, aber nicht die MASTL Kinase, wurden abundant in humanen Thrombozyten detektiert. ENSA, kloniert aus humanen Thrombozyten, wurde in HEK293 Zellen und in *E.coli* BL21 exprimiert und aus *E.coli* als rekombinantes His-getaggtes Protein gereinigt. Die Phosphorylierung von ENSA und ARPP19 wurde in intakten humanen Thrombozyten, in Thrombozytenlysaten und unter Verwendung der rekombinanten Proteine, sowie den S67 und S109 Mutanten von HisENSA untersucht. Die ENSA S67/ARPP19 S62 Phosphorylierung wurde durch die Inhibierung von PP1/PP2A mittels OA für endogenes

ENSA, rekombinantes ARPP19 und ENSA (Wildtyp) in humanen intakten Thrombozyten und in Thrombozytenlysaten stark erhöht. Durch diese Versuche konnte eine MASTL-ähnliche Kinase und ihre Aktivität in humanen Thrombozyten eindeutig nachgewiesen werden. Verschiedene PP2A Holoenzyme wurden in humanen Thrombozyten detektiert. S67 phosphoryliertes rekombinantes ENSA sowie pS62 ARPP19 reduzierten die Aktivität von PP2A in humanen Thrombozytenlysaten um ca. 20% (verglichen mit unphosphoryliertem Protein). Die Hemmung wurde mit Hilfe eines nicht-radioaktiven Serin/Threonin Phosphatase-Aktivitäts-Assays bestimmt. Im Vergleich, 1 nM OA hemmte die PP2A Aktivität in Thrombozytenlysaten vollständig. Bekannte PP2A Substrate („vasodilator-stimulated phosphoprotein“ (VASP) und die mitogen-aktivierte Proteinkinase p38) waren stärker phosphoryliert, wenn isolierte humane Thrombozyten mit geringen Mengen OA inkubiert wurden. Die gleiche Konzentration OA führte zu einer Reduktion der Thrombin-induzierten Aktivierung/Aggregation von humanen Thrombozyten. Dies deutet auf eine Rolle von PP2A innerhalb der Regulierung von humanen Thrombozyten-Aktivierungsmechanismen hin.

Auf Grund der oben genannten Ergebnisse lässt sich schlussfolgern, dass humane Thrombozyten alle Bestandteile des [MASTL-like]-ENSA/ARPP19-PP2A (B55/56) Netzwerks besitzen, welche für die Kontrolle des Zellzyklus essentiell sind und in sich nicht teilenden Thrombozyten eine andere Funktion erfüllen müssen. Für die Zukunft ist es wichtig, die beteiligten Proteine und die Funktionen des [MASTL-like]-ENSA/ARPP19-PP2A Signalwegs in humanen Thromboyzten zu identifizieren und zu erforschen.

1. Introduction

1.1. Platelets, the small blood cells

With a size of only 3.6x0.7 µm, platelets are the smallest human blood cells.[1] These small cells circulate about 10 days in the blood[2] and prevent bleeding, which can be life threatening. Platelets are derived from megakaryocytes, have no nucleus and cell cycle but most other characteristics of a normal cell.[3] Around 150-350*10^9/L of non-dividing platelets are circulating in the blood of a human adult.[4]

Megakaryocytes, located in the bone marrow, produce about 10^{11} platelets each day. This number is only true for normal conditions, if necessary, megakaryocytes can increase platelet production more than 10 times.[2]

Platelets exhibit most of the regular cell organelles including mitochondria, ribosomes and parts of the endoplasmic reticulum, called the platelet dense tubular system,[5] as well as secretory granules, which are derived from megakaryocytes and transported separately between pro-platelets during platelet formation.[6] As platelets do not have a nucleus one could think, they are not able to produce proteins. However, platelets have ribosomes and thousands of translationally active messenger RNAs (mRNAs), both derived from megakaryocytes. This enables platelets to produce proteins using the mRNA, for example when they are activated through thrombin.[7] Platelets contain three types of secretory granules, which are all important for platelet function. The most abundant platelet granules are the α-granules followed by δ-/dense bodies and lysosomes.[8] Upon platelet activation, more than 300 proteins are secreted due to granule exocytosis.[9] α-granules contain for example the adhesion and hemostatic relevant proteins von Willebrand factor (vWF), fibrinogen, thrombospondin-1 (TSP-1) but also receptors that are transported to the platelet surface and remain there for a stronger activation and aggregation of the platelets such as the integrin $\alpha_{IIb}\beta_3$ or the collagen receptor glycoprotein VI (GPVI).[10] Small bioactive molecules like ATP (adenosine 5'-triphosphate), ADP (adenosine 5'-diphosphate), polyphosphates, serotonin, histamines but also cations, such as Mg^{2+} and Ca^{2+}, are cargo of δ-granules. All of these compounds act as positive feedback agonists on platelets for aggregation and coagulation.[9] Lysosomes are releasing acidic hydrolases for thrombus remodeling and antimicrobial response.[5]

Platelets play important roles in inflammation, host defense and tumor development.[1] They are essential for hemostasis (primary and secondary), the process inside a damaged vessel that prevents blood loss from the vessel to the surrounding tissue. During this process, the most common role for platelets is the thrombus formation upon the damage of the vessel wall. Once activated, platelets stimulate other platelets and recruit also other blood and vascular cells into the growing thrombus. [1]

When a circulating platelet is not activated upon its 10 days of life, it is removed through apoptosis.[11]

Patients, who present with relevant mucocutaneous or operative bleeding, often have a defect in platelet granule formation or in the secretory machinery (important for granule secretion).[10] But also defects in other platelet activation steps (e.g. aggregation) or in inhibition (leading to hyper-active platelets and therefore thrombosis), an overproduction of platelets (thrombocytosis)[12] or a reduced platelet count (thrombocytopenia)[13] are known. Therefore, a set of *in vitro* platelet function tests were developed and established for the diagnosis of platelet function disorders.[14]

To study platelets, they are usually isolated from anticoagulated whole blood. However, they cannot be cultured for functional analysis. Functional analysis of platelets should be done directly after isolation, proteins can be studied when platelets are lysed or SDS-PAGE samples are taken during platelet stimulation or inhibition; of course also by fluorochrome-labeling of proteins and subsequent flow cytometric analysis. A 'knock-out' of a protein can only be mimicked using certain inhibitors in living cells or using knock-out (KO) mice with a specific KO only in platelets or megakaryocytes. Mostly mice but also other animal models are used to study platelet function or certain protein functions *in vivo*. If a platelet function related disease is known due to a distinct mutation, this can give also good hints to certain protein functions of platelets.

1.2. Receptor-mediated regulation of platelet functions

Circulating blood platelets are inhibited by nitric oxide (NO) or prostacyclin (PGI_2) derived from endothelial cells under physiological conditions. These inhibitors increase cyclic nucleotide levels (cyclic adenosine monophosphate (cAMP) and cyclic guanosine monophosphate (cGMP)), in the platelet cytoplasm leading to the activation of serine/threonine protein kinases A (PKA) and G (PKG). These kinases phosphorylate many different proteins to prevent spontaneous platelet activation.[15] Therefore, they block important platelet activation pathways. Kinases and phosphatases are prominent substrates of PKA or PKG that are inhibited or activated by PKA/PKG phosphorylation and then phosphorylate/dephosphorylate downstream proteins. A well-known target of both, PKA and PKG, is the vasodilator-stimulated phosphoprotein (VASP).[16] VASP is an actin- and profilin-binding protein important in the negative regulation of myosin-actin dynamics and therefore cytoskeletal rearrangement (platelet shape change).[17]

For *in vitro* experiments in intact human and murine platelets, the stable prostacyclin analog iloprost is used to stimulate PKA. Sodium-nitroprusside (SNP), DEA-NO or S-nitrosocysteine (SNC) are used as NO donors and riociguat is used to stimulate the soluble guanylyl cyclase (sGC) for PKG activation.

In case of a vascular injury, platelets are rapidly activated through different stimuli. The soluble agonists thrombin and ADP as well as the adhesive agonists collagen or vWF are the most common platelet stimuli. Collagen is located as matrix protein in the subendothelium within the vessel wall. The vWF is released by injured endothelial cells or by platelets, but also circulates as plasma protein in the blood. An injury of the endothelium/the vessel wall leads to the exposition of collagen to the blood stream where collagen recruits predominantly the vWF. Once platelets interact with vWF via their surface receptor glycoprotein Ib/IX/V (GPIb/IX/V) or with collagen via GPVI/Fcγ-chain receptor complex,[18] the platelets adhere to the vascular surface, first transiently, then irreversibly[19] due to enhanced vWF-platelet interaction[4] and subsequent activation of integrins such as $\alpha_{IIb}\beta_3$ (GPIIb/IIIa, fibrinogen receptor) and $\alpha_2\beta_1$ (collagen receptor).[18] Collagen-induced platelet activation requires mainly GPVI/Fcγ, which activates phospholipase C γ_2 (PLCγ_2) and increases cytosolic Ca^{2+}-levels.[20]

Thrombin is generated initially on tissue-factor bearing cells, e.g. monocytes, fibroblasts,[18, 21] or amplified on the platelet surface via proteolytic cleavage of prothrombin by factor Xa.[22] Thrombin activates human platelets by extracellular cleavage of the protease-activated receptors PAR1 and PAR4.[23]

Activated platelets change their shape including formation of pseudopodia due to cytoskeletal rearrangement, secrete autocrine agonists, such as ADP or thromboxane A_2 (TXA_2) and present activated integrins on their surface. All these platelet activation responses enable the recruitment of other platelets leading to fibrinogen-mediated platelet-platelet interaction, which is called 'aggregation'. Fibrinogen is cleaved to fibrin by thrombin that stabilizes the platelet thrombus by forming long sticky fibers. Only a stable thrombus is able to stop blood loss completely.[1]

The understanding of the regulation of platelet functions including their activating and inhibitory pathways is very important since platelet hypo- and hyper-reactivity is clinically relevant in platelet-related bleeding, thrombotic and inflammatory diseases, which are often life threatening. The main signaling pathways including the participating receptors, intracellular protein mediators and final functions are often known, but many details of their interactions and relative contribution to the final response remain unknown so far.

1.3. Platelet signal transduction

Receptor-mediated platelet activation in response to agonists is associated with the activation of phospholipase C (PLC) isoforms. The second messenger IP_3 (inositol-1,4,5-triphosphate) is produced by PLC and induces elevation of the cytosolic Ca^{2+}-concentration, important for example for integrin activation through CalDAG-GEFI (Ca^{2+}- and DAG-regulated guanine-nucleotide exchange factor I), Rap1 (Ras-related protein 1) and RIAM (Rap1-GTP-interacting adaptor molecule).[20]

The signal transduction of adhesion receptors, such as GPIb-IX, GPVI/Fcγ and integrins coupled to the FcγIIA receptor often involve ITAM (immunoreceptor tyrosine-based activation motif) signaling pathways, tyrosine kinases of the Src family (SFKs) and phosphoinositide 3-kinases (PI3Ks) and lead to phospholipase Cγ activation although they are activated through different agonists.[24]

The strong platelet agonist thrombin binds to the proteinase-activated receptors PAR1 and PAR4 (human platelets) to induce signaling via G-coupled proteins G12/13α and Gqα. G12/13α activates the Rho-associated protein kinase (ROCK) leading to actin-cytoskeletal remodeling and platelet shape change. Gqα–induced signaling is more involved in Ca^{2+}-dependent integrin $\alpha_{IIb}\beta_3$ activation, granule secretion and phosphatidylserine exposure. Most effects are mediated here by phospholipase Cβ (PLCβ).[23]

TXA_2 and ADP signal also through G-coupled receptors (TXA_2 on thromboxane-prostanoid receptor ,TP, and ADP on $P2Y_1$, $P2Y_{12}$).[25] $P2Y_1$ receptor acts similar to PAR4 via Gqα. $P2Y_{12}$ stimulates phosphoinositide 3-kinase (PI3K) via Giα and PLCβ, activating integrin $\alpha_{IIb}\beta_3$ in an actin cytoskeleton-dependent way. ADP but also ATP, ligand of $P2X_1$ receptor, are released by δ-granules of platelets during activation as autocrine and paracrine less-strong platelet agonists.[26]

Platelets that are inhibited through endothelium-derived PGI_2 exhibit high levels of cytosolic cAMP, the important second messenger for activation of PKA. High cytosolic cAMP levels are produced by the adenylate cyclase, which is activated by Gs-mediated signaling. In contrast, Gi-mediated activating signaling via platelet ADP-$P2Y_{12}$ or epinephrine-α_{2A} interaction.[20, 27] The second major inhibitory pathway in platelets acts through the NO-sensitive guanylyl cyylase (sGC), generating cGMP, resulting in a 10-fold increase of cGMP levels. For activation

of sGC, NO can permeate the plasma membrane. PKGIβ, the only PKG isoform present in platelets, is activated through cGMP and phosphorylates several proteins (for example VASP) to inhibit platelet activatory pathways. cGMP also activates phosphodiesterase (PDE)2A and PDE5A, that degrade cAMP and cGMP again.[28, 29]

Figure 1 demonstrates a recent model of the complex activating and inhibitory signaling network in human platelets.[29]

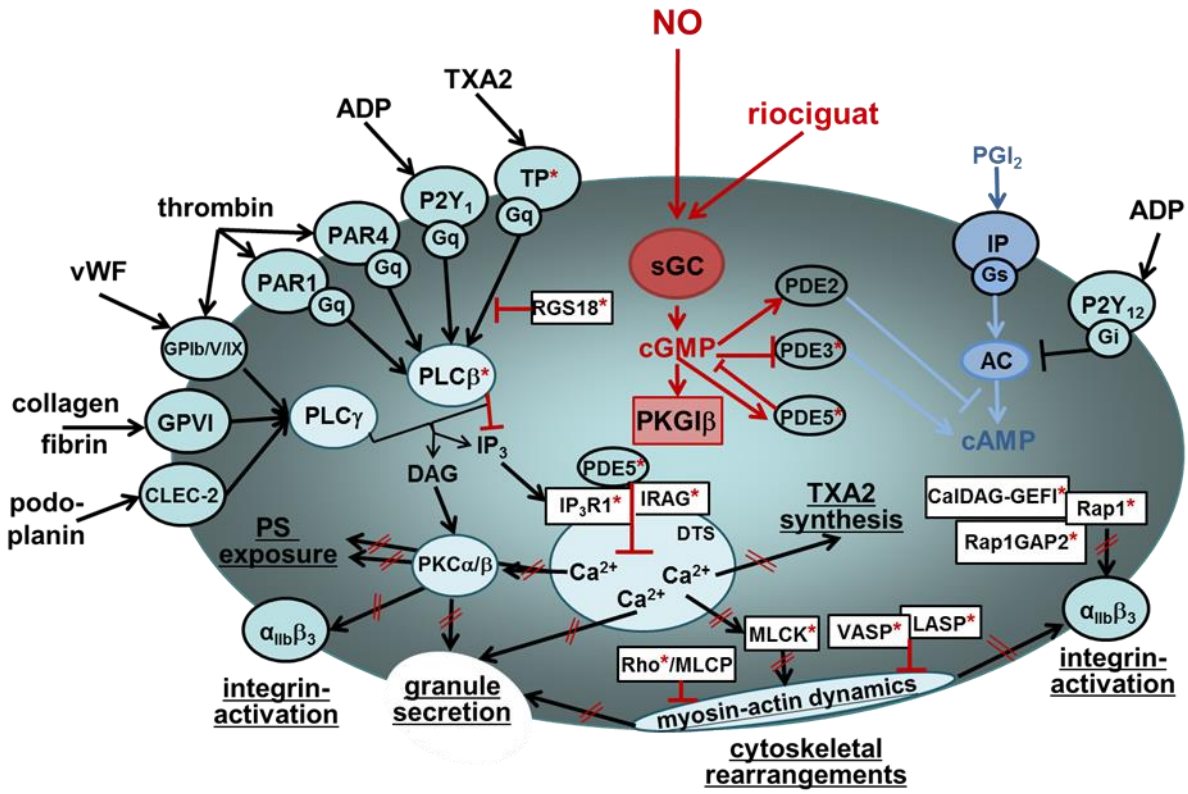

Figure 1: Regulation of protein phosphorylation and function of human platelets by the NO/sGC/cGMP pathways.[29]
Soluble platelet agonists (thrombin, ADP, TXA2) and/or adhesion molecules (vWF, collagen, fibrin, podoplanin), via specific membrane receptors and subsequent signaling pathways, activate various platelet responses, e.g. myosin-actin dynamics with subsequent cytoskeletal rearrangements, integrin activation (e.g. integrin $\alpha_{IIb}\beta_3$), granule secretion (i.e. α-granules, δ-granules/dense bodies, lysosomes) and PS exposure. All these platelet activation responses are crucial for platelet adhesion, aggregation and thrombin generation. NO and sGC stimulators such as riociguat, via sGC/cGMP/PKGIß, inhibit many of these platelet activation responses at several sites of the activation pathways as shown by red blocked arrows. This includes inhibition of Ca^{2+} release from the intracellular Ca^{2+}-store DTS and inhibition of the activating PKCα and PKCβ. Regulation of phosphodiesterases (PDE) by cGMP and phosphorylation modulates this pathway. Platelet proteins shown to be phosphorylated by PKGIβ, as shown in previous studies and ongoing phosphoproteomic analysis, are marked by a red asterisk (*). Phosphorylation of these proteins, e.g. RGS18, PLCβ, IP3R1, IRAG, Rho, MLCK, VASP, LASP, predominantly blocks distinct platelet activation steps (red blockades). In addition to cGMP, inhibitory cAMP is upregulated by the PGI_2/IP/AC pathway and by phosphorylated PDE3 and downregulated by the ADP-mediated pathway and by PDE2 activity. PLC, phospholipase C; RGS18, regulator of G protein signaling 18; IP_3R1, inositol 1,4,5-trisphosphate (IP_3) receptor 1; IRAG (MRVI), IP_3 receptor-associated cGK I substrate protein; small GTPase system: [CalDAG-GEFI/RASGRP2; Rap1; Rap1GAP2]; actin system: [Rho; MLCP; MLCK, VASP, LASP]; vWF, von Willebrand factor; TXA2, thromboxane A2; TP, thromboxane receptor; PGI2, prostacyclin; IP, prostacyclin receptor; PS, phosphatidylserine; PKC, protein kinase C; DTS, dense tubular system.

All of these signaling mechanisms include protein phosphorylation and dephosphorylation catalyzed by corresponding protein kinases and protein phosphatases, respectively. This topic,

with a focus on serine/threonine kinases and phosphatases, will be introduced in the next chapter.

1.4. Protein phosphorylation and dephosphorylation catalyzed by protein kinases and phosphatases

In all eukaryotic cells, signal transduction is regulated by protein kinases and protein phosphatases. 528 different kinase genes (human kinome)[30] and 189 genes for protein phosphatases (human phosphatome) were identified in humans.[31] Serine (Ser/S), threonine (Thr/T) and tyrosine (Tyr/Y) residues of proteins are predominantly phosphorylated. Whereby pSer accounts for 86.4% of all phosphorylations in the human proteome, pThr and pTyr represent 11.9% and 1.8%, respectively.[32] At least 125 different serine/threonine kinases (STKs) exist in the human proteome, which specifically phosphorylate serine and threonine residues.[33] They are activated by different mechanisms such as chemical signals (e.g. Ca^{2+}, cAMP/cGMP) or even by DNA damage. Tyrosine specific kinases (TKs) and dual-specificity kinases (DSKs) that phosphorylate all three different amino acid residues are known. Protein kinases are divided in seven subfamilies (AGC (protein kinase A, G, C family), CaMK (Ca^{2+}/calmodulin-dependent protein kinases), CK1 (cell kinase 1), CMGC (CDK, MAPK, GSK3, CLK family), STE (sterile kinase), TK (tyrosine kinase) and TKL (tyrosine kinase-like)). Kinases can activate themselves by autophosphorylation or they are stimulated by allosteric activators that bind to their regulatory subunits.[34] Important kinases in platelets are serine/threonine kinases like protein kinase C isoforms, Akt/protein kinase B, mitogen activated protein kinases (e.g. p38, Erk1/2) or protein kinase A and G or tyrosine kinases (SFKs like Src, Fyn and Lyn)[35].

Protein phosphatases are divided in three different subfamilies: Phosphoprotein phosphatases, PPP (like PP1, PP2A, PP2B and PP4 to 7), metallo-dependent protein phosphatases (PPM) and protein tyrosine phosphatases (PTP).[36] Important phosphatases in human platelets are serine/threonine phosphatases such as PP1 or PP2A and tyrosine phosphatases such as CD148 and protein tyrosine phosphatase 1B (PTP-1B).[36, 37] Endogenous polypeptide inhibitors are important physiological regulators to control phosphatase activity.[38]

1.5. Protein phosphatase 2A (PP2A)

1.5.1. PP2A – a serine/threonine phosphatase

About 70% of the cellular serine/threonine protein phosphatase PP2A presents as a trimeric holoenzyme that is composed by three different subunits. The scaffolding subunit A, α or β isoform, has a molecular weight of 65 kDa and is also called PR65.[39] Together with the catalytic subunit C (α or β isoform) it is forming the core enzyme of PP2A. Only in the dimeric version (about 30% in cells), the A subunit is acting as regulatory subunit.[40] The Aα and Aβ isoforms share 86% of amino acid similarity.[41] The Aα isoform is likely to be more abundantly expressed than the Aβ isoform in cells and tissues (90% of PP2A assemblies contain Aα; only 10% contain the Aβ subunit).[42]

The catalytic subunit (36 kDa[39]) of PP2A has 50% similarity in amino acid sequence compared to PP1, 40% similarity compared to PP2B. The two isoforms of PP2A C subunit are

97% identical. The α isoform is mainly a plasma membrane-associated protein, the β isoform is mainly expressed in the cytoplasm and the nucleus.[43]

The third component of the PP2A trimeric enzyme is the regulatory subunit B. B consists of four families (B/B55, B‘/B56, B‘‘, B‘‘‘), and each family presents with up to 5 isoforms with different splice variants.[44, 45] The PP2A regulatory subunit is thought to determine intracellular localization and substrate specificity of the trimeric holoenzyme.

In total, there are more than 100 different PP2A holoenzymes possible.[45, 46] This number at least gives an idea of the number of proteins that are substrates and are dephosphorylated by PP2A in cells.

Until today, the major, widely accepted role of PP2A in *Drosophila*, *Xenopus*, yeast and man, is the control of the cell cycle. Here, PP2A B55α is important for the exit from mitosis, by dephosphorylating CDK1 substrates.[47] Further important PP2A substrates are Akt (dephosphorylated on threonine 308, therefore negatively regulated by PP2A-B55) and MAP-kinases, which play important roles in cell proliferation and survival[48, 49]

In addition, PP2A is involved in apoptosis with its substrates Bcl-2 –associated agonist of cell death (BAD, dephosphorylated by PP2A, direct pro-apoptotic activity), Bcl-2 (dephosphorylation suppresses anti-apoptotic activity).[50] On the other hand, PP2A has been described as substrate of the apoptotic caspase-3.[51, 52]

In mammalian systems, PP2A acts as a tumor suppressor. Mutations in the different subunits, leading to altered, often impaired PP2A activity support tumor development.[53, 54] But also other inflammatory and autoimmune diseases such as Alzheimer’s disease (AD) are related to altered PP2A activity.[55]

The PP2A activity is regulated by distinct cellular endogenous inhibitors and activators. PP2A B55δ is inhibited by the small proteins α-endosulfine (ENSA) or cAMP-regulated phosphoprotein 19 (ARPP19) (that are phosphorylated through the microtubule associated serine/threonine kinase like (MASTL) at S67/62) during the mitotic entry of the cell.[56, 57] PP2A B56 is inhibited by Bod1 (biorientation of chromosomes in cell division protein 1) in HeLa cells at the mitotic kinetochors.[58]

Also pharmacological inhibitors like okadaic acid (OA), calyculin A, fostriecin and others are known that inhibit PP2A with different IC_{50}. The toxin okadaic acid is produced in *Dinophysis* and accumulates in shellfish and marine sponges.[59] Calyculin A is a toxin derived from *Discodermia calyx.*[60] Fostriecin is a polyketide synthase, derived originally from the soil bacterium *Streptomyces pulveraceus*.[61] OA interacts with the catalytic subunit (active site) of PP2A (α and β), but it does not differ between the different PP2A enzymes.[62] Therefore, OA inhibits all PP2A enzymes.[63]

PP2A activity and substrate specificity through certain regulatory subunits is also regulated by the leucine carboxyl-methyl transferase 1 (LCMT1) that methylates the C-subunit on leucine 309[64, 65] and the PP2A-specific methyl esterase 1 (PME-1) that removes the methylation again.[66] This regulatory process influences the substrate specificity of PP2A and the holoenzyme formation, which is important for cell survival and cell cycle regulation.[39, 67]

The PP2A activator PTPA (protein phosphatase 2A phosphatase activator, earlier named phosphotyrosyl phosphatase activator) plays an important role in the activation of PP2A.[68] PTPA activates PP2A by activating PTP-1B, which dephosphorylates tyrosine 307 on the

PP2A C-subunit. p-Y307 disturbs the interaction of C-subunit and B-subunits (PR55/B, PR61/B') and therefore inhibits PP2A.[69-71]

1.5.2. PP2A in human platelets and its inhibition

Protein serine/threonine phosphatases including PP2A in human platelets have not been studied in detail so far and the role of PP2A is completely unknown in murine platelets. However, studies with pharmacological inhibition of PP2A by the use of the marine toxin OA revealed the importance of PP2A in regulating distinct functions of human platelets.

The dephosphorylation of p38 mitogen-activated protein kinase (p38) was studied in human platelets by using 1 µM of OA (IC_{50} for PP2A=0.1 nM)[72] to inhibit phosphatase activity. MAPK p38 is phosphorylated and therefore activated with collagen (or collagen-related peptide) during platelet activation, as already described above. Pre-incubation of intact human platelets with 1 µM of OA increased p38 phosphorylation upon collagen stimulation. As the cell permeable OA can also inhibit PP1 at higher concentrations (IC_{50}=20-50 nM)[72], the group wanted to exclude an effect of PP1 on p38 dephosphorylation. Therefore they treated platelet lysates with fostriecin, a very specific inhibitor of PP2A (IC_{50}=3.2 nM) that inhibits PP1 only at very high concentrations (IC_{50}=131 µM). The group suggested that fostriecin is not cell permeable, but another group had different observations.[73] 5 µM of fostriecin and 1 µM of OA in platelet lysates led to an increase in p38 phosphorylation. Sundaresan et al. concluded that this effect was PP2A dependent and PP1 independent.[74] As p38 is phosphorylated and therefore activated upon platelet activation, the phosphorylation is used nowadays as a marker for platelet activation.

A pre-incubation of human platelets with 500 nM of OA inhibited the TXA_2 synthesis upon activation with high doses of thrombin (1 U/mL). Platelet aggregation was significantly reduced and granule secretion (monitored by serotonin release) as well. The inhibition in TXA_2 synthesis was directly related to an inhibition of the thrombin-induced increase of cytosolic Ca^{2+}-levels, according to an inhibition of Ca^{2+} influx (through the plasma membrane) and also of Ca^{2+} release from intracellular platelet stores. In parallel, OA increased tyrosine phosphatase activity detected as decrease of tyrosine phosphorylated proteins using immunoblotting. Therefore, Moscardó et al. concluded that PP1 or PP2A affects TXA_2 synthesis and Ca^{2+}- levels upon platelet activation. But as they used 500 nM OA, a concentration that still could inhibit PP2A and PP1 as well, they referred the effect to PP2A and PP1.[75]

When PP2A is studied in human platelets using specific inhibitors such as OA, it is important to carefully choose the OA concentration to exclude an effect on PP1. As both phosphatases are present in platelets (in the membrane and in cytosolic fractions), both phosphatases can be affected.[76]

Therefore, Moscardé et al. studied in 2013 two different concentrations of OA (100 nM and 500 nM) in human platelets. Low and high concentrations of OA inhibited integrin $\alpha_{IIb}\beta_3$-dependent clot retraction upon activation with a high concentration of thrombin (1 U/mL), but only the high concentration of OA inhibited $\alpha_{IIb}\beta_3$ receptor activation and platelet aggregation. 100 nM of OA inhibited in intact platelets most likely only PP2A, but control experiments with other phosphatase inhibitors were missing.[77]

Once a group tried to study the role of PP1 in platelets. They used a KO mouse model for a platelet specific KO of one isoform of the catalytic subunit of PP1 (PP1cγ) and studied the effect of this KO on thrombin-induced platelet activation. They observed mild inhibitory effects upon platelet activation with low concentrations of thrombin (0.01 U/mL) on integrin $\alpha_{IIb}\beta_3$ activation, soluble fibrinogen binding, platelet aggregation and thrombus stabilization.[78]

A possible regulator of PP2A in human platelets was found in 2016 by Kathlani et al. They identified the adaptor protein CIN85 (SH3 domain-containing kinase binding protein 1), which reduced PP2A activity, by interacting with the catalytic subunit of PP2A. They suggested an integrin-related platelet function of the PP2A-CIN85 complex. Their main studies were done in human embryonic kidney 293 cells (HEK293).[79]

By trying to find substrates of PP2A and therefore proofs for PP2A activity in human platelets, Abel et al. studied in 1995 VASP (vasodilator-stimulated phosphoprotein) phosphorylation and dephosphorylation *in vitro* with recombinant proteins and in human platelets with OA pre-incubation. VASP is a target of protein kinases A and G for different phosphorylation sites. The group could show that PP2A dephosphorylates the PKA site S157 with higher priority than the PKG site S239 after platelet inhibition. Therefore, they pre-incubated human platelets with 50 nM OA, leading to a strong VASP phosphorylation at S157 and less at S239. This observation was similar to platelet inhibition by iloprost or NO-donors.[80]

So far, most functional studies for PP2A in human platelets used OA to inhibit the phosphatase. As the differentiation of OA inhibitory effects on PP1 or PP2A is difficult, nearly nothing is known in human platelets about the role of PP1. The experiments performed with OA only addressed the effects on PP2A and/or PP1, as they could not be sure, which kinase was inhibited. Strong endogenous inhibitors of human platelet PP2A holoenzymes are not known until now. In platelet lysates, 1 nM of OA is able to completely inhibit PP2A (my experiments and Moscardó et al. 2013[77]). For intact platelets, as described above, higher concentrations are needed, impeding specific studies on PP2A functions in human platelets. Until today, among pharmacological inhibitors of PP2A, OA is the most specific one. With an IC_{50} of 0.1 nM, OA inhibits PP2A much stronger than fostriecin (IC_{50}=3.2 nM).

When studying substrates of PP2A in platelets, these proteins are always part of a complex network. Therefore, differences in the phosphorylation patterns or in platelet functions can always be due to interaction partners of the PP2A substrates. It is very difficult to relate an effect on a protein or a cell function directly to PP2A.

1.6. The Gwl/MASTL-ENSA/ARPP19-PP2A regulatory system in the cell cycle control

Protein phosphatase 2A is part of a regulatory system that controls the cell cycle in many different organisms.

The small, 121 amino acid long, cytosolic protein α-endosulfine (ENSA or ARPP19e) was first discovered 30 years ago as sulfonylurea-sensitive K_{ATP} channel regulator.[81] ENSA is expressed in many human tissues and also found in *Xenopus laevis*,[56] *Drosophila*[82] and yeast.[83] A protein very similar to ENSA is the cAMP-regulated phosphoprotein 19 (ARPP19). It shares many structure similarities with ENSA and is also found in mammalian cells[84] and *Xenopus*.[57] ARPP19 and ENSA have both a molecular weight of about 12 to 13 kDa[85-87] and in the brain, ENSA and ARPP19 are expressed in different regions (ENSA mainly in the

striatum).[84] The paralog proteins are encoded by different genes.[87] A third important protein of the ARPP-family is ARPP16, a smaller isoform of ARPP19 (16 amino acids are missing at the N-terminus), running in a gel with a size of 16 kDa,[86] being mainly expressed in brain tissue.[85] For ENSA, eight different isoforms (also called splice variants) are known so far (according to uniprot.org). The variants differ in their number of amino acids. The canonical sequence of ENSA is isoform 1 (according to uniprot.org).

In mammalian cells, the three ARPP family proteins have two important phosphorylation sites. One is a PKA site (S109 human ENSA, S104 human ARPP19 and S88 human ARPP16).[84] The second phosphorylation site (S67 mammalian ENSA, S62 mammalian ARPP19 and S46 mammalian ARPP16) was discovered, first in *Xenopus* and HeLa cells, in 2010 for ARPP19 and ENSA to play an important role in the cell cycle regulation.[56, 57] This site is phosphorylated by microtubule-associated serine/threonine kinase-like (MASTL) in mammalian cells,[88] called Greatwall kinase in yeast,[89] *Xenopus*[90] and *Drosophila*,[91] converting ENSA and ARPP19 to strong inhibitors of the protein phosphatase PP2A. ARPP16 was identified in neurons to be phosphorylated at S46 by a kinase similar to MASTL, called MAST3 (microtubule-associated serine/threonine kinase 3).[92] The different small proteins prefer, when phosphorylated through MASTL or MAST3, different PP2A complexes. pS62 ARPP19 and pS67 ENSA prefer PP2A B55δ for inhibition. pS67 ENSA has a remarkable IC_{50} of around 0.47 nM for PP2A B55δ (tight binding inhibitor).[93] pS46 ARPP16 in brain mainly interacts and inhibits PP2A B55α and B56δ.[94] The inhibition of PP2A supports the cell to enter into mitosis.[56, 57]

This part of the cell cycle regulation is schematically shown for ENSA and MASTL in the following figure.

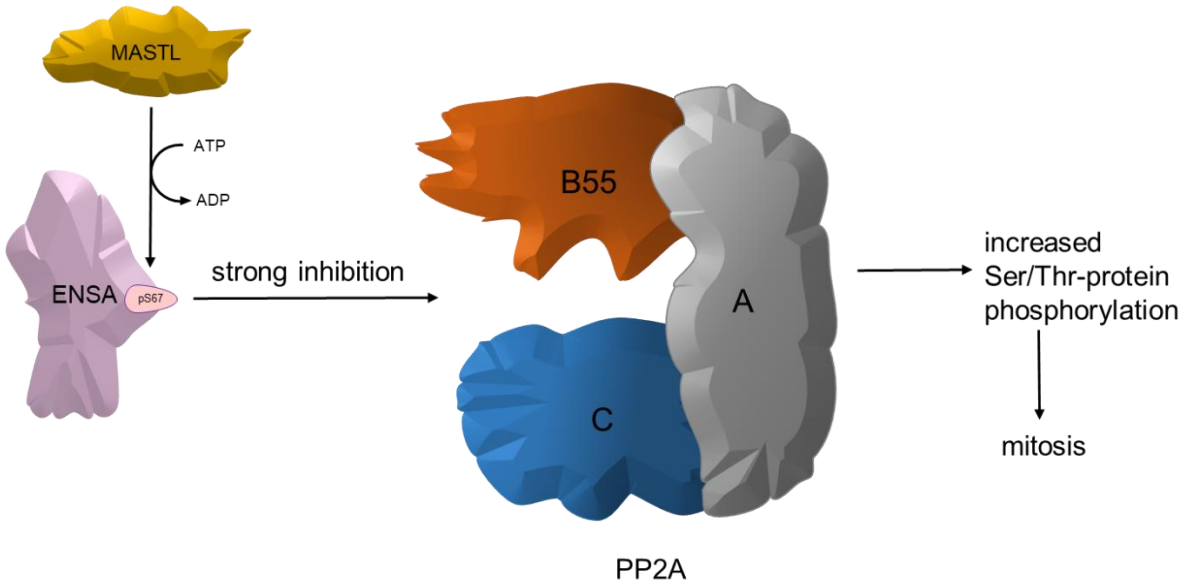

Figure 2: The cell cycle regulatory system MASTL-ENSA-PP2A.
Scheme of the inhibition of PP2A via pS67 ENSA in mammalian cells leading to an increase in phosphorylated serine/threonine residues of many proteins, helping the cell to enter into mitosis. Modified from Mochida 2014.[93]

The MASTL kinase as well as PKA, PKG, Akt, MAST and LATS (large tumor suppressor kinase) kinases belong to the class of AGC kinases (in total 60 members).[30, 95, 96] The MASTL kinase comprises two parts in the overall amino acid sequence that are important for its kinase activity. They are located on the N- and the C-terminus.[97] MASTL/Greatwall kinase was discovered in 2004 in *Drosophila*, as part of the cell cycle.[98] It is promoting mitotic progression

but it also helps the cell to re-enter into the cell cycle after DNA damage.[99] For the phosphorylation of ENSA/ARPP19, MASTL needs to be activated most likely through the phosphorylation by cyclin-dependent kinase 1 (CDK1).[100]

The other way around, active PP2A B55δ dephosphorylates substrates of CDK1, therefore promoting exit from mitosis. Cdk1 and PP2A are counter players (and master regulators) in the cell cycle control. MASTL and ENSA/ARPP19 are acting in between.[101] The inhibition of the tumor suppressor PP2A influenced by MASTL kinase may explain, why in some cancer types upregulated MASTL is detected.[99]

The inhibitory mechanism of MASTL-ENSA/ARPP19-PP2A has been well studied in *Drosophila*, *Xenopus*, yeast, zebrafish, mammalian cells and even in plants.[89, 102]

ENSA is also a substrate of PP2A and can be dephosphorylated by this phosphatase. The dephosphorylation process is much slower than the one of other substrates of PP2A. ENSA inhibits the dephosphorylation of CDK1 substrates through a competition for the active site of PP2A B55.[103]

ENSA and ARPP19 are both targets of protein kinase A, which phosphorylates these proteins at a second phosphorylation site (S109 for ENSA and S104 for ARPP19).[84] This phosphosite has been discovered and studied earlier than the MASTL-site, but so far, the functional role of the PKA phosphorylation is unknown. Recently, the PKA phosphorylation was found for ARPP16 in brain tissue to reciprocally regulate/inhibit the pS46 phosphorylation and therefore the PP2A inhibition.[94, 104] PKA is known to phosphorylate PP2A B56δ, increasing PP2A activity.[105] Therefore, PKA works as a PP2A activator, ENSA/ARPP19/16 as PP2A inhibitors.

A possible interaction partner of ENSA and ARPP19 was detected in earlier studies via NMR analysis of proteins in the brain. ENSA and also ARPP19 only interacted with specific residues in the N-terminal helical domain of α-synuclein, when ENSA or ARPP19 and α-synuclein were both bound to the surface of SDS micelles.[106] A mutation inserted in ENSA, mimicking PKA phosphorylation (S109E) disturbs the helix around S109 and therefore disrupts the interaction with α-synuclein.[107]

In relation to AD, ENSA protein levels in the brain of AD patients was found to be strongly decreased.[108] The same group found ARPP19 and PKA expression levels to be decreased in patients with down-syndrome and AD patients.[109]

A relation of the cell cycle regulatory machinery through MASTL to platelet function was made in 2009 by Johnson et al., who showed that the *in vivo* inactivation of MASTL kinase induced by a single amino acid mutation (E167D) in zebrafish results in thrombocytopenia (reduced platelet count). MASTL seems to influence platelet development in megakaryocytes.[97]

1.7. Aims of the thesis

The fact that the PP2A–ENSA/ARPP–Greatwall (MASTL) system is conserved from yeast to man[110], these components may certainly regulate pathways and functions distinct from the cell cycle control. ENSA and ARPP19/16 are also well expressed in the brain, especially in neurons [94, 104], which are post-mitotic, non-dividing cells. However, the functions of ENSA/ARPP19/16 in neurons have not been well established.

Platelets are also post-mitotic, non-dividing specialized cells with a broad spectrum of cell-biological and functional responses except mitosis/cell division. The observation that both ENSA and ARPP19 are expressed in both human and murine platelets[111, 112] and phosphorylated in response to cAMP-elevating platelet inhibitors[113] led to our working hypothesis that the Greatwall/MASTL-ENSA/ARPP19-PP2A regulatory system is present and regulated in human platelets. It was therefore the aim of my thesis to obtain further evidence for this hypothesis. In particular, the following major questions were addressed:

a) Are both ENSA and ARPP19 phosphorylated in intact human platelets at their established PKA site (S109, S104) in response to a cAMP-elevating platelet inhibitor?

b) In human platelets, cAMP/PKA with its multiple substrates represents one major inhibitory pathway. A second major inhibitory pathway is provided by NO/cGMP/PKG signaling, which is less characterized but overlaps with the cAMP/PKA pathway.[29, 114] Therefore, are ENSA and ARPP19 also targets of the cGMP/PKG pathway in human platelets?

c) In *Drosophila*, *Xenopus* and other species, ENSA and ARPP19 when phosphorylated at S67 and S62, respectively, by Greatwall or MASTL represent potent PP2A inhibitors. Is there S67 ENSA and/or S62 ARPP19 phosphorylation in human platelets; is there a corresponding ENSA/ARPP19-kinase and what is the effect on PP2A kinase activity?

d) In addition to ENSA/ARPP19 and their S67/S62 protein kinases, are the typical PP2A targets of ENSA/ARPP present in human platelets, and can they be functionally assessed?

2. Materials

2.1. Bacterial strains

2.1.1. ONE SHOT© TOP10 *E.coli*

Chemically competent *E.coli* strain used for cloning and plasmid replication.
Transformation efficiency: $1*10^9$ KbE/µg plasmid-DNA

Genotype: F- *mcrA* Δ(*mrr-hsd*RMS-*mcr*BC) Φ80*lac*ZΔM15 Δ *lac*X74 *rec*A1 *ara*D139 Δ(*araleu*)7697 *gal*U *gal*K *rps*L (StrR) *end*A1 *nup*G

Company: Invitrogen

2.1.2. BL21 (DE3) *E.coli*

Chemically competent *E.coli* strain used for protein expression.
Transformation efficiency: $1\text{-}5*10^7$ cfu/µg pUC19 DNA

Genotype: *fhuA2 [lon] ompT gal (λ DE3) [dcm] ΔhsdSλ DE3 = λ sBamHIo ΔEcoRI-B int::(lacI::PlacUV5::T7 gene1) i21 Δnin5*

Company: New England Biolabs

2.2. Cell line - Human embryonic kidney cells 293 (HEK293)

HEK293 cells are easy to transfect adherent growing cells. Originally they were derived from human embryonic kidney cells (HEK), that were exposed to sheared fragments of adenovirus type 5 DNA, performed by F.L. Graham in the lab of Alex van der Eb in Leiden published in 1977. Cells continue dividing after reaching confluence.[115]

2.3. Plasmids

2.3.1. pCMV-3Tag-1A

CMV promoter 1–602
3× FLAG tag 682–753
multiple cloning site 754–828
BGH polyA signal 908–1134
f1 origin 1273–1579
***bla* promoter** 1604–1728
SV40 promoter 1748–2086
neomycin/kanamycin resistance ORF 2121–2912
HSV-TK polyA signal 2916–3371
pUC origin 3500–4167

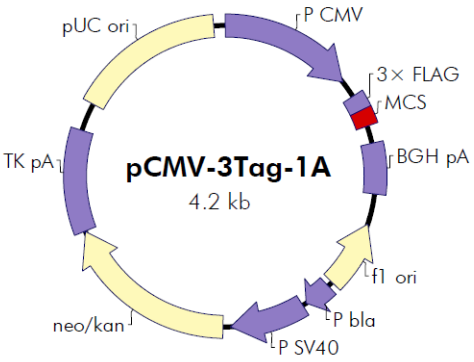

pCMV-3Tag-1A Multiple Cloning Site Region
(sequence shown 620–893)

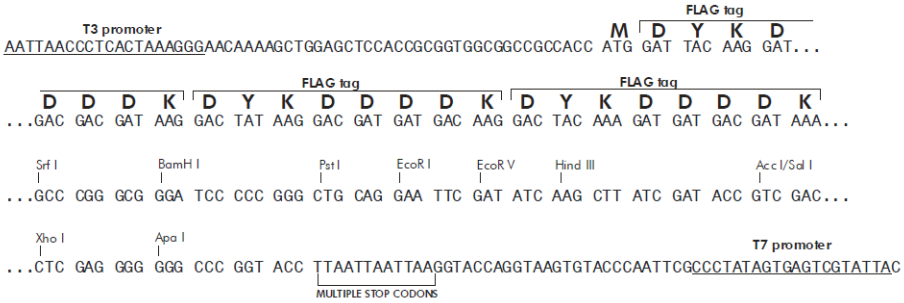

Figure 3: Vector map and sequence of pCMV-3Tag-1A vector.[117]

The pCMV-3Tag-1A vector is a commercially available vector from Agilent Technologies, including an N-terminal FLAG-tag, a neomycin/kanamycin resistance ORF and an ampicillin resistance (bla).

2.3.2. pET28a

pET-28a(+) sequence landmarks	
T7 promoter	370-386
T7 transcription start	369
His•Tag coding sequence	270-287
T7•Tag coding sequence	207-239
Multiple cloning sites	
(*Bam*H I - *Xho* I)	158-203
His•Tag coding sequence	140-157
T7 terminator	26-72
lacI coding sequence	773-1852
pBR322 origin	3286
Kan coding sequence	3995-4807
f1 origin	4903-5358

The maps for pET-28b(+) and pET-28c(+) are the same as pET-28a(+) (shown) with the following exceptions: pET-28b(+) is a 5368bp plasmid; subtract 1bp from each site beyond *Bam*H I at 198. pET-28c(+) is a 5367bp plasmid; subtract 2bp from each site beyond *Bam*H I at 198.

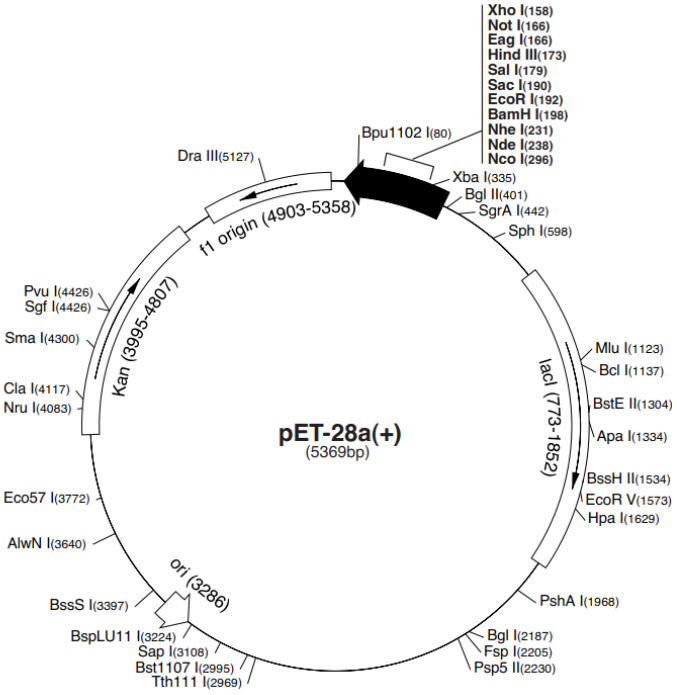

Figure 4: Vector map of pET28a-plasmid. (novagen cat.-no. 69864-3)

pET28a(+) is a commercially available vector from Novagen. It includes a kanamycin resistance gene (KanR), sequence for an N-terminal His-tag and an optional C-terminal His-tag. When inserting a stop-codon between the sequence of the protein of interest and the C-terminal His-tag sequence, the protein is only expressed with an N-terminal His-tag.

2.4. Buffers and stock solutions

DNA purification from agarose gel

Binding buffer - 50 mL
17.2 mM $NaClO_4$ solved in ddH_2O, 50 mM tris/HCL (pH 8.0) and 10 mM EDTA (pH 8.0)

Washing buffer - 50 mL
50 mM Tris/HCL (pH 8.0), 2 mM EDTA (pH 8.0), 0.4 M and 25 mL of 100% ethanol (50% (v/v) final)

Buffer for agarose gel electrophoresis

TAE, 50x
2 M tris/acetate (121.1 g tris, 25.5 mL acetic acid (100%)), 50 mM EDTA, pH 8.0 in a final volume of 500 mL ddH_2O

TAE 1x
50xTAE diluted 1:50 with ddH_2O, pH 8.3

6x loading buffer
40% (w/v) sucrose and 0.05% (w/v) bromphenol blue are solved in 10 mL ddH_2O, sterile filtered and stocks are stored at -20°C

***E.coli* buffers and media**

Lysis buffer for *E.coli* lysis
50 mM NaH_2PO_4, 300 mM NaCl, 1 mM $MgCl_2$, 15 mM imidazol (can be up to 20 mM, depending on purification results), including cOmplete™ mini protease inhibitor cocktail, Roche), pH 8.0

LB-broth medium
2% (w/v) LB broth in ddH_2O, autoclave at 121°C for sterilization, antibiotics are added directly before use

LB-broth medium with agar (Lennox) for agar plates
3.5% (w/v) LB broth (with agar) in ddH_2O, autoclaved at 121°C for sterilization or heated a few times in the microwave, antibiotic solutions are added in warm (but not hot) solution

Ampicillin 100 mg/mL stock
Solved in ddH_2O, sterile filtered, used 1:1000 diluted

Kanamycin 50 mg/mL stock
Solved in ddH_2O, sterile filtered, used 1:1000 diluted

Cell culture buffers

1x DMEM (Dulbecco's Modified Eagle Medium) complete medium – 450 mL (final volume 500 mL)
4.5 g/L D-glucose (0.45% (w/v)); 0.11 g/L sodium pyruvate (0.011% (w/v)) and phenol red. Added: 10% (v/v) heat-inactivated (30 min. at 65°C in the water bath) fetal bovine serum (FBS), 1% (v/v) L-glutamine (stock: 200 mM) and 1% (v/v) pen/strep (stock: penicillin (5000U/mL)/streptomycin (5000 µg/mL)). Stored at 4°C, small amounts were sterile filtered before use

DMEM serum-free medium – 450 mL
4.5 g/L D-glucose (0.45% (w/v)); 0.11 g/L sodium pyruvate (0.011% (w/v)) and phenol red. 1% (v/v) pen/strep (stock: penicillin (5000U/mL)/streptomycin (5000 µg/mL)) were added. Stored at 4°C, small amounts were sterile filtered before use

2x HEK293 cell lysis buffer
0.1 M tris, 0.3 M NaCl, 10 mM $MgCl_2$*8 H_2O, 2% (v/v) triton in ddH_2O, pH 7.5

1xDulbeccos PBS (phosphate buffered saline) pH 7.0-7.3
Without Calcium, Magnesium, phenol red. Stored at 4°C, sterile filtered before use

Platelet isolation buffers

Apyrase 500 U/mL
500 U/mL in ddH_2O, aliquoted and stored at -20°C

EDTA 0.5 M pH 7.4
0.5 M EDTA solved in ddH_2O, sterile filtered and stored at 4°C

CGS-buffer pH 6.5
120 mM NaCl, 12.9 mM $Na_3C_6H_5O_7$ *2 H_2O (trisodium citrate dihydrate), 30 mM D-glucose in ddH_2O, pH 6.5, stored in 50 mL aliquots at -20°C

HEPES-buffer pH 7.4
150 mM NaCl, 5 mM KCl, 1 mM $MgCl_2$*8 H_2O, 10 mM D-glucose, 10 mM HEPES in ddH_2O, adjust pH 7.4, stored maximum 4 weeks at 4°C

4xplatelet lysis buffer pH 7.5
50 mM tris, 150 mM NaCl, 4% (w/v) SDS solved in ddH_2O, pH 7.5

Platelet lysate generation

Lysis buffer with EDTA/EGTA pH 7.4
50 mM tris, 150 mM NaCl, 1 mM EDTA, 0.1 mM EGTA, 0.25% (v/v) NP-40, 30 ng/µl BSA, pH 7.4

Lysis buffer without EDTA/EGTA pH 7.4
50 mM tris, 150 mM NaCl, 0.25% (v/v) NP-40, 30 ng/µl BSA, pH 7.4

Gel-electrophoresis and western blotting buffers

3xLaemmli sample buffer
200 mM tris/HCl, 15% (v/v) glycerol, 6% (w/v) SDS, 0.06% (w/v) bromphenol blue in ddH_2O

3xLaemmli sample buffer for phostag SDS-PAGE
200 mM tris, 15% (v/v) glycerol, 6% (w/v) SDS, 2% (w/v) bromphenol blue in ddH_2O

APS 10% (w/v) solution
10% (w/v) APS was solved in ddH_2O. Aliquots of 1 mL were stored at -20°C

Bromphenol blue stock, 1% (w/v)
1% (w/v) bromphenol blue solved in ddH_2O

20% (w/v) SDS
40 g (20% (w/v)) SDS-pellets solved to a final volume of 200 mL ddH_2O

Tris 1 M, pH 6.8
1 M tris solved in ddH_2O, pH adjusted to 6.8

Tris 1 M, pH 8.8
1 M tris solved in ddH_2O, pH adjusted to 8.8

10xTBS, pH 7.4
1.37 M NaCl, 0.2 M tris solved in ddH_2O, pH 7.4

1xTBST
10 mM tris, 150 mM NaCl, 0.1 % (v/v) Tween®-20; 100 mL 10xTBS solved in 900 mL of ddH_2O, 1 mL Tween®-20 was added, pH 7.4

10x TGS Running buffer (BioRad)
25 mM tris, 192 mM glycine, 0.1% (w/v) SDS, pH 8.3

1x TGS Running buffer
2.5 mM tris, 19.2 mM glycine, 0.01% (w/v) SDS; 100 mL 10xTGS running buffer (BioRad) solved in 900 mL ddH_2O, pH 8.3

10x Transfer buffer
1.92 M glycine, 0.25 M tris solved in ddH_2O

1x Transfer buffer
192 mM glycine, 25 mM tris, 20% (v/v) methanol; 300 mL 10x transfer buffer, 600 mL methanol (pure) and 2100 mL ddH_2O, pH 8.4.

5x Phostag running buffer
0.5 M tris, 0.5 M MOPS, 0.5 % (w/v) SDS; solved in ddH_2O, pH 7.8 (do not adjust!), stored at 4°C

1x Phostag running buffer
0.1 M tris, 0.1 M MOPS, 0.1 % (w/v) SDS, 5 mM sodium bisulfite; 100 mL of 5x running buffer were diluted with 395 mL ddH_2O and 5 mL of 0.5 M sodium bisulfite solution, pH 7.8

1x Phostag transfer buffer
25 mM tris, 192 mM glycine, 10% (v/v) methanol in ddH_2O: 400 mL of 10xtransfer buffer, 400 mL methanol (pure), 20 mL of 20% (w/v) SDS solution, 3180 mL ddH_2O, pH 8.4

$ZnCl_2$ solution 10 mM
10 mM $ZnCl_2$ solved in ddH_2O, needs to be prepared fresh before each use!

Phostag solution 5 mM
10 mg phostag acrylamide (AAL-107) were solved in 100 µL methanol (pure), thoroughly vortexed, 1 mL ddH_2O added, vortexed, 2.2 mL ddH_2O added, vortexed until clear solution was obtained; stored protected from light at 4°C

Sodium bisulfite solution 0.5 M
0.5 M sodium metabisulfite solved in 100 mL ddH_2O, stored at 4°C; stable around 3 to 4 weeks

Silver staining buffers

Gel fixation solution
12.5 M (40% (v/v)) methanol, 1.67 M (10% (v/v)) acetic acid in ddH_2O

Wash solution
30% (v/v) ethanol in ddH_2O

Thiosulfate solution
0.02% (w/v) $Na_2S_2O_3$*5 H_2O in ddH_2O

Silver nitrate staining solution
0.2% (w/v) $AgNO_3$, 2 mM formaldehyde in ddH_2O

Developing solution
6% (w/v) Na_2CO_3, 16 µM $Na_2S_2O_3$*5 H_2O, 5 mM formaldehyde in ddH_2O

Stop solution
0.5% (w/v) EDTA in ddH_2O

Protein purification buffers

Binding buffer, pH 7.4
20 mM Na_3PO_4*12 H_2O, 500 mM NaCl, 30 mM imidazole in ddH_2O, pH 7.4

Elution buffer, pH 7.4
20 mM Na_3PO_4*12 H_2O, 500 mM NaCl, 500 mM imidazole in ddH_2O, pH 7.4

1xTBS, pH 7.4
0.137 M NaCl, 0.02 M tris, 100 mL of 10xTBS diluted in 900 mL ddH_2O

Recombinant protein phosphorylation in platelet lysis - buffers

10x kinase phosphorylation buffer pH 7.4
100 mM HEPES, 50 mM $MgCl_2$, 10 mM DTT (0.2 mM EDTA, if needed)

ATP 10 mM
10 mM ATP solved in ddH_2O, aliquoted and stored at -20°C. One aliquot is only used once

Recombinant protein phosphorylation with recombinant kinase - buffers

Kinase assay buffer (5x kinase dilution buffer)
25 mM MOPS, 25 mM $MgCl_2$*8 H_2O, 5 mM EGTA, 2 mM EDTA in ddH_2O, pH 7.2, stored at 4°C

Kinase dilution buffer III
5 mM MOPS, 5 mM $MgCl_2$*8 H_2O, 1 mM EGTA, 0.4 mM EDTA, 0.05 mM DTT, 100 ng/µL bovine serum albumin (BSA) in ddH_2O, pH 7.2. DTT and BSA were always added fresh on the day of the experiment. Stored at 4°C or aliquoted and stored at -20°C

Immunoprecipitation – Dynabeads™ protein A - buffers

1xPBS
137 mM NaCl, 2.6 mM KCl, 8 mM Na_2HPO_4*2 H_2O, 1.4 mM KH_2PO_4 solved in 1 L ddH_2O, pH 7.4

Washing buffer
1xPBS, 0.01 % (v/v) Tween®-20, pH 7.4

Elution buffer
50 mM glycine solved in ddH_2O, pH 2.8

Dynabeads™ His-tag isolation&pulldown - buffers

Binding/wash buffer
0.1 M NaH_2PO_4, 0.6 M NaCl, 0.02% (v/v) Tween®-20, pH 8.0

Elution buffer - 10xPP2A reaction buffer
500 mM imidazole, 2 mM EGTA, 0.2% (v/v) 2-mercaptoethanol, 1 mg/mL BSA solved in ddH_2O, pH 7.2. Stored at 4°C, used maximum 5 days

PP2A activity assay – buffers

5xPP2A reaction buffer
250 mM imidazole, 1 mM EGTA, 0.1% (v/v) 2-mercaptoethanol, 0.5 mg/mL BSA solved in ddH_2O, pH 7.2. Stored at 4°C, used maximum 5 days

2.5. Chemical substances

Table 1: Chemical substances used.

name	manufacturer
1 kb plus DNA ladder (1 µg/µL)	Invitrogen, USA
100 bp DNA ladder (0.5 µg/µL)	New England Biolabs, USA
6x DNA loading dye	Thermo Fisher Scientific, USA
8-Bromo-cGMP	Cayman chemical, USA
accutase solution	Sigma-Aldrich GmbH, (now part of Merck KGaA, Darmstadt, Germany)
acetic acid (AcOH) 96 % (v/v)	Carl Roth® GmbH&Co. KG, Karlsruhe
acrylamide (Rotiphorese® gel (acrylamide/bisacrylamide 30%/0.8%))	Carl Roth® GmbH&Co. KG, Karlsruhe
adenosine 5'-diphosphate-sodium salt (ADP)	Sigma-Aldrich GmbH, (now part of Merck KGaA, Darmstadt, Germany)

name	manufacturer
adenosine 5‘-triphosphate (ATP)	Sigma-Aldrich GmbH, (now part of Merck KGaA, Darmstadt, Germany)
adenosine 5‘-[3-γ-thio]triphosphate (thioATP) (1 mM)	Roche Diagnostics international AG, Switzerland
agarose standard (Roti®garose)	Carl Roth® GmbH&Co. KG, Karlsruhe
ammonium acetate ($CH_3CO_2NH_4$) (3 M, pH 5.5)	Invitrogen, USA
ammonium persulfate (APS)	Carl Roth® GmbH&Co. KG, Karlsruhe
ampicillin sodium salt (antibiotics; powder)	Fisher Scientific; USA
apyrase grade VII from potatoe	Sigma-Aldrich GmbH, (now part of Merck KGaA, Darmstadt, Germany)
bovine serum-albumin fraction V (BSA), pH 7.0	Capricorn Scientific, Ebsdorfergrund, Germany
bromphenol blue sodium salt	Merck KGaA, Darmstadt, Deutschland
calcium chloride ($CaCl_2$)	Carl Roth® GmbH&Co. KG, Karlsruhe
chloroform (trichloromethane) ($CHCl_3$)	Merck Millipore, Darmstadt, Germany
Clarity™ Western ECL Substrate	BioRad Laboratories, Hercules, USA
guanosine 3’,5’-cyclic monophosphate (cGMP)	Sigma-Aldrich GmbH, (now part of Merck KGaA, Darmstadt, Germany)
complete mini protease inhibitor tablets	Roche Deutschland Holding GmbH, Mannheim
complete mini protease inhibitor tablets (EDTA-free)	Roche Deutschland Holding GmbH, Mannheim
dimethyl sulfoxide (DMSO)	Merck KGaA, Darmstadt, Germany
disodium-dihydrogen-phosphate (Na_2HPO_4-*2 H_2O)	Carl Roth® GmbH&Co. KG, Karlsruhe
D(+)-Glucose (Glc)	Carl Roth® GmbH&Co. KG, Karlsruhe
dNTPs (dATPs, dCTPs, dGTPs, dTTPs), each 10 mM	Thermo Fisher Scientific, USA
1,4-Dithiothreitol (DTT)	Carl Roth® GmbH&Co. KG, Karlsruhe
ethylenediaminetetraacetic acid - disodiumsalt-dihydrate (EDTA-Na_2*2 H_2O)	Carl Roth® GmbH&Co. KG, Karlsruhe
ethylenediaminetetraacetic acid (EDTA 0.5 M solution)	AppliChem GmbH, Darmstadt, Germany
ethylene glycol-bis(β-aminoethyl ether)-*N*,*N*,*N*′,*N*′-tetraacetic acid (EGTA)	Carl Roth® GmbH&Co. KG, Karlsruhe
ethanol (EtOH) 99,5 % (v/v), pure	Carl Roth® GmbH&Co. KG, Karlsruhe
ethydiumbromide	Carl Roth® GmbH&Co. KG, Karlsruhe

name	manufacturer
fetal bovine serum (FBS) from South America	Thermo Fisher Scientific, USA
formaldehyde (FA) 37 % (v/v)	Carl Roth® GmbH&Co. KG, Karlsruhe
forskolin from *coleus forskohlii*	Sigma-Aldrich GmbH, (now part of Merck KGaA, Darmstadt, Germany)
fostriecin sodium salt	Cayman chemical, USA
L-glutamine (Gln) (200 mM)	GE Healthcare, Chalfont St Giles, UK
glycerol	Carl Roth® GmbH&Co. KG, Karlsruhe
glycine	Carl Roth® GmbH&Co. KG, Karlsruhe
glycogen (5 mg/mL)	Thermo Fisher Scientific, USA
2-(4-(2-hydroxyethyl)-1-piperazineethanesulfonic acid (HEPES)	Carl Roth® GmbH&Co. KG, Karlsruhe
hydrochloric acid (HCl)	Carl Roth® GmbH&Co. KG, Karlsruhe
Ilomedin 20µg/ml® (iloprost)	Jenapharm, Jena
imidazole	Carl Roth® GmbH&Co. KG, Karlsru
isopropyl β-D-1-thiogalactopyranoside (IPTG)	Thermo Fisher Scientific, USA
isopropanol (2-propanol, IPA) 99.9 % (v/v)	Carl Roth® GmbH&Co. KG, Karlsruhe
kanamycin sulfate (antibiotics; powder; for research use only)	Fisher Scientific, USA
LB broth	Sigma-Aldrich GmbH, (now part of Merck KGaA, Darmstadt, Germany)
LB broth with agar (Lennox)	Sigma-Aldrich GmbH, (now part of Merck KGaA, Darmstadt, Germany)
magnesium chloride ($MgCl_2$)	Carl Roth® GmbH&Co. KG, Karlsruhe
magnetic beads (Dynabeads®) His-tag isolation & pulldown	Novex®, life technologies, Thermo Fisher scientific, USA
magnetic beads (Dynabeads®) Protein A	Novex®, life technologies, Thermo Fisher scientific, USA
methanol (MeOH) 99,9 % (v/v)	Carl Roth® GmbH&Co. KG, Karlsruhe
β-mercaptoethanol	BioRad Laboratories, Hercules, USA
MOPS (3-(N-morpholino) propane sulphonic acid)	Carl Roth® GmbH&Co. KG, Karlsruhe
NP-40 alternative	Merck Millipore, Darmstadt, Germany
okadaic acid ammonium salt (OA)	Enzo Life sciences, Lörrach, Germany
penicillin (5000U/mL)/streptomycin (5000 µg/mL) (P/S) antibiotics	Thermo Fisher scientific, USA

name	manufacturer
PhosStop (phosphatase inhibitor cocktail tablets)	Roche Deutschland Holding GmbH, Mannheim
phostag™ AAL-107	Wako Chemicals, Germany
PolyJet™	SignaGen Laboratories, Rockville, USA
potassium chloride (KCl)	Carl Roth® GmbH&Co. KG, Karlsruhe
Precision Plus Protein Dual Color Standard	BioRad Laboratories, Hercules, USA
Quick Start™ Bradford 1x Dye Reagent	BioRad Laboratories, Hercules, USA
riociguat	Bayer AG, Leverkusen, Germany
Roti®-Phenol for nucleic acid extraction	Carl Roth® GmbH&Co. KG, Karlsruhe
Rp-8-Br-PET-cGMPS sodium salt	BioLog life science institute, Bremen, Germany
Sephadex® G-25	Promega, USA
silver nitrate ($AgNO_3$)	Carl Roth® GmbH&Co. KG, Karlsruhe
sodium azide (NaN_3)	Carl Roth® GmbH&Co. KG, Karlsruhe
sodium chloride (NaCl)	Carl Roth® GmbH&Co. KG, Karlsruhe
sodium chloride, isotonic solution 0.9% (w/v), sterile	B. Braun Melsungen AG, Melsungen
sodium carbonate (Na_2CO_3)	Merck KGaA, Darmstadt, Germany
sodium dihydrogen phosphate monohydrate ($NaH_2PO_4*H_2O$)	Carl Roth® GmbH&Co. KG, Karlsruhe
sodium hydroxide (NaOH) (32% (v/v))	Carl Roth® GmbH&Co. KG, Karlsruhe
sodium disulfite (sodium metabisulfite) $Na_2S_2O_5$)	Merck KGaA, Darmstadt, Germany
sodium dodecyle sulfate (SDS)	Carl Roth® GmbH&Co. KG, Karlsruhe
sodium hydrogen carbonate ($NaHCO_3$)	Carl Roth® GmbH&Co. KG, Karlsruhe
sodium perchlorate ($NaClO_4$)	Carl Roth® GmbH&Co. KG, Karlsruhe
sodium thiosulfate pentahydrate ($Na_2S_2O_3*5\ H_2O$)	Merck KGaA, Darmstadt, Germany
staurosporine	Abcam®, Cambridge, UK
tautomycetin	Tocris, USA
TEMED (N, N, N', N' tetramethyl-ethyldiamine)	Sigma-Aldrich GmbH, (now part of Merck KGaA, Darmstadt, Germany)
terralin	Schülke, Norderstedt
triethylamine ($C_6H_{15}N$)	Sigma-Aldrich GmbH, (now part of Merck KGaA, Darmstadt, Germany)

name	manufacturer
tris-(hydroxymethyl)-aminomethan (tris)	Carl Roth® GmbH&Co. KG, Karlsruhe
trisodium citrate dehydrate ($Na_3C_6H_5O_7$ *2 H_2O)	Carl Roth® GmbH&Co. KG, Karlsruhe
trisodium phosphate dodecahydrate (Na_3PO_4*12 H_2O)	Carl Roth® GmbH&Co. KG, Karlsruhe
Triton™X-100	Carl Roth® GmbH&Co. KG, Karlsruhe
Tween®-20	Sigma-Aldrich GmbH, (now part of Merck KGaA, Darmstadt, Germany)
zinc chloride (ZnCl2)	Honeywell, Germany

2.6. DNA and protein ladders

Size standards were used for agarose gel electrophoresis (DNA) but also for SDS-PAGE (proteins).

For DNA ladders, a mix of DNA fragments are used.

1 kb plus DNA Ladder and 100 bp DNA ladder (Invitrogen)

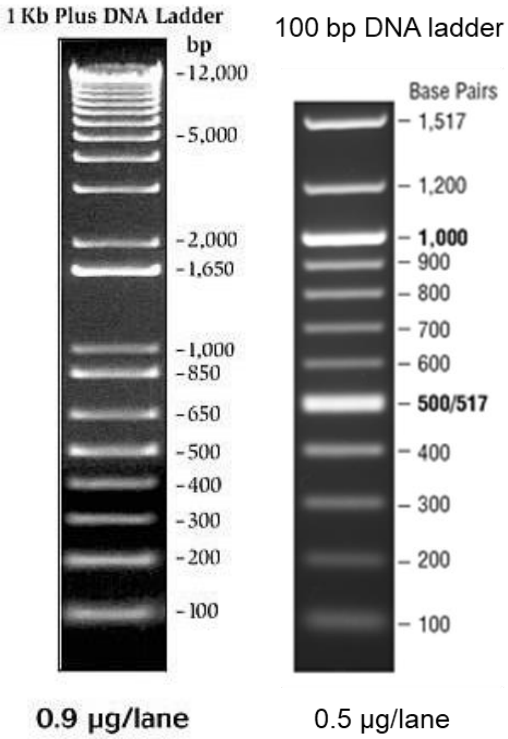

Figure 5: DNA size standards 1 kb (Invitrogen, datasheet Doc.Rev.:021802) and 100 bp (new england biolabs, international.neb.com) from NEB.
Depending on the percentage of the gel (1 kb shown for 0.9% (w/v) agarose gel; 100 bp for 1.3% (w/v) agarose; both are shown for ethidium bromide staining) and the amount of standard added, the thickness of the lanes and the spreading is differing. The mass intervals of 1 kb above 2000 bp are 1000 bp each band. Intervals for 100 bp ladder are 100 bp per band.

Precision Plus Protein Dual Color Standard, BioRad

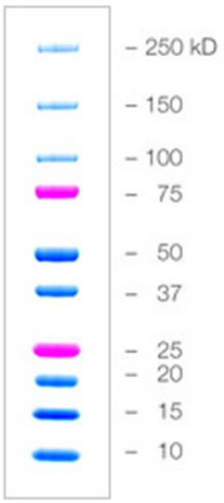

Figure 6: Molecular weight protein standards from BioRad.
The standard was used as marker for SDS-PAGE. 10 different sized proteins are included in the standard. Band heights is depending on the gel percentage.[118]

2.7. Consumables

Table 2: Consumables used.

material	description	manufacturer
14 mL PP tubes with round bottom and cup	14 mL tubes with two-position vent stopper; polypropylene	Greiner Bio-One GmbH, Frickenhausen
6-well cell culture plate	Cellstar® sterile, flat bottom, with lid, PS, clear	Greiner bio-one GmbH, Frickenhausen
affinity purification columns	HisTrap™ HP 1 mL	GE Healthcare, Chalfont St Giles, UK
desalting/buffer exchange columns PD-10	Sephadex™ G-25M	GE Healthcare, Chalfont St Giles, UK
blotting filter paper	Whatman™ 17CHR	GE Healthcare Life Sciences, Amersham, UK
citrate monovettes	Monovette® 10 mL 9NC, with anticoagulant 0.106 M citrate	Sarstedt AG&Co KG, Nümbrecht
cannual with tube for blood collection	Safety-Multifly®-Set 21G with tube and adapter 0.8x19 mm	Sarstedt AG&Co KG, Nümbrecht
cannual blue (23G)	BD Microlance™ 3 number 14, 0.6 mmx30 mm	Becton, Dickinson and Company Limited, Drogheda, Ireland
cell culture dish	20 mm, polystyrene, sterile	Greiner bio-one GmbH, Frickenhausen
cell culture flask	25 cm², 75 cm², with filter cupl	Greiner bio-one GmbH, Frickenhausen
cell scraper	M, length 300 mm, swiveling blade, blade with 200 mm, sterile	TPP®, Trasadingen

material	description	manufacturer
centrifugal filter units, Amicon® Ultra-4	Ultracel® 3K	Merck Millipore, Darmstadt, Germany
Costar® Assay plate 96 well	Flat bottom, half area, high binding, clear, polystyrene	Corning, USA
cuvettes for LTA measurement	Mikro-cuvettes with stirring bar for APACT 4 dispo-system	DiaSys Greiner, Flacht
cuvettes for OD measurement Rotilabo®	Single-use cells, polystyrene, semi micro 1.6 mL	Carl Roth® GmbH&Co. KG, Karlsruhe
cryo tubes	CryoTube™ Vials 1.8 mL	Nunc™, Sigma Aldrich Chemie GmbH, München
falcon tubes	Cellstar Tubes® polypropylene, conical bottom (15 mL/50 mL) with and without food (only 50 mL)	Greiner Bio-One GmbH, Frickenhausen
filter top 500	‚rapid'-filtermax, 500 mL, sterile, 0.22 µm pore size, PES membrane	TPP®, Trasadingen
filtered pipette tips	Biosphere Filter Tips 1250 µL extra long	Sarstedt AG&Co KG, Nümbrecht
folded qualitative filter paper	313, medium filtration rate, particle retention 5-8 µm, 185 mm	vWR, Darmstadt
micro tubes	Reaction tube, safe seal 1.5 and 2.0 mL	Sarstedt AG&Co KG, Nümbrecht
pasteur pipette (glas)	150 mm, open top	vWR, Darmstadt
PCR reaction tubes	Soft strips + cap strips 0.2 ml, clear	Biozym® Scientific GmbH, Hessisch Oldendorf
pipette tips	Ep T.I.P.S. 50-1000µl	Fisher Scientific GmbH, Nidderau
pipette tips	TipOne 200µl yellow/10 µL graduated tip	StarLab, Hamburg
PVDF (polyvinylidene difluoride) membrane	Amersham™ Hybond™ PVDF blotting membrane 0.45 µm and 0.2 µm	GE Healthcare Life Sciences, Amersham, UK
sealing tape	Optically clear, for 96 well plates	Sarstedt AG&Co KG, Nümbrecht
serological pipettes	Cellstar® sterile, 25/10/5 mL	Greiner bio-one GmbH, Frickenhausen
spin columns (10 mL)	Promega Ser/Thr phosphoatase assay	Promega, USA
sterile filter for syringe	Rotilabo® CA,diameter 25mm, sterile 0.2µm pore size	Carl Roth® GmbH&Co. KG, Karlsruhe
syringe	Discardit™ II (20/10/5 mL)	BD, Heidelberg
transfer pipette	3.5 mL disposable Pasteur pipettes with integral bulb	Sarstedt AG&Co KG, Nümbrecht
Zeba™ spin desalting columns	0.5 mL, 7K MWCO	Thermo Fisher scientific, USA

2.8. Primer for cloning and mutagenesis

Table 3: Primers used for cloning, ordered from Eurofines.

primer name	sequence nucleotides
FLAG-ENSA_forward	5'-AATGAATTCATGTCCCAGAAACAAGAAGAAGAGAACCC-3'
FLAG-ENSA_reverse	5'-AATCTCGAGTCATTCAACTTGGCCACCCGC-3'
His-ENSA_forward	5'-AATGAATTCATGTCCCAGAAACAAGAAGAAGAGAACCC-3'
His-ENSA_reverse	5'-AAT CTCGAGTCATTCAACTTGGCCACCCGCAAGCTTGCTGGTGAC-3'

Table 4: Primer used for mutagenesis, ordered from Eurofines.

primer name	sequence nucleotides
ENSA S109A_ forward	5'-GGATCTGCCCCAGAGAAAGTCCGCGCTCGTCACCAGCAAGCTTGCG-3'
ENSA S109A_ reverse	5'-CGCAAGCTTGCTGGTGACGAGCGCGGACTTTCTCTGGGGCAGAT GGGGCAGATCC-3'
ENSA S109D_ forward	5'-GGATCTGCCCCAGAGAAAGTCCGACCTCGTCACCAGCAAGCTTGCG-3'
ENSA S109D_ reverse	5'-CGCAAGCTTGCTGGTGACGAGGTCGGACTTTCTCTGGGGCAGATCC-3'
ENSA S67A_ forward	5'-AAGGGCAAAAGTACTTTGACGCAGGAGACTACAACATGGC-3'
ENSA S67A_ reverse	5'-GCCATGTTGTAGTCTCCTGCGTCAAAGTACTTTTGCCCTT-3'
ENSA S67D_ forward	5'-AAGGGCAAAAGTACTTTGACGACGGAGACTACAACATGGCCAA-3'
ENSA S67D_ reverse	5'-TTGGCCATGTTGTAGTCTCCGTCGTCAAAGTACTTTTGCCCTT-3'

2.9. Proteins and enzymes

All used recombinant proteins and enzymes are listed in Table 5.

Table 5: List of used proteins and enzymes.

protein	tag	concentration stock	expression system/source	storage	company
ARPP19, human, full length	GST, N-terminal	0.5 µg/µL	*E.coli*	Aliquots, -80°C	SignalChem
DpnI	--	10 U/µL		-20°C	Thermo Fisher scientific, USA
EcoRI	--	15 U/µL	*E.coli*	-20°C	Invitrogen, USA
MASTL, active	GST, N-terminal	0.05 µg/µL; activity: 18 nmol/min/mg	baculovirus-infected Sf9 insect cells	aliquots, -80°C	SignalChem
MASTL, inactive	GST	0.05 µg/µL	baculovirus-infected Sf9 insect cells	aliquots, -80°C	SignalChem (for western blotting)
Pfu polymerase	--	2.5 U/µL	--	-20°C	Thermo Fisher scientific, USA
PKA C-subunit (bovine)	--	30 ng/µL activity: 5.7 U/mg	purified from bovine heart	-20°C	kind gift of Prof. E. Butt, Univ. of Würzburg
PKGIβ (human)	--	120 ng/µL max. activity: 3.7 U/mg (stimulated by cGMP)	baculovirus-infected Sf9 insect cells	-20°C	kind gift of Prof. E. Butt, Univ. of Würzburg
T4 DNA Ligase	--	5 U/µL	--	-20°C	Thermo Fisher scientific, USA
thrombin/ factor IIa (human)	--	10 U/mL in ddH_2O	isolated from human plasma	aliquots at -80°C	Roche Diagnostics international AG, Switzerland
XhoI	--	10 U/µL	--	-20°C	Invitrogen, USA

2.10. Inhibitors

Table 6: List of inhibitors.

name	stock concentration and storage	targets (IC_{50})	company
fostriecin	2 mM in ethanol stored at -20°C, light protected	PP2A (1.5 nM) and PP4 (3 nM); PP1 (131 µM)[119]	Enzo Life sciences, USA
okadaic acid ammonium salt	2 mM in ethanol, stored at -20°C, light protected	PP2A (0.1-0.3 nM); PP1 (20-50 nM)[72]	Enzo Life sciences, USA

name	stock concentration and storage	targets (IC_{50})	company
staurosporine	5 µM in DMSO, stored at -20°C, light protected	PKC (3 nM), cAMP-dependent protein kinase (8 nM), p60v-src (6 nM)[120]	Abcam®, UK
tautomycetin	2 mM in DMSO, stored at -20°C, light protected	PP1 (1.6 nM), PP2 (62 nM)[121]	Tocris, USA
Rp-8-Br-PET-cGMPS, sodium salt	in ddH_2O, aliquoted and lyophilized, stored at -20°C	PKG Iα; Iβ; II (K_i=35; 30; 450 nM)	BioLog Life Science Institute

2.11. Antibodies

2.11.1. Primary antibodies

Table 7: Primary antibodies.

name	detection of	host species	stock [µg/mL]	usage	company
anti-α-actinin	human/mouse/rat/hamster/monkey total α-actinin-1 protein (carboxy-terminal binding), cross reaction with isoform 2 and 4	rabbit polyclonal	--	WB: 1:2000 in 3% (w/v) skimmed milk-TBST	Cell Signaling®, USA
anti-ENSA antibody	human/monkey/(rat/mouse) ENSA: amino acids near carboxy-terminus	rabbit polyclonal	1	WB 1:500 in 5% (w/v) BSA-TBST IP test (20 µg)	Cell Signaling®, USA
anti-ENSA antibody	human/mouse/rat ENSA, not defined	rabbit mono-clonal	--	WB: 1:1000-1:100000	Abcam®, UK
anti-ENSA antibody	human/mouse/rat ENSA, not defined	mouse mono-clonal	--	WB 1:100 – 1:5000 in 5% (w/v) BSA-TBST IP 1-2 µg per 100-500 µg protein	Santa Cruz®, USA
anti-pS67 ENSA/ pS62 ARPP19 antibody	human/rat/(mouse) residues surrounding pS67/S62–phospho-specific	rabbit polyclonal	--	WB platelets 1:250 recomb. proteins 1:500 in 5% (w/v) BSA-TBST	Cell Signaling®, USA

name	detection of	host species	stock [µg/mL]	usage	company
anti-pS109 PAN ENSA antibody	human pS109 ENSA pS104 ARPP19	rabbit polyclonal	94	WB 1 µg/mL in 5% (w/v) BSA-TBST	Custom prepared by Immuno-Globe® Himmelstadt, Germany
anti-pS109 ENSA antibody	*Xenopus*/human pS109 HisENSA	rabbit polyclonal	--	WB 1:300 in 5% (w/v) BSA-TBST	Prof. Dr. S. Mochida, Japan (kind gift)
anti-FLAG antibody	DYKDDDDK-tag	rabbit polyclonal	--	WB 1:3000 in 5% (w/v) BSA-TBST	Cell Signaling®, USA
G153 serum anti-ARPP19 antibody	recomb. human ARPP19 and HisENSA	rabbit polyclonal, serum	--	WB 1:2000 in 5% (w/v) BSA-TBST	Prof. Dr. A. Nairn, USA (kind gift)
anti-MASTL antibody	residues 550-600 of human MASTL kinase	rabbit polyclonal	1000	WB 1:500	Bethyl Laboratories, USA
anti-P-p38 MAP kinase (T180/Y182) (12F8) antibody	human/mouse/ rat/monkey/ *D.melanogaster* activated pT180/pY182 p38 MAP kinase	rabbit polyclonal	--	WB 1:1000 in 5% (w/v) BSA-TBST	Cell Signaling®, USA
anti-pS239 VASP antibody	human/mouse/ rat/monkey pS239 VASP	rabbit polyclonal	--	WB 1:1000 in 5% (w/v) BSA-TBST	Cell Signaling®, USA

2.11.2. Secondary antibodies

Table 8: Secondary HRP-conjugated antibodies used.

name	detection of	species	usage	company
HRP-conjugated anti-rabbit IgG (H+L)	rabbit IgG	goat polyclonal	WB: 1:5000 in 5% (w/v) BSA-TBST	BioRad Laboratories, USA
HRP-conjugated anti-mouse IgG (H+L)	mouse IgG	goat polyclonal	WB: 1:5000 in 5% (w/v) BSA-TBST	BioRad Laboratories, USA

2.12. Equipment

Table 9: Equipment used.

device name	type	manufacturer
autoclave	VX-150	Systec GmbH, Linden, Germany
automated hematology analyzer	KX-21N Sysmex ®	Sysmex Corporation Japan/Sysmex Germany GmbH
blot chamber	Trans-Blot® Cell	BioRad Laboratories, Hercules, USA
centrifuge 1	Allegra X-30R (Rotor: SX4400)	Beckmann Coulter GmbH, Krefeld, Germany
centrifuge 2, tabeltop (for 1.5 and 2 mL reaction tubes)	5418 R	Eppendorf AG, Hamburg, Germany
chromatography system (liquid) with fraction collector	ÄKTA™ Pure with fraction collector F9-R	GE Healthcare, Chalfont St Giles, UK
CO_2-incubator (cell culture)	INCO 153	Memmert GmbH & Co. KG, Schwabach, Germany
cryo freezing device	Mr. Frosty	Nalgene®, Thermo Fisher, Dreieich
electrophoresis system agarose gel	mini/midi-sized gel horizontal electrophoresis system	Cole-Parmer, Wertheim, Germany
electrophoresis system SDS-PAGE	mini-PROTEAN Tetra Cell	BioRad Laboratories, Hercules, USA
ELISA reader used for PP2A assay	Opsys MR™ Microplate Reader	Dynex Technologies Inc, USA
FACS tubes (polystyrol tubes)	5 mL, 75x12 mm	A. Hartenstein GmbH, Würzburg
freezer (4°C/-20°C)	divers	Liebherr
freezer (-80°C)	ultra-low Temp. freezer U725	Eppendorf AG, New Brunswick, USA
gel casting module for SDS-PAGE	mini-Protean Tetra Cell Casting Module	BioRad Laboratories, Hercules, USA
gel casting module for agarose gel	mini/midi-sized gel casting module	Cole-Parmer, Wertheim, Germany
gel documentation system	Gel Doc™ EZ Reader	BioRad Laboratories, Hercules, USA
incubator (37°C)	Heratherm Incubator	Thermo Fisher scientific, USA
laminar flow cabinet (cell culture)	Hera safe	Thermo Fisher scientific, USA
light microscope (cell culture)	Diaphot 300	Nikon, Düsseldorf, Germany
light transmission aggregometer	APACT 4S PLUS	DiaSys Diagnostics, Flacht, Germany
magnet for Dynabeads	DynaMag™-2	Invitrogen by Thermo Fisher Scientific life technologies, Norway
magnetic stirrer with/without heating	neoMag® D-6010/D-6011	neoLab Migge GmbH, Heidelberg, Germany

device name	type	manufacturer
microwave	studio 4in1 MD12801	MEDION AG, Essen, Germany
orbital shaker	RM Multi-1 with PRs-26	StarLab, Hamburg
PCR-cycler	mastercycler pro S	Eppendorf AG, Hamburg, Germany
pH-meter	HI 2211 pH/ORP meter	HANNA Instruments Deutschland GmbH, Vöhringen, Germany
pipette	divers	Eppendorf AG, Hamburg, Germany
pipet Filler (pipette boy)	S1	Thermo Fisher scientific, USA
power supply	PowerPac™ HC	BioRad Laboratories, Hercules, USA
precision balance	CPA 1003P	Sartorius AG, Göttingen, Germany
sonicator	Q700	QSonica, Newtown, USA
shaker (horizontal)	shaker DOS-10L	neoLab® Migge GmbH, Heidelberg, Germany
shaker (horizontal *E.coli*)	Certomat® H	Sartorius AG, Göttingen, Germany
spectrophotometer	NanoDrop2000c	Thermo Fisher scientific, USA
thermomixer	thermomixer compact 5350	Eppendorf AG, Hamburg, Germany
rock'n roller	SU1400	SunLab, Mannheim, Germany
vortex mixer 1	lab dancer	VWR International GmbH, Darmstadt, Germany
vortex mixer 2	neoVortex® mixer D-6012	neoLab® Migge GmbH, Heidelberg, Germany
water bath	ED-AP (042) (5A max. 60°C)	Julabo GmbH, Seelbach, Germany
water purification device	Milli-Q® advantage and Q-POD® element	Merck Millipore, Darmstadt, Germany
western blot chemiluminescence detection	Fusion FX7	Vilbert Lourmat GmbH, Eberhardzell, Germany

2.13. Kit-systems

- GeneJet Plasmid Miniprep Kit – Thermo Fisher Scientific
- Serine/threonine phosphatase activity assay - Promega

2.14. Software and databases

Software

- Graphs and statistics:

  GraphPad Prism 7

- Reverse primer design:

  Ualberta (http://www.ualberta.ca/~stothard/javascript/rev_comp.html)

- Test for proper cutting of protein sequence with used enzyme = webcutter

  http://heimanlab.com/cut2.html; (earlier: http://rna.lundberg.gu.se/cutter2/index.html)

- Translation of sequences

  Expasy (http://web.expasy.org/translate/)

- Sequence alignment (e.g. to compare a sequencing result and the expected sequence)

  Clustal Omega (clustal.org/omega or ebi.ac.uk/Tools/msa/clustalo/)

Databases

- Uniprot for protein information and sequences (uniprot.org)
- PhosphoSitePlus for phosphorylation sites of proteins and known references or antibodies (phosphosite.org)
- PhosphoNet:Kinexus for the search of human protein kinases, phosphorylation sites, substrates and inhibitors (phosphonet.ca)

3. Methods

3.1. Handling of *Escherichia coli (E.coli)*

3.1.1. Storage of *E.coli*

Bacterial cultures, which were frequently used, were plated on a LB-agar-antibiotic-plate, incubated overnight at 37°C in an incubator and stored for a maximum of four weeks at +4°C. For long-term storage, cryo-stocks of the *E.coli* strains were prepared by inoculating 10 mL of LB-broth-antibiotics medium and overnight cultivation at 37°C and 250 rpm. 1 mL of culture was added to glycerol (final concentration of 20% (v/v) glycerol) in a cryo-tube, strongly vortexed and directly frozen in liquid nitrogen. The stocks were stored at -80°C.

3.1.2. Cultivation of *E.coli*

E.coli TOP10 and BL21 were cultivated at 37°C and 225 rpm in a "shaking incubator" in LB-medium. Depending on antibiotic resistances of the used plasmid, the needed antibiotics were added.

3.1.3. Determination of cell density

The cell density of the *E.coli* culture was determined by measuring the optical density (OD) at a wavelength of 600 nm in a 1.5 mL cuvette using NanoDrop2000c. Therefore, a 1:10 dilution of the *E.coli* culture was prepared by adding 100 µL of *E.coli* suspension to 900 µL of culture medium. The OD_{600} was determined at least three times and a mean was calculated. As blank value, 1 mL of the same LB-medium was used.

3.1.4. Transformation of One Shot® TOP10 *E.coli* with heat shock

Transformation of One Shot® TOP10 *E.coli* was performed for DNA reproduction and isolation. To transform chemically competent One Shot® TOP10 *E.coli* with the plasmid (containing the sequence for the protein of interest (ENSA)), one vial per transformation (50 µL of *E.coli*) was thawed on ice. 1-5 µL of the plasmid solution were added into the vial directly after thawing the whole suspension and mixed by tapping gently on the vial. The mix was left on ice for 30 minutes (min.), each 10 min. the tube was carefully tapped for mixing. After incubation, the vial was placed for exactly 30 seconds (sec.) in a 42°C water bath and then placed back on ice for around 2 min. 250 µL of 37°C pre-heated S.O.C medium were added per vial. The vial was placed in a thermomixer and incubated for 1 to 2 hours at 300 rpm shaking at 37°C.

100 µL of the reaction mixture were placed on a 37°C pre-heated LB-agar plate containing kanamycin for selection (or ampicillin, depending on the used plasmid). With a new pipette tip, a small part was taken from the liquid spot of *E.coli* suspension and placed next to the first, by spreading the liquid with the tip. The same procedure was repeated with a fresh tip from the second spot. In the end, there were three places on the plate, filling nearly the whole surface, containing different concentrations of cells. The plate was converted and incubated over night at 37°C.

It was expected that only successfully transformed *E.coli* containing the (ENSA) plasmid grow on the plate.

3.1.5. Transformation of *E.coli* BL21 (DE3) via heat shock

For each protein expression, one tube of *E.coli* BL21 (DE3) was thawed on ice for 10 min. 1-5 µL with a maximum of 100 ng (usually around 90 ng) of plasmid containing the HisENSA protein sequence were added to the cells and the tube flicked carefully up to 5 times. The tube was kept on ice for 30 min. The heat shock was performed at 42°C in a water bath for exact 10 sec. Afterwards, the tube was placed on ice again for 5 min. 950 µL of S.O.C medium having room temperature (RT) were added and the tube was placed for 60 min. at 37°C and 300 rpm in the thermomixer. Agar selection plates containing ampicillin were heated to 37°C. The transformed cells were spread in dilutions on the plates (procedure as described in 3.1.4.) and incubated overnight at 37°C.

It was expected that only successfully transformed *E.coli* containing the (ENSA) plasmid grow on the plate.

3.1.6. Isolation of plasmid-DNA from *E.coli* TOP10 (mini-prep)

For DNA isolation, the geneJET Plasmid mini-prep kit (Thermo Scientific) was used.
E.coli were plated on selection plates. On the next day, a single colony was picked and placed into 5 mL of LB medium including the selection antibiotics. After overnight incubation at 37°C with 200 rpm shaking, the bacteria were harvested by centrifugation using at 8,000 rpm for 2 min. at RT in 2 mL reaction tubes with a tabletop 5418R Eppendorf centrifuge. The supernatant was discarded and the pellet was solved in 250 µL of ‘resuspension solution’ (including RNase A), the suspension was placed in a new reaction tube. 250 µL of ‘lysis solution’ were added and the suspension mixed by inverting the tube 4 to 6 times, the solution became viscous. 350 µL of ‘neutralization solution’ were added and the tube immediately inverted 4 to 6 times for mixing.

The solution was centrifuged for 5 min. at 14,000 rpm (tabletop 5418R Eppendorf centrifuge) to pellet cell debris and chromosomal DNA. The supernatant was transferred to the supplied GeneJET columns by pipetting, without taking the white precipitate. The column was centrifuged in the supplied tube for 1 min. The flow-through was discarded and the column was placed back in the collection tube. 500 µL of ‘wash solution’ (diluted with ethanol) were added to the column and the column was centrifuged for 1 min. at 14,000 rpm (tabletop 5418R Eppendorf centrifuge). The flow-through was discarded and the column was placed again back to the collection tube. The wash procedure was repeated once. The flow-through was discarded, the column centrifuged for 1 min. to remove all remaining ‘wash solution’, so no ethanol was remaining on the column and the sample.

The column containing the DNA was placed in a new 1.5 mL reaction tube, 50 µL of ‘elution buffer’ (water) were placed in the middle of the spin column membrane, incubated for 2 min. at RT and the column centrifuged for 2 min. at 14,000 rpm (tabletop 5418R Eppendorf centrifuge). The column was discarded and the purified plasmid DNA stored at -20°C.

3.1.7. Protein expression in *E.coli* BL21

A pET28-vector including the sequence for α-endosulfine isoform 1 (according to uniprot.org) was transformed into the chemically competent BL21 *E.coli* according to 3.1.5. A starter culture was prepared by picking a clone from a fresh agar-plate or placing a part of a glycerol-stock into 10 mL of LB-medium containing 30 µg/mL kanamycin. The culture was incubated over night at 37°C and 250 rpm shaking.

The next day, all 10 mL of starter culture were added to 500 mL of LB-medium also containing 30 µg/mL kanamycin (1:50 dilution). If a higher amount *E.coli* was needed, higher volumes were used.

The suspension was shaken for about 5 hours at 37°C, until OD_{600} of 0.6 was reached. Protein expression was induced by adding IPTG at a final concentration of 0.1 mM (stock: 0.1 M IPTG). The culture was incubated at 250 rpm for 20 hours at 20°C. Optional, to fastly cool down the *E.coli* suspension, the Erlenmeyer flask including the suspension could be placed on ice before adding IPTG.

After 20 hours of incubation, the bacterial suspension was transferred into 50 mL falcons and pelleted at 4,225 xg for 10 min. at 4°C. The supernatant was removed and the pellets stored at -20°C, if not needed immediately.

For protein purification (3.5.5.), one pellet was resuspended in 5 mL of ice-cold lysis buffer. To completely lysate the cells, the suspension was placed into 2 mL reaction tubes and sonicated using U700 sonicator. Therefore, two to three times sonication of 10 sec. with amplitude 75% and two times sonication of 15 sec. with amplitude 50% with intermitted 30 sec. incubation on ice was performed. The lysate was then centrifuged for 45 min. at 14,000 rpm and 4°C in a table top-centrifuge from Eppendorf 5418R to remove all cell pieces that were left. Only the supernatant was used for protein purification. For western blotting, 50 µL of the lysate were used and mixed with 25 to 50 µL of 3xlaemmli sample buffer and heated for 5 min. at 95°C and 350 rpm shaking.

3.2. Molecular biology methods

3.2.1. Determination of DNA concentration using NanoDrop2000c

To determine the concentration of a DNA solution, the absorption of the solution in a UV range was measured using the spectrophotometer NanoDrop2000c.

As blank value, 1.5 µL of ddH_2O (buffer, where the DNA was solved in), were used. 1 to 1.5 µL of the sample were placed on the measuring point. The lid was closed and the concentration was measured using a filter wavelength of 260 nm. A minimum of three absorption measurements per solution were performed, and the mean of the measurements in arbitrary units was calculated as concentration.

3.2.2. Cloning of plasmid-DNA using PCR (polymerase chain reaction)

The idea of a PCR-reaction is to amplify a small amount of DNA and produce thousands to millions of copies of the DNA. In this reaction, a polymerase is used, that produces the new

DNA by using the old one as a template. The polymerization reaction is performed by a DNA polymerase that starts the reaction at a pre-existing 3'-OH group. Therefore, certain primers (always forward and reverse) can be designed to amplify a certain DNA sequence from a template. For amplification, nucleotides need to be added. By using the same system, mutations can be inserted specifically in a DNA sequence that is amplified. Polymerases are working with different speed and different accuracy. Depending on the aim of the PCR (DNA amplification (e.g. for genotyping) or mutagenesis), different polymerases can be used. For a mutagenesis, a accurate working polymerase, like the Pfu-polymerase, should be used. For genotyping for example, the less accurate working Taq-polymerase is sufficient.

In this thesis, PCR was used for DNA amplification (insert or vector) and mutagenesis.

First, the insert needed to be amplified via PCR by using Pfu-Polymerase and primers containing overhangs with the appropriate sites for restriction enzyme digestion. The standard PCR-reaction mix was prepared on ice containing the reagents listed in Table 10.

Table 10: PCR reaction mix for PCR-cloning.

	standard mix (50 µL per sample)	**control (50 µL)**
10xPfu-buffer	5 µl	5 µl
forward primer	1 µL (10 µM)	1 µL (10 µM)
reverse primer	1 µL (10 µM)	1 µL (10 µM)
dNTP mix	1 µL (10 mM each)	1 µL (10 mM each)
Pfu-polymerase	1 µL	1 µL
ddH_2O	40 µL	41 µL
template (added last)	1 µL (10 ng)	--

One control (standard mix without template, as mentioned in Table 10) was always included per run. The heating block of the PCR machine was pre-heated to 95°C and the samples were placed on the hot block to directly start the reaction. The following PCR-program was used.

Table 11: Steps of used PCR-program.

step	**step in one cycle**	**temperature [°C]**	**time**
denaturation of template		95	2 min.
cycle	start of cycle	95	25 sec.
	annealing	55-65	25 sec.
	elongation	68	n min. (n=size of insert [kb] x2; 1 min. for ~500 kb)
total number of cycles: 25			
final elongation		68	15 min.
cool down		to 4	infinity

10% (v/v) of the reaction sample (5 µL) were checked via agarose gel. When one clear band appeared, the rest of the reaction was purified via phenol/chloroform extraction.

Phenol/chloroform extraction:

The reaction was placed in a 1.5 mL reaction tube, mixed with ddH_2O to a final volume of 300 µL, an equal volume (300 µL) of phenol/chloroform/isopropanol (25:24:1) was added, the reaction tube vortexed for 30 sec., centrifuged for 8 min. at maximum speed (16,900 xg) using a table top Eppendorf 5148R centrifuge and the upper, aqueous phase removed. Now the DNA inside the aqueous phase was precipitated with ethanol. 300 µL of DNA solution were used, 12 µL glycogen (5 mg/mL), 30 µL ammonium acetate, $CH_3CO_2NH_4$, (3 M, pH 5.5) and 940 µL of ice cold 100% ethanol were added, the tube inverted for mixing and vortexed for 30 sec. The solution was centrifuged in a table top centrifuge for 15 min. at 16,900 xg and RT. The supernatant was removed with a pipette, 500 µL of 75% (v/v) ethanol added, the sample vortexed for 30 sec., centrifuged for 5 min. at 16,900 xg, the supernatant removed, again 500 µL of 75% (v/v) ethanol added, 30 sec. vortexed, 5 min. centrifuged and the supernatant again removed. All remaining fluidics were carefully removed with a yellow pipette tip.

The remaining DNA pellet was solved in 10 µL of ddH_2O. The DNA concentration was measured using the NanoDrop2000c.

The insert DNA then was digested by using two enzymes also suitable for the target plasmid. Therefore, 1 µL per enzyme was added to the insert-DNA in a total volume of 50 µL. The digestion was incubated at 37°C for 1 to 2 hours in a thermomixer. The whole reaction sample was placed on an agarose gel to separate digested from non-digested DNA by size. The digested PCR-product was cut out of the gel and isolated using the purification method explained in 3.2.4.

The target vector was also digested with the same two enzymes used for the insert DNA. This digesting method has the advantage that the insert is fitting exactly in the gap of the vector.

3.2.3. Ligation reaction of vector and insert

To place the certain DNA sequence including the sequence of the gene of interest (insert) into a certain vector, ligation was performed. Vector and insert were digested with the same restriction enzymes before starting the ligation. The volume of insert and vector together was 10 µL, including a maximum of 100 ng DNA (vector plus insert). 10 µL of thawed 2xligation buffer were added, and the solution mixed. 1 µL of T4 ligase was added, mixed by tipping and incubated for 2 to 3 hours at RT.

With this ligation mix, transformation of chemically competent *E.coli* (TOP10) was performed. Clones were picked and DNA was isolated via mini-prep (Thermo Fisher). A test digestion with 3 µL of DNA and enzymes used already for insert digestion was performed and an agarose gel was run to look if insert DNA appears after digesting the new vector.

3.2.4. DNA purification from agarose-gel

The bands including the DNA were cut out of the agarose gel and placed in a reaction tube, 600 µL of binding buffer (6 M sodium perchlorate, 50 mM tris pH 8.0, 10 mM EDTA) were added and the gel piece incubated at 50°C and 500 rpm shaking with in between vortexing, until the gel was solved.
After having a clear solution, 5 µL of 'prep-a-gene matrix' (BIORAD; stock of 166 mg/mL, solved in water and washed before use 5 to 10 times with water; stored at 4°C and vortexed before use), were added and incubated for 10 min. at RT. The mix was centrifuged a table top Eppendorf 5148R centrifuge at 13,000 rpm for 1 min. at RT, the supernatant was discarded and the pellet resuspended in 1.0 mL of wash buffer (20 mM tris pH 8.0, 2 mM EDTA, 400 mM NaCl, 50% (v/v) ethanol).
The centrifugation and resuspension were repeated. The mix was then centrifuged (Eppendorf 5148R) at 13,000 rpm for 1 min. at RT, the supernatant discarded, the pellet centrifuged again and all remaining liquid removed. The pellet was now solved in 10 µL of ultrapure water (ddH_2O) and incubated for 10 min. at 37°C with 400 rpm shaking.
The mix was centrifuged again (Eppendorf 5148R) at 13,000 rpm for 1 min. at RT. The supernatant now contained the purified DNA and was transferred into a new reaction tube. The DNA concentration was determined as mentioned in 3.2.1.

3.2.5. Mutagenesis of DNA

To insert a mutation into the DNA of the protein of interest, mutagenic primers were designed that include the nucleotide mutation and around 20 nucleotides 3' and 5' next to the mutation site. The size of the primers should be a minimum of 40 basepaires (bp). A sense and a reverse primer were designed. To ensure, the sequence of the primers is correct, 'Expasy translate tool' was used, translating the nucleotide sequence into the amino acid sequence. The mutation was inserted via PCR and the mutagenic primers (sequence shown in 2.8.). Only mutated PCR should be amplified. The PCR reaction was pipetted as presented in Table 12, Table 13 presents the performed PCR program.

Table 12: PCR reaction mix for mutagenesis using PCR.

	standard mix (50 µL per sample/per mutation)
10xPfu-buffer	5 µl
sense mutagenic primer	1 µL (10 µM stock)
antisense primer	1 µL (10 µM stock)
dNTP mix	1 µL (10 mM each dNTP)
Pfu-polymerase	1 µL
ddH_2O	40 µL
template DNA (added last)	1 µL (20 - 100 ng)

Table 13: Steps of mutagenesis PCR-program.

step	step in one cycle	temperature [°C]	time
denaturation of template		95	1 min.
cycle	start of cycle	95	50 sec.
	annealing	60	50 sec.
	elongation	68	n min. (n=size of complete plasmid DNA [kb] x2
total number of cycles: 18			
final elongation		68	7 min.
cool down		to 4	infinity

To digest the non-mutated DNA, also called 'parental-DNA' after the PCR-run, 25 µL of the sample were used and 1 µL of the restriction enzyme DpnI (10 U/µl stock) was added. DpnI only cuts DNA derived from *E.coli* but not PCR-produced DNA. DpnI is methylation sensitive. It only cuts DNA that presents with methylated bases. Methylation does not exist on PCR-produced DNA, but indeed on *E.coli*-produced DNA.

The solution was incubated without shaking for one hour at 37°C.

2 µL of the digestion solution were directly used for transforming chemically competent *E.coli* (TOP10) according to the Invitrogen™ transformation protocol. The pre-incubation step was performed in medium without antibiotics to increase the clone yield.

Two colonies were picked, the DNA was isolated as described (3.1.6.) and the DNA was sent for sequencing. Sequencing was performed by the manufacturer 'Eurofines'.

3.2.6. Agarose gel electrophoresis (for verification of PCR, DNA digestion and DNA purification)

Agarose gel electrophoresis is used to separate DNA fragments by size from each other, varying from 100 bp to 25 kbp.[122] Agarose molecules form stable polymers during gelation. The helical polymers are forming supercoiled bundles leading to a three-dimensional structure of the agarose gel, including pores and channels. The pore size of the gel is variable depending on the concentration of the agarose.

DNA is negatively charged due to its phosphate backbone. When DNA is loaded on an agarose gel and an electric field is applied, the negatively charged DNA is moving towards the positively charged cathode, whereby the speed is depending on the size of the fragment. The bigger the fragments the slower they run in the gel. DNA fragments can be visualized after agarose gel electrophoresis is completed by staining DNA with ethidium bromide (potentially carcinogenic, should be always handled with care) using UV light.

Procedure:
A 1.5% (w/v) agarose gel was prepared by adding 1.5 g of ultrapure agarose to 100 mL of gel running buffer TAE (40 mM tris-acetate, 1 mM EDTA, pH 8.3). The mix was heated in the microwave until all agarose powder was completely solved. The solution was kept at RT to cool down by gentle swirling. Ethidium bromide (2.5 µL of 10 mg/mL stock added to 50 mL gel)

was added and the solution was placed inside a horizontal gel box, including a suitable comb. Bubbles were removed and the gel polymerized at RT until the gel was completely polymerized within one hour. The gel was placed with its surrounding plastic box inside a horizontal gel-chamber, already being filled with TAE running buffer. Care was taken that the gel was completely covered with buffer.

Sample preparation for agarose gel electrophoresis:
5 µL sample + 5 µL 6xloading buffer in one PCR tube

Running procedure:
The samples were loaded on the gel (10 µL per pocket), a suitable DNA size marker was used (100 bp or 1 kbp ladder). The power was placed to 80-100 Volt, the gel ran about 30 min. By checking the height of the dye running front, the gel was stopped before the front reached the end of the gel.

The gel was taken out of the running chamber and was placed inside a gel documentation machine from BioRad. By switching on UV light, the DNA lanes were detected and a picture was taken for documentation.

3.3. Cell culture

All working steps with a human cell line were performed under sterile conditions if not mentioned otherwise, using a sterile workbench, sterile pipettes and sterile buffers, media, solutions and reagents.

3.3.1. Cultivation and storage of the human embryonic kidney cell line HEK293

Human embryonic kidney cells 293 are adherent cells. They were cultured in 75 cm^2 cell culture flasks in DMEM complete medium (high glucose) containing fetal bovine serum (FBS), the antibiotics pen/strep and the amino acid L-glutamine. Cells were split 1:10 every 3rd to 5th day. Between the 5 days, the medium was exchanged by 9 to 10 mL of fresh medium. Cells were cultivated in an incubator with water-saturated atmosphere and 5% (v/v) CO_2 at 37°C.

3.3.2. Splitting of HEK293 cells

To split the cells, 1-2 mL of accutase were used to detach the adherent cells. Therefore, the old medium was removed, the cells once washed with 10 mL of 1xDulbeccos PBS and then accutase was added. After about 2 min., the cells detached from the flask surface. 8 mL of fresh medium were added and the mix was well resuspended by pipetting on the flask wall. 1 mL of the suspension was placed into a new flask containing 9 mL of fresh medium. If accutase has to be removed completely, the cell suspension was placed into a 15 mL falcon and centrifuged at 2,000xg for 5 to 10 min. The supernatant was removed and the pellet was resuspended in 10 mL fresh medium. 1 mL of the suspension was placed in a new flask containing 9 mL of fresh medium.

For transfection-experiments, HEK293 cells were placed in a 6-well plate. First, 1.8 mL of fresh complete DMEM medium were added per well. The cells grown in a 75 cm^2 flask were removed from the surface as described above. Therefore, the centrifugation step was performed, the pellet resuspended in 10 mL of fresh complete DMEM medium, 200 µL of this

mix were added drop-wise per well. The cells were cultured overnight in an incubator with water-saturated atmosphere and 5% (v/v) CO_2 at 37°C.

3.3.3. Transient transfection of HEK293 cells

To insert DNA into the nucleus of HEK293 cells via transient transfection and to induce a non-stable overexpression of the protein of interest (FLAG-ENSA), 'PolyJet™ DNA In Vitro Transfection Reagent' was used.

The polymer based PolyJet™ reagent is encasing the DNA within 5 min. of incubation. The DNA-PolyJet™ complex enters the cell via endocytosis. Inside the cell, the DNA is set free, enters the nucleus and the polymer reagent is completely degraded in the cytoplasm.

Transfection was performed with cells cultured in 6-well plates with 2 mL complete medium per well. About 80% of the well bottom should be covered with cells. 30 to 60 min. before planned transfection, the old medium was removed and 1 mL of fresh pre-heated to 37°C complete DMEM medium was added per well.

Per well, 1 µg of DNA (pCMV-3Tag-1A including ENSA sequence) should be added. Therefore, 1 µg of DNA was placed into 50 µL of serum-free medium (final DNA concentration 20 ng/µL). In a second reaction tube, 3 µL of PolyJet™ reagent were mixed with 50 µL of serum-free DMEM-medium. The PolyJet™ mix was then added to the DNA-containing medium (final DNA concentration 10 ng/µL), for mixing, the tube was only once carefully placed upside down. The reaction was incubated for 15 min. at RT without shaking.

The whole 100 µL mix was then added to the cells by placing it drop-wise inside the 1 mL of medium inside the well (final DNA concentration 1 µg/mL).

The mix was incubated for 4 to 5 hours with the cells while they were incubated at 37°C with 5% (v/v) CO_2 in the humidified incubator. Then, the medium mix was removed gently with a pipette and 2 mL of fresh complete DMEM-medium were added per well.

Cells can be treated and harvested next day.

3.3.4. Stimulation of HEK293 cells

Transient transfected HEK293 cells overexpressing FLAG-ENSA or the mutant S67A FLAG-ENSA were treated with forskolin, to stimulate adenylyl cyclase and protein kinase A signaling pathways.

The complete medium was removed again on the day after transfection. Cells were washed once with 1 mL of serum-free DMEM medium. 1 mL serum-free DMEM including 10 µM forskolin (1 µL from 10 mM stock solution) was placed on the cells, the vehicle control includes 1 µL of 100% DMSO stock (final concentration: 0.1% (v/v) DMSO/well). To the untreated control (basal), 1 mL of serum-free DMEM was added.

The cells were incubated for 15 min. in an incubator with water-saturated atmosphere and 5% (v/v) CO_2 at 37°C. After incubation, the medium was removed and the cells washed twice with ice-cold 1xTBS-buffer on ice. All following steps were performed on ice. 125 µL of 2xHEK293

lysis buffer were placed on the cells. With a scraper, the adherent cells were removed from the bottom of the well. 125 µL of 3xSDS-laemmli buffer were added and the mix placed in a 1.5 mL reaction tube. The mix was heated for 10 min. at 95°C and 350 rpm shaking in a thermomixer. Samples were cooled to RT and stored at -20°C.

3.4. Platelet isolation and experiments

3.4.1. Blood drawing

After written informed consent was given, blood was taken from healthy volunteers who did not take platelet-affecting drugs (e.g. aspirin, ibuprofen) for at least 10 days before. Blood was drawn from a vein in the antecubital fossa or forearm via venipuncture using a cannula with tube into monovettes (5 or 10 mL) containing 3.2% (v/v) tri-sodium-citrate (1:10) to prevent blood coagulation. During blood drawing, care was taken, that the blood was not drawn too fast and that no bubbles appeared, to prevent pre-activation of platelets by enhanced shear stress. Blood cells were counted automatically using a Sysmex® KX-21N analyzer.

Studies of human platelets from healthy volunteers were approved by the ethics committee of the University Mainz (Study No. 837.302.12; 25.07.12).

3.4.2. Isolation of human platelets from anticoagulated whole blood

Washed human platelets were isolated from citrate-anticoagulated whole blood. After drawing the blood as described in 3.4.1., EGTA (Stock solution 0.5 M) was added to each 10 mL whole blood citrate tube with a final concentration of 3 mM.

For proteomic or phosphoproteomic samples, 0.2 U/mL apyrase (final concentration) were also added per tube.

The tubes were centrifuged at 200xg for 10 min. at RT with decel 2 in a Hereaus Alegra® centrifuge. The resulting upper layer, which included the yellow platelet-rich plasma (PRP), was separated from the lower buffy coat (leukocytes and erythrocytes) by careful transfer with a 2.5 mL transfer pipette into a new 14 mL Greiner® tube with lid and diluted 1:1 with CGS-buffer. The platelets in the PRP kept 5 to 10 min. for resting at RT.

The diluted PRP was then centrifuged at 69xg for 10 min. at RT with decel 1 to remove the remaining leukocytes from the PRP. The supernatant was transferred into a new 14 mL Greiner® tube without leukocyte contamination.

The leukocyte-free PRP was centrifuged at 400xg for 10 min. at RT with decel 2 to pellet the platelets. The supernatant was removed and the tube shortly placed upside-down on a tissue, to remove all liquid leftovers.

The white and fluffy platelet pellet was then solved in 1 mL of CGS-buffer with a 3.5 mL transfer pipette. 2 mL of CGS-buffer were added on top and the suspension was let to rest for 5 to 10 min.

After a final centrifugation, again at 400xg for 10 min. at RT with decel 2, the cell pellet was resuspended in a small amount of HEPES-buffer (0.8 to 1 mL for all pooled pellets), depending on the cell pellet size and the target platelet concentration.

The platelet concentration was determined in a 100 µL 1:10 platelet:HEPES dilution using a Sysmex KX-21N analyzer. The platelet concentration was adjusted to $2*10^8$ platelets/mL or up to $2*10^9$ platelets/mL.

3.4.3. Analysis of platelet aggregation by light transmission aggregometry according to Born[123]

Agonist-induced platelet aggregation can be measured using light transmission aggregometry (LTA) according to Born.[123] PRP is incubated in a cuvette at 37°C under stirring conditions. The cuvette is placed between a light course and a photocell. The absorbance of the plasma is measured over time during the whole experiment. A platelet agonist is added to induce platelet aggregation. Activated platelets are forming aggregates, more light can pass through the plasma, therefore the transmission increases and the photocell is detecting this increase. The signal is converted in a graphic curve. The transmission ranges from 0% (maximal optical density of PRP) to 100% (no optical density of autologous platelet-poor plasma (PPP)). The used instrument, e.g. APACT 4, measures the latency time (lag time), the maximum of aggregation and the slope of the curve automatically. The primary (reversible aggregation) and the secondary (irreversible aggregation) wave of platelet aggregation can be detected and seen in the curve, depending on the agonist. A wide panel of agonists can be used for the LTA, e.g. thrombin, collagen, ADP, therefore, different receptor-mediated platelet activation pathways can be investigated with this method.[124, 125] Effectors that influence (reduce) platelet aggregation can also be tested using LTA.

Procedure:
Washed human platelets were generated as described in 3.4.2. For aggregation measurement, micro-cuvettes with stirring bars from Diasys® were used.

First, the blank value was measured using 200 µL of HEPES buffer (pH 7.4). Then, 200 µL of washed human platelets solved in HEPES buffer ($2*10^8$ platelets/mL) were placed in a cuvette in the channel. 1 mM of Ca^{2+} was added. The reaction was started by pressing ‘start’ and adding the agonist 11 sec. after starting. OA pre-incubation was performed with the platelet sample (inside the cuvette) by first adding 1 mM of Ca^{2+}, then OA and then incubating the sample for 10 min. at 37°C without stirring. After incubation, the cuvette was placed in the channel and the activation was started by pressing ‘start’ and by adding thrombin after 11 sec. Control samples for OA incubation were treated without or with vehicle (ethanol 0.01%) and Ca^{2+} and incubated for 10 min. at 37°C without stirring.

3.4.4. Stimulation of human platelets

Depending on the stimulus and which proteins should be analyzed via western blotting, the amount of platelet varied between $2*10^8$ to $2*10^9$ platelets/mL. Platelet stimulation or inhibition was performed at 37°C in the water bath. Before stimulation, platelets should rest at least 15 min. at 37°C. Stimulation time and agonist-concentration varied depending on the agonist used for stimulation or inhibition, shown in Table 14.

Table 14: Reagents used for platelet activation or inhibition.

agonist/inhibitor	final concentration	incubation time at 37°C	stock concentration	buffer used for dilution	effect on platelets
α-thrombin (human)	0.1 U/mL	1 to 3 min.; 5 min. for aggregometry	10 U/mL	HEPES-buffer, pH 7.4	activation
iloprost	5 nM	15,30,120 sec.	55 µM	HEPES-buffer, pH 7.4	inhibition
riociguat	10 µM	1,2,5,10 min.	10 mM	HEPES-buffer, pH 7.4	inhibition

3.4.5. Generation of platelet lysates

Washed human platelets were isolated from citrated whole blood as described in 3.4.2. and resuspended in HEPES buffer, pH 7.4. The platelet concentration was adjusted to $1*10^9$ platelets/mL. Platelets were rested at 37°C in a water bath for 15 min. without shaking. 1 mM of Ca^{2+} (from 1 M stock of $CaCl_2$) and optional okadaic acid (pre-incubation of intact platelets) was added and the samples were incubated again at 37°C in the water bath for about 15 min. without shaking. After incubation, samples were centrifuged for 1 min. at 4°C and maximum speed (16900xg) at RT. The supernatant was removed and the platelet pellet was solved in 50% (v/v) of the original volume of extraction buffer including a 1:100 dilution of protease inhibitor cocktail (cOmplete™ protease inhibitor cocktail, Roche). To supend the platelet pellet completely, the pellet-buffer mix was strongly resuspended, vortexed and kept on ice.

3.4.6. Removal of free phosphate and salts from platelet lysates

Lysates, generated as described in 3.4.5., needed to be phosphate-free when used in the non-radioactive serine/threonine phosphatase assay (Promega).

According to the assay protocol, 10 mL of deionized water were added to a provided spin column, it was allowed to drain in a waste 50 mL falcon, after applying slight pressure to the column with a 10 mL syringe plunger to start draining. The Sephadex® G-25 resin was resuspended with a 25 mL wide-mouth pipette and then 10 mL of the resin were added to the spin column. The liquid was allowed to drain by gravity into a 50 mL falcon.

10 mL of lysis buffer as used for lysis generation were added carefully on the column and the buffer was allowed to drain by gravity.

Buffer leftovers were removed by centrifugation of the column placed in a 50 mL falcon with adaptor at 600 xg for 5 min. and 4°C.

The sample (500 to 1000 µL) was placed on the column. The column was placed in a new 50 mL falcon with adaptor and centrifuged again at 600 xg for 5 min. and 4°C, to elute the sample.

3.4.7. Phosphorylation of recombinant proteins in lysates of isolated human platelets

Lysates were generated as described in 3.4.5. with and without 2 µM okadaic acid pre-incubation. 2 µM okadaic acid were also added to the lysis buffer, for samples with and without OA pre-incubation in intact platelets. As control, lysates without OA and also without OA pre-incubation of intact platelets were used.

250 nM of His-tagged ENSA protein or 87 nM of GST-tagged ARPP19 were added to the lysate. 10x kinase phosphorylation buffer were added, to be diluted in the final volume to 1x buffer.

The phosphorylation reaction was started by adding 1 mM ATP or 1 mM thio-ATP (final concentration). The mix was incubated in the water bath at 30°C. Samples for western blotting were taken before ATP addition, after 3, 10 and 30 min. or 10, 20 and 40 min. after ATP addition. Samples were mixed 1:1 with 3xSDS-laemmli buffer to stop the reaction and directly heated for 5 min. at 95°C and 350 rpm. The samples were examined in western blot for ENSA or ARPP19 signal and for pS62 ARPP19 or pS67 ENSA protein signal.

3.4.8. Protein phosphatase 2A activity assay with lysates of isolated human platelets

The non-radioactive serine/threonine protein phosphatase assay (Promega) was used to investigate platelet PP2A activity. The assay is specific for PP2A, PP2B and PP2C, as the provided phosphopeptide serves as a substrate of PP2A, PP2B or PP2C, but not of protein phosphatase 1 (PP1). The sample, including the active phosphatase (e.g. cell lysate), is added to the phosphopeptide. The active phosphatase dephosphorylates the peptide and phosphate is set free in the sample. The free phosphate performs a color reaction with an added molybdate dye from yellow to green. With a filter wavelength of 630 nm, the absorbance can be measured and the amount of free phosphate can be measured (as a standard is used for each experiment and 0 minute controls also). The free phosphate reflects the phosphatase activity. The buffer is chosen depending on the phosphatase that should be measured. The samples need to be phosphate free when added to the phosphopeptide. Inhibition of the phosphatase (e.g. PP2A inhibited with OA) can be detected. The principle of the assay is shown for platelet lysate containing PP2A in Figure 7.

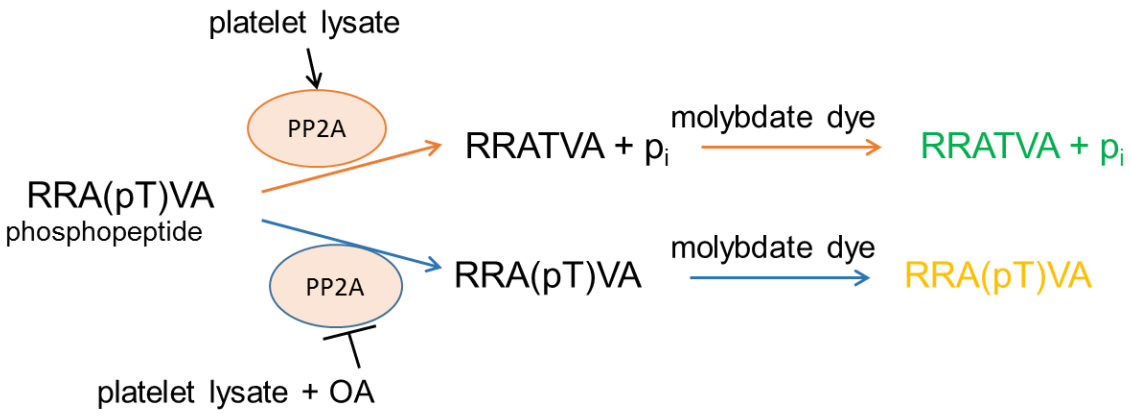

Figure 7: Principle of the serine/threonine phosphatase assay for platelet lysate and PP2A. Modified after Promega protocol S/T phosphatase assay.

The reaction was performed in a 1/2-well low affinity binding 96-well plate (polypropylene, clear, flat bottom).

Washed platelet lysates were generated as mentioned in 3.4.6. For storage, the lysates were aliquoted and frozen at -20°C.

Platelet lysate was diluted with phosphatase lysis buffer, after thawing on ice, to a platelet count of $1*10^8$ platelets/mL.

Preparation of standard-samples:
The provided standard was diluted 1:20 and 5xPP2A reaction buffer was diluted 1:5 with phosphate-free water. The amount of needed dye was prepared. Per 1.5 mL reaction tube, 1 mL of molybdate dye was mixed with 10 µL of molybdate additive and mixed well.

After preparation was finished, first the standard was pipetted on the plate starting at A1, going to E1. Therefore, the needed amount of 1:20 dilution was mixed with 1xreaction buffer to a final volume of 50 µL/well. Standard should have the following concentrations: 20,000; 10,000; 5,000; 2,500 and 1,000 pmol/µL. Blank was placed at F1 and consist of 50 µL 1xreaction buffer.

5 µL of provided peptide (stock:1 mg, M=754 kDa; powder solved in 1.33 mL of phosphate-free water to 1 mM solution) were placed per well. For control samples without peptide, 5 µL of phosphate-free water were used.

The needed amount of 5xPP2A reaction buffer was added per well (final 10 µL/well). If recombinant protein samples re-buffered in 5xPP2A reaction buffer were used, the missing volume of 5xPP2A reaction buffer to fill up to 10 µL was added.

Recombinant protein samples were placed inside the wells, the plate was closed with sealing foil and was placed for 3 min. at 37°C inside an incubator to heat it up.

35 µL of diluted platelet extract were added to start the reaction. As control, 0 min. samples were stopped immediately with 50 µL/well of the prepared dye solution. For incubation, the plate was placed at 37°C in an incubator.

Other time samples were performed as needed (20, 30, 40 or 60 min.; each sample had its own well) and also stopped with 50 µL of the prepared dye solution. When the last samples were stopped, 50 µL per well of dye solution were also added to the standard samples and the blank, when the experiment was finished.

After additional 15 min. of incubation in the dark at RT and the removal of bubbles with a cannual, the samples were measured in a plate reader (Optisys MR™) at a wavelength of 630 nm. Prior to measurement, the plate was shaken for 2 sec. by the plate reader.

3.4.9. Immunoprecipitation of endogenous ENSA from platelet lysates using magnetic Dynabeads™

50 µL (1.5 mg) of Protein A Dynabeads™ were placed in a 2.0 mL reaction tube after vortexing the Dynbeads™ stock minimum 30 sec. The tube was placed on a Dyna-2 magnet for 2 min. The supernatant was discarded. 2 µL of an anti-ENSA antibody (monoclonal, mouse) from Santa Cruz® in 200 µL PBST (0.02% (v/v) Tween®-20) were added to the beads and the mix was resuspended. The tube was placed on an orbital rotator and incubated upon over-head

rotation for 10 min. at RT. After the incubation time, the supernatant was removed, 50 µL of the supernatant were mixed with 50 µL of 3xSDS-laemmli loading buffer and heated for 5 min. at 95°C and 350 rpm. The beads were once washed with 200 µL PBST.

In the meantime, human platelets were isolated from citrated whole blood as described in 3.4.2. The isolated platelets were placed in the water bath at 37°C for resting (15 min.). Afterwards they were centrifuged in a small tabletop centrifuge at 16,900xg for 1 min. at RT. The supernatant was removed and the platelet pellet was resuspended in a similar volume of 1xplatelet/HEK293 lysis buffer (stock 2x, diluted 1:1 with ddH_2O).

1 mL of platelet lysate was added to 1.5 mg beads. The sample was incubated for one hour with over-head rotation in an orbital shaker at RT. The supernatant was removed after incubation and 50 µL were mixed with 50 µL 3xSDS-laemmli loading buffer for SDS-PAGE. The beads were washed, as recommended, three times with 200 µL washing buffer (PBST) by gentle resuspending and placing the tube again on the magnet. Afterwards, the beads were resuspended in 100 µL washing buffer and transferred to a new reaction tube. The supernatant was removed and bound platelet ENSA was eluted with 20 µL elution buffer (50 mM glycine solution, pH 2.8) by gently pipetting to resuspend the bead-antibody-protein complex. The sample was incubated for max. 5 min. at RT. After elution, the suspension was mixed with 40 µL 3xlaemmli loading buffer and heated at 95°C for 5 min. at 350 rpm of shaking.

3.4.10. Phosphorylating magnetic Dynabeads™ bound recombinant His-tagged ENSA at S67 in platelet lysate

Co^{2+}-coupled magnetic Dynabeads™ (Invitrogen) were used to bind His-tagged proteins. After vortexing the tube with Dynabeads™ for a minimum of 30 sec., 2 mg (50 µL) of beads were placed in a 2 mL reaction tube. The tube was placed on a Dyna-2 magnet for 2 min. The supernatant was discarded. The protein (40 µg of His-tagged ENSA) in a 1:1 dilution with 2xbinding/wash buffer (0.1 M sodium phosphate, 0.6 M NaCl, 0.02% (v/v) Tween®-20) in a total volume of 700 µL (if volume was missing to reach 700 µL, it was filled with 1xbinding/wash buffer) was added to the beads and the suspension was well solved by pipetting up and down. A control without protein was always performed. The mix was incubated for 10 min. at RT and 450 rpm horizontal shaking. The tube was placed on the magnet for 2 min. again and the supernatant removed. The beads were washed twice with 300 µL of 1xbinding/was buffer and twice with 300 µL of lysis buffer (without EDTA/EGTA). The platelet lysate was in lysis buffer (without EDTA/EGTA) and therefore, the buffer conditions for the beads should be similar. The beads were solved in 85 µL of lysis buffer (without EDTA/EGTA).

Isolated human platelets and platelet lysates were generated as described in 3.4.2. and 3.4.5. with 15 min. of incubation with 1 µM of okadaic acid in $5x10^8$/mL intact human platelets.

The beads with bound protein were incubated with 1.0 to 1.4 mL of platelet lysate ($1x10^9$plateles/mL), 10x kinase phosphorylation buffer without EDTA/EGTA in the presence of 200 nM okadaic acid. A sample was used for SDS-PAGE/western blotting before starting the reaction. 1 mM thio-ATP (Roche) was added to lead to a stable phosphorylation of the protein. After 100 min. of incubation, 50 µL were used for SDS-PAGE/western blotting. The tube with the mix was placed on a magnet for 2 min., the supernatant was removed and again a sample for SDS-PAGE/western blotting was taken from the supernatant. The beads were washed twice with 300 µL of lysis buffer (without EDTA/EGTA). The HisENSA proteins were eluted

from the beads with 10xPP2A reaction buffer with EDTA/EGTA by incubating for 10 min. at 30°C and 450 rpm of shaking. The tube with the suspension was applied on a magnet for 2 min. and the eluate was transferred into a fresh tube. 2 µL of the eluate were mixed with 80 µL of 3xSDS-laemmli sample loading buffer and heated for 5 min. at 95°C and 350 rpm. 100 µL of 3xSDS-laemmli loading buffer were also added to the beads, resuspended and the sample heated for 5 min. at 95°C and 350 rpm.

3.5. Protein biochemical methods

3.5.1. Gel electrophoresis – SDS-PAGE

Sodium dodecyl sulfate polyacrylamide gel electrophoresis (SDS-PAGE) is used to separate proteins in solution only by their molecular weight and independent of their charge.[126]

Sodium dodecyl sulfate (SDS) is added to a protein sample. SDS works as an anionic surfactant, binding two amino acids per one SDS-molecule. Therefore, SDS is able to cover the charge of the protein, giving all proteins the same negative charge. To ensure, the proteins are also unfolded, a reducing agent as β-mercaptoethanol or dithiothreitol (DTT) is added to the sample loading buffer (3x SDS-laemmli buffer) and the samples are heated for about 5 min. at 95 - 99°C. By placing a constant electric field on a polyacrylamide gel the negatively charged proteins migrate towards the positively charged electrode. So, the migration distance within the polyacrylamide gel depends only on the size (molecular weight) of the proteins, but not on their charge.[126]

Acrylamide was the basis of the used gels, which undergoes a radical polymerization reaction with other acrylamide molecules. A catalytic substance (usually N,N,N',N'-tetramethylethylene-1,2-diamine, TEMED) and a radical reaction initiator such as ammonium persulfate (APS) are necessary for this reaction. For SDS-PAGE, a solution of acrylamide and bisacrylamide is used. These molecules perform a copolymerization reaction. The first step of this reaction is the generation of free radicals by ammonium persulfate; TEMED accelerates this reaction. A basic pH between 8 and 9 is most efficient for the radical formation reaction. Then, the free radicals convert acrylamide monomers into free radicals, which are able to react with other monomers, building polymer chains. These polymer chains are also crosslinked to bisacrylamide molecules. This crosslinking stabilizes and determines the pore size of the gel.[127]

The buffer system is usually a tris-glycine-SDS-buffer system (TGS).

Procedure:

Sample preparation
A 1:10 mix of β-mercaptoethanol:3xSDS-laemmli buffer was prepared fresh before use. For most experiments, the sample was mixed 1:1 with the prepared β-mercaptoethanol/laemmli buffer mix. It was heated at 95°C for 5 min. with 350 rpm shaking in a thermomixer. Only HEK293 cell samples were heated for 10 min. at 95°C with 350 rpm shaking. The samples were stored at -20°C.

Gel preparation
1.5 mm thick, self-made polyacrylamide mini-gels were used for SDS-PAGE. The percentage of the acrylamide in the gel depended on the molecular weight of the protein(s) of interest. For ENSA (13 kDa, runs at 16 kDa; HisENSA at around 19 kDa), 13 or 14% (v/v) acrylamide gels

were used, for GST-ARPP19 (46 kDa) 10% (v/v) acrylamide gels, for proteins like VASP (46-50 kDa) or p38 MAP-kinase (38 kDa) 8% (v/v) acrylamide gels were used.

For the preparation of the stacking (4% (v/v)) and separating (8 to 14% (v/v)) gel, first tris, SDS and water were mixed in a falcon. Acrylamide (as it is harmful) was added under the hood and the solution was mixed well by turning the falcon upside down. The stacking gel mix was stored in the fridge at 4°C until needed. Directly before placing the separating gel mix in between the glass plates, ammonium persulfate (APS) and N,N,N',N'-tetramethylethylene-1,2-diamine (TEMED) were added to start the polymerization reaction. The solution was mixed well by inverting the falcon and then the mix was placed between the glass plates. To get a homogenous border on the gel top, 1 mL of 2-propanol (isopropyl alcohol) was placed on top of each gel.

After 30 to 45 min. of polymerization, the gels were solid. The 2-propanol was removed, APS and TEMED were added to the stacking gel mix, the falcon converted for mixing and the gel-mix placed on top of the separating gel. A comb with 15 pockets and 1.5 mm thickness was placed inside the stacking gel. After 45 min., the stacking gel was also solid and the gels could be used directly or stored in wet tissues at 4°C in a horizontal position until they were needed (up to one week).

Table 15: Protocol for the preparation of a standard mini polyacrylamide gel (separating gel).

substance	8% (v/v) acrylamide	10% (v/v) acrylamide	13% (v/v) acrylamide	14% (v/v) acrylamide
30% (v/v) acrylamide: 0.8% (v/v) bisacrylamide	2 mL	2.5 mL	3.25 mL	3.5 mL
1.0 M tris, pH 8.8	3 mL	3 mL	3 mL	3 mL
20% (w/v) SDS	38 µL	38 µL	38 µL	38 µL
ddH_2O	2.4 mL	1.9 mL	1.15 mL	0.9 mL
10% (w/v) APS	36 µL	36 µL	36 µL	36 µL
TEMED	5 µL	5 µL	5 µL	5 µL

Table 16: Protocol for the preparation of a standard mini polyacrylamide gel (stacking gel).

substance	4% (v/v) acrylamide
30% (v/v) acrylamide: 0.8% (v/v) bisacrylamide	660 µL
1.0 M tris, pH 6.8	630 µL
20% (w/v) SDS	25 µL
ddH_2O	3.6 mL
10% (w/v) APS	25 µL
TEMED	5 µL

Gel running

The samples were thawed on ice. The gels were placed in a BioRad mini-gel vertical running chamber, 1xTGS running buffer (1:10 dilution of 10xTGS running buffer (BioRad) and ddH_2O) was placed inside the gasket between the gels, the chamber was filled with running buffer until the mark of the used numbers of gels (2 or 4). The combs were removed. 5 µL of marker (BioRad prestained Precision plus dual color standards) were placed in the first pocket of each gel. 20 µL of sample (or less, depending on the amount of protein in the sample) were placed in each pocket. Empty pockets were filled with 20 µL of 3xlaemmli loading buffer (as used for sample preparation).

The gel was run at constant 80 V until the marker started separating (15 to 20 min.), the voltage was increased to constant 120 V. The gel was run in total for around 1.5 hours until the blue running front (containing bromphenol blue, negatively charged ions from the buffer and proteins smaller than 5 kDa) reached nearly the end of the gel.

After stopping the run, the gel was taken out of the glasses, the stacker gel and a 1 mm long part of the end of the gel were removed. The gel was then used for silver staining or protein transfer to a membrane with subsequent immunostaining (western blotting).

3.5.2. Silver staining of proteins in SDS-PAGE gels according to Blum et al. 1987[128]

Proteins separated by gel electrophoresis can be visualized in the gel by staining with color reagents or by using reduction of silver ions. Silver staining is a very sensitive protein detection method, even low concentrations (ng) of proteins are sufficient to be detected.[129-131]

Silver ions are interacting with negatively charged side chains of proteins. These ions and therefore the protein can be visualized by reduction to metallic silver in an additional step.

Procedure:
The protein gel was incubated for at least one hour (shaking on a horizontal shaker) or overnight in gel fixation buffer containing acetic acid and methanol, to immobilize protein bands and to remove interfering substances like SDS, buffers and salts. The fixation buffer was removed, the gel was washed three times for 20 min. on a shaker in 30% (v/v) ethanol-ddH_2O solution. The gel was placed for 1 min. in thiosulfate solution to reduce unspecific background staining, washed three times for 20 sec. with ddH_2O and then impregnated with silver staining solution (formaldehyde was added to the staining solution directly before use) for 20 min. and shaking at RT.

The staining solution was removed, the gel was washed two times for 20 sec. with ddH_2O and then the developing solution (formaldehyde was added directly before use) was placed on the gel. Under shaking by hand, the gel was developed. When the color of the protein bands was strong enough, the staining solution was removed and stop solution (containing EDTA) was added.

A picture of the silver stained gel was performed using BioRad ImageLab and a BioRad signal detection machine (Gel Doc™ EZ Reader).

3.5.3. Western blotting and densitometric protein detection

To detect proteins and phosphorylated proteins with specific antibodies, western blotting was performed. Therefore, protein samples ran on polyacrylamide gels are transferred on a membrane by placing an electrical field. The negatively charged proteins run to the positively charged electrode. The membrane needs to be placed between the gel and the electrode.

PVDF (polyvinylidene difluoride) membranes were activated directly before usage, by placing them in 100% methanol for a few seconds. The blotting sandwich (with filters outside, the gel and the activated membrane) was made directly in the 1xtransfer buffer. The transfer was performed at constant 0.8 A at 4°C for 1 hour 10 min. (8% (v/v) acrylamide gel), 1 hour 20 min.

(13% (v/v) acrylamide gel) or maximum 1.5 hours (14% (v/v) acrylamide gel and phostag gel). The higher the percentage of acrylamide in the gel, the longer the transfer time.

After transfer, the membrane was placed in 5% (w/v) BSA-TBST for blocking and preventing unspecific binding of the antibody. Blocking was performed minimum 45 min. on a horizontal shaker. After blocking, the membranes were incubated overnight at 4°C with the primary antibodies in 5% (w/v) BSA-TBST. Usually, one or two membranes were sealed in a foil with 4 mL of antibody solution on a vertical rotator. If the antibody was incubated with skimmed milk-TBST, the membrane was blocked with skimmed milk-TBST.

On the next day, the membrane was washed three times for minimum 5 min. each with 1xTBST. Afterwards, it was incubated for minimum 1 hour with the secondary-HRP (horseradish peroxidase)-conjugated antibody directed against the species, in which the first antibody was produced. After incubation, the membrane was washed again three times for minimum 10 min. each with 1xTBST.

Then the membrane was developed by adding ECL (1:1 mix of two solutions (BioRad) freshly made before use) on the membrane and looking for the chemiluminescence signal using the western blot detection device (Fusion FX7). By varying the exposure times, the best exposure time for a clear signal was chosen.

3.5.4. Zn^{2+}-Phostag™ gel electrophoresis

With a phostag™ gel electrophoresis, proteins are separated by their number of phosphorylated sites and not by their molecular weight. Even with the same level of phosphorylation on different phosphorylation groups of one protein, different bands occur, as long as the phosphorylation sites are different. This method has the advantage, that only one general antibody is needed against the protein of interest. If no antibody directed against the phosphorylation sites of the protein is available, the phosphorylation can still be detected via phostag gel electrophoresis.

Phostag™ is a molecule that captures phosphorylated amino acids as Ser/Thr/Tyr or His/Asp/Lys, sold by a company called WAKO. The phostag™ compound is added to acrylamide of the separating gel during gel preparation. Two divalent metal ions are needed for the core of the phostag™ molecule. These ions are also added during gel-preparation and can be Zn^{2+} or Mn^{2+}, added as $ZnCl_2$ or $MnCl_2$. As Zn^{2+} has a higher resolving capability and is able to better separate a wider range of proteins as Mn^{2+}, I used Zn^{2+}-phostag gel electrophoresis. Phostag™ shows the highest phosphoric acid groups capturing at neutral pH, therefore, the pH of the separating gel and the samples is 6.8. As EDTA is a chelator of positively charged ions, it is disturbing. Samples should not include any EDTA. A protein size marker does not help to detect the proteins. The method was established for platelet lysates in our lab by our master student Stephanie Dorschel.

Procedure:

Sample preparation

Sample preparation was similar to standard SDS-PAGE. Only the 3xlaemmli buffer differed. And no EDTA should be present in the samples. A 1:10 mix of β-mercaptoethanol:3xlaemmli-buffer was prepared fresh before use. Depending on the experiment, the experimental sample was mixed 1:1 with the prepared β-mercaptoethanol/laemmli-buffer mix. It was heated for 5 min. at 95°C with 350 rpm shaking in a thermomixer.

Gel preparation

1.5 mm thick, self-made polyacrylamide mini-gels were used for Zn^{2+}-phostag™ gel electrophoresis. The big difference was that no SDS was added to the gel itself, but to the running buffer. Therefore, the phostag™ compound and $ZnCl_2$ were added to the separating gel. The percentage of the acrylamide in the gel depended on the molecular weight of the protein of interest. But it was not similar to the percentage of standard SDS-PAGE for the same protein. Some tries needed to be performed to find the right acrylamide percentage and also phostag™ concentration for each new protein that should be investigated. For recombinant GST-ARPP19 (46 kDa), 6% (v/v) acrylamide and 35 µM phostag™ were most suitable.

For separating (6% (v/v) acrylamide) gel preparation, first tris, ddH_2O, $ZnCl_2$-solution and phostag™ solution were mixed in a falcon, acrylamide (as it is harmful) was added under the hood and the solution was mixed well by vortexing. For the stacker gel mix (4% (v/v) acrylamide), only tris, ddH_2O and acrylamide were used and the mix was stored in the fridge at 4°C until needed. Directly before use, APS and TEMED were added to start the polymerization reaction. The solution was strongly vortexed and placed between the glass plates. To get a homogenous border, 1 mL of 2-propanol was placed on top of each gel.

After 45 min. to one hour of polymerization, the gels were solid. The 2-propanol was removed, APS and TEMED were added to the stacker gel mix, the falcon inverted for mixing and the gel mix placed on top of the separating gel. A comb with 15 pockets was placed inside the stacker gel. After 45 min., the stacker gel was solid and the gels could be used directly or stored in wet tissues at 4°C in a horizontal position until they were needed (up to three months).

Table 17: Protocol for the preparation of one phostag mini polyacrylamide gel (separating gel).

substance	**6% (v/v) acrylamide, 35 µM phostag**
30% (v/v) acrylamide: 0.8% (v/v) bisacrylamide	1.5 mL
1.0 M tris, pH 6.8	3 mL
ddH_2O	2.93 mL
5 mM phostag solution	52.5 µL
10 mM $ZnCl_2$ solution	52.5 µL
10% (w/v) APS	36 µL
TEMED	5 µL

Table 18: Protocol for the preparation of a 4% (v/v) acrylamide stacker gel for phostag mini polyacrylamide gel electrophoresis.

substance	**4% (v/v) acrylamide**
30% (v/v) acrylamide: 0.8% (v/v) bisacrylamide	660 µL
1.0 M tris, pH 6.8	630 µL
ddH_2O	3.6 mL
10% (w/v) APS	25 µL
TEMED	5 µL

Gel running

Only one gel was run at the same time. The samples were thawed on ice. The gel was placed in a BioRad mini-gel vertical running chamber. 500 mL 1xrunning buffer was prepared fresh

and mixed well, directly before running the gel. 7 µL of marker were placed in the first pocket of the gel, only to visualize the forefront on the membrane after transfer. As mentioned above, a marker does not help to identify the proteins when running a phostag-gel, but it helps to identify the front of the membrane after western blotting.

10 to 12 µL of sample were placed in one pocket depending on the protein amount. The pocket between marker and sample was filled with loading buffer, when enough pockets without sample were left. Also empty pockets behind the samples were filled with loading buffer. The gel was run at constant 30 mA for 3.5 to 4 hours until the blue running front reached nearly the end of the gel. The running chamber was placed on ice under a hood.

After the run was complete, the Zn^{2+}-ions were removed by washing the gel twice 10 min. in 50 mL of 1xtransfer buffer containing 1 mM EDTA. A third washing step with 50 mL of 1xtransfer buffer under shaking was performed for 10 min. Then the gel was ready for western blotting as described in 3.5.3. Only the 1xtransfer buffer for phostag gels is different, it contains SDS and less methanol.

3.5.5. Protein purification of His-tagged recombinant proteins via immobilized metal ion affinity chromatography (IMAC)

The metal ion affinity chromatography is a purification method, where proteins or peptides are separated by their different affinity to metal ions. Therefore, metal ions are immobilized on an insoluble matrix by chelation. The matrix including the ions can be packed e.g. inside a column. This method is very helpful, when a protein was expressed in *E.coli* or a human cell line and should now be isolated/purified, by separating it from all other proteins in the cell lysate.[132, 133]

For this project, His-tagged proteins were purified via the high affinity of histidine to Ni^{2+}-ions. Therefore, columns including crosslinked agarose beads coupled to a chelating group that is pre-charged with nickel ions were used, trapping only proteins including exposed histidine groups (e.g. as a His-tag (6xhistidine)). For captured protein removal, a competing agent is added that competes with the histidine residues for the Ni^{2+}-ions. Imidazole suits best for this competition. The higher the imidazole concentration in the buffer, the higher the competition and the more proteins are eluted from the column.

Procedure:
After His-tagged ENSA proteins were expressed in BL21 and the cells lysed as described in 3.1.7., the proteins were purified using HisTrap HP 1 mL columns (GE Healthcare) with Ni^{2+}-ions for histidine interaction according to the manufactures protocol.

One or two pellets of *E.coli* BL21 expressing HisENSA, were lysed after protein expression (each in a 50 mL falcon) in 5 to 10 mL of lysis-buffer and used for one purification. The machine used for purification was ÄKTA Pure (GE Healthcare), the software was 'Unicorn™ 6.3.2.' (GE Healthcare) HisTrap HP columns were used up to five times for a similar protein.

All bubbles in the pump system were first removed by performing a pump wash. The ÄKTA Pure was always cleaned before use by running cleaning programs with 1 M NaOH, ddH_2O and 20% (v/v) ethanol solution. All buffers and samples were first sterile filtered using filter top 500 filters for the buffers or sterile filters for syringes for the sample to remove particles from the solutions that could disturb the machine.

Step 1: Column insertion
The used HisTrap HP 1 mL column was inserted into the system without placing bubbles inside. The machine should be in 20% (v/v) ethanol solution, a constant down flow of 1 mL/min was induced and the column placed on position 1. A pre-column alarm was set on 0.5 MPa to ensure, that the column is not destroyed because of too high pressure during insertion.

Step 2: Column washing and preparation
The column was now first washed with 20% (v/v) ethanol solution and then with the same amount of ddH_2O.

The whole system was washed with the used binding buffer (pH 7.4) containing 30 mM imidazole. In the end, the system was filled completely with binding buffer.

Step 3: Protein loading
The protein sample (centrifuged and filtered lysate) was loaded with a syringe (10 mL) on the, binding buffer filled 'superloop', a 50 mL glass column used for automated sample loading during the purification process. It should be as less bubbles in the loop as possible.

Step 4: Protein purification program
The program, constructed with the Unicorn program, was run to purify the protein sample. For the sample loading procedure, the volume of sample was adjusted for each new run.

First, the system was shortly prepared, then the sample was loaded. Protein passing the UV sensor was visualized in a curve in the software. During sample loading, a high amount of proteins passed through the column without binding (except of the His-tagged protein). After finishing the loading, the system and the column was washed until the UV signal was stable at 0 mAU.

Then the elution was started by directly adding 100% elution buffer to the system and the column. As soon as a peak in the UV signal started, the machine collected the sample in a new 15 mL Falcon using the fraction collector. During elution, fractions of 2 mL were collected with a total column volume of 12 to 16 (equals 12 to 16 mL).

Samples for SDS-PAGE followed by silver staining or western blotting were collected from the sample loading, the washing procedure and of fractions of the eluate.

After the run was finished, the fractions of the eluate were united in a 15 mL or 50 mL falcon.

The used column was washed with ddH_2O and 20% (v/v) ethanol for re-use. Columns were stored in 20% (v/v) ethanol in a horizontal position, closed up and down with caps at 4°C. For each different protein (wild type and mutants), a different column was used.

The purified protein was re-buffered in 1xTBS, as described in the following section.

3.5.6. Buffer replacement of recombinant proteins via PD-10 columns

To change the buffer of the purified proteins, PD-10 desalting columns packed with Sephadex™ G-25 resin (GE Healthcare) were used. Sephadex™ is made by crosslinking dextran with epichlorohydrin. The G-type is defined by the degree of crosslinking, swelling and the molecular fractionation range. When the sample is placed on the column (up to 2.5 mL are possible), small contaminants such as salts are entering the pores of the resin, are retained and move slow, whereas large molecules such as big proteins directly run through the column

and move faster than the smaller molecules. With this method, buffers can be exchanged and small contaminants can be removed by gravity flow or centrifugation.

Procedure:
The sealed end of the column was cut, the cap removed and the storage buffer was removed by letting it drop out by gravity.
The column was filled with 5 mL of equilibration buffer (1xTBS, pH 7.4), the flow through was discarded. This procedure was repeated in total 5 times (25 mL of equilibration buffer ran through the column). 2.5 mL of sample were placed on the column (if the volume was less, the volume was adjusted to 2.5 mL with equilibration buffer), the flow through was collected and a sample for SDS-PAGE was taken to ensure, no HisENSA protein passed through the column.
The column was placed in a new falcon or in the first well of a 96 well plate, 3.5 mL of equilibration buffer were added to the column to elute the protein. The eluate was collected.
If a 96-well plate was used: five drops per well were collected. After elution was finished (around 16 wells were filled), the fractions were tested for protein via Bradford test on a separate 96-well plate as described in 3.5.9.
The fraction containing protein on the elution-plate were united in a new 15 mL falcon. Usually, well 3 to 14 contained protein (in total about 70 drops). With this method it could be shown that protein elution was finished after 3.5 mL of elution buffer ran through the column.
Later, the eluate was collected in a new 50 mL falcon instead of the 96-well fractionation.

In most cases, the total protein volume after purification was higher than 2.5 mL. A second column was used. Additionally, the columns could be re-used by adding 25 mL of equilibration buffer on the column after elution. 2.5 mL of sample as described before could be re-buffered again.

3.5.7. Concentration of protein solutions using amicon ultra-4 centrifugal filter units

To concentrate the purified recombinant protein samples after buffer exchange, 3K amicon ultra-4 centrifugal filter units (Merck Millipore) were used. The filter units are suitable for a volume of up to 4 mL of sample. 3K defines the smallest size of protein (3 kDa) that is able to pass through the filter membrane.

The filter unit is built out of a cap, a filter device and a centrifugal tube, where the flow through is collected.

Maximum 4 mL of sample were placed inside the filter device at the same time, placed inside the centrifuge tube. The cap was closed and the sample centrifuged at 4000xg for 10 to 15 min. The flow through was always removed after centrifugation and the samples in the filter device resuspended, when new sample was added. After nearly the whole sample (up to 18 mL) were placed on the filter device and about 2 mL of sample remained, 2 mL of 1xTBS were added and the centrifugation repeated. This step was repeated up to 4 times to get rid of probably remaining imidazole left overs. In the end, a volume of 2 to 3 mL of purified protein in 1xTBS remained. The sample was resuspended well in the filter device and then placed into a new 15 mL falcon. A sample for SDS-PAGE was taken from the re-buffered protein. The proteins were stored at 4°C.

3.5.8. Determination of protein concentration in solutions via NanoDrop2000c

The protein concentration in the re-buffered protein samples was determined by using the NanoDrop2000c.

1.5 µL of the buffer, where the protein was solved in, were used as blank. 1 to 1.5 µL of the sample were used to measure the concentration using a filter wavelength of 280 nm. A minimum of three measurements per solution were performed, and the mean of the measurements in arbitrary units was calculated as concentration.

3.5.9. Protein quantification via the Bradford assay

The colorimetric protein assay, developed by Marion M. Bradford, is a fast method to determine a protein concentration in solution. The dye Coomassie Brilliant Blue G-250 induces an absorbance shift from red (465 nm) to blue (595 nm) in the presence of proteins, that can be measured with a spectrometer.[134]

Bradford was for this thesis only used to detect proteins but not to determine the protein concentration. Therefore, the absorbance was not measured, it was only looked for the color change.

5 µL of purified and re-buffered protein were placed in a well of a 96-well plate. 250 µL of Bradford reagent were added. If color changed from red to blue, the fraction contained protein.

3.5.10. Phosphorylation of recombinant HisENSA/GST-ARPP19 proteins by protein kinase A or G at S109/S104 or by the MASTL-kinase at S67/S62

Recombinant HisENSA or GST-ARPP19 protein was mixed with 'kinase dilution buffer III', MASTL kinase/C-subunit of protein kinase A or PKGIβ (and Bromo-cGMP for PKGIβ). ddH_2O was added to fill the missing volume. A sample was taken for SDS-PAGE (0 min.) and the phosphorylation reaction was started by adding 1 mM γ-thio-ATP or ATP. The reaction was incubated in the water bath at 30°C and time samples for SDS-PAGE were taken (5, 10, 20, 30 min.).

When the phosphorylated protein should be used in further experiments (PP2A activity assay), γ-thio-ATP was used and the amount of sample was chosen, that 130 µL were left after 20/30 min., after taking all SDS-PAGE samples. The reaction was stopped by adding 6 mM EDTA (1.3 µL of 0.5 M EDTA stock). These 130 µL were then desalted (also free phosphate was removed and the buffer was changed), by using Zeba™ spin desalting columns, 7K MWCO (Thermo Fisher) as described in 3.5.11.

When both phosphorylation sites of ENSA or ARPP19 should be phosphorylated simultaneously, both kinases were added at the same time and time samples were taken as above for SDS-PAGE and western blot analysis.

When both phosphorylation sites of ENSA or ARPP19 should be phosphorylated consecutively, first one kinase was added, the reaction was run as described above, and after 20 min., the second kinase was added and time samples were taken again for 5, 10 and 20 min. (called 25, 30 and 40 min. for the first kinase).

3.5.11. Removal of free phosphate and salts from phosphorylated recombinant proteins

For desalting/phosphate removal, Zeba™spin desalting columns (7K MWCO, 0.5 mL) were used. The columns can be used for up to 130 µL of a solution, where salts or free phosphate should be removed. In the same time, the exchange of the buffer is possible. The work principle is similar to PD-10 columns, also Sephadex® G-25 is used. Only the sample and column volume is much smaller.

The columns were prepared by first removing the plastic closing the column on the end of the column and by opening the cap a bit. Each column was placed in a 1.5 mL reaction tube and then the tube placed in a small tabletop centrifuge (5418R) to remove the storage buffer. The flow through was discarded, 300 µL of 5xPP2A reaction buffer were placed carefully on top or the resin inside the columns, the column was centrifuged at 1500xg for 1 min. at RT and the flow through discarded. The column had to be placed back into the reaction tube in the same direction as before, the cap was always placed back on the column and turned half. The procedure was repeated two to three times.

The columns then were placed in a new 1.5 mL reaction tube. Maximum 120 µL of the sample were placed on the column, 10 µL of stacker (5xPP2A reaction buffer) were placed on top. The cap was placed back on the column but not completely closed and the sample was centrifuged at 1500xg for 2 min. at RT. A small amount of desalted sample was used for SDS-PAGE analysis. The sample was now ready for further experiments (PP2A activity assay with platelet extract). For each sample, a different column was used.

To see how much protein stayed on the columns after sample elution, 100 µL of 5xPP2A reaction buffer were placed on the columns, and the columns were centrifuged at 1500xg for 2 min. at RT in a new reaction tube. The flow through was mixed with 100 µL of 3xSDS-laemmli sample loading buffer and also placed on a SDS-PAGE. The purity of the eluate was controlled via SDS-PAGE followed by silver staining. The higher the protein concentration and the higher the sample volume (best 120 µL), the higher the purity of the sample after elution and the more protein was recovered after elution.

3.6. Production of a polyclonal rabbit antibody directed against human pS109 ENSA

A company (ImmunoGlobe® Antikoerpertechnik GmbH, Germany) produced an antibody directed against the phosphorylation site of human ENSA at S109 for this project. Therefore, two rabbits were immunized with the specific peptide (CPQRKS-pS-LVTSK; also in different variations). After isolation and purification, only one rabbit showed promising antibody results, detecting recombinant pS109 HisENSA specifically via western blotting. This anti-pS109 ENSA polyclonal rabbit antibody (called anti-pS109 PAN ENSA antibody) was in most cases used for the detection of recombinant pS109 HisENSA/pS104 GST-ARPP19. However, until today, the successful use of this and other antibodies directed against pS109 ENSA for detecting this phosphosite in platelet lysates remains problematically.

4. Results

4.1. Regulation of ENSA/ARPP19 phosphorylation by PKA and PKG in human platelets - (phospho)proteomic data of human platelets

Earlier cAMP/PKA phosphoproteome studies of our group and collaborators initiated this project to compare the established cAMP/PKA phosphoproteome of human platelets obtained in response to the prostacyclin analog iloprost[113, 135] with the phosphoproteome of human platelets obtained in response to cGMP-elevating platelet inhibitors. First, the effects of iloprost (cAMP-pathway) were compared with the ones of NO donors often used to elevate cGMP in human platelets (S-nitrosocysteine (SNC), sodium nitroprusside (SNP), diethylamine NONOate (DEA-NO)) and the soluble guanylyl cyclase (sGC) stimulator riociguat. In these experiments, riociguat and the three NO donors stimulated the phosphorylation of more than 150 proteins (>1.5 fold above control) and, interestingly, decreased the phosphorylation of more than 60 proteins (<0.66 below control).[29]

Both the cAMP-elevating iloprost and the cGMP-elevating NO-donors and riociguat stimulated the phosphorylation of vasodilator-stimulatd phospoprotein (VASP) at S239 (an established excellent phosphosite for PKG, but less also for PKA) and α-endosulfine (ENSA) at S109. At the same time, the phosphorylation of another known phosphorylation site of ENSA, S67, was reduced (Table 19).

Table 19: Effect of cGMP-elevating (NO donors, riociguat) and cAMP-elevating (iloprost) platelet inhibitors on the phosphorylation of VASP and ENSA.

acc. number	gene	p-site	av. ratio DEA-NO	av. ratio iloprost	av. ratio SNP	av. ratio riociguat	av. ratio SNC	copy number/ platelet
P50552	VASP	S239	12.19	7.17	6.93	9.22	7.67	44600
O43768	ENSA	S109	14.04	17.97	12.46	16.03	13.88	7800
O43768	ENSA	S67	0.82	0.53	0.82	0.62	0.72	7800

Washed human platelets were incubated without and with diethylamine NONOate (DEA-NO 5 µM, 2 min.); iloprost (5 nM, 2 min); sodium nitroprusside (SNP, 5 µM, 2 min); riociguat (10 µM, 5 min) or sodium S-nitrosocysteine (SNC, 5 µM, 2 min). The reaction was stopped with 4xlysis buffer, samples were shock frozen in liquid nitrogen and analyzed by quantitative phosphoproteomics as described. The change of various phosphosites (p-sites) compared to control (increase or decrease) is shown as average ratio (av. ratio). The copy number indicates the number of molecules of a given protein per platelet obtained in earlier studies (Burkhardt et al 2012).[111]

While the prostacyclin analog iloprost, which activates the prostacyclin receptor-sensitive adenylate cyclase (sAC), is well established as specific activator of the cAMP-pathway in platelets, less was known about the soluble guanylyl cyclase (sGC) stimulator riociguat. Previously, our group characterized riociguat in detail as a cGMP-specific inhibitor of murine and human platelets.[136] Importantly, all tested riociguat effects were abolished in murine platelets obtained from platelet-specific sGC knock-out mice. Then, in the absence of cAMP-elevating agents, riociguat did not affect cAMP levels and PKA substrates in both murine and human platelets but increased the phosphorylation of established PKG substrates such as VASP (S239) and PDE5A (S102). To provide further, additional evidence for the specificity of the cGMP/PKG pathway in our conditions, I analyzed the effect of the PKG inhibitor Rp-8-Br-PET-cGMPS[137] on riociguat-induced phosphorylation of VASP S239 (a PKG site) and on iloprost-induced phosphorylation of VASP S157 (a PKA site) in human platelets (Figure 8).

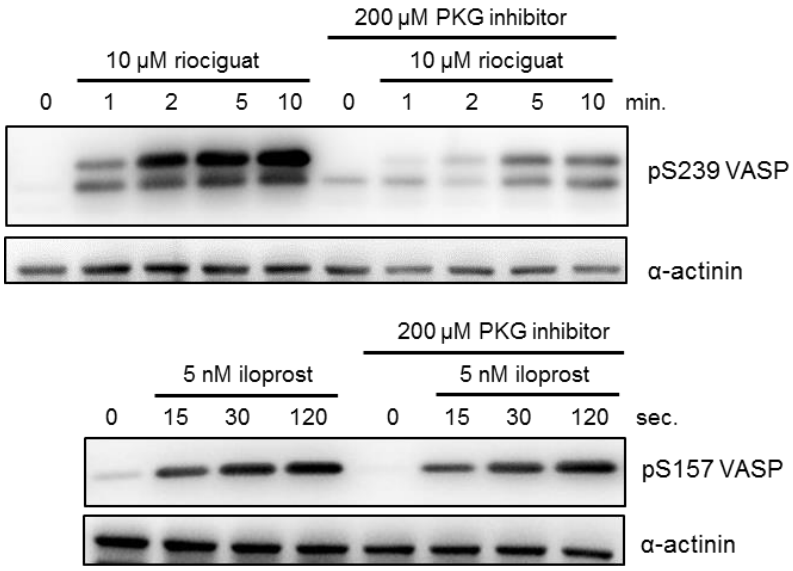

Figure 8: The PKG inhibitor Rp-8-Br-PET-cGMPS strongly inhibits riociguat-induced VASP S239 phosphorylation but not iloprost-stimulated VASP S157 phosphorylation.
Washed human platelets were pre-incubated with the PKG inhibitor (200 µM, 20 min) and then treated with riociguat (10 µM, samples after 1, 2, 5, and 10 minutes) or iloprost (5 nM, time samples after 15, 30 and 120 seconds). As loading control α-actinin was used. Anti-pS239 VASP antibody (Cell Signaling®) was used 1:1000 in 5% (w/v) BSA-TBST, anti-pS157 VASP antibody (ImmunoGlobe®) was used 1:2000 in 5% (w/v) BSA-TBST; anti-α-actinin antibody (Cell Signaling®) was used 1:2000 in 3% (w/v) skimmed milk-TBST. The data shown here are representative for n=3 independent experiments.

The data showed that riociguat–induced VASP S239 phosphorylation but not iloprost-induced VASP S157 phosphorylation is inhibited by the PKG inhibitor. Therefore, for further phosphoproteomic and functional experiments with riociguat and iloprost, conditions were selected that produced maximal increase of platelet cGMP levels/VASP 239 phosphorylation or cAMP levels/VASP S157 phosphorylation in order to study other substrates such as ENSA or ARPP19. Thus, a full phosphoproteomic study headed by PD Dr. K. Jurk and Dr. R. Zahedi was performed, in which I participated. The data are unpublished so far. Currently, a manuscript for publication is in preparation. From this study, data concerning ENSA/ARPP19 were extracted and presented in Table 20.

Table 20: Regulation of selected phosphosites of ENSA, ARPP19, PP2A subunit B56δ, and VASP in human platelets by riociguat and iloprost.

						riociguat (cG)		iloprost (cA)	
uniprot	**gene**	**protein name**	**CN/ plt**	**# pep-tides**	**p-site**	**↑phospho rylation**	**p-value fraction**	**↑phospho rylation**	**p-value fraction**
O43768	ENSA	α-endosulfine (ARPP19e)	7800	3	S109	3.75	100%	4.81	100%
P56211	ARPP19	cAMP-regulated phosphoprotein 19	2500	1	S104	2.18	100%	3.53	100%
Q14738	PPP2R5D	ser/thr-protein phosphatase 2A 56 kDa reg. subunit δ (PP2A B subunit B'-δ)	1300	1	S573	2.13	100%	4.52	100%
P50552	VASP	vasodilator-stimulated phosphoprotein	44600	1	S157*	1.67	100%	2.03	100%
P50552	VASP	vasodilator-stimulated phosphoprotein	44600	4	S239	4.52	100%	3.92	100%

*** all trypsin digests except VASP S157 (subtilisin)**

Washed human platelets from 3 healthy donors (3 biological replicates) were incubated with buffer (control), riociguat (10 µM, 5 min.) or iloprost (5 nM, 2 min.). After incubation, samples were stopped by the addition of 4xlysis buffer, shock frozen in liquid nitrogen and analyzed by quantitative phosphoproteomics as described.[135] The fold increase of phosphorylation of various phosphosites compared to control is shown as average ratio of all quantified peptides bearing the corresponding site. As a measure of reliability, the "p-value fraction" (∑peptides p<0.05/∑ site-bearing peptides) and # of averaged peptides is given in the table. The p-value fraction of all sites shown here is 100%, which is an excellent measure of reliability of these phosphosite (p-site) measurements.

These phosphoproteomic data demonstrate that ENSA (at S109) and ARPP19 (at S104) are phosphorylated in response to cAMP/PKA as well as to cGMP/PKG stimulation in intact human platelets, similar to VASP (Table 20). Interestingly, while all cAMP- and cGMP-elevating platelet inhibitors increased ENSA S109 and ARPP19 S104 phosphorylation, they decreased ENSA phosphorylation at another site, serine 67 (Table 19).

It should be noted here that this phosphosite S67 is within the central part of ENSA, which is identical in both ENSA and ARPP19. Therefore, phosphopeptides derived from ENSA (around S67) or ARPP19 (S62) are identical and could be from either protein. However, ENSA is clearly the more abundant protein in human platelets.

The S67 ENSA/S62 ARPP19 phosphosites are functionally important sites, which will be presented and discussed later. To study phosphorylation and regulation of the human ENSA/ARPP19 family in more detail, human platelet ENSA was cloned, mutated and expressed for further studies and compared to commercially available ARPP19, as described in the following chapters.

4.2. α-endosulfine (ENSA) – from DNA to (purified) proteins

As human platelets cannot be studied in cell culture due to a missing cell cycle, other strategies to study certain protein functions are needed. One possibility is to produce the protein of interest as recombinant protein in *E.coli* including a tag for protein purification and then to use it in further experiments as phosphorylation experiments and to study the influence of the phosphorylated protein on other proteins in human platelets. For this reason, the human ENSA protein was cloned in a suitable vector, purified and studied.

The DNA-sequence of ENSA included in a vector was kindly provided by Dr. Sabine Herterich (Medical Center, Central laboratory, University of Würzburg), who isolated ENSA RNA from human platelets and synthesized the cDNA using the RNA. She used the cDNA as a template for PCR. By using different primer pairs to identify different ENSA isoforms, she found mainly ENSA isoform 1, 2, 5 and 6 in washed human platelets (isoform numbers are according to uniprot.org/uniprot/O43768). The ENSA DNA I obtained was part of the sequencing vector pCR™4-TOPO, which is predominantly used for sequencing.

Then first, I cloned the sequence of ENSA isoform 1 (canonical sequence) into an expression vector pCMV-3Tag-1A that includes a sequence for an N-terminal FLAG-tag on the ENSA protein.

4.2.1. Cloning ENSA DNA into pCMV-3Tag-1A expression vector

The DNA-sequence of ENSA isoform 1 (also in the following called ‘insert’) was amplified via PCR, using suitable primers (forward and reverse) for the sequence and Pfu-polymerase. The amplification was confirmed by running a small amount of sample on an agarose gel. The size of the insert was 384 bp. The used ladder was a 100 bp ladder, each gap between the lines equals 100 bp. The ladders consisted of DNA fragments with different but specified sizes.

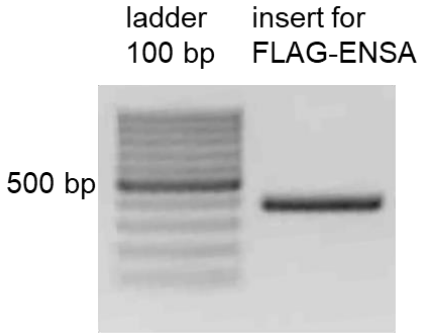

Figure 9: Amplification of FLAG-ENSA insert (size: 384 bp) confirmed by agarose gel.

After successful PCR, the DNA was purified via phenol/chloroform purification to remove the polymerase, and then digested with the two restriction enzymes EcoRI and XhoI.

EcoRI is cleaving double stranded DNA on the following specific site, resulting in four nucleotides sticky ends with 5’end overhangs AATT:

5’ …G↓AATTC… 3’

3’ …CTTAA↑G… 5’

XhoI is cleaving also double stranded DNA on the following specific site, resulting also in four nucleotides sticky ends with 5’end overhangs TCGA:

5’ …C↓TCGAG… 3’

3’ …GAGCT↑C… 5’

The overhanging parts have the advantage that, if a vector and the insert are both digested with the EcoRI and XhoI enzymes, they are easy to connect to each other.

After digestion, the whole sample was purified by agarose gel electrophoresis. The pCMV-3Tag-1A vector was also digested with the same enzymes and purified by agarose gel electrophoresis. The correct fragments were cut from the gel and purified (according to 3.2.4.). Figure 10 shows the map of the pCMV-3Tag-1A vector including the amino acids, where the enzymes are cutting the DNA (dark blue).

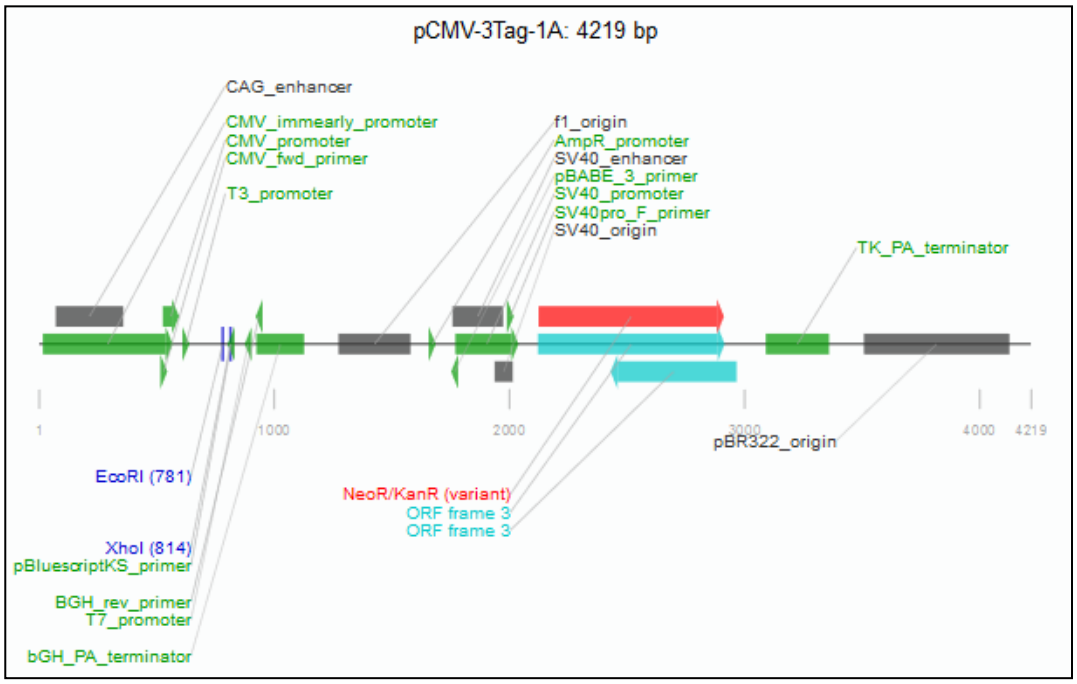

Figure 10: Linear map of pCMV-3Tag-1A showing the cutting points of the used enzymes.[116] EcoRI and XhoI are marked in blue. The ENSA insert is located between the two cutting positions of EcoRI and XhoI.

The digested vector and insert on the agarose gel are shown in Figure 11. The 100 bp and 1 kb ladders, used in Figure 11, are described in 2.6. in more detail. In Figure 11, the 1kb ladder starts with 500 bp (lower bands are not seen because TAE was used as running buffer, following bands are 650, 850, 1000, 1600, 2000, 3000, 4000, 5000 and 6000 bp), the 100 bp ladder starts with 100 bp.

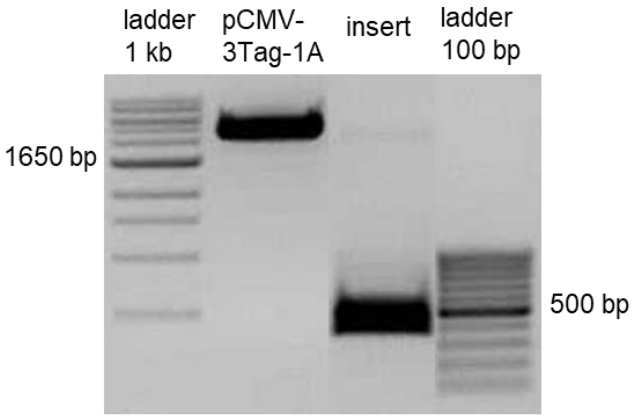

Figure 11: Digested pCMV-3Tag-1A vector and ENSA-insert (384 bp) placed on an agarose gel for purification.

After determining the concentration of insert and vector, the ligation was started. Amplification, vector digestion and ligation were controlled via agarose gel electrophoresis. Chemically competent bacteria (TOP10) were transformed with the resulting DNA. The DNA of six clones was isolated via mini-prep (Thermo Fisher) (screening of clones) and for verification, plasmid DNA (3 µL) of all clones was digested with EcoRI and XhoI. The presence of the correct insert was checked via agarose gel electrophoresis (Figure 12).

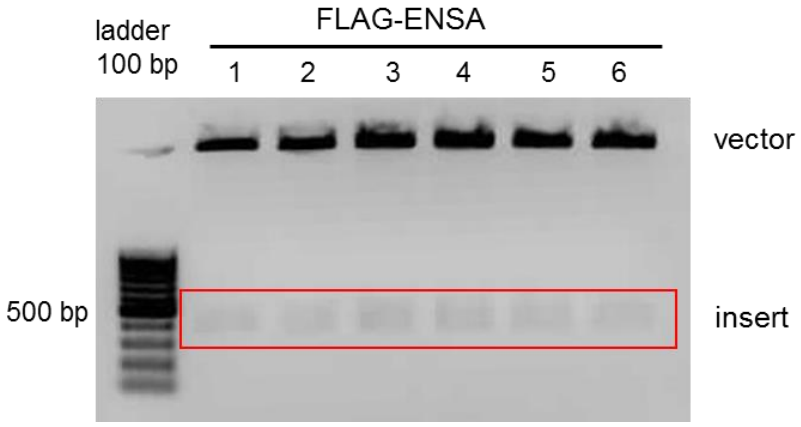

Figure 12: Digestion of pCMV-3Tag-1A containing ENSA insert.
Agarose gel of digested vector (upper black band) containing the insert. The insert (384 bp) is marked with a red square. 1: clone 1; 2: clone 2; 3: clone 3; 4: clone 4; 5: clone 5; 6: clone 6. Ladder is described in more detail in chapter 2.6.

Afterwards, DNA was isolated of clone 1 of FLAG-ENSA via maxi-prep to have more plasmid for the following experiments. The following table shows the concentration, measured via NanoDrop2000c, of the plasmid after the preparation.

Table 21: Concentration of FLAG-ENSA DNA containing vector of clone 1.

plasmid	concentration [ng/µl]
FLAG-ENSA1 (pCMV-3Tag-1A)	1020

The success of cloning was verified via sequencing by the company 'Eurofins'. Nucleotide sequence analysis was first translated to amino acid sequence using ‘expasy translate’ and then compared with the expected FLAG-ENSA amino acid sequence using ‘clustal omega’.

```
FLAG-ENSA       DYKDDDDKDYKDDDDKARAGSPGLQEFMSQKQEEENPAEETGEEKQDTQEKEGILPERAE
expected        DYKDDDDKDYKDDDDKARAGSPGLQEFMSQKQEEENPAEETGEEKQDTQEKEGILPERAE
                ****************************************************************

FLAG-ENSA       EAKLKAKYPSLGQKPGGSDFLMKRLQKGQKYFDSGDYNMAKAKMKNKQLPSAGPDKNLVT
expected        EAKLKAKYPSLGQKPGGSDFLMKRLQKGQKYFDSGDYNMAKAKMKNKQLPSAGPDKNLVT
                ************************************************************

FLAG-ENSA       GDHIPTPQDLPQRKSSLVTSKLAGGQVE
expected        GDHIPTPQDLPQRKSSLVTSKLAGGQVE
                ****************************
```

Figure 13: Sequencing data (FLAG-ENSA) compared with expected FLAG-ENSA sequence (expected).
The FLAG-tag is marked in red. The nucleotide translation was done using ‘expasy translate’; the comparison was done using ‘clustal omega’ (1.2.1).

This vector could now be used for transient transfection of HEK293 cells leading to an over-expression of FLAG-tagged ENSA.

4.2.2. Cloning ENSA DNA into pET28a expression vector

For cloning ENSA isoform 1 DNA into the pET28a vector, to have the possibility, to express His-tagged ENSA isoform 1 in *E.coli* and study the recombinant protein in more detail, a similar procedure was done as described above (4.2.1.). Insert and vector were also purified after digestion via agarose gel electrophoresis and cutting the correct bands.

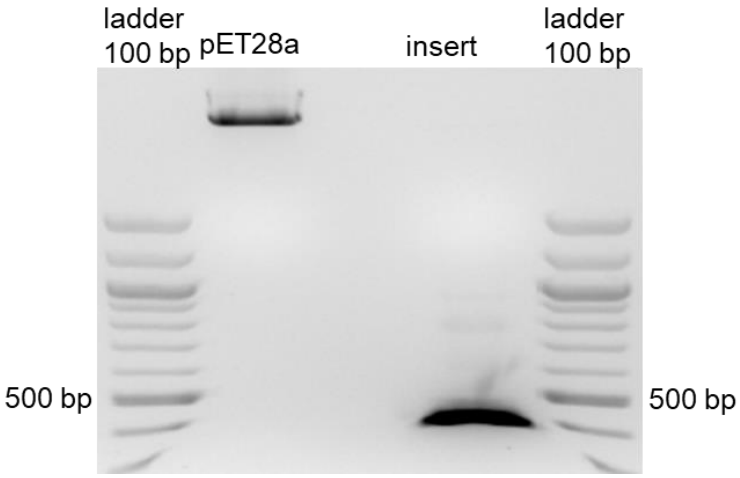

Figure 14: Digestion of pCMV-3Tag-1A vector and ENSA-insert.
Agarose gel of digested vector and insert for purification via agarose gel electrophoresis. Ladder is described in more detail in chapter 2.6.

The concentration after DNA-extraction was determined for insert and vector using NanoDrop2000c.

Table 22: Concentration of vector and insert after digestion and DNA-extraction from agarose gel electrophoresis.

plasmid	concentration [ng/µl]
pET28a	13.9
ENSA insert	13.0

Ligation was done with a ratio of vector:insert of 1:3, *E.coli* TOP10 were transformed with the ligation product and 4 clones were picked, the plasmid-DNA isolated using a mini-prep-kit and the DNA, as described above, first test digested by taking 3 µL per sample and checked via agarose gel electrophoresis. As control, DNA of clone 2 was also taken as non-digested version and placed in a separate pocket (equals sample 1).

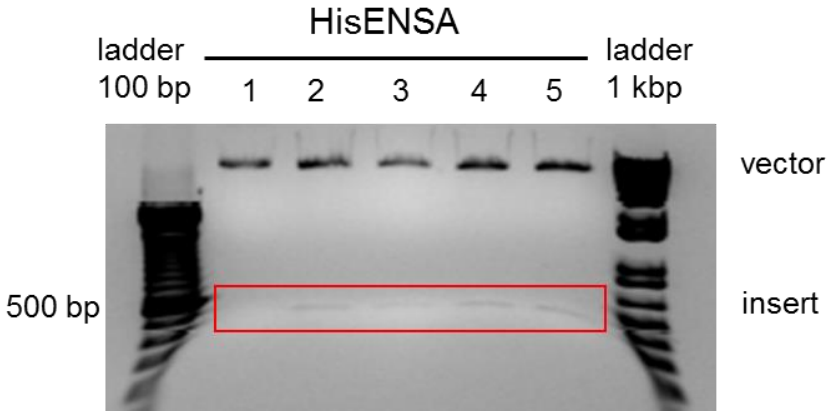

Figure 15: Digestion of pET28a-plasmid containing the ENSA insert.
Agarose gel with digested pET28a vector (upper black band) including the insert for ENSA (bands in the red square). 1: clone 2 without enzymes; 2: clone 1; 3: clone 2; 4: clone 3; 5: clone 4. Ladders are described in more detail in chapter 2.6.

Clone 1 was sent for sequencing ('Eurofines') to verify successful cloning. Nucleotide sequence analysis was first translated to amino acid sequence using ‘expasy translate’ and then compared with the expected HisENSA amino acid sequence using ‘clustal omega’.

```
HisENSA       MGSSHHHHHHSSGLVPRGSHMASMTGGQQMGRGSEFMSQKQEEENPAEETGEEKQDTQEK
expected      MGSSHHHHHHSSGLVPRGSHMASMTGGQQMGRGSEFMSQKQEEENPAEETGEEKQDTQEK
              ************************************************************

HisENSA       EGILPERAEEAKLKAKYPSLGQKPGGSDFLMKRLQKGQKYFDSGDYNMAKAKMKNKQLPS
expected      EGILPERAEEAKLKAKYPSLGQKPGGSDFLMKRLQKGQKYFDSGDYNMAKAKMKNKQLPS
              ************************************************************

HisENSA       AGPDKNLVTGDHIPTPQDLPQRKSSLVTSKLAGGQVE
expected      AGPDKNLVTGDHIPTPQDLPQRKSSLVTSKLAGGQVE
              ************************************
```

Figure 16: Sequencing data (HisENSA) compared with expected HisENSA sequence (expected).
The His-tag is marked in red. The nucleotide translation was done using ‘expasy translate’; the comparison was done using ‘clustal omega’ (1.2.1).

Now, this vector could be used for transformation of *E.coli* BL21 leading to an over-expression of His-tagged ENSA followed by protein isolation.

4.2.3. Mutagenesis of ENSA DNA inserted in pCMV-3Tag-1A and pET28a vector

The interesting phosphorylation sites of ENSA (S67 and S109) should be mutated to alanine (A) and aspartic acid (D) for further studies. Such mutational studies are important to validate the described phosphosites. The A mutant cannot be phosphorylated. The D mutant can also not be phosphorylated but is mimicking the phosphorylation, so the D mutant was used as a phosphomimetic.

Therefore, according to 3.2.5., the primers generated for these mutations were used for both vectors, including ENSA-sequence, to insert a mutation at S67 or S109 to A or D. Each mutated DNA was sent for sequencing to ‘Eurofines’, all mutations were successful. The sequencing results are shown as amino acid sequences in the following figures (Figure 17 - Figure 21).

```
HisENSA S109A     MGSSHHHHHHSSGLVPRGSHMASMTGGQQMGRGSEFMSQKQEEENPAEETGEEKQDTQEK
expected          MGSSHHHHHHSSGLVPRGSHMASMTGGQQMGRGSEFMSQKQEEENPAEETGEEKQDTQEK
                  ************************************************************

HisENSA S109A     EGILPERAEEAKLKAKYPSLGQKPGGSDFLMKRLQKGQKYFDSGDYNMAKAKMKNKQLPS
expected          EGILPERAEEAKLKAKYPSLGQKPGGSDFLMKRLQKGQKYFDSGDYNMAKAKMKNKQLPS
                  ************************************************************

HisENSA S109A     AGPDKNLVTGDHIPTPQDLPQRKSALVTSKLAGGQVE
expected          AGPDKNLVTGDHIPTPQDLPQRKSALVTSKLAGGQVE
                  ***************************************
```

Figure 17: Sequencing data of the HisENSA S109A mutant.
The S109A mutation is marked in red. The His-tag sequence is marked in blue. Clustal Omega (1.2.1) was used for sequence alignment.

```
HisENSA S67A      ------------------------------------------------------DTQEK
expected          MGSSHHHHHHSSGLVPRGSHMASMTGGQQMGRGSEFMSQKQEEENPAEETGEEKQDTQEK
                                                                       *****

HisENSA S67A      EGILPERAEEAKLKAKYPSLGQKPGGSDFLMKRLQKGQKYFLAGDYNMAKAKMKNKQLPS
expected          EGILPERAEEAKLKAKYPSLGQKPGGSDFLMKRLQKGQKYFLAGDYNMAKAKMKNKQLPS
                  ************************************************************

HisENSA S67A      AGPDKNLVTGDHIPTPQDLPQRKSSLVTSKLAGGQVE
expected          AGPDKNLVTGDHIPTPQDLPQRKSSLVTSKLAGGQVE
                  ***************************************
```

Figure 18: Sequencing data of HisENSA S67A mutant.
The S67A mutation is marked in red. Clustal Omega (1.2.1) was used for sequence alignment of sequencing result compared to the expected amino acid sequence.

For the S67A mutant the sequencing started not in front of the His-tag but behind because of some sequencing primer binding problems (Figure 18). However, the mutation was successfully detected and sequenced. The sequencing for the D mutants was also correct (data not shown)

```
HisENSA S67D      MGSSHHHHHHSSGLVPRGSHMASMTGGQQMGRGSEFMSQKQEEENPAEETGEEKQDTQEK
expected          MGSSHHHHHHSSGLVPRGSHMASMTGGQQMGRGSEFMSQKQEEENPAEETGEEKQDTQEK
                  ************************************************************

HisENSA S67D      EGILPERAEEAKLKAKYPSLGQKPGGSDFLMKRLQKGQKYFDDGDYNMAKAKMKNKQLPS
expected          EGILPERAEEAKLKAKYPSLGQKPGGSDFLMKRLQKGQKYFDDGDYNMAKAKMKNKQLPS
                  ************************************************************

HisENSA S67D      AGPDKNLVTGDHIPTPQDLPQRKSSLVTSKLAGGQVE
expected          AGPDKNLVTGDHIPTPQDLPQRKSSLVTSKLAGGQVE
                  ***************************************
```

Figure 19: Sequencing data of HisENSA S67D mutant.
Clustal Omega (1.2.1) was used for sequence alignment of sequencing result compared to the expected amino acid sequence. The His-tag sequence is marked in blue. The S67D mutation is marked in red.

```
HisENSA S109D     MGSSHHHHHHSSGLVPRGSHMASMTGGQQMGRGSEFMSQKQEEENPAEETGEEKQDTQEK
expected          MGSSHHHHHHSSGLVPRGSHMASMTGGQQMGRGSEFMSQKQEEENPAEETGEEKQDTQEK
                  ************************************************************

HisENSA S109D     EGILPERAEEAKLKAKYPSLGQKPGGSDFLMKRLQKGQKYFDSGDYNMAKAKMKNKQLPS
expected          EGILPERAEEAKLKAKYPSLGQKPGGSDFLMKRLQKGQKYFDSGDYNMAKAKMKNKQLPS
                  ************************************************************

HisENSA S109D     AGPDKNLVTGDHIPTPQDLPQRKSDLVTSKLAGGQVE
expected          AGPDKNLVTGDHIPTPQDLPQRKSDLVTSKLAGGQVE
                  ***************************************
```

Figure 20: Sequencing data of HisENSA S109D mutant.
Clustal Omega (1.2.1) was used for sequence alignment of sequencing result compared to the expected amino acid sequence. The His-tag sequence is marked in blue. The S109D mutation is marked in red.

```
FLAGENSA S67A     MDYKDDDDKDYKDDDDKDYKDDDDKARAGSPGLQEFMSQKQEEENPAEETGEEKQDTQEK
expected          MDYKDDDDKDYKDDDDKDYKDDDDKARAGSPGLQEFMSQKQEEENPAEETGEEKQDTQEK
                  ************************************************************

FLAGENSA S67A     EGILPERAEEAKLKAKYPSLGQKPGGSDFLMKRLQKGQKYFDAGDYNMAKAKMKNKQLPS
expected          EGILPERAEEAKLKAKYPSLGQKPGGSDFLMKRLQKGQKYFDAGDYNMAKAKMKNKQLPS
                  ************************************************************

FLAGENSA S67A     AGPDKNLVTGDHIPTPQDLPQRKSSLVTSKLAGGQVE
expected          AGPDKNLVTGDHIPTPQDLPQRKSSLVTSKLAGGQVE
                  ************************************
```

Figure 21: Sequencing data of FLAG-ENSA S67A mutant.
The S67A mutation is marked in red. Clustal Omega (1.2.1) was used for sequence alignment of sequencing result compared to the expected amino acid sequence. The FLAG-tag sequence is marked in blue. The S67A mutation is marked in red.

4.2.4. Expression and purification of His-tagged ENSA

For protein expression and purification, *E.coli* BL21 were transformed as described in 3.1.5. with the HisENSA pET28a vector and all mutant vectors.

Protein expression and purification were performed as described in 3.1.7. and 3.5.5.

For protein isolation, the purification profile of all proteins looked very similar. The sample loading leaded always to a strong increase of the UV signal. After loading, the signal decreased to 0 again. The column was washed and subsequently the elution was started. When the protein of interest was eluted, the UV line showed a peak. As an example, the purification profile of wildtype HisENSA protein is shown in Figure 22.

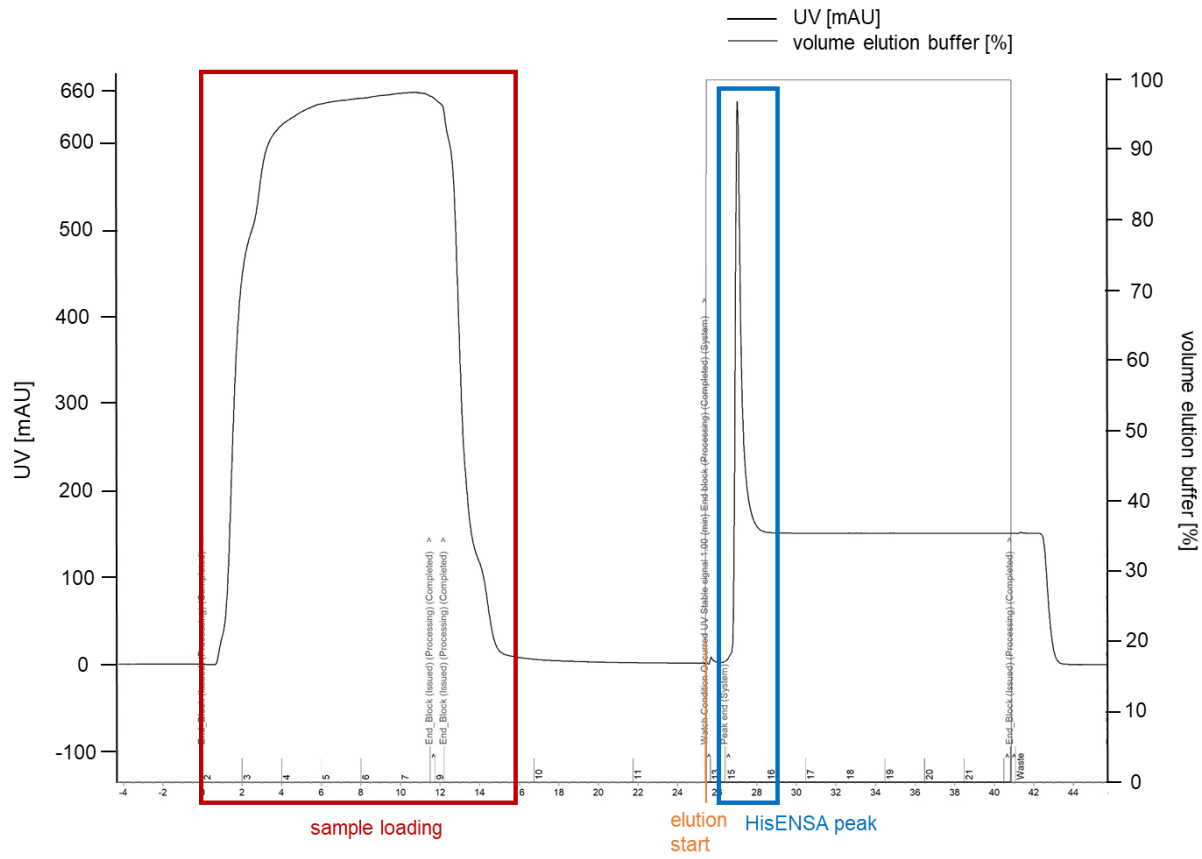

Figure 22: Protein purification profile for HisENSA WT.
Sample loading is marked in red, the start of the protein elution in orange (addition of elution buffer) and the protein peak in blue. The plateau after the protein peak always appeared, which contained small amounts of the purified protein. All fractions until the plateau ended/purification finished were collected, re-buffered and concentrated. This elution profile is representative for at least three purifications of wildtype HisENSA and S67A/D and S109A/D HisENSA mutants.

All collected fractions of the eluate of one protein were pooled, the buffer was exchanged using PD-10 columns and the sample was concentrated using amicon ultra-4 centrifugal units. The total amount of protein in the sample after concentrating depended mostly on the fact, if one pellet or two pellets of *E.coli*-expression solution were selected for purification.

SDS-PAGE, western blotting (using the Cell Signaling® anti-ENSA antibody) and silver staining were performed for all proteins (Figure 23, Figure 24, Figure 25).

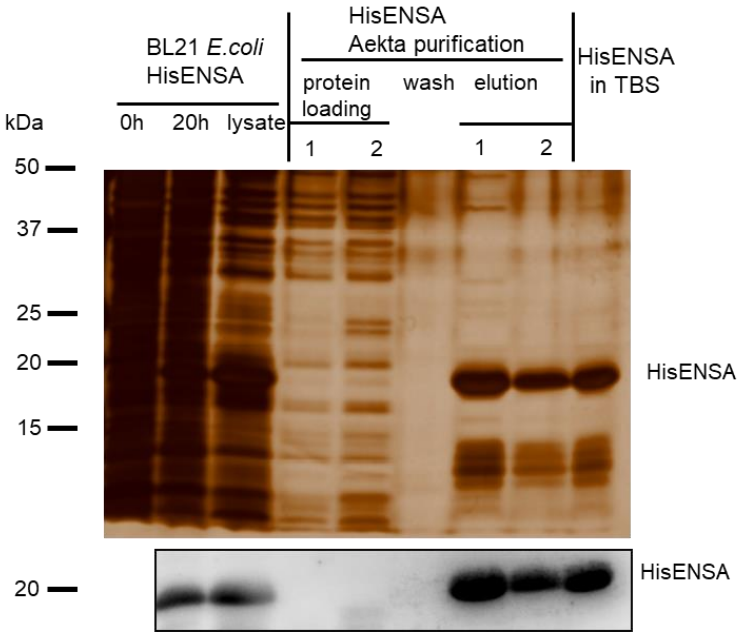

Figure 23: Purification results of HisENSA wildtype.
Silver staining (13% (v/v) acrylamide SDS-PAGE) and western blot of HisENSA wildtype expression, purification and buffer exchange. 0h: before IPTG addition, 20h: 20 hours after IPTG addition and incubation overnight at 20°C, the SDS-PAGE *E.coli* samples equal an OD_{600} of 1; 1 and 2 are the numbers of fractions that were taken. For western blot, anti-ENSA antibody (Cell Signaling®) was used 1:500 in 5% (w/v) BSA-TBST.

ENSA protein was detected after 20h of incubation (after expression induction) in the lysed *E.coli* and in the elution fractions as well as in the re-buffered protein sample (Figure 23). This shows that no ENSA protein was lost during sample loading and washing of the column.

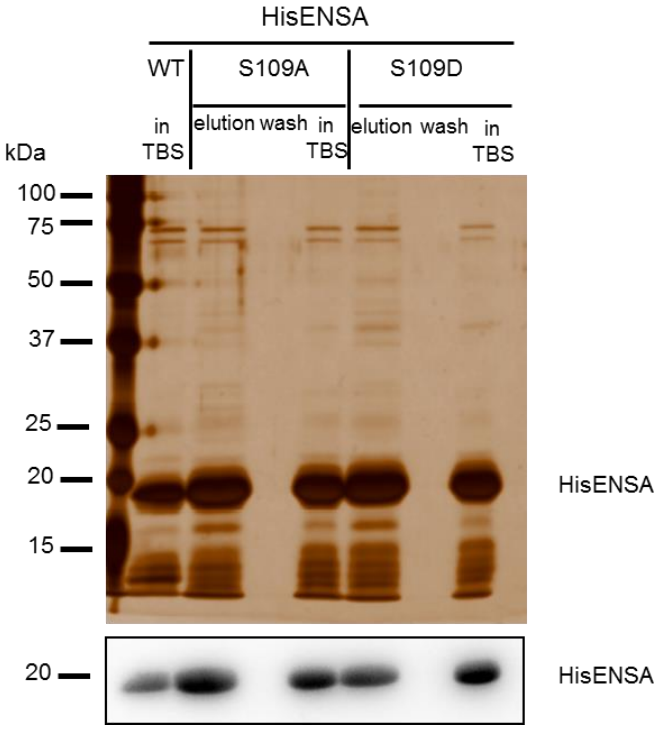

Figure 24: Purification results of HisENSA S109A and S109D mutants.
Silver staining (13% (v/v) acrylamide SDS-PAGE) and western blot of HisENSA wildtype (WT) in TBS and the S109 mutants (purification and buffer exchange (in TBS)). For western blot, anti-ENSA antibody (Cell Signaling®) was used 1:500 in 5% (w/v) BSA-TBST.

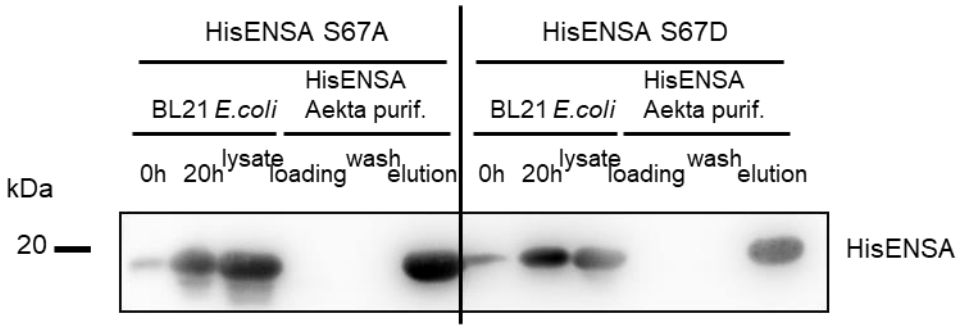

Figure 25: Purification results of HisENSA S67A and S67D mutant.
Western blot of HisENSA S67 mutants expression and purification. 0h: before IPTG addition, 20h: 20 hours after IPTG addition and incubation overnight at 20°C, the *E.coli* samples equal an OD_{600} of 1. Anti-ENSA antibody (Cell Signaling®) was used 1:500 in 5% (w/v) BSA-TBST.

The silver stains show that the purifications worked well with only very low contamination of other proteins (Figure 23, Figure 24). HisENSA was expressed in high amounts in *E.coli* after protein expression induction with IPTG (seen in Figure 25 for 20h samples).

The recombinant proteins were used after purification for further experiments as described in the following chapters. They were stored in 1xTBS at 4°C.

4.3. Phosphorylation of recombinant human His-tagged ENSA and GST-tagged ARPP19 protein by PKA and PKG

To characterize the purified proteins as protein kinase substrates, HisENSA wildtype, S109A, S109D mutants and the S67A mutant (shown in 4.10.) were incubated under phosphorylating conditions with purified bovine protein kinase A (C-subunit of PKA was used for phosphorylation) and recombinant human protein kinase G (PKGIβ).

Wildtype HisENSA and S67A mutant (shown in 4.10.) were phosphorylated at S109, both S109 mutants were not, showing that S109 of the ENSA protein is phosphorylated and not S108 (directly next to S109) and also that the anti-pS109 ENSA antibody from S. Mochida (generated for *Xenopus* ENSA) detects S109 phosphorylation of human ENSA and not another amino acid phosphorylation of the protein.

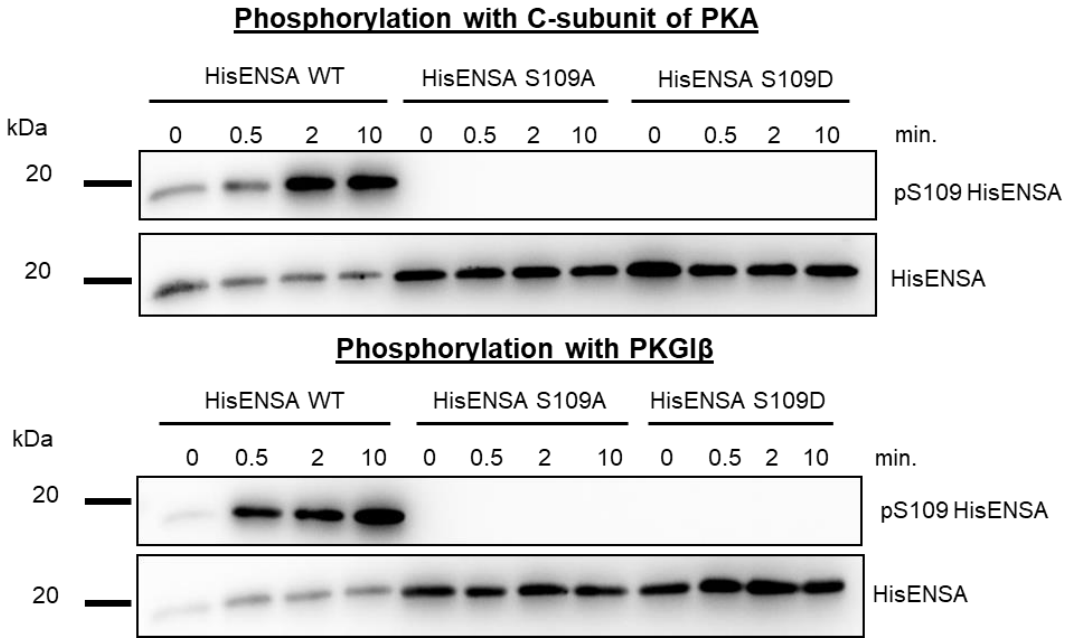

Figure 26: HisENSA wildtype (WT) is phosphorylated at S109 by protein kinase A and G.
HisENSA proteins were phosphorylated in the presence of C-subunit of PKA or PKGIβ and 1 mM ATP (and 5 µM cGMP for PKG). Western blots are showing that the S109 HisENSA mutant proteins are not phosphorylated at S109. For HisENSA signal, the anti-ENSA antibody (Cell Signaling®) was used 1:500 in 5% (w/v) BSA-TBST, for pS109 the anti-pS109 ENSA antibody (S. Mochida) was used (1:300) in 5% (w/v) BSA-TBST. The western blots are representative for n=3 independent experiments.

These results support our phosphoproteomic data and show that ENSA S109 is a specific substrate for both PKA and PKG in human platelets and as recombinant protein.

As our proteomic data also found ARPP19 to be phosphorylated in response to both cAMP- and cGMP-elevating platelet inhibitors, I analyzed whether commercially available recombinant GST-tagged human ARPP19 protein is phosphorylated on S104 (similar to S109 of ENSA) by PKA and PKG. As shown in Figure 27, phosphorylation of the recombinant ARPP19 protein worked well by both protein kinases.

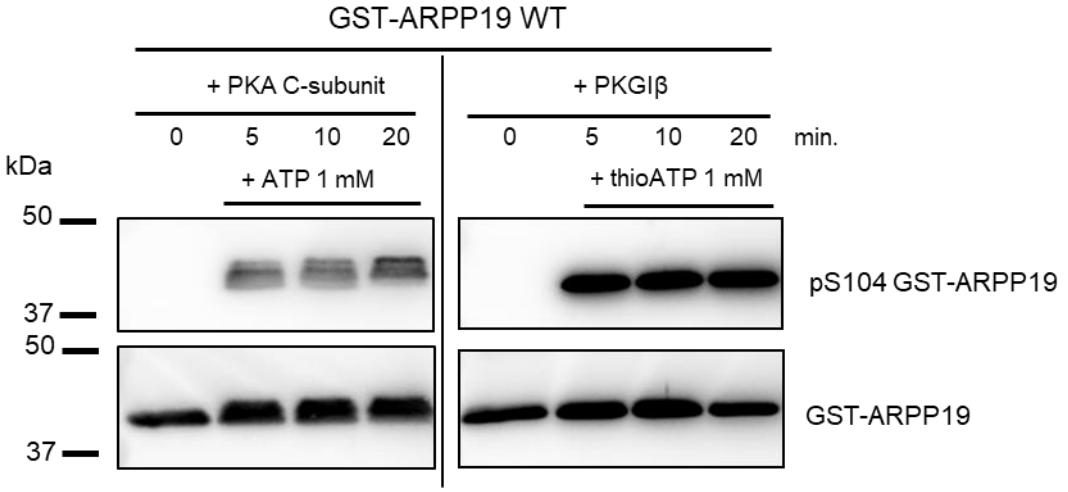

Figure 27: GST-ARPP19 wildtype (WT) is phosphorylated by protein kinase A and G at S104.
GST-ARPP19 protein was phosphorylated in the presence of C-subunit of PKA or PKGIβ and 1 mM ATP or thio-ATP (and 5 µM cGMP for PKG). For detection of the ARPP19 protein, the G153 serum antibody, directed against ARPP19, was used 1:2000 in 5% (w/v) BSA-TBST, for pS104 the anti-pS109 PAN ENSA antibody (ImmunoGlobe®) was used 1 µg/mL in 5% (w/v) BSA-TBST. The western blots are representative for n>3 independent experiments.

These results show, that both PKA and PKG phosphorylate well recombinant ENSA and ARPP19 at a closely related, but distinct phosphorylation site within the C-terminal region of these two proteins (S109 ENSA/ S104 ARPP19).

For PKA phosphorylation of ARPP19 a closely co-migrating double band appeared for the pS104 signal and with the general antibody (also when thio-ATP was used). There is no real explanation for this until now, as I also did not see this for PKG phosphorylation of the same site. As thio-ATP induces a stable phosphorylation (thio-phosphate, which cannot be removed by a phosphatase), it was used when the protein was phosphorylated for further experiments (for example inhibitory experiments).

To better demonstrate the similarity of ARPP19 and ENSA, an amino acid sequence alignment for both human proteins (ENSA isoform 1 (uniprot.org) and ARPP19) is presented in Figure 28.

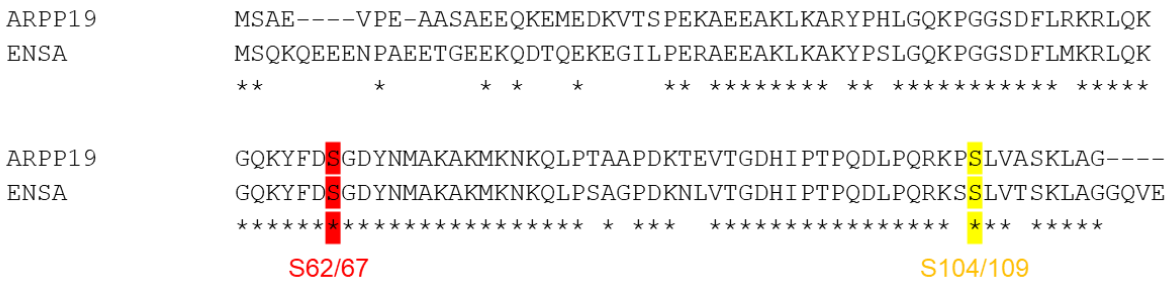

Figure 28: Amino acid sequence alignment of ENSA isoform 1 and ARPP19.
Clustal Omega (1.2.1) was used for sequence alignment. S62/67 is marked in red, S104/109 in yellow. Stars show that both amino acids are identical. Empty space shows that there is no amino acid sequence similarity between ARPP19 and ENSA.

4.4. Overexpression of FLAG-tagged ENSA in HEK293 cells and endogenous ENSA in HEK293 cells compared to human platelets

For the analysis of ENSA phosphorylation in other human cells, human embryonic kidney 293 cells were transiently transfected (using PolyJet™) with the pCMV-3Tag-1A plasmid containing the sequence for FLAG-tagged ENSA. The phosphorylation of FLAG-ENSA was investigated using the adenylate cyclase activator forskolin (10 µM, 15 minutes), DMSO (0.1% (v/v)) was used as vehicle control (protein phosphorylation results shown later).

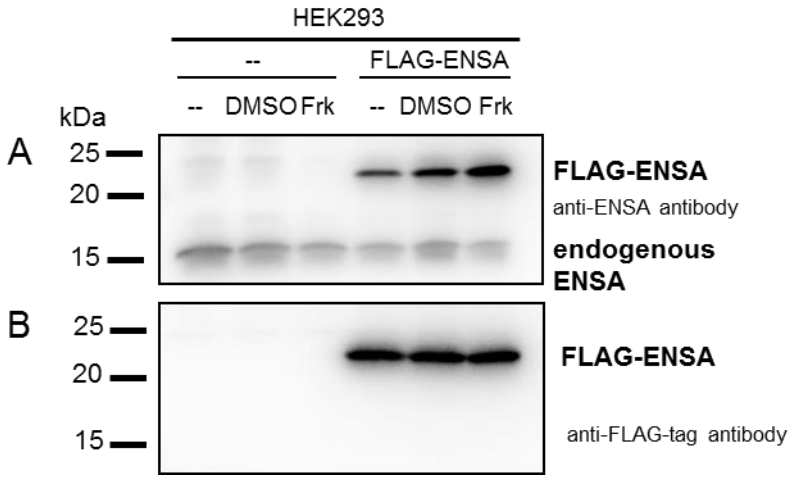

Figure 29: Overexpression of FLAG-ENSA in transfected HEK293 cells.
A: Western blot showing a strong signal for FLAG-tagged ENSA using the general anti-ENSA antibody (Cell Signaling®, 1:500 in 5% (w/v) BSA-TBST) also signal of endogenous ENSA. B: anti-FLAG-tag antibody (Cell Signaling®, 1:3000 in 5% (w/v) BSA-TBST) showing only a signal for FLAG-ENSA. Frk: 10 µM forskolin; DMSO: vehicle control 0.1% (v/v); --: untreated.

Transfection was successful (see Figure 29). The anti-ENSA antibody also detected a signal for endogenous ENSA in HEK293 cells of about 16 kDa.

For comparison, the following blot (Figure 30) shows endogenous ENSA present in HEK293 cells and human platelets of very similar size (~16 kDa). Overexpressed FLAG-tagged ENSA is larger as expected (~22 kDa) and also well-recognized by the anti-ENSA antibody. Expression levels did not change upon treatment with thrombin, iloprost or SNP.

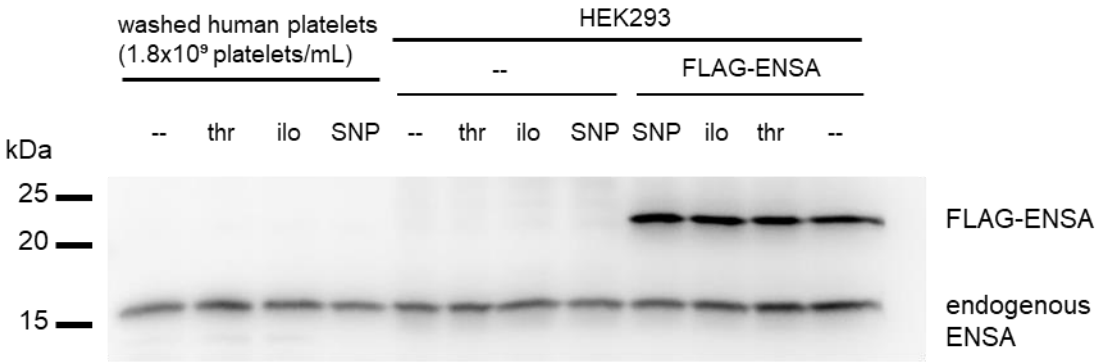

Figure 30: Endogenous ENSA in human platelets and in HEK293 cells, compared to FLAG-ENSA overexpressed in HEK293 cells.
Western blot showing washed human platelets and HEK293 cells, treated with thrombin (thr), iloprost (ilo), sodium-nitroprusside (SNP) or untreated (--). Anti-ENSA antibody (Cell Signaling®) was used 1:500 in 5% (w/v) BSA-TBST.

The treatment of HEK293 cells with forskolin and therefore the activation of PKA led to a phosphorylation of FLAG-ENSA at serine 109 (S109) and a decreased phosphorylation of serine 67 (S67), shown in the following western blots (Figure 31). The vehicle (DMSO) did not influence the phosphorylation. A similar phosphorylation pattern was observed for endogenous ENSA in HEK293 cells, also shown in the following blots (Figure 31).

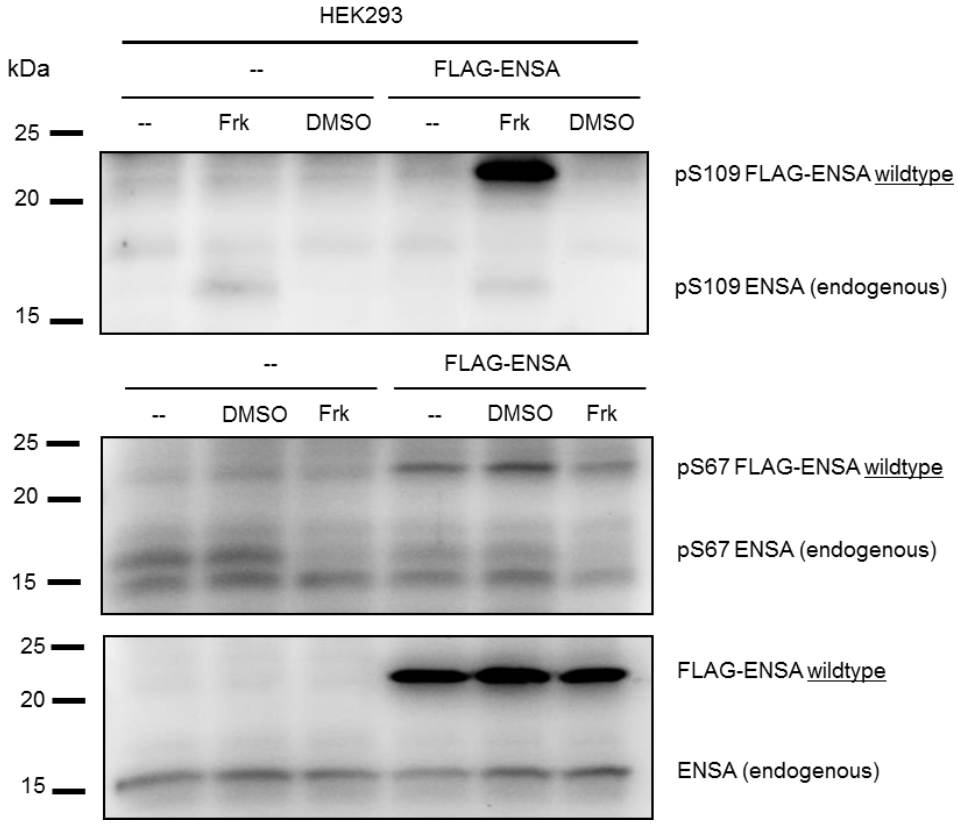

Figure 31: Phosphorylation pattern of endogenous ENSA of forskolin-treated HEK293 cells compared to FLAG-ENSA.
Western blots showing HEK293 cells expressing endogenous ENSA (16 kDa) and FLAG-tagged ENSA (about 22 kDa), treated with 10 µM forskolin (Frk), with vehicle (DMSO) or without treatment (--). Anti-ENSA antibody (Cell Signaling®) was used 1:500 in 5% (w/v) BSA-TBST; anti-pS67 ENSA antibody (Cell Signaling®) was used 1:250 in 5% (w/v) BSA-TBST; for pS109 ENSA detection, anti-pS109 PAN ENSA antibody (ImmunoGlobe®) was used with 1 µg/mL in 5% (w/v) BSA-TBST.

In HEK293 cells, endogenous ENSA was already phosphorylated at S67 under basal conditions. The same effect was seen for FLAG-ENSA expressed in HEK293 cells. In contrast, endogenous ENSA of washed human platelets did not show a phosphorylation at S67 under basal conditions by immunoblotting. Figure 32 shows a comparison for FLAG-ENSA, FLAG-ENSA S67A mutant, human platelets and the recombinant His-tagged ENSA protein (general ENSA signal and pS67 ENSA signal). Phosphorylation of endogenous platelet ENSA at S67 was induced by an incubation of intact human platelets with 10 µM okadaic acid (OA) for 40 minutes. OA is a very potent inhibitor of the protein phosphatase 2A (PP2A). This effect will be discussed in more detail in the following sections.

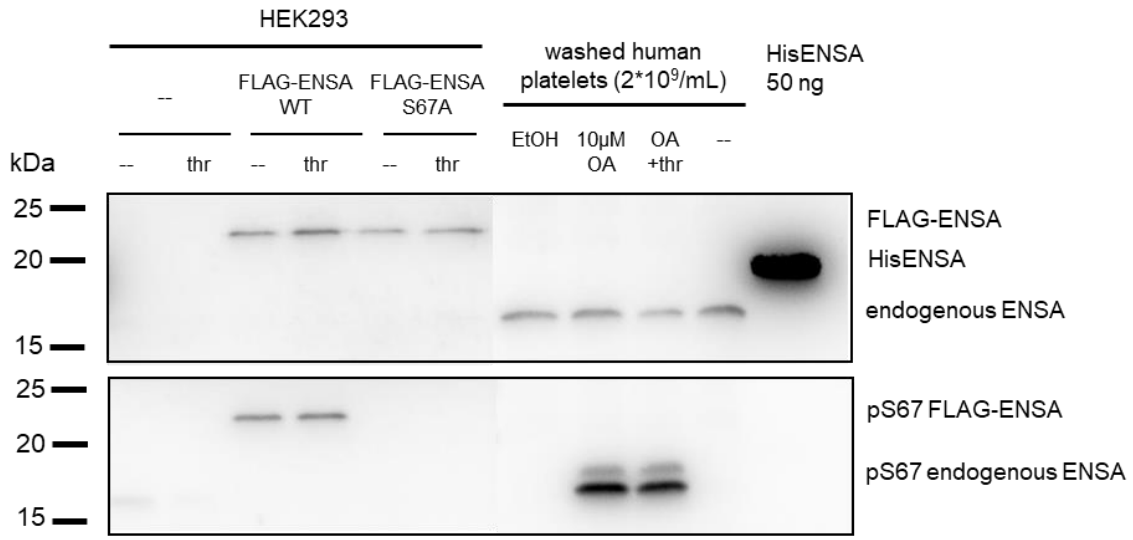

Figure 32: Phosphorylation of endogenous platelet ENSA and FLAG-ENSA in HEK293 cells at S67.
Wildtype FLAG-ENSA shows under basal conditions (--) a phosphorylation at S67 in the western blot. Human platelet endogenous ENSA only shows S67 phosphorylation when platelets were incubated with the PP2A inhibitor okadaic acid (OA) for 40 minutes. The addition of thrombin 0.1 U/mL and 1 minute of incubation on top did not change the S67 phosphorylation of ENSA. Recombinant HisENSA was not detected by the anti-pS67 ENSA antibody. Anti-ENSA antibody (Cell Signaling®) was used 1:500 in 5% (w/v) BSA-TBST; anti-pS67 ENSA antibody (Cell Signaling®) was used 1:250 in 5% (w/v) BSA-TBST.

These data indicate that both, the dividing HEK293 cells and the non-dividing platelets present a kinase that is able to phosphorylate ENSA at S67. This kinase is active in HEK293 cells under basal conditions. In platelets, the kinase has to be activated or a phosphatase needs to be inhibited to detect this kinase-mediated phosphorylation signal.

As mentioned before, ENSA and ARPP19 are paralogs, encoded by distinct genes but show highly conservation, especially around the central region of the S67 phosphorylation site. The anti-S62/67 ENSA/ARPP19 phospho-antibody cannot distinguish whether the signal is due to ENSA S67 or ARPP19 S62. Here, the blots showed that OA leads to two pS67 signal bands (Figure 32 and others), a more prominent one at ~16 kDa and a minor one at ~19 kDa, suggesting that the upper band is ARPP19 (with a mass of 13 kDa), which is known to migrate unusually high (~19 kDa, see its name) in SDS PAGE. In comparison, ENSA migrates at ~16 kDa.

4.5. Phosphorylation of endogenous ENSA at S67 in human platelets

As shown before, endogenous ENSA in human platelets is not phosphorylated at S67 under basal conditions. This result suggests that there is no phosphorylation of S67 ENSA under basal conditions (no active kinase). Another explanation could be that the used western blotting method is not sensitive enough to detect low phosphorylation of S67 ENSA. A third possibility could be that pS67 ENSA is dephosphorylated again very fast under basal conditions (active phosphatase), so we are not able to detect the phosphorylation via western blotting.

To find out whether S67 phosphorylation of ENSA could be induced in human platelets, isolated intact human platelets were incubated with the protein phosphatase 2A (PP2A)

inhibitor OA, as mentioned in the chapter before. The inhibition of PP2A resulted in phosphorylation at S67 of endogenous ENSA as detected by immunoblotting. This phosphorylation was dependent on the concentration of OA and the incubation time of washed human platelets with OA (Figure 33). However, 200 nM OA and 10 minutes of incubation were already sufficient to detect a clear pS67 signal.

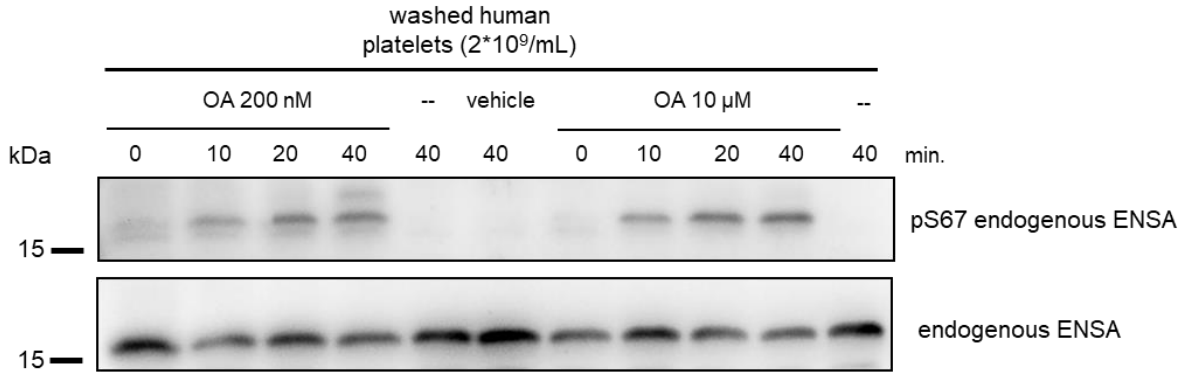

Figure 33: Phosphorylation of endogenous ENSA in intact human platelets incubated with OA. As control, washed human platelets were incubated without or with ethanol (vehicle 0.1% (v/v)) for 40 minutes. Anti-ENSA antibody (Cell Signaling®) was used 1:500 in 5% (w/v) BSA-TBST; anti-pS67 ENSA antibody (Cell Signaling®) was used 1:250 in 5% (w/v) BSA-TBST.

Obviously, as seen for the controls in the western blot, the pS67 ENSA signal was related to OA incubation and therefore seems to be related to inhibited phosphatase(s) or/and more active kinase(s).

As already seen in Figure 32, two bands were detected for the pS67 ENSA signal, which appeared with time. Probably, the upper band at 19 kDa is the phosphorylated S62 ARPP19. ARPP19 is less abundant than ENSA in human platelets and does not run as fast as ENSA.

The kinase phosphorylating ENSA at S67 or other possible interaction partners in human platelets are not known so far but of great interest. Therefore, immunoprecipitation of endogenous ENSA in lysates of human platelets was performed to potentially catch the unknown kinase responsible for S67 ENSA phosphorylation. The identification of such kinase would be helpful for understanding ENSA function in human platelets.

4.6. Immunoprecipitation (IP) of endogenous human platelet ENSA

To better study ENSA and its interaction partners in human platelets, the idea was to immunoprecipitate ENSA from platelet lysates using protein A magnetic beads, called protein A Dynabeads™ (Invitrogen), and an antibody against ENSA, bound to the beads.

All commercially available antibodies directed against general ENSA were not recommended to be used for IP, except of a monoclonal mouse anti-ENSA antibody from Santa Cruz®. First, I probed three different anti-pan ENSA antibodies for ENSA detection in western blot and then for the IP. The polyclonal rabbit anti-ENSA antibody from Cell Signaling® that I generally used for western blot detection of endogenous and recombinant ENSA worked well for western blotting (see for example Figure 26 and Figure 33). The second antibody I probed was a monoclonal rabbit anti-ENSA antibody from Abcam®. The third and last antibody I probed was the monoclonal mouse anti-ENSA antibody from Santa Cruz®, which is recommended to be used for IP. In comparison, the best western blot signal of endogenous ENSA for washed

human platelets was detected with the polyclonal rabbit anti-ENSA antibody from Cell Signaling®. Therefore, this antibody was used for western blot detection.

The coupling of the antibodies to the Dynabeads™ worked well for all antibodies, but none of the antibodies bound endogenous ENSA in platelet lysates in several experiments.

As an example, the silver stain and the western blot of the monoclonal mouse anti-ENSA antibody from Santa Cruz®, are shown in Figure 34. The polyclonal rabbit anti-ENSA antibody from Cell Signaling® was used as primary antibody upon western blotting, to detect the general ENSA signal. To visualize also the monoclonal mouse antibody in the blot, anti-rabbit and anti-mouse-HRP-conjugated antibodies were used as secondary antibodies.

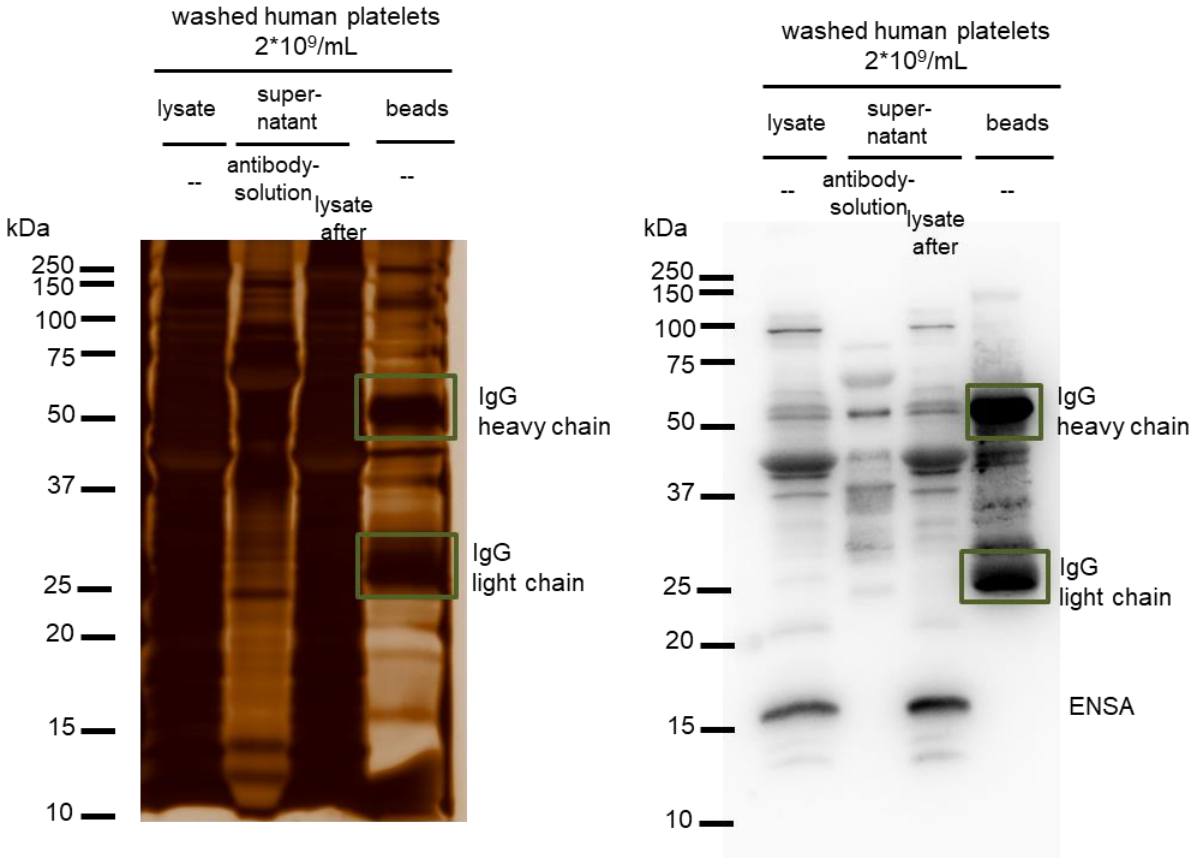

Figure 34: Silver stain and western blot of ENSA immunoprecipitation from human platelet lysates.
Lysate: before incubation with beads; supernatant antibody-solution: antibody solution after bead incubation; supernatant lysate after: lysate after bead incubation; beads: beads after incubation with antibody solution and platelet lysate treated with sample loading buffer. Anti-ENSA antibody (Cell Signaling®) was used 1:500 in 5% (w/v) BSA-TBST. The blot/silver stain are representative for n>3 independent experiments.

Endogenous ENSA was always detectable in the lysate (supernatant), but there was no detection after immunoprecipitation, suggesting that all anti-ENSA antibodies are only able to bind denatured ENSA in western blot analysis but not native ENSA. This could be because ENSA undergoes a change in its secondary structure, when it interacts with membranes or proteins or when it is phosphorylated and therefore, the antibodies are not able to bind the protein in the lysate. Alternatively, the conditions I chose were not perfect for ENSA IP and need to be improved.

4.7. Phosphorylation of recombinant compared to endogenous ENSA at S67 in lysates of human platelets

To find out, if the phosphorylation of ENSA S67 also appears for the recombinant His-tagged ENSA protein when incubated with human platelet lysate, intact platelets were pre-incubated for 15 to 20 minutes with OA, lysate generated as described in 3.4.5. and incubated with the recombinant protein. Platelets without OA pre-incubation and also the HisENSA S67A mutant that cannot be phosphorylated at S67 were used as negative control. The phosphorylation reaction was started with the addition of 1 mM ATP.

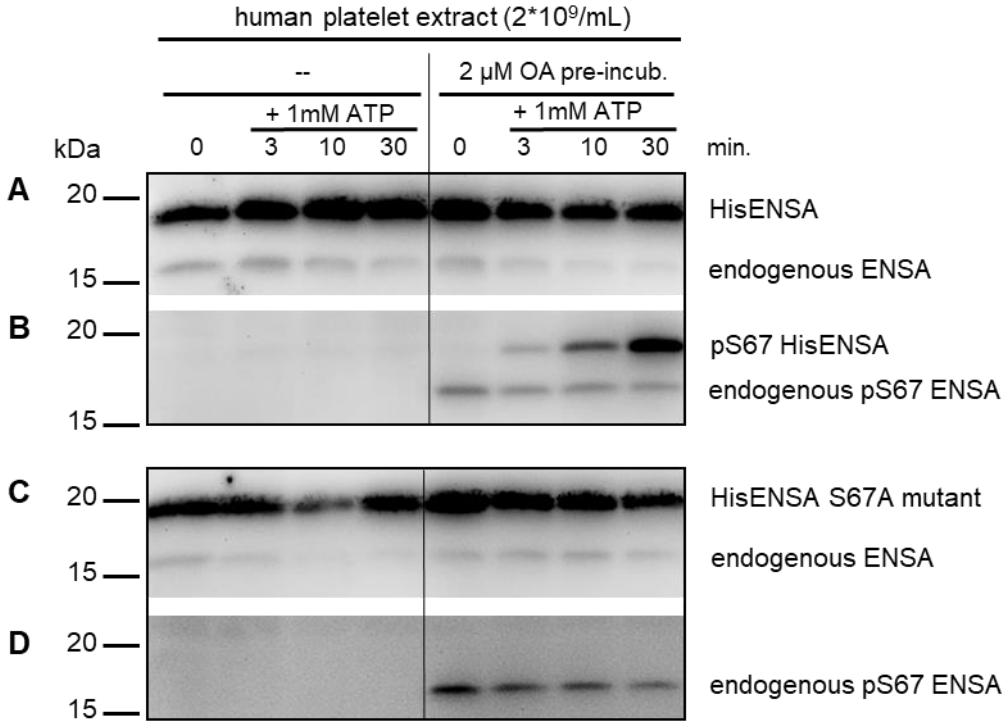

Figure 35: Time-dependent phosphorylation of HisENSA at S67 in the presence of 2 µM OA. Washed human platelets, pre-incubated without and with 2 µM OA for 15 min., reaction was started with the addition of 1 mM ATP. S67A HisENSA mutant was used as negative control. Anti-ENSA antibody (Cell Signaling®) was used 1:500 in 5% (w/v) BSA-TBST; anti-pS67 ENSA antibody (Cell Signaling®) was used 1:250 in 5% (w/v) BSA-TBST. These blots are representative for n>3 independent experiments.

The representative western blot in Figure 35 shows clearly a time-dependent phosphorylation of recombinant wildtype HisENSA at S67 induced by a kinase present in human platelets. Endogenous ENSA was already phosphorylated at S67 after the pre-incubation of intact platelets with OA, indicating that there is a kinase present in human platelets phosphorylating ENSA at S67.

Phosphorylation of recombinant HisENSA at S67 was also detected when OA (2 µM) was directly added in the phosphorylation buffer/platelet lysate without OA-pre-incubation of intact platelets. This has been probed for HisENSA and also for recombinant GST-ARPP19, shown in Figure 36.

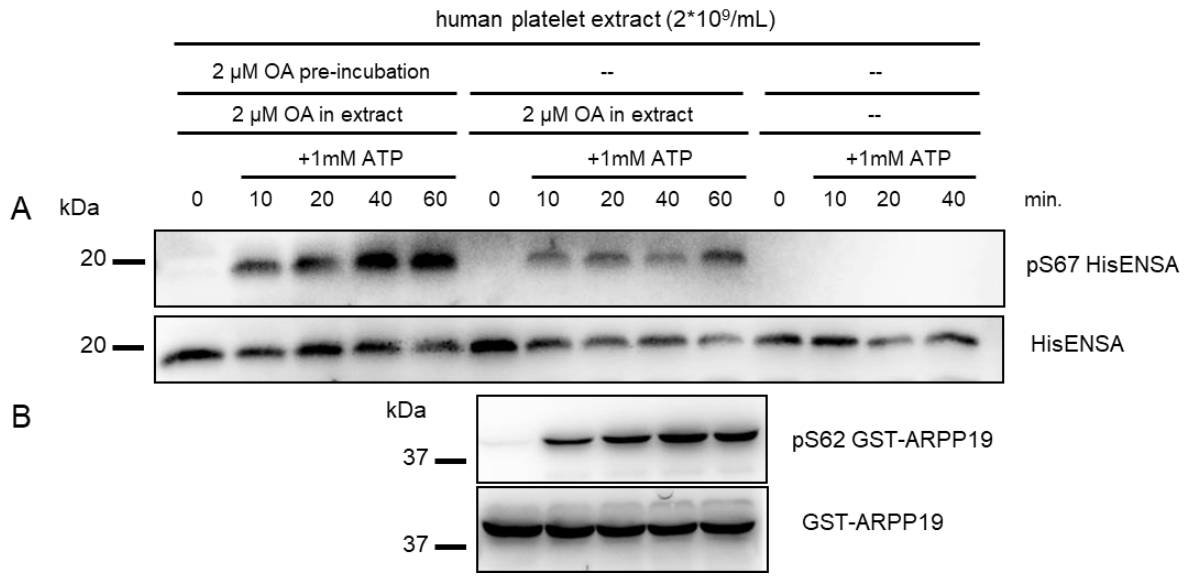

Figure 36: HisENSA and GST-ARPP19 phosphorylation at S67/62 by a kinase present in human platelet lysate in the presence of OA.
A shows that S67 ENSA was phosphorylated when PP2A was inhibited, even if OA was added only to platelet lysate. The pS67 HisENSA signal was weaker without OA pre-incubation. **B**: ARPP19 was phosphorylated at S62 upon PP2A inhibition with OA in platelet lysate. Washed human platelets were pre-incubated with or without 2 µM OA for 20 minutes, and/or 2 µM OA was added to platelet lysate. Reaction was started by the addition of 1 mM ATP. The G153 serum antibody, directed against ARPP19 but also detecting recombinant ENSA, was used 1:2000 in 5% (w/v) BSA-TBST for general ENSA and ARPP19 detection; anti-pS67 ENSA/pS62 ARPP19 antibody (Cell Signaling®) was used 1:500 in 5% (w/v) BSA-TBST.

HisENSA and also GST-ARPP19 were phosphorylated at S67/S62 in OA containing platelet lysates without pre-incubating intact human platelets with OA. The S67 kinase and PP2A are both active in platelet lysate and the inhibition of PP2A by OA also worked in platelet lysate. To investigate PP2A inhibition, thio-pS67 HisENSA was used instead of OA to inhibit PP2A trimeric holoenzymes containing distinct regulatory B-subunit isoforms in platelet lysate (results shown later).

The pS67 signal of HisENSA was decreased when PP2A was only inhibited in platelet lysate compared to the pre-incubated platelet samples. This could be explained by the fact that the platelet protein concentration including PP2A in platelet lysate ($2*10^9$/mL) was two-fold higher than the protein concentration of used intact platelets with OA pre-incubation ($1*10^9$/mL). Therefore, the used OA concentration in higher concentrated platelet lysates has less inhibitory capacity for PP2A than in the lower ones.

4.8. How to identify the ENSA S67 protein kinase(s) in human platelets

Proteomic analysis by our group (Burkhart et al.[111], Beck et al.[113], unpublished) and others[138] did not detect the prominent MASTL kinase in human and murine platelets so far, which is known to phosphorylate ENSA at S67 in dividing mammalian (e.g. HeLa) cells.

Using SDS-PAGE and western blotting, I investigated whether the MASTL kinase is present/detectable in human platelets and HEK293 cells (Figure 37). Endogenous MASTL of mammalian cells has a size of about 100 kDa (uniprot.org/uniprot/Q96GX5). The antibody against MASTL (from Bethyl laboratories) is known to detect the recombinant protein in

western blot running in a range of about 100 kDa.[139] Inactive recombinant GST-tagged MASTL kinase (derived from baculovirus infected Sf9 insect cells, SignalChem) was used as positive control for the antibody. Figure 37 shows that the anti-MASTL antibody detects recombinant GST-tagged kinase (~150 kDa) and MASTL kinase in HEK293 cells (100 kDa). In contrast, no signal similar to the size of endogenous MASTL kinase in HEK293 cells (~100 kDa) could be detected in lysates of human platelets.

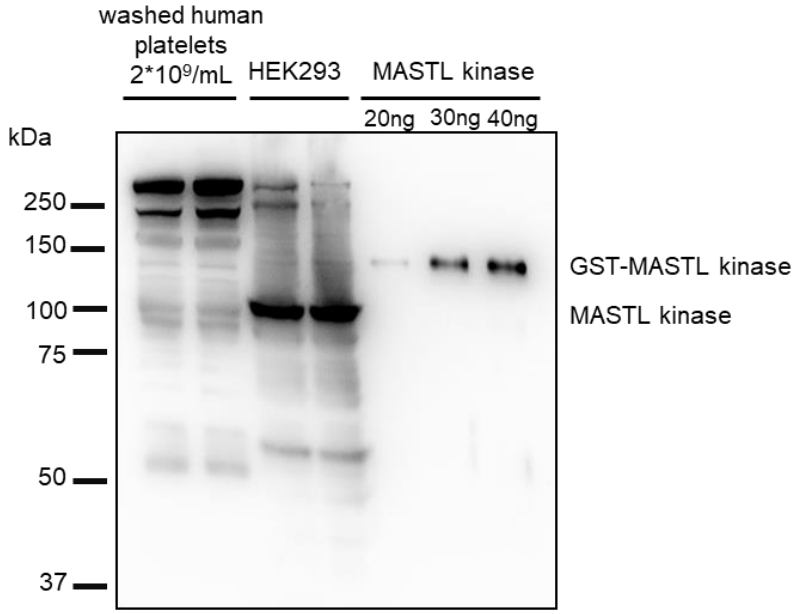

Figure 37: Detection of MASTL kinase using washed human platelets, HEK293 cells and recombinant MASTL kinase.
Endogenous MASTL was detected in HEK293 cells (100 kDa) but not in human platelets by the anti-MASTL antibody from Bethyl laboratories. Anti-MASTL antibody (Bethyl laborytories) was used 1:500 in 5% (w/v) BSA-TBST.

The interesting question now concerns the nature/identity of the kinase present in human platelets that is able to phosphorylate ENSA on S67. The results from chapter 4.7. clearly demonstrate the presence of an ENSA S67 protein kinase activity in platelets with little evidence that it is the MASTL kinase.

To get a better idea whether another kinase present in human platelets could phosphorylate ENSA at S67, a blast analysis by similarity was performed for both active sites of the human MASTL kinase protein (N- and C-terminal), defining the activity of the kinase. Figure 38 shows a scheme of human MASTL kinase.

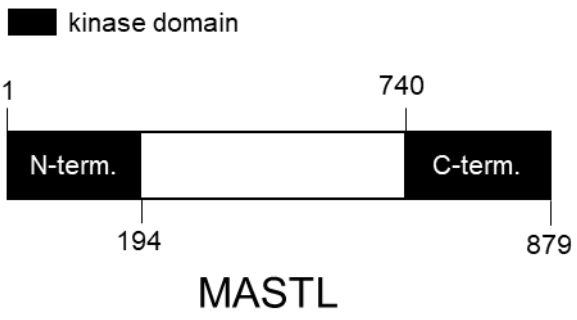

Figure 38: Structure of human MASTL kinase with the two sites important for kinase activity. (Adapted from Yu et al. 2004[140]/uniprot.org/uniprot/Q96GX5 and Ocasio et al. 2016[141])

A few kinases were identified showing structural similarity up to 48% (only isoforms of the Greatwall/MASTL kinase share 93-99% similarity with MASTL). However, only some of them are known to be present in human platelets (Table 23). C or N shows, which site of the MASTL kinase shares the similarity with the kinases.

Table 23: Amino acid sequence similarity blast analysis, copy number (CN) per platelet and transcriptomic data of identified kinases present in human platelets and in comparison to the murine platelet proteome.

kinase (protein name)	**uniprot accession number human[142]**	**site similarity**	**human platelet proteome:** CN/platelet	**human platelet transcriptome** reads/platelet	**murine platelet proteome** CN/platelet
MASTL	Q96GX5	100%	n.d.	333.00	n.d.
MAST1	Q9Y2H9	C – 46.5%	n.d.	0.89	n.d.
MAST2	Q6P0Q8	C – 45.2%	n.d.	18.50	21
MAST3	O60307	C – 45.2%	n.d.	239.00	n.d.
MAST4	O15021	C – 39.4%	n.d.	3,015.00	n.d.
LATS1	O95835	C – 48.3%	n.d.	Not tested	n.d.
LATS2	Q9NRM7	C – 48.3%	found only in TiO_2 enrichment	Not tested	n.d.
STK38 (NDR1)	Q15208	N – 47.3%	2,500	1,822.00	4,388
STK38L (NDR2)	Q9Y2H1	N – 45.9%	1,200	100.00	98
Ribosomal protein s6 kinase α3 (KS6A3)	P51812	C – 44.6%	1,300	Not tested	1,041

Human proteomic data: Burkhart et al. 2012[111]; human transcriptome: unpublished, generated by Dr. S. Schubert, values are mean reads of resting platelets from 10 individuals; murine proteomic data: Zeiler et al. 2014.[138] N.d.: not detected; C: C-terminal; N. N-terminal; CN: copy number

For comparison, the copy numbers of well-known proteins and of ENSA and ARPP19 from unstimulated human and murine platelets predicted by quantitative phosphoproteomics[111, 138] and the relating results (reads/platelet) of human platelet mRNA transcripts determined by Dr. S. Schubert (CTH, Mainz) are listed in Table 24.

Table 24: Proteome and transcriptome data of certain platelet proteins compared to the murine proteome.

kinase (protein name)	uniprot accession number human[142]	human platelet proteome: CN/platelet	human platelet transcriptome reads/platelet	murine platelet proteome CN/platelet
GPIb α-chain	P07359	18,900	13,260	46,154
GPVI	Q9HCN6	9,600	3,609	7,822
vWF	P04275	11,100	3,142	67,353
Integrin $\alpha_{IIb}\beta_3$	P08514	83,300	48,053	106,624
ENSA	O43768	7,800	624	1,241
ARPP19	P56211	2,500	2,822	1,364

Human proteomic data: Burkhart et al. 2012[111]; human transcriptome: unpublished, generated by Dr. S. Schubert, values are means of resting platelets from 10 individuals; murine proteomic data: Zeiler et al. 2014.[138] N.d.: not detected. CN: copy number

The transcriptomic and proteomic data were generated for resting platelets. Detected mRNA and protein levels implicate importance for the protein in resting platelets. For the MAST4 protein, only mRNA was detected in resting platelets, showing no need for the protein under these conditions but a potential need of translated protein via mRNA upon platelet activation. If mRNA and protein are found, it can be concluded that the protein has a function in platelets.

In a pilot protein kinase inhibitor experiment, lysates of washed human platelets supplemented with recombinant HisENSA were pre-incubated with OA in the presence or absence of the kinase inhibitor staurosporine (an ATP-competitive kinase inhibitor predominant of protein kinase C (IC_{50}=3 nM) and cAMP-dependent kinases (IC_{50}=8 nM)[120]). The reaction was started by adding 1 mM ATP (Figure 39).

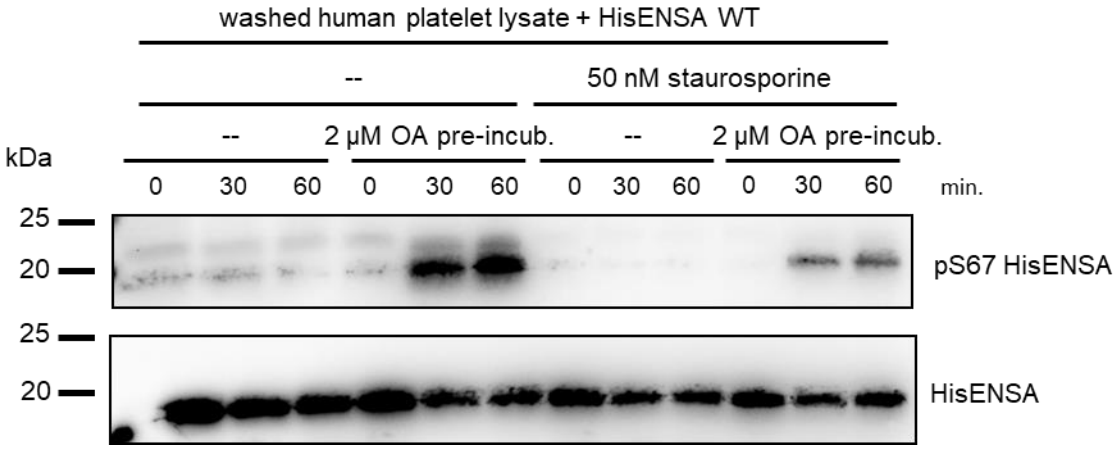

Figure 39: Reduced OA-induced pS67 ENSA kinase activity in human platelet lysate upon staurosporine (50 nM) treatment.
Anti-ENSA antibody (Cell Signaling®) was used 1:500 in 5% (w/v) BSA-TBST; anti-pS67 ENSA antibody (Cell Signaling®) was used 1:250 in 5% (w/v) BSA-TBST.

OA-induced phosphorylation of recombinant S67 HisENSA in lysates of human platelets was diminished by the treatment with 50 nM of staurosporine in a time dependent manner despite constant HisENSA protein content per sample (Figure 39). These data indicate that the kinase (or a related activating kinase) is sensitive to 50 nM of staurosporine, seen as reduced kinase activity. Kinases that are sensitive to small amounts of staurosporine are PKC ((IC_{50}=3 nM), cAMP-dependent kinases like PKA/PKG (IC_{50}=8 nM)[120], MINK1 (IC_{50} = 0.49 nM)[143], KS6A3 (IC_{50} = 0.5 nM) and STK38L/NDR2 (K_D = 28 nM)[144]. STK38/NDR1 kinase is inhibited by concentrations of staurosporine higher than 50 nM.[144]

To obtain further insights concerning the unknown ENSA S67 protein kinase of human platelets, we performed a pilot protein kinase screen by a protein kinase biotech company (‘Reaction Biology Corporation’, Malverne, Pennsylvania, USA), using a small peptide mimicking the phosphorylation site of S67 of ENSA. A peptide with a S67A exchange served as negative control. Both peptides were solved in water to a concentration of 1 mM.

S67 peptide: RLQKGQKYFDSGDYNMAKAKMK

S67A peptide: RLQKGQKYFDAGDYNMAKAKMK

A standard peptide, called Reaction Biology Corporation (RBC) standard substrate, was used for each protein kinase tested as positive control.

The company measured the phosphorylation of the two peptides in the presence of a kinase and, as positive control, a standard peptide (RBC standard substrate for a given protein kinase). This method was based on radioisotope labeling with ^{32}P-γ-ATP or ^{33}P-γ-ATP called filtration binding assay as the radiolabeled products were finally bound to filters.[145] First, ten kinases (AKT1, GRK1, LATS1, MINK/MINK1, MRCKa/CDC42BPA, PKA, PKCa, ROCK1, RSK1, SGK1) were tested as selected candidates, as they are all staurosporine-sensitive kinases. Only the LATS1 kinase showed some phosphorylation activity of the S67 peptide (data not shown). But LATS1 was not found in human platelets in our proteomic study.

In a second experiment, two kinases belonging to the same family as LATS1, STK38/NDR1 and STK38L/NDR2, were tested in comparison to PKA for the phosphorylation of the two peptides (plus positive control (RBC substrate); plus protein kinase (enzyme) alone as negative control) in three independent experiments. The results are shown in the following figures.

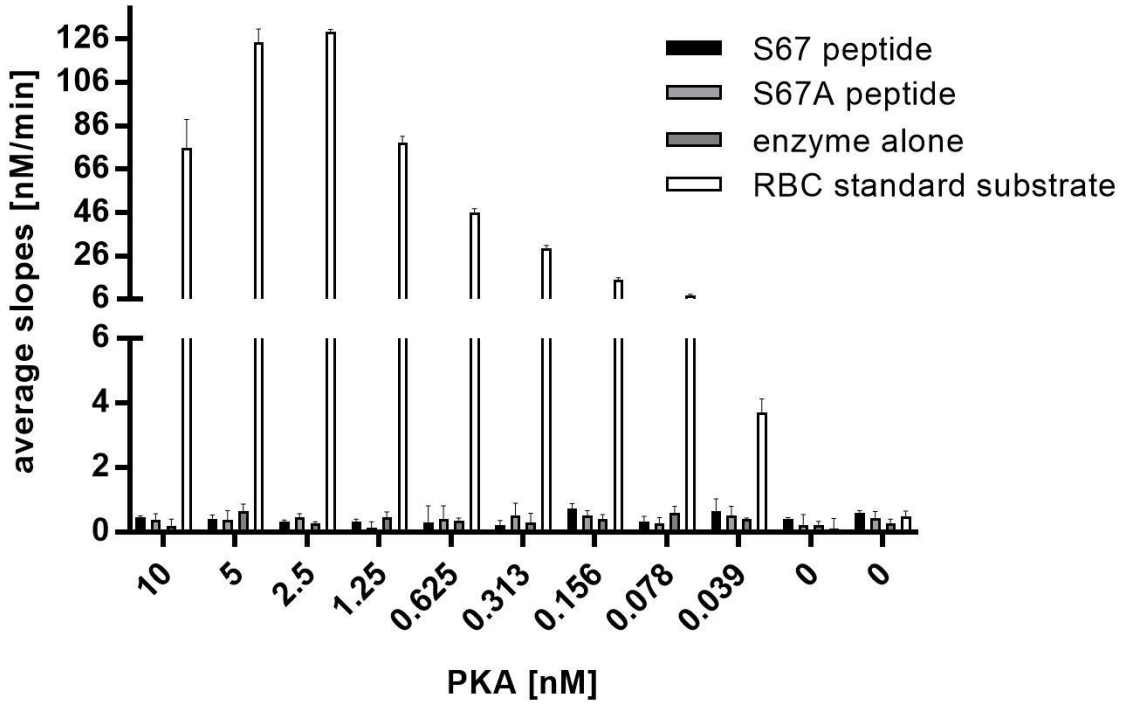

Figure 40: PKA does not phosphorylate the ENSA related S67 peptide.
The used PKA kinase is active as shown with the positive control 'RBC standard substrate'. The shown values are mean values (± SD) of three independent experiments. RBC: reaction biology corporation

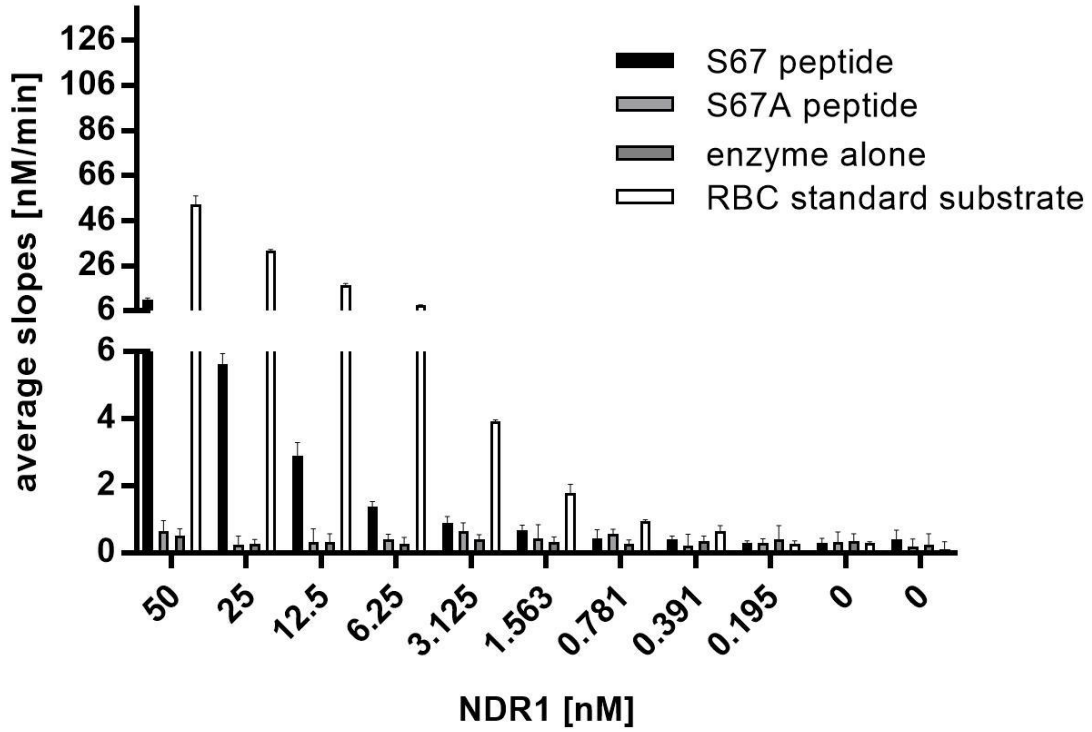

Figure 41: NDR1 (STK38) phosphorylates moderately the ENSA related S67 peptide.
The used NDR1 kinase is active as shown with the positive control 'RBC standard substrate'. It does not phosphorylate the S67A peptide (negative control). The shown values are mean values (± SD) of three independent experiments. RBC: reaction biology corporation

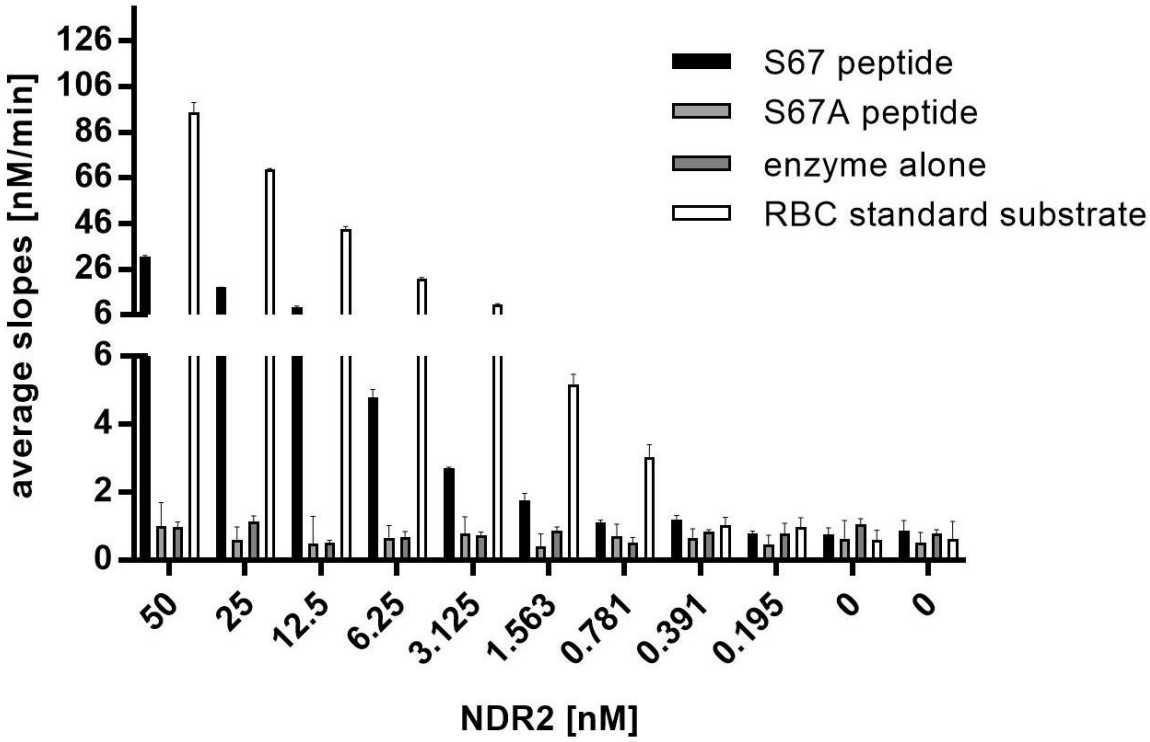

Figure 42: NDR2 (STK38L) phosphorylates strongly the ENSA related S67 peptide.
The used NDR2 kinase is active as shown with the positive control 'RBC standard substrate'. It does not phosphorylate the S67A peptide (negative control). The phosphorylation is stronger than the one of NDR1. The shown values are mean values (± SD) of three independent experiments. RBC: reaction biology corporation

The average slopes (nM/min) represent the kinase activity towards the peptide. The higher the value the stronger the peptide is phosphorylated. As shown in Figure 40, protein kinase A (PKA) did not phosphorylate S67 of the ENSA S67 peptide. PKA only phosphorylated the RBC standard substrate (serving as positive control), as high average slope values were calculated. A phosphorylation of the standard substrate showed that the used kinase is active. The observation that PKA does not phosphorylate S67 ENSA or S62 ARPP19 will also be demonstrated in the following chapter.

The average slope values of NDR1 for the S67 peptide were higher compared to the negative controls S67A peptide and enzyme alone (Figure 41) and also compared to PKA (Figure 40). The RBC substrate was phosphorylated by NDR1 but less than the RBC standard for PKA, indicating a general lower activity of the used NDR1 kinase compared to PKA.

Average slope values of NDR2 (Figure 42) for S67 peptide were higher compared to negative controls for the same kinase and also compared to NDR1 and PKA. The values for the RBC substrate were higher compared to NDR1 pointing to a general higher activity of the NDR2 kinase compared to NDR1.

4.9. Phosphorylation of Dynabeads™-bound HisENSA at S67 in platelet lysate

For the development of a pull-down assay, which enables catching of endogenous platelet ligands to beads with immobilized recombinant and S67 phosphorylated ENSA, the ability of OA-treated platelet lysate was tested for phosphorylation of recombinant wildtype HisENSA

and the recombinant S67A HisENSA mutant bound to magnetic beads. Therefore, Co^{2+}-coupled Dynabeads™ were used to bind specifically the His-tag of the recombinant ENSA proteins (wildtype and S67A mutant).

The HisENSA proteins bound to the Dynabeads™ were incubated in platelet lysate in the presence of OA (and thio-ATP) to yield kinase activity for ENSA S67 phosphorylation. The experimental procedure is described in detail in 3.4.10.

Figure 43 shows that after coupling to the beads, some protein still remained in the supernatant (called 'supernatant'). pS67 of wildtype HisENSA was present after 100 min. of incubation with platelet lysate, after the incubation time of 100 min., no protein was present in the supernatant. The elution of HisENSA protein was successful, but high amounts of protein also remained on the beads.

The HisENSA protein bound to beads was well phosphorylated at S67 compared to the unbound protein in other experiments (e.g. Figure 35). The beads did not sterically block the S67 phosphorylation in platelet lysate. The S67A mutant bound as well to the beads but was not phosphorylated, as expected.

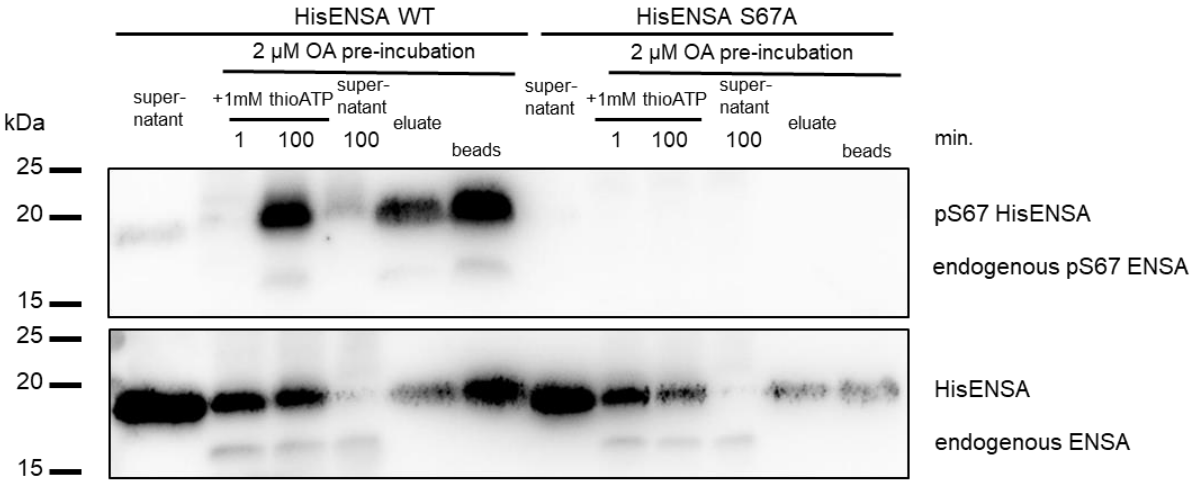

Figure 43: Phosphorylation of HisENSA bound to Dynabeads in human platelet lysate.
Anti-ENSA antibody (Cell Signaling®) was used 1:500 in 5% (w/v) BSA-TBST; anti-pS67 ENSA antibody (Cell Signaling®) was used 1:250 in 5% (w/v) BSA-TBST. The western blots are representative for n>3 independent experiments, all showing similar results.

The elution of coupled HisENSA was more complicated, pointing to a strong interaction of HisENSA with the Co^{2+}-ions and maybe improper elution conditions. 10xPP2A reaction buffer with 500 mM imidazole was used as elution buffer. For HisENSA protein purification with HisTrap columns in 3.5.5., 500 mM imidazole were sufficient to elute the proteins. Higher concentrations than 500 mM of imidazole are not recommended for His-tagged protein elution.

The HisENSA protein eluted from the Dynabeads™ contained free phosphate. It was planned to test these phosphorylated proteins in a PP2A activity assay, measuring free phosphate as PP2A activity. Therefore, high concentrations of free phosphate disturbed the experiment and the pS67 HisENSA protein could not be used for further experiments.

Thus, for the PP2A assay, recombinant HisENSA and also recombinant GST-ARPP19 were phosphorylated with recombinant active MASTL kinase as described in the following chapters.

4.10. Recombinant MASTL and PKA/PKG-mediated phosphorylation of recombinant HisENSA at S67 and S109

Recombinant HisENSA protein was phosphorylated with recombinant MASTL kinase, PKA and PKG, to investigate the different phosphorylation sites of HisENSA in more detail. A phostag based SDS-PAGE assay was established to analyze the efficiency (stoichiometry) of the phosphorylation for the distinct sites. The phosphorylated proteins were used in further experiments, for example for the PP2A activity assay (3.4.8. and 4.12.2.).

First, only one site of HisENSA was phosphorylated with MASTL, PKA or PKG (Figure 44; Figure 1); the reaction was started by adding ATP, samples were taken after 5, 10 and 20 minutes. Then, both phosphorylation sites of HisENSA were phosphorylated consecutively or simultaneously with MASTL and PKG (Figure 45; Figure 46). MASTL and PKA were used for consecutive and simultaneous phosphorylation of HisENSA (Figure 47, Figure 48). As negative control, the mutant S67A was used.

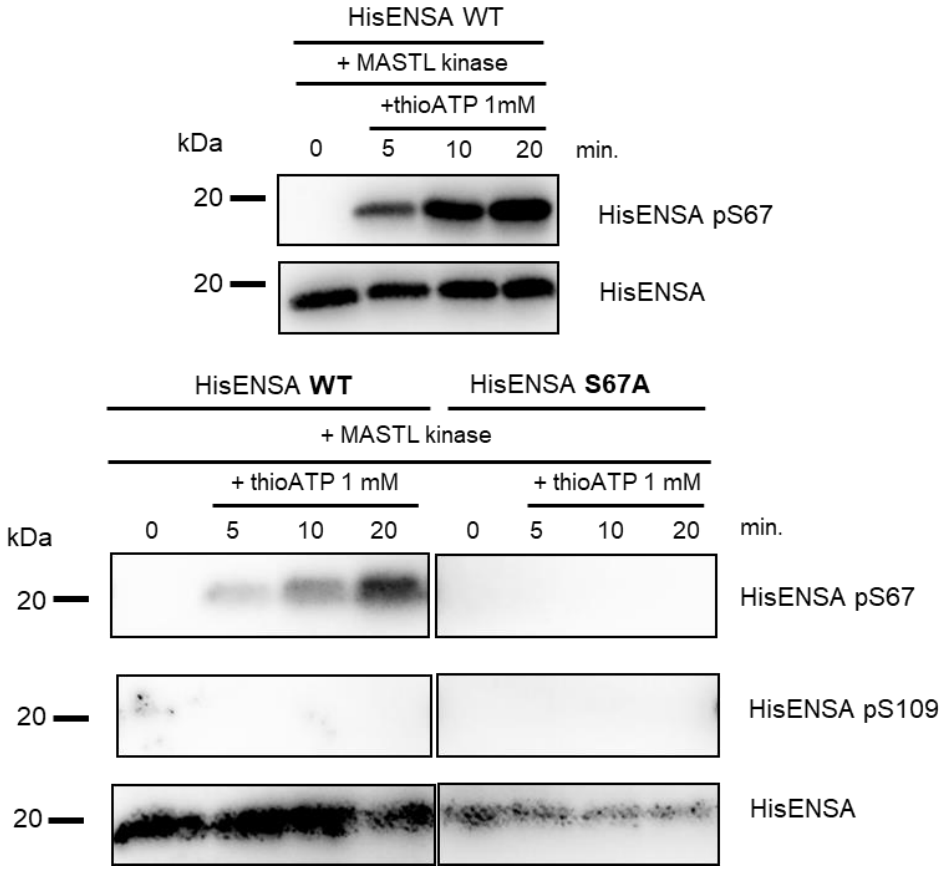

Figure 44: Recombinant MASTL-kinase phosphorylates wildtype HisENSA at S67 but not at S109. HisENSA protein was phosphorylated in the presence of MASTL and 1 mM thio-ATP. The anti-ENSA antibody (Cell Signaling®) was used 1:500 in 5% (w/v) BSA-TBST for ENSA detection; anti-pS67 ENSA/pS62 ARPP19 antibody (Cell Signaling®) was used 1:500 in 5% (w/v) BSA-TBST; anti-pS109 PAN ENSA antibody (ImmunoGlobe®) was used 1 µg/mL in 5% (w/v) BSA-TBST. The western blots are representative for n=3 independent experiments, all showing similar results.

MASTL kinase phosphorylated HisENSA at S67 in a time dependent manner. The second phosphorylation site S109 was not phosphorylated by the MASTL kinase (Figure 44, Figure 45). The general anti-ENSA antibody from Cell Signaling® did not show clear bands for HisENSA, when the protein was already stored a longer time at 4°C (as seen above). The change of the acrylamide percentage of the gel from 13 to 14% and the usage of another

antibody (G153 serum, produced for the detection of general ARPP19) improved the general ENSA signal also of the protein when long-term stored (Figure 46, Figure 47, Figure 48). The Cell Signaling® anti-ENSA antibody detects the C-terminal region of the ENSA protein. Less clearly detected bands could be due to a change in the C-terminal region of the HisENSA protein upon storage conditions and therefore due to a weaker binding of the antibody to the protein.

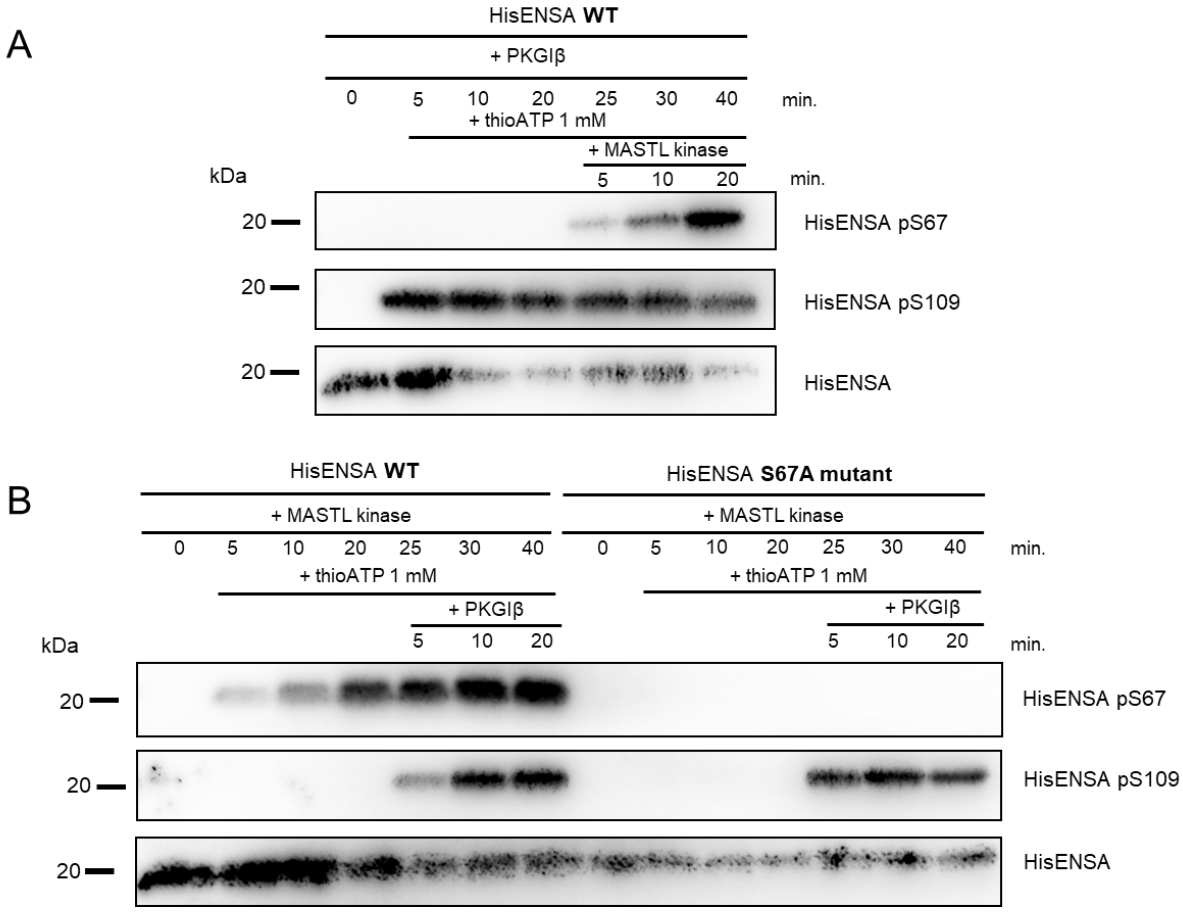

Figure 45: MASTL and PKG phosphorylate HisENSA at S67 and S109, respectively, independent of the presence of the other phosphorylated site.
HisENSA proteins (WT and S67A) were phosphorylated in the presence of MASTL, PKGIβ and 1 mM thio-ATP (and 5 µM cGMP for PKG). The anti-ENSA antibody (Cell Signaling®) was used 1:500 in 5% (w/v) BSA-TBST for ENSA detection; anti-pS67 ENSA/pS62 ARPP19 antibody (Cell Signaling®) was used 1:500 in 5% (w/v) BSA-TBST; anti- pS109 PAN ENSA antibody (ImmunoGlobe®) was used 1 µg/mL in 5% (w/v) BSA-TBST. The western blots are representative for n=3 independent experiments, all showing similar results.

MASTL and PKG phosphorylated the HisENSA proteins site-specifically (Figure 45). The S67A mutant was only phosphorylated at S109.

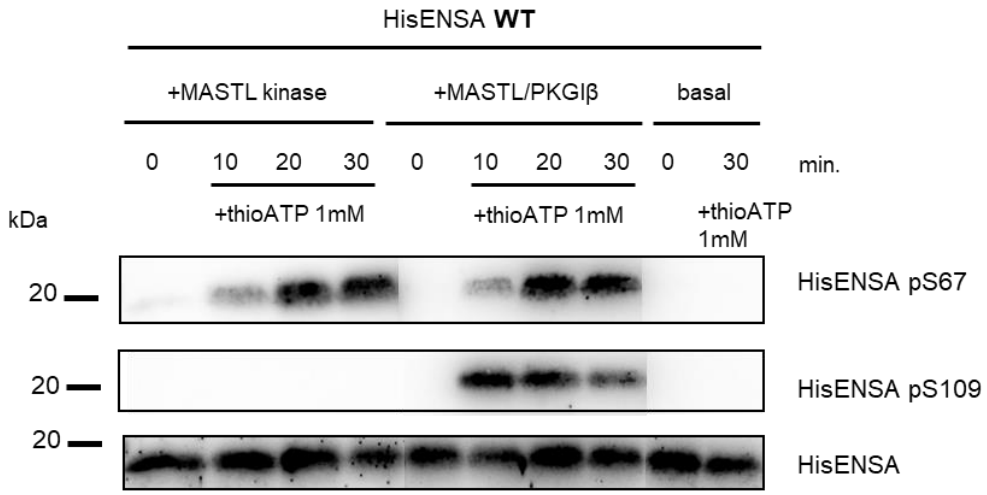

Figure 46: MASTL kinase and PKG phosphorylate HisENSA simultaneous at S67 and S109, respectively.
HisENSA protein was phosphorylated in the presence of MASTL and/or PKGIβ and 1 mM thio-ATP (and 5 µM cGMP for PKG). The G153 serum antibody, directed against ARPP19 but also working for ENSA, was used 1:2000 in 5% (w/v) BSA-TBST for ENSA and ARPP19 detection; anti-pS67 ENSA/pS62 ARPP19 antibody (Cell Signaling®) was used 1:500 in 5% (w/v) BSA-TBST; anti-pS109 PAN ENSA antibody (ImmunoGlobe®) was used 1 µg/mL in 5% (w/v) BSA-TBST. The western blots are representative for n=3 independent experiments, all showing similar results.

MASTL kinase and PKG phosphorylated the HisENSA wildtype (WT) protein simultaneously at both phosphorylation sites, indicating that both phosphorylation sites are accessible independent of phosphorylation of the other site (Figure 46).

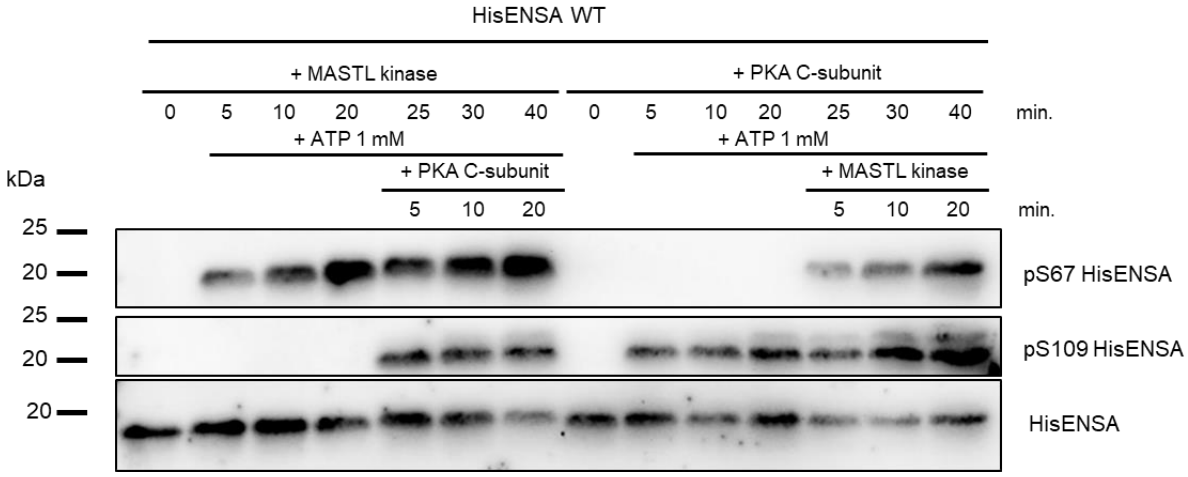

Figure 47: MASTL and PKA phosphorylate HisENSA at S67 and S109, respectively, independent of the presence of the other phosphorylated site.
HisENSA protein was phosphorylated in the presence of MASTL and C-subunit of PKA and 1 mM thio-ATP. The G153 serum antibody, directed against ARPP19 but also working for ENSA, was used 1:2000 in 5% (w/v) BSA-TBST for ENSA and ARPP19 detection; anti-pS67 ENSA/pS62 ARPP19 antibody (Cell Signaling®) was used 1:500 in 5% (w/v) BSA-TBST; anti-pS109 PAN ENSA antibody (ImmunoGlobe®) was used 1 µg/mL in 5% (w/v) BSA-TBST. The western blots are representative for n=3 independent experiments, all showing similar results.

MASTL and PKA phosphorylated the HisENSA proteins site-specifically. The order of kinase addition did not influence the site-specific phosphorylation. PKA phosphorylation at S109 led to the appearance of two bands (Figure 47). The second band could not be identified so far.

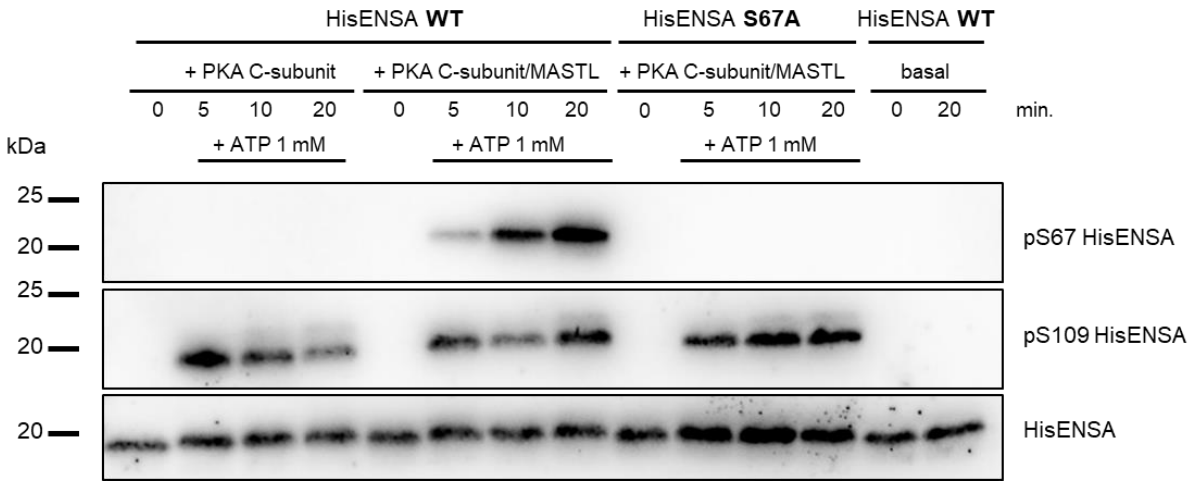

Figure 48: MASTL kinase and PKA phosphorylate HisENSA simultaneously at S67 and S109, respectively.
HisENSA proteins (WT and S67A) were phosphorylated in the presence of MASTL and/or C-subunit of PKA and 1 mM thio-ATP. S67A mutant was only phosphorylated at S109. The G153 serum antibody, directed against ARPP19 but also working for ENSA, was used 1:2000 in 5% (w/v) BSA-TBST for ENSA and ARPP19 detection; anti-pS67 ENSA/pS62 ARPP19 antibody (Cell Signaling®) was used 1:500 in 5% (w/v) BSA-TBST; anti-pS109 PAN ENSA antibody (ImmunoGlobe®) was used 1 µg/mL in 5% (w/v) BSA-TBST. The western blots are representative for n=3 independent experiments, all showing similar results.

MASTL kinase and PKA phosphorylated the HisENSA wildtype (WT) protein simultaneously at both phosphorylation sites (Figure 48), suggesting that phosphorylation sites are accessible independent of phosphorylation of the other site (similar as MASTL and PKG phosphorylation). PKA phosphorylated the S67A HisENSA mutant only at S109, leading to two bands as also observed for wildtype ENSA.

The established phostag-based SDS-PAGE was applied to the phosphorylated HisENSA samples to analyze the efficiency of the phosphorylation of proteins, but the separation of differentially phosphorylated proteins did not work for His-tagged ENSA. This could be due to the histidine-tag of the protein, as histidine residues interact with cations and the phostag SDS-PAGE works with Zn^{2+}-ions.

4.11. Recombinant MASTL and PKA/PKG-mediated phosphorylation of recombinant wildtype GST-ARPP19 at S62 and S104

In our phosphoproteomic analysis of human platelets ARPP19 was phosphorylated in a similar manner as ENSA. Therefore, corresponding phosphorylation experiments were performed for recombinant GST-ARPP19 as performed for HisENSA. The phostag-based SDS-PAGE assay was also established to investigate GST-ARPP19 stoichiometric phosphorylation. The phosphorylated protein was used in further experiments (for example the PP2A activity assay (3.4.8. and 4.12.2.)).

First, only one site of GST-ARPP19 was phosphorylated with MASTL, PKA or PKG (Figure 49); reaction was started by adding ATP, samples were taken after 5, 10 and 20 minutes for kinase phosphorylation detection.

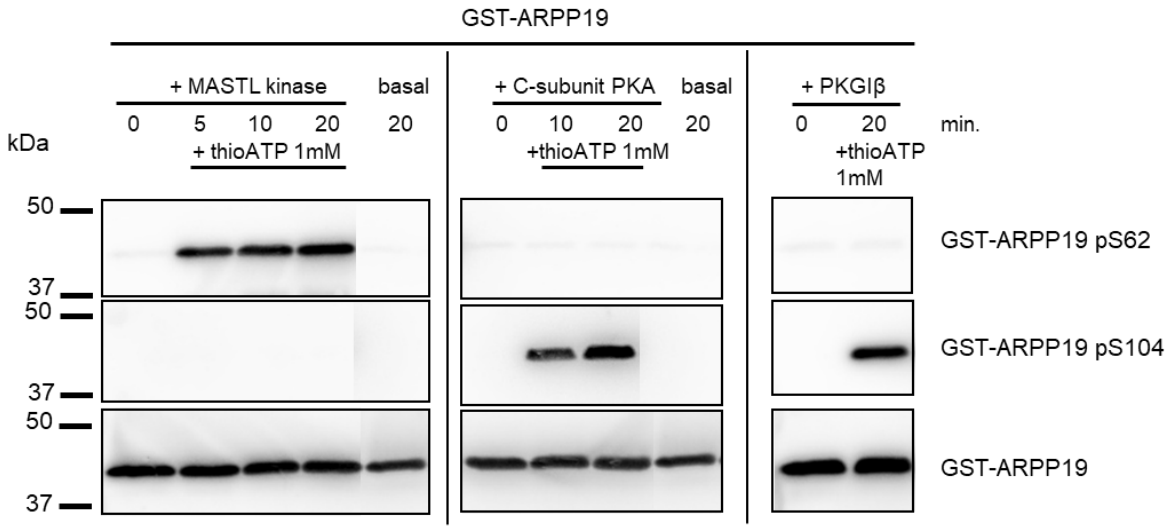

Figure 49: Recombinant MASTL-kinase phosphorylates wildtype GST-ARPP19 at S62 but not at S104, recombinant PKA and PKG phosphorylate wildtype GST-ARPP19 at S104 but not at S62. GST-ARPP19 protein was phosphorylated in the presence of MASTL, C-subunit of PKA or PKGIβ and 1 mM thio-ATP (and 5 µM cGMP for PKG). For ARPP19 signal, the G153 serum antibody, directed against ARPP19, was used 1:2000 in 5% (w/v) BSA-TBST, anti-pS67 ENSA/pS62 ARPP19 antibody (Cell Signaling®) was used 1:500 in 5% (w/v) BSA-TBST for pS104 the anti-pS109 PAN ENSA antibody (ImmunoGlobe®) was used 1 µg/mL in 5% (w/v) BSA-TBST. The western blots are representative for n=3 independent experiments.

Figure 49 shows, similar to the HisENSA phosphorylation experiment, that the MASTL kinase/PKA C-subunit or PKGIβ phosphorylated GST-ARPP19 at S62/S104 in a time dependent manner. The second phosphorylation site (S62 or S104) was not phosphorylated by PKA/PKG or the MASTL kinase, respectively.

GST-ARPP19 was phosphorylated consecutively first with MASTL and PKGIβ (Figure 50) and then with MASTL and PKA C-subunit (Figure 51). For both experiments, ARPP19 phosphorylation was analyzed using the phostag-based SDS-PAGE assay.

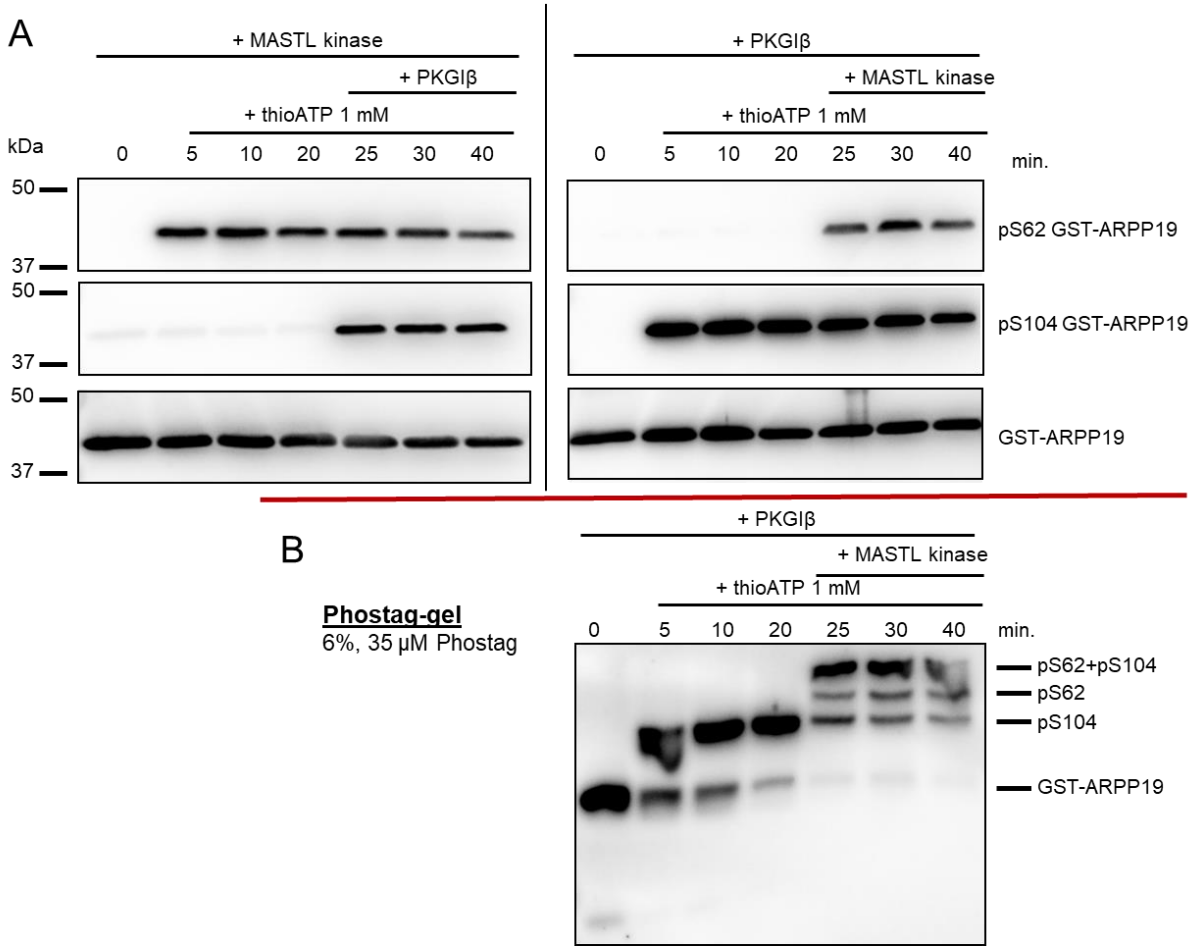

Figure 50: MASTL and PKG phosphorylate GST-ARPP19 at S62 and S104, respectively, independent of the presence of the other phosphorylated site.
A: standard SDS-PAGE and western blot. B: Phostag gel (6% (v/v) acrylamide including 35 µM phostag), separating the proteins by their number of phosphorylated sites. GST-ARPP19 protein was phosphorylated in the presence of MASTL, PKGIβ and 1 mM thio-ATP (and 5 µM cGMP for PKG). For ARPP19 signal, the G153 serum antibody, directed against ARPP19, was used 1:2000 in 5% (w/v) BSA-TBST, anti-pS67 ENSA/pS62 ARPP19 antibody (Cell Signaling®) was used 1:500 in 5% (w/v) BSA-TBST for pS104 the anti-pS109 PAN ENSA antibody (ImmunoGlobe®) was used 1 µg/mL in 5% (w/v) BSA-TBST. The western blots are representative for n=3 independent experiments. For phostag, the G153 antibody was used.

MASTL and PKG phosphorylated the GST-ARPP19 protein site-specifically (Figure 50). The phostag-based SDS-PAGE revealed a high efficiency of the phosphorylation reaction of ARPP19 with PKGIβ and the MASTL kinase (Figure 50 B). After the addition of the second kinase MASTL, three bands appeared in the phostag-gel. Based on our phostag-gel studies, it is very likely that the highest band reflects the doubled phosphorylated protein, the other two bands single phosphorylated protein on two different phosphorylation sites.

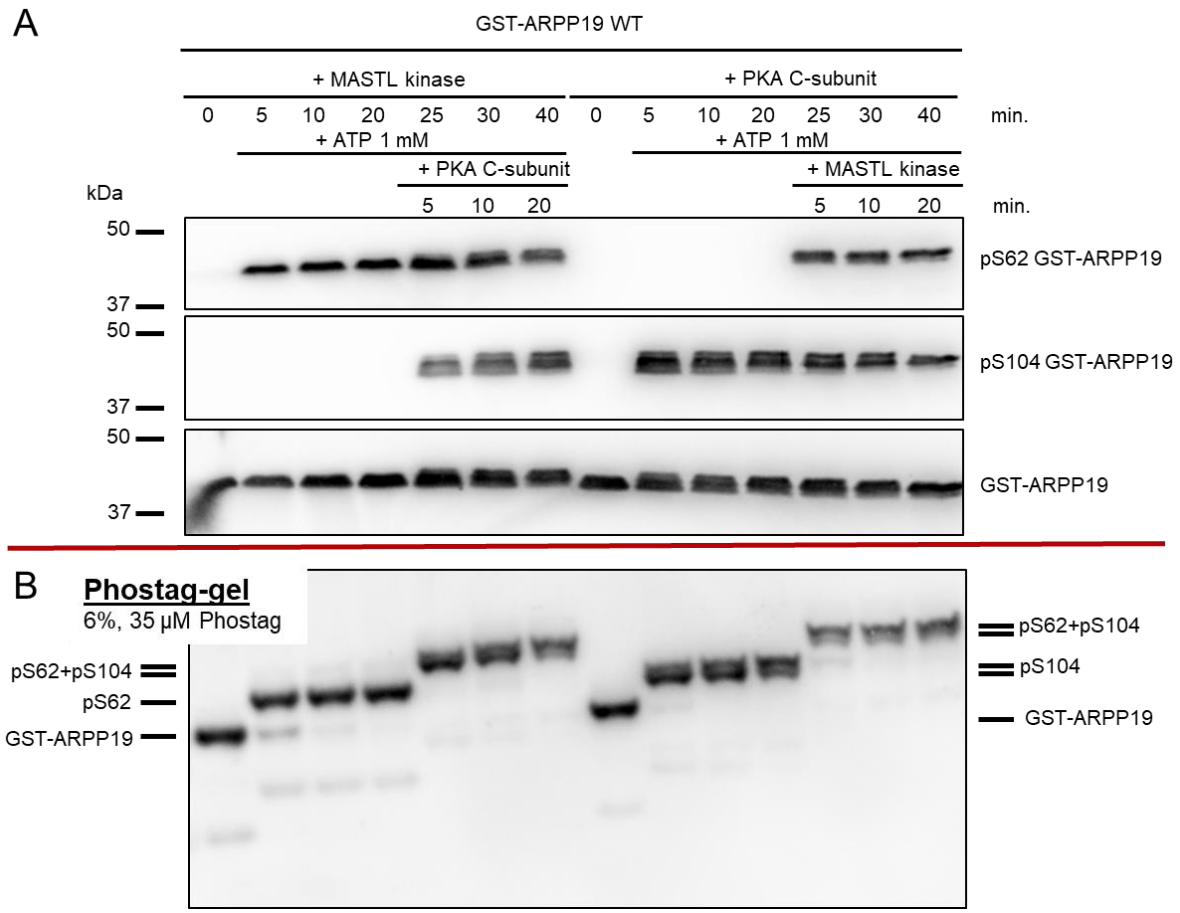

Figure 51: MASTL and PKA phosphorylate GST-ARPP19 at S62 and S104, respectively, independent of the presence of the other phosphorylated site.
A: standard SDS-PAGE and western blot. B: Phostag gel (6% (v/v) acrylamide including 35 µM phostag), separating the proteins by their number of phosphorylated sites. GST-ARPP19 protein was phosphorylated in the presence of MASTL, PKA C-subunit and 1 mM thio-ATP. For general ARPP19 signal, the G153 serum antibody, directed against ARPP19, was used 1:2000 in 5% (w/v) BSA-TBST, anti-pS67 ENSA/pS62 ARPP19 antibody (Cell Signaling®) was used 1:500 in 5% (w/v) BSA-TBST for pS104 the anti-pS109 PAN ENSA antibody (ImmunoGlobe®) was used 1 µg/mL in 5% (w/v) BSA-TBST. The western blots are representative for n=3 independent experiments. For phostag, the G153 antibody was used.

MASTL and PKA phosphorylated the GST-ARPP19 protein in a site-specific manner (Figure 51). The phostag-based SDS-PAGE revealed a high efficiency of the phosphorylation reaction of ARPP19 with PKA and the MASTL kinase (Figure 51 B). No unphosphorylated protein remained after kinase addition. The addition of PKA C-subunit led to the appearance of two bands of pS104 GST-ARPP19 in normal SDS-PAGE and also in the phostag SDS-PAGE. The phosphorylation of ARPP19 on S62 only led to a single band or a single shift in phostag SDS-PAGE. After addition of the second kinase (MASTL or PKA C-subunit), a higher band appeared, reflecting double-phosphorylated GST-ARPP19 (pS62 and pS104).

In the following part (Figure 52, Figure 53), GST-ARPP19 was phosphorylated by MASTL kinase and PKA C-subunit/PKGIβ simultaneously on both phosphorylation sites (S62, S104).

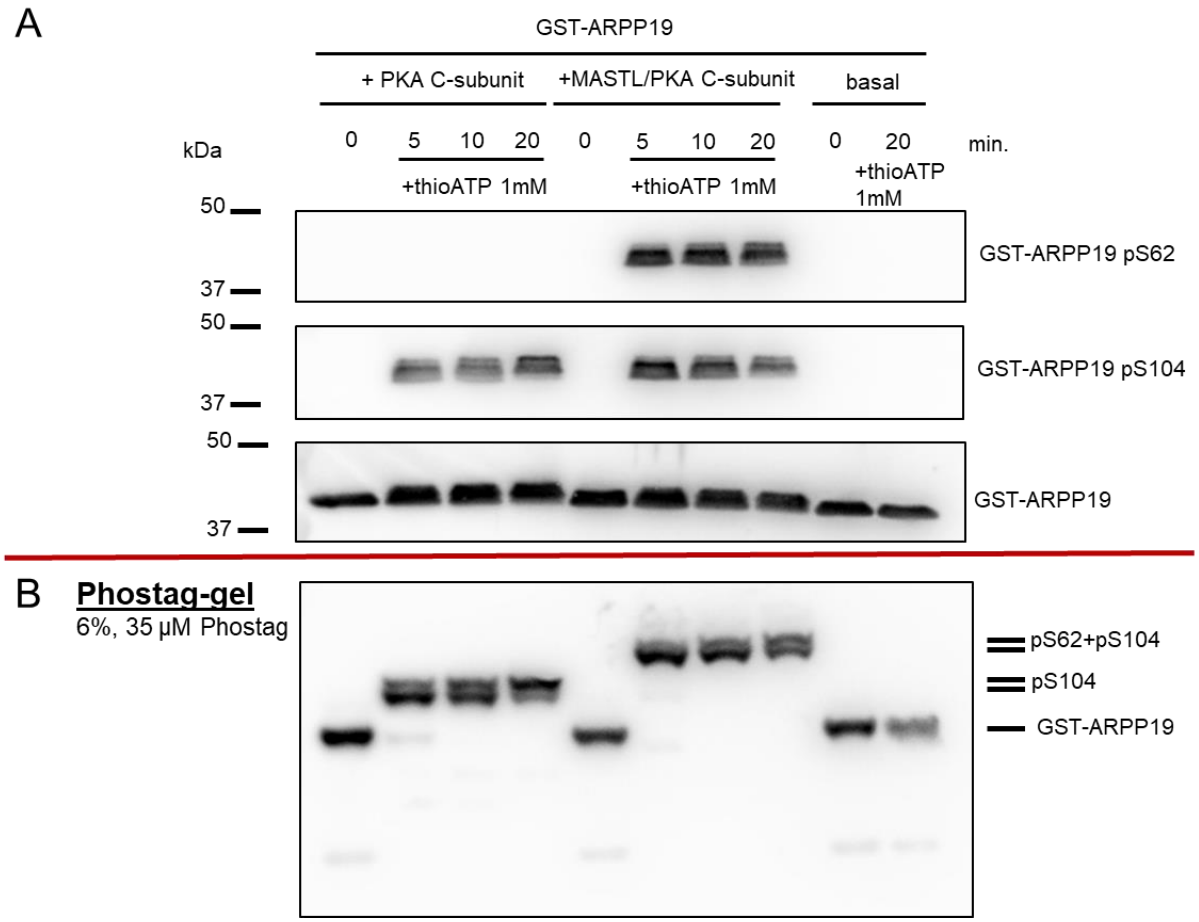

Figure 52: MASTL kinase and PKA phosphorylate GST-ARPP19 simultaneously at S62 and S104, respectively.
A: standard SDS-PAGE and western blot. B: Phostag gel (6% (v/v) acrylamide including 35 µM phostag), separating the proteins by their number of phosphorylated sites. GST-ARPP19 protein was phosphorylated in the presence of MASTL, PKA C-subunit and 1 mM thio-ATP. For ARPP19 signal, the G153 serum antibody, directed against ARPP19, was used 1:2000 in 5% (w/v) BSA-TBST, anti-pS67 ENSA/pS62 ARPP19 antibody (Cell Signaling®) was used 1:500 in 5% (w/v) BSA-TBST for pS104 the anti-pS109 PAN ENSA antibody (ImmunoGlobe®) was used 1 µg/mL in 5% (w/v) BSA-TBST. The western blots are representative for n=3 independent experiments. For phostag, the G153 antibody was used.

MASTL kinase and PKA phosphorylated the GST-ARPP19 protein simultaneously at both phosphorylation sites, showing the accessibility of both sites independent of the phosphorylation of the other site (Figure 52). The phostag based SDS-PAGE revealed a high efficiency of the simultaneous phosphorylation reaction of ARPP19 with PKA and the MASTL kinase (Figure 52 B), showing no unphosphorylated protein band after kinase addition. Only two close bands appear for the double-phosphorylated ARPP19 protein (at S62 and 104). The second band that appeared is likely to be related to PKA C-subunit phosphorylation.

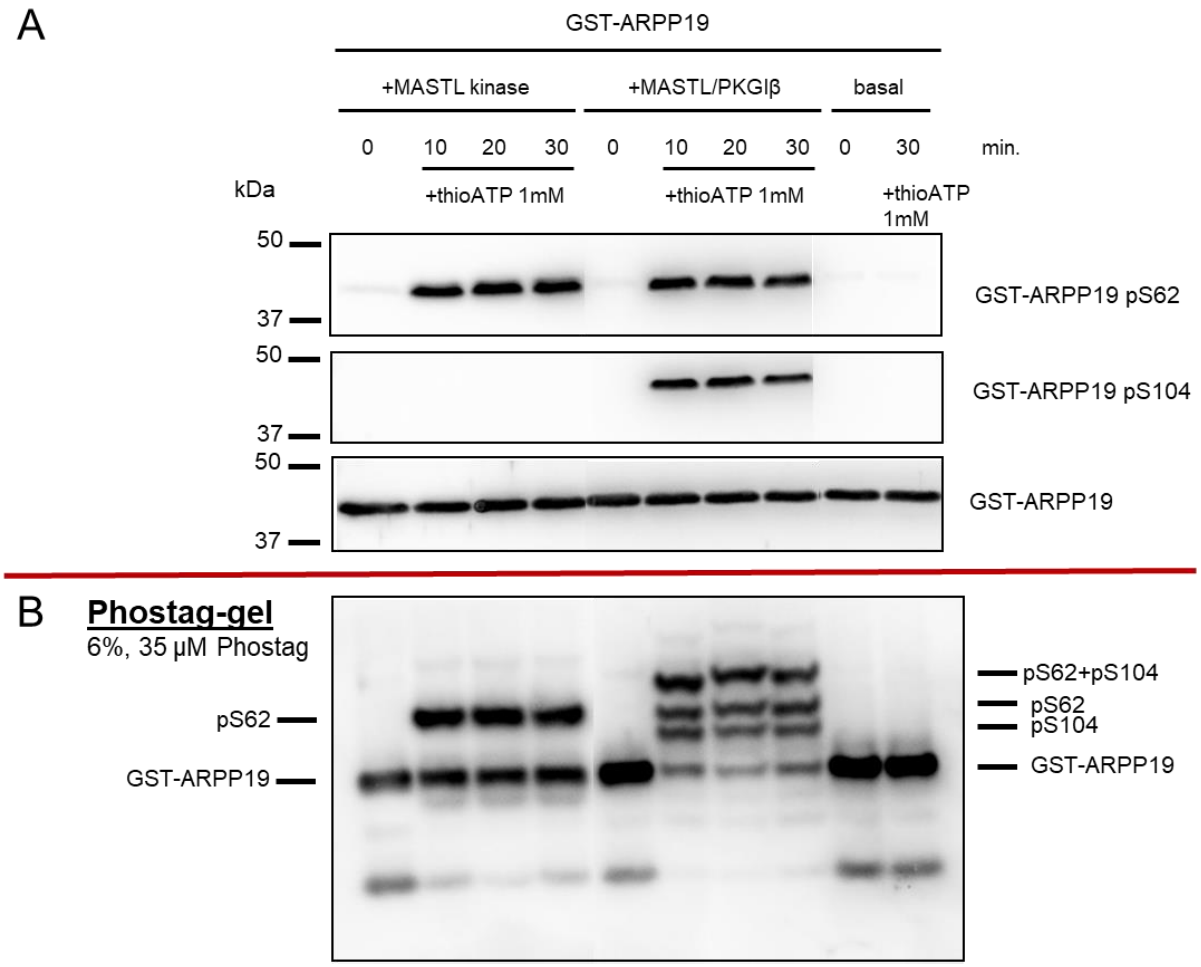

Figure 53: MASTL kinase and PKG phosphorylate GST-ARPP19 simultaneously at S62 and S104, respectively.
A: standard SDS-PAGE and western blot. B: Phostag gel (6% (v/v) acrylamide including 35 µM phostag), separating the proteins by their number of phosphorylated sites. GST-ARPP19 protein was phosphorylated in the presence of MASTL, PKGIβ and 1 mM thio-ATP (and 5 µM cGMP for PKG). For ARPP19 signal, the G153 serum antibody, directed against ARPP19, was used 1:2000 in 5% (w/v) BSA-TBST, anti-pS67 ENSA/pS62 ARPP19 antibody (Cell Signaling®) was used 1:500 in 5% (w/v) BSA-TBST for pS104 the anti-pS109 PAN ENSA antibody (ImmunoGlobe®) was used 1 µg/mL in 5% (w/v) BSA-TBST. The western blots are representative for n=3 independent experiments. For phostag, the G153 antibody was used.

MASTL kinase and PKG phosphorylated the GST-ARPP19 protein simultaneously on both phosphorylation sites, showing the accessibility of both sites independent of the phosphorylation of the other site (Figure 53). The phostag based SDS-PAGE still revealed a high efficiency of the simultaneous phosphorylation reaction of ARPP19 with PKG and the MASTL kinase (Figure 53 B), even though some unphosphorylated protein remained after 30 minutes of incubation. The phosphorylation pattern in phostag SDS-PAGE of MASTL/PKG phosphorylation was similar to Figure 50, with also three different bands upon PKG and MASTL phosphorylation. It is very likely that the three bands reflect single-site phosphorylated ARPP19 (pS62 or pS104) and two-site phosphorylated protein (pS62 and pS104). The single phosphorylated GST-ARPP19 protein maybe appears because the phosphorylation of the first site of ARPP19 blocks the phosphorylation of the second site of the protein.

4.12. Analysis of protein phosphatase 2A in human platelets

4.12.1. Proteomic data

Our proteomic studies of human platelets demonstrated abundant expression of the majority of important PP2A subunits (Table 25). For comparison, copy numbers per platelet are also shown for ENSA, ARPP19 and VASP.

Table 25: Estimated copy numbers per platelet of PP2A subunits, ENSA, ARPP19 and VASP in human and murine (C57BL/6 strain) platelets.

	human platelet PP2A subunits (Burkhart JM et al. Blood 2012)		**murine platelet PP2A subunits (Zeiler M et al. MCP 2014)**
gene	**protein name**	**CN/platelet**	**CN/platelet**
PPP2CA	PP2AA_HUMAN Serine/Threonine-protein phosphatase 2A **catalytic** subunit α isoform (bu)	3,205	9,176
PPP2CB	PP2AA_HUMAN Serine/Threonine-protein phosphatase 2A **catalytic** subunit β isoform (bu)	3,126	779
PPP2R1A	2AAA_HUMAN Serine/Threonine-protein phosphatase 2A 65 kDa regulatory subunit A α isoform **scaffold** (bu)	10,118	16,089
PPP2R1B	2AAA_HUMAN Serine/Threonine-protein phosphatase 2A 65 kDa **regulatory** subunit A β isoform	not detected	787
PPP2R2A	2ABA_HUMAN Serine/Threonine-protein phosphatase 2A 55 kDa **regulatory** subunit B α isoform (bu)	2,214	1,739
PPP2R2D	2ABD_HUMAN Serine/Threonine-protein phosphatase 2A 55 kDa **regulatory** subunit B δ isoform (bu)	1,332	363
PPP2R4	PTPA_HUMAN Serine/Threonine-protein phosphatase 2A activator (bu)	3,995	8,863
PPP2R5A	2A5A_HUMAN Serine/Threonine-protein phosphatase 2A 56 kDa **regulatory** subunit α isoform (bu)	1,578	1,975
PPP2R5B	2A5B_HUMAN Serine/Threonine-protein phosphatase 2A 56 kDa **regulatory** subunit β isoform (bu)	917	101
PPP2R5G	2A5G_HUMAN Serine/Threonine-protein phosphatase 2A 56 kDa **regulatory** subunit γ isoform (bu)	1,408	2,955
PPP2R5D	2A5D_HUMAN Serine/Threonine-protein phosphatase 2A 56 kDa **regulatory** subunit δ isoform (bu)	1,294	631
PPP2R5E	2A5E_HUMAN Serine/Threonine-protein phosphatase 2A 56 kDa **regulatory** subunit ε isoform (bu)	1,725	1,240
ENSA	ENSA_HUMAN α-endosulfine	7,800	1,241
ARPP19	ARPP19_HUMAN cAMP-regulated phosphoprotein 19	2,500	1,364
VASP	VASP_HUMAN Vasodilator-stimulated phosphoprotein	44,600	36,153

CN: copy number

Proteomic analysis of platelets from C57BL/6 mice demonstrated the expression of the same PP2A subunits as identified in human platelets as well as of ENSA and ARPP19 (Table 24).[138] So far, there are no PP2A functional data in murine platelets.

4.12.2. Establishment of a PP2A-optimized serine/threonine-phosphatase assay for the quantification of PP2A activity in human platelet lysates

To investigate, if HisENSA or GST-ARPP19 are able to influence platelet PP2A activity, when they are phosphorylated at S67 or S62, I used the commercially available, non-radioactive serine/threonine protein phosphatase assay and established the assay in our lab for platelet lysates. Depending on the chosen buffer, this assay is optimized for PP2A, PP2B or PP2C. However, it cannot be excluded that activities of PP5 and PP6, phosphatases that are also present in human platelets, are also detected by this assay. The provided phosphopeptide served as a substrate of PP2A, PP2B or PP2C, but not of protein phosphatase 1 (PP1).

Platelet lysates were generated and free phosphate was removed as described in 3.4.5. and 3.4.6. PP2A activity was measured and quantified as described in 3.4.8. When phosphorylated recombinant proteins were used to investigate their potential to inhibit platelet PP2A activity in the platelet lysate, they were pipetted in the well, together with the peptide and 5xPP2A reaction buffer before platelet lysate was added. Each experiment was done at least three times. The platelet concentration used for the assay was $1*10^8$ platelets/mL (generated platelet lysate was diluted 1:20 with extraction buffer).

To validate that the assay reflects serine/threonine-phosphatase activity by PP2A and not by PP1, the three inhibitors for PP1 or PP2A, okadaic acid, fostriecin and tautomycetin were used. Depending on the concentration, the inhibitors are specific for only PP2A or PP1 inhibition.

OA was tested first. In very low concentrations (reported IC_{50} = 0.1-0.3 nM)[72], only PP2A is inhibited by OA (IC_{50} of OA for PP1 is 20-50 nM).[72]

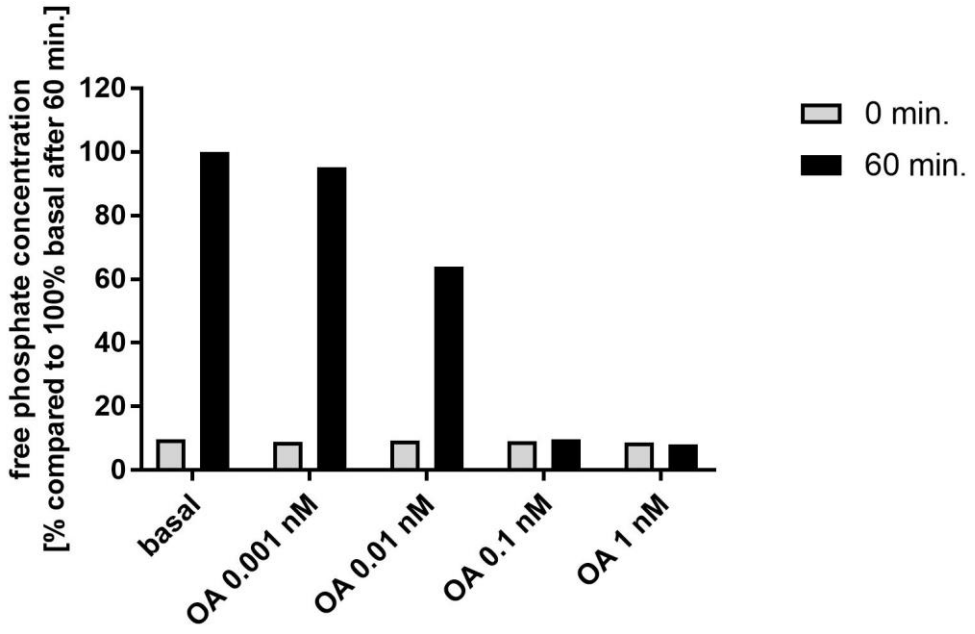

Figure 54: PP2A activity is reduced by OA in a dose dependent manner.
PP2A activity in lysates of human platelets after 0 or 60 min under basal conditions or in the presence of OA (different concentrations). 0.1 nM and 1 nM of OA inhibited PP2A activity completely in platelet lysate. Data are expressed as percentage of free phosphate concentration compared to 100% basal free phosphate concentration after 60 min. Data are shown as mean of technical triplicates and are representative for three independent experiments.

The inhibitory effect of OA on PP2A in platelet lysate was very strong (reported IC_{50}=0.1-0.3 nM).[72] 0.1 nM of OA was sufficient to inhibit completely PP2A in $1*10^8$ platelets/mL after 60 minutes without any pre-incubation in intact human platelets. The IC_{50} of OA for PP1 is 20-50 nM.[72] As phosphatase activity was already inhibited completely with 0.1 nM of OA, the activity can only be due to PP2A, as PP1 is still active when using 0.1 nM OA.

Fostriecin and tautomycetin were used in different concentrations to further investigate PP2A and PP1 inhibition.

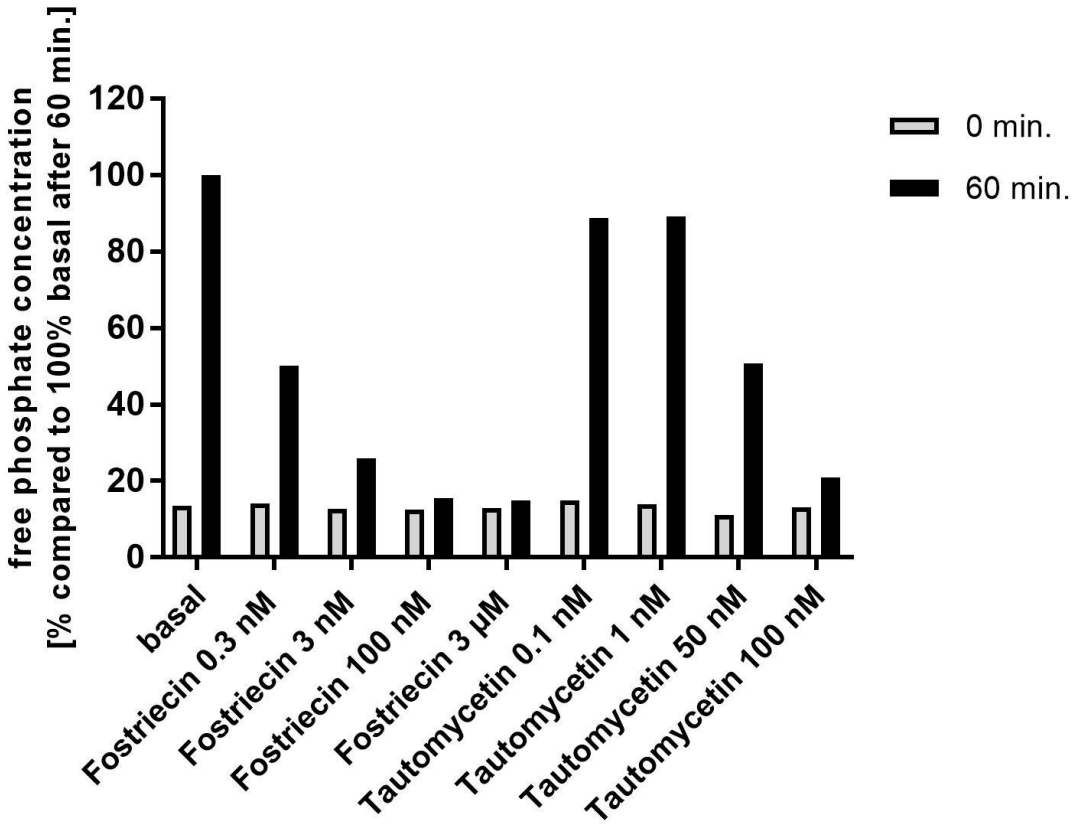

Figure 55: Reduction of PP2A activity by fostriecin and tautomycetin in a dose dependent manner.
PP2A activity in lysates of human platelets after 0 or 60 min under basal conditions or in the presence of fostriecin or tautomycetin (different concentrations). PP2A activity was inhibited completely in platelet lysate with 100 nM and 3 µM fostriecin and also nearly completely with 100 nM of tautomycetin. Data are expressed as percentage of free phosphate concentration compared to 100% basal free phosphate concentration after 60 min. Data are shown as mean of technical triplicates and are representative for three independent experiments.

Low concentrations of fostriecin are inhibiting PP2A activity completely (IC_{50}=1.5 nM)[119], PP1 is only inhibited with high concentrations of fostriecin (IC_{50}=131 µM).[119] Therefore, fostriecin is a very specific inhibitor of PP2A when low concentrations of fostriecin are used. The results in Figure 55 show that the measured phosphatase activity was only inhibited with high concentrations (100 nM and 3 µM) of fostriecin.

The third inhibitor, tautomycetin, is in low concentration specific for PP1 inhibition (IC_{50}=1.6 nM)[121], it inhibits PP2A only when higher concentrations are used ((IC_{50}=62 nM)[121]. The data of Figure 55 show clearly a reduction of measured phosphatase activity for concentrations higher than 50 nM.

All data shown in Figure 55 rule out PP1 activity as the predominantly measured phosphatase activity.

After PP1 was excluded as major acting phosphatase in the S/T-phosphatase activity assay, the measured phosphatase activity is most likely due to PP2A activity (the used buffer excludes PP2B and PP2C). Only PP5 and PP6 activity has to be checked in future experiments.

To investigate the effect of phosphorylated ENSA and ARPP19 on platelet PP2A activity, recombinant pS67 HisENSA and pS62 GST-ARPP19 (phosphorylated with the recombinant MASTL kinase and desalted with Zeba^{TM}spin columns according to 3.5.10. and 3.5.11.) were used in different concentration in the serine/threonine phosphatase activity assay.

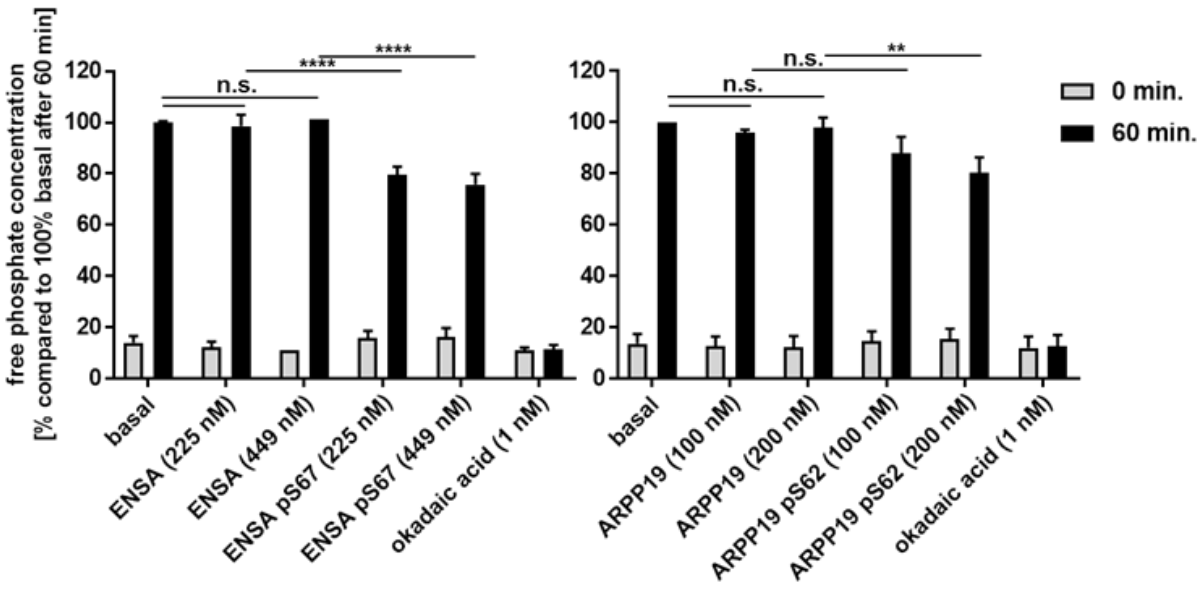

Figure 56: Phosphorylation of ENSA at S67 or ARPP19 at S62 reduces PP2A activity in human platelets.
PP2A activity in lysates of human platelets after 0 and 60 min under basal conditions or in the presence of OA, recombinant HisENSA, HisENSA pS67, recombinant GST-ARPP19 and GST-ARPP19 pS62, respectively, as determined by a PP2A specific *in vitro* Ser/Thr-phosphatase assay. Data are expressed as percentage of free phosphate concentration compared to 100% basal free phosphate concentration after 60 min, mean ± SD of three different experiments. **P<0.01; ****P<0.0001; n.s.: not significant.

Phosphorylated recombinant ENSA at S67 or ARPP19 at S62 inhibited dose-dependently PP2A activity in lysates of human platelets (Figure 56). PP2A activity was reduced up to 20% compared to basal conditions when pS67 ENSA or pS62 ARPP19 were added.

These data indicate that PP2A is active in non-activated human platelets, which leads to dephosphorylation of its own inhibitors ENSA and ARPP19 (when no OA is added).

In chapter 4.7., I showed that PP2A inhibition by OA led to a phosphorylation of recombinant and endogenous ENSA at S67. Now, the PP2A activity assay results show vice versa that pS67 ENSA or pS62 ARPP19 inhibits platelet PP2A activity, which is shown for the first time.

4.13. The effect of low and high doses of the marine toxin okadaic acid (OA) on human platelets

PP2A inhibition by OA led to endogenous ENSA phosphorylation at S67 in human platelets (chapter 4.5., Figure 33) in a dose dependent manner. On the other hand, pS67 ENSA or pS62 ARPP19 led to a reduction of platelet PP2A activity in platelet lysates (chapter 4.12.2., Figure 56). OA, according to the PP2A activity assay, inhibited PP2A in human platelet lysate completely with a concentration of only 0.1 nM (chapter 4.12.2., Figure 54).

To investigate the effect of OA pre-incubated with intact washed human platelets on substrates of PP2A (also platelet activation/inhibition markers), SDS-PAGE/western blot samples of intact washed human platelets incubated with low and high concentrations of OA (200 nM and 10 µM) for 10, 20 and 40 minutes (according to samples of Figure 33 in chapter 4.5.) were analyzed for VASP and p38 MAPK phosphorylation (Figure 57). The incubation of washed human platelets with OA led to a phosphorylation of VASP S239 and also S157 (detected as upper band in the blot) and of the MAP-kinase p38. VASP pS239/pS157 are used as typical marker for platelet inhibition (PKG/PKA activity), p38 phosphorylation is used as a marker of platelet activation. Both proteins are known to be substrates of PP2A.[80, 146] PP2A inhibition led to an increase in p38 and VASP phosphorylation, without any additional stimulus.

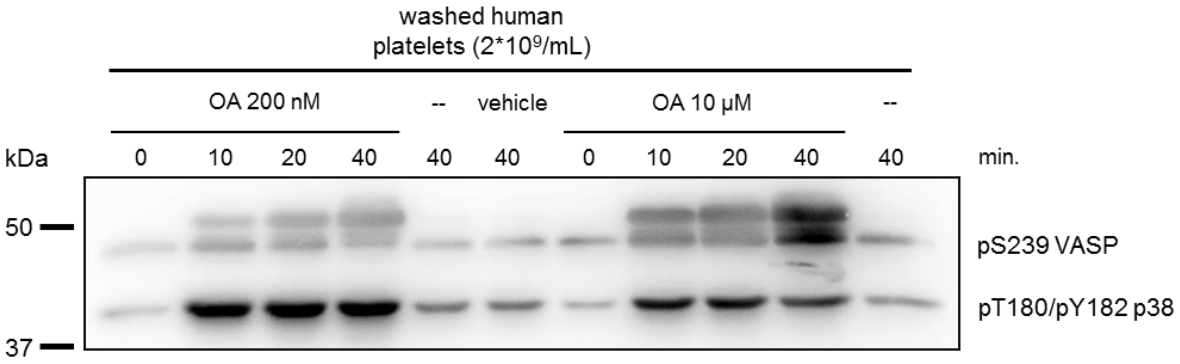

Figure 57: The MAP kinase p38 and VASP at S239/S157 are targets of PP2A in human platelets. Both proteins were phosphorylated when PP2A is inhibited. Anti-pS239 VASP antibody (Cell Signaling®) was used 1:1000 in 5% (w/v) BSA-TBST; anti-pT180/pY182 p38 antibody (Cell Signaling®) was used 1:1000 in 5% (w/v) BSA-TBST.

200 nM OA led to a strong phosphorylation of p38. Upon VASP phosphorylation, two bands appeared according to a PKA phosphorylation of S157 (upper band, 50 kDa) and PKG phosphorylation of S239 (both bands, as the antibody is detecting pS239 VASP).[16, 147] Longer incubation of intact platelets with OA led to a stronger PKA phosphorylation (stronger upper band), suggesting a PP2A effect on VASP S157 dephosphorylation, as already reported by Abel et al. in 1995.[80]

10 µM of OA induced a stronger phosphorylation of VASP on both sites. Higher concentrations of OA induce PP1 inhibition, that can also dephosphorylate VASP.[80] But these effects will be discussed in more detail later.

In the following experiment it was investigated how ENSA S67 phosphorylation in human platelets is related to platelet activation. As 200 nM of OA were sufficient to mediate strong phosphorylation of the PP2A substrates VASP and p38, only low doses (200 nM) OA were used in this experiment.

Washed human platelets were incubated without and with 200 nM of OA for 10 minutes (phosphorylation of PP2A substrates already appeared for a pre-incubation time of 10 min.), then thrombin (0.1 U/mL) was added to activate the platelets. Samples were analyzed before thrombin addition and after 1 and 3 minutes of incubation with thrombin by immunoblotting. 10 minutes of OA pre-incubation led to a detectable phosphorylation of S67 ENSA on the western blot (Figure 58).

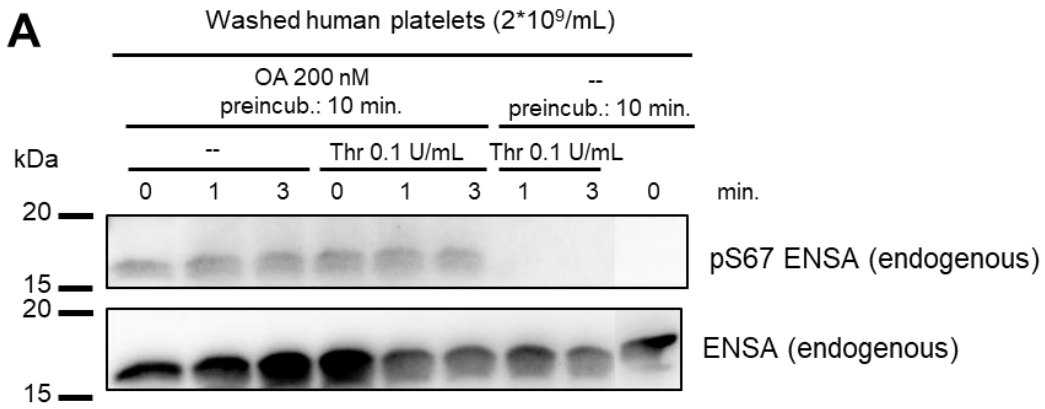

Figure 58: Low concentration of the PP2A-inhibitor OA mediates enhanced phosphorylation of ENSA S67. Representative western blot of endogenous ENSA and endogenous ENSA S67 phosphorylation in lysates of washed human platelets pre-treated without (-) or with 200 nM okadaic acid (OA), in the absence or presence of thrombin (0.1 U/ml). The anti-ENSA antibody (Cell Signaling®) was used 1:500 in 5% BSA-TBST for ENSA detection; anti-pS67 ENSA/anti-pS62 ARPP19 antibody (Cell Signaling®) was used 1:250 in 5% BSA-TBST.

The western blot data demonstrate, that even short-term treatment of washed human platelets with OA at low dose (200 nM for specific inhibition of PP2A) resulted in pronounced phosphorylation of endogenous ENSA at S67 (Figure 58). Thrombin treatment did not change the ENSA S67 phosphorylation pattern.

Early studies reported that pharmacological PP2A inhibition using OA diminished agonist-induced activation of human platelets.[148, 149] Therefore, I investigated the effect of low doses of OA on thrombin-induced activation/aggregation of washed human platelet function by using light transmission aggregometry (LTA).

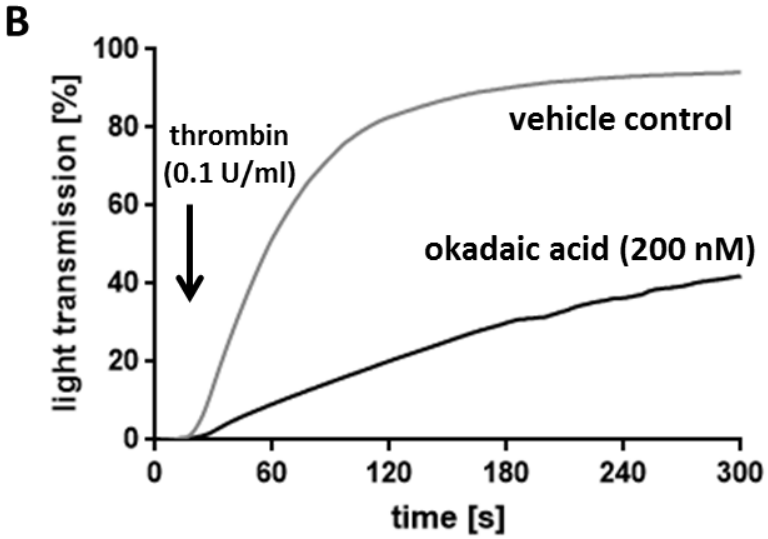

Figure 59: Low concentration of the PP2A-inhibitor OA inhibits thrombin-induced aggregation of washed human platelets.
Representative platelet aggregation curves of washed human platelets ($2x10^8$/ml) pretreated with vehicle control (ethanol) or 200 nM OA for 10 min. at 37°C and stimulated with 0.1 U/ml thrombin at 37°C under stirring conditions. Platelet aggregation is presented as percentage of light transmission monitored for 5 min.

The inhibition of PP2A with 200 nM of OA led to a reduced aggregation of platelets stimulated with 0.1 U/mL thrombin suggesting that OA-mediated decrease in platelet aggregatory capacity is associated with increased ENSA S67 phosphorylation (Figure 59).

5. Discussion

5.1. PKA-/PKG-mediated phosphorylation of the cell cycle regulators ENSA and ARPP19 in human platelets

Preliminary proteomic and phosphoproteomic studies of our group with human platelets detected significant expression of both ENSA and ARPP19 in these small non-dividing blood cells.[111] In subsequent studies addressing the cAMP/PKA phosphoproteome (more than 130 cAMP/PKA regulated phosphoproteins) we could demonstrate that ENSA (at S109) and ARPP19 (at S104) are phosphorylated in intact human platelets in response to the cAMP-elevating platelet inhibitor iloprost.[113] Furthermore, this increased ENSA (S109) phosphorylation was down-regulated by the platelet activator ADP, due to the known inhibition of the iloprost-induced cAMP increase by ADP.[135] Human platelets are strongly inhibited by both cAMP- and cGMP-elevating agents, and the corresponding cAMP- and cGMP-dependent protein kinases (PKA/PKG), which have overlapping effects but distinct substrate specificity.[29] Therefore, I investigated the effect of the cGMP/PKG–pathway on ENSA/ARPP19 phosphorylation using various NO-donors and the sGC stimulator riociguat in comparison to iloprost (cAMP pathway) and VASP (S239/S157) as established PKG/PKA substrate (Table 19, Table 20). ENSA (at S109) was strongly phosphorylated (several-fold stimulated over basal, often more than the excellent PKG substrate VASP S239) in response to several different cGMP-elevating agents as well as in response to the cAMP-elevating iloprost (Table 19, Table 20). These data and additional experiments with a PKG inhibitor (Figure 8) indicate that both ENSA and ARPP19 are phosphorylation targets of the platelet inhibitory pathways cAMP and cGMP, most likely phosphorylated by PKA and PKG, respectively.

The cAMP-regulated phosphoproteins (ARPP) ENSA (also known as ARPP19e or α-endosulfine) and ARPP19 and its isoform ARPP16 have been discovered earlier and studied since a long time as PKA substrates with little functional information.[84] This dramatically changed when two independent groups in 2010 established for *Xenopus* that both ENSA and ARPP19 inhibit PP2A, and thereby control mitosis, when phosphorylated by a special kinase called Greatwall (Gwl).[56, 57] Whereas PKA phosphorylated ENSA at the C-terminal site S109, ENSA S67 phosphorylation by Gwl was required for the potent inhibition of PP2A.[93] ENSA and ARPP19 are highly conserved, including the C-terminal PKA phosphorylation site (S109 ENSA, S104 ARPP19) and the central Gwl phosphorylation site (S67 ENSA, S62 ARPP19), in a broad spectrum of systems such as plants, *Xenopus*, *Drosophila*, yeast and a wide range of eukaryotes including humans.[150] Since the original demonstration in 2010, multiple studies established that the Gwl-ENSA/ARPP19–PP2A pathway is essential for controlling mitosis and its M and S phases from yeast to man[151] but ENSA/ARPP19 were not investigated in platelets until now.

It is indeed surprising to find the important phosphoproteins and cell cycle regulators ENSA and ARPP19 in the non-dividing human platelets, which perhaps suggests that they may have other functions outside of the cell cycle control (discussed later). Phosphorylation of both platelet ENSA (S109) and ARPP19 (S104) was strongly increased in our phosphoproteomic studies when the cAMP/PKA or cGMP/PKG pathway was stimulated. Further evidence for PKA-/PKG-specific phosphorylation of human ENSA and ARPP19 was obtained by experiments with recombinant HisENSA (also with its phosphosite mutants) and GST-ARPP19 using purified or recombinant protein kinases A and G (Figure 26, Figure 27; also Figure 44-53). ENSA and ARPP19 were strongly phosphorylated by both PKA and PKG, which was

abolished in the case of ENSA by S109A and S109D mutations. Other data showed that the PKA- and PKG-induced phosphorylation of ARPP19 caused a complete shift of ARPP19 in phostag-gels, indicating stoichiometric phosphorylation of ARPP19 at S104 (Figure 50-52).

All data obtained with intact human platelets and with recombinant proteins establish that ENSA and ARPP19 are not only targets of PKA, but also excellent PKG targets. In fact, the extent of S109 ENSA phosphorylation in response to various cGMP-elevating platelet inhibitors (Table 19) and compared to many other phosphoproteins[29] places especially ENSA among the best PKG targets studied. On a practical level, my experiments with recombinant ENSA and its phosphosite mutants also validated the various phospho-antibodies used including their application for ARPP19. It is of special interest that cGMP- and cAMP-elevating platelet inhibitors increased the phosphorylation of S109 ENSA while they decreased S67 ENSA phosphorylation (Table 19). I observed such reciprocal phosphorylation of ENSA also with HEK293 cells (treated with forskolin for PKA activation), which I used as additional human cellular model suitable for transfection (Figure 31). The endogenous ENSA in HEK293 cells and human platelets presents as only major band of similar size on the western blot (using the general Cell Signaling® anti-ENSA antibody). The properties of S67 ENSA and S62 ARPP19 phosphorylation will be discussed next, later the functional implication of ENSA and ARPP19 phosphorylation in human platelets.

5.2. MASTL-related protein kinases in human platelets

Considering the important functional role of S67 ENSA/S62 ARPP19 phosphorylation and the detection of these phosphoproteins in platelets by phosphoproteomics (Table 19), I investigated the possible S67 ENSA phosphorylation in human platelets and HEK293 cells (Figure 31, Figure 32, Figure 33). The Cell Signaling® anti-pS67 ENSA/anti-pS62 ARPP19 phospho-antibody, which recognizes both pS67 ENSA and pS62 ARPP19, detected a signal in HEK293 cell samples but not in samples obtained from non-stimulated (basal) or stimulated platelets. It has been reported in other systems that Gwl-phosphorylated ENSA/ARPP19 is dephosphorylated by PP2A and perhaps by another phosphatase, which can be prevented by the PP2A inhibitor okadaic acid (OA).[103] Therefore, I tested the effect of okadaic acid on S67 ENSA/S62 ARPP19 phosphorylation in experiments with intact human platelets and platelet lysates. Both, with intact platelets and with platelet lysates, OA induced a strong phosphorylation of endogenous S67 ENSA/S62 ARPP19 and added recombinant HisENSA or GST-ARPP19 at the same sites (Figure 32, Figure 33, Figure 35 and Figure 36). As important control and validation of the phosphorylation site and phospho-antibodies studied, the S67A HisENSA mutant was not phosphorylated (Figure 35). These experiments with intact human platelets and their lysates established for the first time without any doubt that human platelets express significant activities of a protein kinase, which phosphorylates endogenous and/or added HisENSA/GST-ARPP19 at the sites S67/S62 known in other systems to be responsible for PP2A inhibition. With platelets, the absent S67 ENSA phosphorylation under basal conditions but clearly detectable pS67 ENSA when PP2A is inhibited (Figure 33 and Figure 35) could indicate that the S67 kinase or a related one is inhibited by PP2A dephosphorylation, which is reversed by PP2A inhibition. An additional possibility is a very fast dephosphorylation of pS67 ENSA under basal conditions in human platelets, which is inhibited by OA. These results are in line with the observation that S67 phosphorylation of ENSA is also not detectable in western blots when platelets are inhibited by iloprost or activated by thrombin (Figure 58). The sensitive phosphoproteome analysis detected a decrease in S67 ENSA phosphorylation

upon platelet inhibition, suggesting that the amount of pS67 ENSA is too low for western blot detection but sufficient for detection via mass spectrometry.

The fact that ENSA is phosphorylated at S67 in HEK293 cells under basal conditions (the S67 kinase is active) and in human platelets only detectable with OA treatment (S67 kinase needs to be activated) suggests a different regulation/role of S67 ENSA phosphorylation in dividing HEK293 cells and non-dividing human platelets. This could be due not only to a different regulation/role, but also to a different kinase, that phosphorylates S67 ENSA/S62 ARPP19 in the different cell types.

In mammalian cells, only two protein kinases were described so far, which have the capacity to phosphorylate S67 ENSA/S62 ARPP19: MASTL (the human orthologue of Greatwall, Gwl)[88, 152] and the related microtubule-associated serine/threonine kinase 3 (MAST3).[94, 104] However, neither our proteomic nor transcriptomic studies detected traces of MASTL or MAST3 in human platelets. In addition, I did not detect MASTL kinase in platelets by western blot analysis (Figure 37). Interestingly, quantitative analysis of the murine platelet proteome did also not detect MASTL or MAST3 protein kinase.[138] Therefore, I performed a BLAST analysis by similarity to search for other human MASTL-related protein kinases (Figure 38, Table 23). I found several protein kinases, which showed a MASTL similarity of 40-50%, including the recently described ARPP16 kinase MAST3.[94] However, with the exception of STK38 (nuclear Dbf2-related protein kinase 1, NDR1) and STK38L (NDR2), these MASTL related kinases were not detectable in the human[111] and mouse[138] platelet proteome (Table 23). This motivated us to perform a small kinase screening experiment in collaboration with the biotech company ‘Reaction Biology Corporation’. NDR1 and especially NDR2 were able to phosphorylate the wildtype S67 peptide, but not the mutant S67A peptide of the conserved 22 amino acid sequence around the MASTL phosphorylation site of ENSA and ARPP19 (Figure 40, Figure 41, Figure 42). Therefore, our biochemical data with platelets and the data from the kinase screen reveal a possible role for the STK38/NDR kinases in human platelets. This is also supported by my observation that the OA-induced S67 ENSA phosphorylation in platelet lysates is potently inhibited by 50 nM staurosporine (Figure 39). However, an important caveat is that staurosporine is a very potent inhibitor of NDR1/2 but also inhibits many other protein kinases such as PKA, PKG and PKC.[120]

The serine/threonine kinases NDR1 and 2 belong to the NDR (nuclear Dbf2-related) family (members are LATS1/2 and NDR1/2) and, similar to MASTL, PKA and PKG, they are part of the AGC kinase family. NDRs are conserved in *Drosophila*, *Caenorhabditis elegans*, yeast and mammalian cells (also humans). NDR kinases are activated through multi-site phosphorylation (auto-phosphorylation and through other kinases) and through their co-activator MOB (Mps1-one binder), by binding to the N-terminus of the kinases. For my results it is of considerable interest that PP2A was shown to dephosphorylate and inactivate NDR kinases[153, 154], which was prevented by the PP2A inhibitor OA.[155] In my experiments with human platelets, it is certainly possible that OA mediated activation of NDR kinases and subsequently S67 ENSA/S62 ARPP19 phosphorylation. NDR kinases play important roles in the cell cycle progression, apoptosis, autophagy, DNA damage signaling, centrosome biology and neurobiology.[156] In mice hippocampal neurons (also non-dividing cells) NDR2 kinase has been shown to control integrin-dependent dendritic and axonal growth.[157] So far, nothing is known about the NDR kinases in platelets except that both NDR1 and 2 were detected in our human platelet proteomic analysis as well as the mouse platelet proteomic analysis.[138]

In other mammalian cells (rat/mouse brain), the group of Professor Angus Nairn (Yale University) showed that ARPP16 (shorter isoform of ARPP19) is phosphorylated at S46

(similar to S67 ENSA or S62 ARPP19) by MAST3 instead of the MASTL kinase.[94, 104] This phosphorylation converts ARPP16 to a strong inhibitor of PP2A B55α but also of PP2A B56δ. These data suggest that in different cells different kinases could phosphorylate ENSA/ARPP proteins at the MASTL-phosphorylation site. Interestingly, PKA phosphorylated and inhibited MAST3 as discussed below.

The discovery of MASTL as human Gwl orthologue[88] led to the recognition that a defined MASTL E167D mutation in humans is associated with thrombocytopenia.[88, 152, 158] Very recently, Hurtado et al. described the megakaryocyte specific MASTL mutation (E167D knock-in) and complete MASTL KO in mice, reporting a reduced platelet count and decreased half-life of platelets in KO and mutant mice. They observed increased annexinV-levels, probably associated with platelet apoptosis or platelet activation, increased bleeding times and defective clot retraction.[159] Overall, they interpreted MASTL mutation as a gain of kinase function for the MASTL kinase, leading to a stronger inhibition of PP2A. Unfortunately, this group did not provide any biochemical data for the presence of MASTL protein or activity in platelets.

At present, I conclude that there are two interesting options for the detected S67 ENSA/S62 ARPP19 protein kinase activity in human platelets:

a) Despite the negative protein expression data so far, there are perhaps low, not yet detectable expression levels of MASTL (or MAST3), which support the clearly observed S67 ENSA/S62 ARPP19 phosphorylation. I am aware of the difficulty to exclude low, undetectable levels of an enzyme/protein kinase as functionally important.

b) Biochemical and functional data clearly suggest that NDR1/NDR2 or perhaps related protein kinases are expressed in human platelets, which catalyze the detected ENSA/ARPP19 phosphorylation.

Future approaches will have to clarify this important point.

5.3. Phosphorylation of recombinant HisENSA and GST-ARPP19 by recombinant human MASTL, recombinant human PKG1β and purified bovine PKA (C-subunit)

Since the various MASTL- and PKA/PKG-phosphorylation sites of ENSA and ARPP19 may affect the properties of these proteins and their interactions with other regulators such as kinases and phosphatases, I studied theses phosphorylations with recombinant proteins in more detail (Figure 44-53). Here, I summarize the results and their implications.

a) PKA/PKG: HisENSA and GST-ARPP19 were strongly and time-dependently phosphorylated by both kinases at a site recognized by various phospho-antibodies raised against pS109 ENSA. This ENSA phosphorylation was abolished with ENSA S109A/D mutants but not with the S67A ENSA mutant. Importantly, PKA and PKG phosphorylation of GST-ARPP19 caused a time-dependent complete mobility shift of ARPP19 in phostag-gels, demonstrating stoichiometric (complete) phosphorylation of the PKA/PKG site. Whereas phostag-gel analysis worked very well with GST-ARPP19, this was, for unknown reasons, not the case with HisENSA. Perhaps, this was due to the His-tag of the ENSA protein since His-tags interact with positively charged ions (e.g. Ni^{2+} or Co^{2+}, as used for the purification of His-tagged proteins). In phostag-gels, Zn^{2+} is used for the phostag component, which may disturb the gel running procedures.

However, some groups reported successful (at least qualitatively) phostag blots with His-tagged proteins.

b) MASTL: HisENSA and GST-ARPP19 were strongly and time-dependently phosphorylated by MASTL at a site recognized by the Cell Signaling® anti-pS67 ENSA/anti-pS62 ARPP19 antibody. The ENSA phosphorylation by MASTL was abolished in the S67A ENSA mutant but not with the S109A ENSA mutant. With GST-ARPP19, MASTL phosphorylation caused a time-dependent complete mobility shift of ARPP19 in phostag-gels, demonstrating stoichiometric (complete) phosphorylation of the MASTL site.

c) MASTL+PKA or PKG: The studies with the simultaneous or consecutive phosphorylation of HisENSA or GST-ARPP19 by kinase combinations (MASTL+PKA; MASTL+PKG) showed that the two important phosphorylation sites (MASTL: S67/S62; PKA/PKG: S109/S104) were similarly phosphorylated by the responsible kinases with or without the other kinase. In other words, MASTL had no major effect on PKA/PKG mediated ENSA/ARPP19 phosphorylation, and PKA/PKG had no major effect on the MASTL-mediated ENSA/ARPP19 phosphorylation. At present, I cannot rule out smaller effects in these interaction studies since detailed kinetics were not performed. In addition, the experiments were carried out with tagged ENSA/ARPP19 proteins, which may affect phosphorylation and interactions. Finally, the effects may be different in intact cells and may be cell type-/system-specific (see subsequent discussion).

S. Mochida (one of the original discoverers of *Xenopus* ENSA/PP2A) reported in 2014 the different phosphorylation sites of ENSA in *Xenopus laevis* and their influence on PP2A inhibition.[93] Whereas human ENSA (and ARPP19) apparently only have two major phosphorylation sites (S67/S62 for MASTL, S109/S104 for PKA), *Xenopus* ENSA and ARPP19 have a third site, T28 for ENSA/S28 for ARPP19. Mochida concluded that the phosphorylation of all three sites influences PP2A inhibition. However, pS67 ENSA is the most potent PP2A inhibitor and interacts with both B55- and C-subunit, blocking the catalytic center of PP2A. The phosphorylation of the other sites (T28/S28, S109/S104) influences the PP2A interaction via occupying the catalytic center of PP2A (pT28) or interaction of the N-terminal region of ENSA with another surface of the PP2A heterotrimer (not the catalytic center), transforming 'ENSA into a 'stepwise turner' that modulates PP2A-B55 activity to several discrete levels'.[93] Mochida calculated the IC_{50} values for pENSA PP2A B55 inhibition for his experiments with *Xenopus* components and obtained an IC_{50} of 0.47 nM for pS67 ENSA, an IC_{50} of 0.52 nM for pS67+pS109 ENSA and much higher values for pS109 ENSA alone.[93] Apparently, PKA phosphorylation of *Xenopus* ENSA S109 had little effect in these systems.

Andrade et al. showed in 2017 that brain ARPP16 phosphorylation sites (the shorter isoform of ARPP19) are reciprocally phosphorylated when forskolin is added to striatal slices.[92] These conditions induced a reduced phosphorylation of the MASTL/MAST sites (S46, similar to S62 ARPP19/S67 ENSA) and stimulated S88 phosphorylation via PKA (similar to PKA sites S104 ARPP19/S109 ENSA). These authors provided for their system (rat and mouse striatum, MAST3 kinase and ARPP16) several mechanisms how S46 ARPP16 phosphorylation was inhibited, which would result in decreased inhibition of PP2A:

a) PKA phosphorylation of ARPP16 inhibited the extent of PP2A inhibition by S46-phosphorylated ARPP16.

b) PKA phosphorylated and inhibited MAST3.

c) Forskolin/cAMP/PKA activated PP2A via direct phosphorylation of PP2A B56δ[160] or additional mechanisms.

Some or all of these effects may perhaps be specific for brain and have been recently reviewed.[161] In our phosphoproteomic analysis, we also found PP2A B56δ in human platelets to be phosphorylated upon platelet inhibition/PKA activation (Table 20).

Dupré et al. recently studied the interaction of PKA and Gwl regulating ARPP19/ENSA phosphorylation in the *Xenopus* system. They did not observe any major effect of PKA on ARPP19 phosphorylation by Greatwall and on the ability of Gwl phosphorylated ARPP19 to inhibit PP2A B55δ. Overall, they concluded that the effect of S67 phosphorylation is dominant over the negative-function of S109-phosphorylation.[162]

There are additional mechanisms of possible interaction of these components. Mochida et al. showed in 2015, that protein phosphatase 1 (PP1) is inhibited by CDK1 kinase which, on the other hand, phosphorylates/activates Greatwall/MASTL kinase resulting in PP2A inhibition. PP1 is able to dephosphorylate itself to reactivate its phosphatase activity, which includes the dephosphorylation/inactivation of the Greatwall/MASTL kinase. This shifts the balance to dephosphorylated ENSA/ARPP19 and will initiate the exit from mitosis.[163] Since many components of PP1 are also present in human platelets,[111, 164, 165] the regulatory mechanism enabling PP2A to dephosphorylate ENSA/ARPP19 may include PP1.

I did not detect PKA effects on human S67/S62 ENSA/ARPP19 phosphorylation and function *in vitro* with recombinant proteins. However, in intact platelets and HEK293 cells I found ENSA to be strongly phosphorylated at S109 when PKA and PKG are activated and, at the same time, down-regulation of S67 ENSA phosphorylation. Although the exact mechanism has not been elucidated, several promising pathways exist based on earlier and recent studies:

1. The MASTL/Greatwall homolog in yeast, Rim15, is phosphorylated and inhibited by PKA.[166] The same has been shown for MAST3 (phosphorylating ARPP16 at S46) in rat striatal neurons.[104] Our data can be explained if the MASTL-like kinase in human platelets is also phosphorylated/inhibited by PKA. In addition, (as mentioned before) PP2A B56δ is activated by PKA-mediated phosphorylation. Activated PKA (in response to cAMP-elevating platelet inhibitors) may inhibit the MASTL-like kinase and activate PP2A. As a result, ENSA is less phosphorylated at S67, PP2A is less inhibited and can dephosphorylate pS67 ENSA or other substrates, protein phosphatases or kinases. Also, we cannot rule out for our system that pS67 ENSA is dephosphorylated by another PP2A holoenzyme, which is not inhibited by ENSA/ARPP19.

2. There is a reciprocal relation between the two phosphorylation sites of ENSA. Phosphorylation of S67 ENSA is leading to a reduced phosphorylation of S109 and the other way around. This reciprocal relation was shown for ARPP16 in brain tissue, where MAST3 (instead of MASTL) was used to phosphorylate ARPP16.[104] However, these *in vitro* findings have not been reported in other studies. Maybe one site phosphorylated blocks the accessibility of the second phosphorylation site for kinases by conformational changes of ENSA or the interaction of phosphorylated ENSA with other proteins.

5.4. Protein phosphatase 2A – PP2A

Protein phosphatase 2A (PP2A) and in particular PP2A-B55/B56 (PP2A holoenzymes containing the B55/B56 regulatory subunits) bind and are strongly inhibited by S67-/S62-phosphorylated ENSA/ARPP19.[93, 94, 151, 161]

It has been known for a long time that PP2A is expressed in most cells from yeast to man and that it exists in the cell predominantly as a heterotrimeric holoenzyme composed of a catalytic subunit (C), a scaffolding subunit (A) and a targeting/regulatory subunit (B). However, the full extent of the diversity and functional role of the regulatory B subunits was not appreciated until recently.[167, 168] In humans, A and C subunits of PP2A each have two possible variants (α,β) whereas the B subunits are encoded by 15 different genes, which may yield 23 isoforms due to alternative promoters and alternative splicing. Based on this, human tissues/cells may contain up to 92 different trimeric PP2A holoenzymes and additional 4 dimeric (AC) forms.[168]
Based on sequence homology, B subunits are subdivided into four distinct families called

- B (or B55,or PR55,or by gene name: *PPP2R2*)
- B´ (or B56,or PR61,or by gene name: *PPP2R5*)
- B´´ (or PR72,or by gene name: *PPP2R3*)
- B´´´ (or the striatins, *STRN*)

The different B subunits are further subdivided, for example B55 α,β,γ,δ and B56 α-ε, which have sequence similarity but exhibit distinct patterns of expression and subcellular localization. Overall, the B-type subunits are true “regulatory” subunits, determining substrate specificity of the associated PP2AC subunit and modulating PP2A catalytic activity. They are often expressed in a specific way and also determine the intracellular locations of the PP2A holoenzymes.[168] The limited data published so far suggest that *Xenopus* ENSA prefers trimeric PP2A containing the B55δ subunit[93] whereas ARPP16 in brain interacts and inhibits PP2A B55α and B56δ.[94]
Considering the enormous heterogeneity of PP2A composition and function, it was very important for my human platelet project to have some information on the expression level of PP2A and other phosphatases in these cells. Fortunately, I could extract these data from our proteomic databases as summarized in Table 25. Human platelets contain the two catalytic subunits (α,β), only one of the two scaffolding A (α), two B55 subunits (α,δ), five B56 subunits (α,β,γ,δ,ε) and the PP2A activator, which is known to activate PP2A by dephosphorylating tyrosine 307.[70] Interestingly, the distribution of PP2A isoforms in human platelets is similar to the one in murine platelets, although some quantitative differences exist. For the scaffolding subunit A, only the α-isoform was found in human platelets, similar to other human cells.[42] The proteomic data suggest that 14 different PP2A trimeric holoenzymes and 2 different dimeric forms could exist in human platelets, perhaps even more due to the splice variants of the regulatory subunits.

It is of interest to note here that human platelets contain the **B55α**, **B55δ**, B56α, B56β, B56γ, **B56δ** and B56ε subunits, but only some of them (in bold) are known so far to be ENSA/ARPP targets.

5.5. PP2A activity in platelet lysates and intact platelets: Effects of MASTL-phosphorylated HisENSA and GST-ARPP19 on PP2A

The results discussed so far suggest a major role of ENSA/ARPP19 in regulating PP2A activity in platelets. To test this, I established a well-described, very sensitive PP2A assay, which measures the release of free phosphate by the absorbance of a molybdate:phosphate complex. This assay can be specific for PP2A activity by optimizing the assay conditions and by using a selective substrate (only dephosphorylated by PP2A, PP2B and PP2C). The assay is very sensitive to low phosphate concentration changes, can be used with cell lysates but is also susceptible to interferences (see methods/results). Most importantly, all free phosphate in solutions, lysates and protein-solutions has to be removed completely before use. With these precautions in mind, I established an assay specific for PP2A activity in lysates of human platelets. This activity was potently inhibited by OA with concentrations of 1 nM and below in agreement with the reported IC_{50} of 0.1-0.3 nM[72] whereas the PP1 inhibitor tautomycetin (reported IC_{50} for PP2A: 62 nM)[121] had inhibitory effects on measured phosphatase activity only at concentrations of 50 nM and higher (Figure 54, Figure 55). These data and other controls, such as concentration- and time-dependency of the PP2A assay with platelet lysates (data not shown), established the conditions to study the effects of known (OA) and putative inhibitors of PP2A in human platelet lysates. I therefore tested the effect of HisENSA/GST-ARPP19 phosphorylated by MASTL at S67/S62 *in vitro*.

I observed a clear and significant reduction (~20%) in platelet PP2A activity when pS67 HisENSA and pS62 GST-ARPP19 were added to the assay, compared to the non-phosphorylated proteins (no inhibition) and 1 nM OA (complete inhibition) (Figure 54, Figure 56). These results together with the other data obtained show for the first time a role for phosphorylated ENSA and ARPP19 in the inhibition of PP2A in human platelets. However, the effects observed so far were small. It is very likely that ENSA/ARPP19 inhibit only some of the PP2A holoenzymes present in human platelet lysates in contrast to OA that binds to and inhibits all PP2A catalytic subunits independent of the other subunits. ENSA and ARPP19 are thought to achieve their inhibitory effects, as far as known, via a limited number of B subunits (B55/B56 subfamily). However, there is very limited number of studies and data available on the regulation of mammalian/human PP2A by the ENSA/ARPP family. The complete inhibition of PP2A with OA in platelet lysates or washed platelets also explains why we observe a signal for pS67 ENSA. All PP2A complexes are inhibited, no active complex is left that could dephosphorylate pS67 ENSA. Endogenous inhibitors of PP2A, like ENSA, only inhibit some complexes of PP2A. Therefore, other PP2A complexes stay active and continue dephosphorylating their substrates.

My results set the stage to study the role of PP2A and its regulation by ENSA/ARPP19 in more detail in the future. For example, it would be important to elucidate, which platelet PP2A subtypes bind to and are inhibited by phosphorylated S67/S62 ENSA/ARPP19. This question could be addressed by immunological and/or proteomic approaches that would also be important for the identification of specific substrates of PP2A in human platelets.

5.6. Biochemical and functional effects of low dose OA on human platelets

To obtain further insights into PP2A function in intact human platelets, I studied, in washed human platelets, the effects of low dose OA (200 nM) on the phosphorylation of S67 ENSA, S157/S239 VASP and T180/Y182 p38 MAP kinase as well as on platelet aggregation upon activation with thrombin (Figure 57, Figure 58, Figure 59). Strikingly, 200 nM OA increased phosphorylation of S67 ENSA, p38 and VASP (primarily the S157 site) within 10 minutes.

Higher amounts of OA (10 µM) revealed a stronger phosphorylation of VASP. This points to an additional effect of PP1 inhibition upon VASP (de)phosphorylation. The data relate MAP kinase p38 dephosphorylation only to PP2A activity, as higher concentrations of OA, which additionally inhibit PP1, did not lead to an increase of p38 phosphorylation.

On top, S67 ENSA phosphorylation upon OA incubation was not affected by treatment of washed human platelets with thrombin (Figure 58). The increased S67 ENSA phosphorylation with 200 nM of OA could be due to the inhibition of the pS67 ENSA phosphatase (primarily PP2A) and/or to the activation of the corresponding S67 ENSA kinase, as discussed earlier. Since both effects are due to PP2A inhibition, pS67 ENSA could serve as marker for PP2A inhibition in human platelets.

The observed increased phosphorylation of p38 with 200 nM of OA is of considerable interest, since it is well known that there is an extensive crosstalk between p38, other MAP kinases and PP2A.[146] Platelet p38 phosphorylates and activates downstream transcriptional regulatory proteins such as IKKβ (inhibitor of nuclear factor kappa-B kinase subunit β), cytosolic phospholipase A_2 ($cPLA_2$) and so called MAP kinase activated protein kinases (MAPKAPK). The $cPLA_2$ pathway leads to TXA_2 generation, which facilitates granule secretion, aggregation and integrin outside-in signaling.[165]

Other groups showed that PP2A regulates PLA_2 phosphorylation and activity in human platelets upon platelet activation with thrombin[75] and that p38 is dephosphorylated and therefore inactivated by PP2A.[74] PLA_2 is a Ca^{2+}-sensitive lipase, PP2A is increasing the Ca^{2+}-concentration upon thrombin stimulation.[75]

It is of interest to note that the low dose OA, increasing p38 phosphorylation, decreased thrombin-induced platelet activation/aggregation. The detected phosphorylation of p38 (T180/Y182) is, upon platelet stimulation, a well-known marker of platelet activation.[169] The reduced platelet aggregation response upon OA pre-incubation could be mediated by phosphoproteins, which are also regulated by PKA/PKG substrates such as VASP and others. Phosphorylation of S157 and S239 VASP is a typical response of PKA and PKG activation in platelets but there are many other proteins phosphorylated.[29] Although OA increased the phosphorylation of the PKA/PKG substrate VASP, this does not indicate that OA stimulates PKA/PKG phosphorylation/activation, which is not known for these kinases. It is more likely that there is in platelets always an equilibrium of protein phosphorylation/protein dephosphorylation, which can be altered by kinase activators, protein phosphatase inhibitors or both. However, many other protein kinases and especially MAPK are regulated by phosphorylation/dephosphorylation and are often indirectly activated by OA through PP2A inhibition.[74, 170]

The observed OA reduction of thrombin-stimulated platelet aggregation and OA induced (T180/Y182) p38 phosphorylation (which leads to platelet activation) is at first sight a paradox.

However, both the OA target PP2A and the MAPK p38 are components of large modular networks, which may have different functional endpoints. In support of this view it was recently summarized that protein phosphatases and in particular PP2A were initially envisioned as tumor suppressors. But it has now become clear that several of them are oncogenes and some have both tumor suppressive and oncogenic characteristics, depending on the cellular context or other unknown factors.[171] In fact, multiple signaling/MAPK components are regulated by PP2A in human tissues/cell types including the serine/threonine kinase Akt, which is negatively regulated through PP2A-B55α.[48] Both proteins are present in human platelets.

Functionally, PP2A appears also to be involved in clot retraction through outside-in $\alpha_{IIb}\beta_3$ integrin signaling in human platelets[77, 79] perhaps at a later phase of platelet activation.

One important point needs to be mentioned: OA incubation does not lead to the same inhibitory pathway as the inhibition of human platelets by NO or iloprost. All three conditions (OA, NO, iloprost) cause increased phosphorylation of multiple platelet proteins in human platelets due to inhibited dephosphorylation (OA) or activated PKG (NO) or activated PKA (iloprost). The spectrum of these regulated phosphoproteins, which mediate functional effects, only partially overlaps, as far as known. In addition, there is a crosstalk between the various protein kinases and phosphatases. For example, phosphorylation of PP2A S573 B56δ was detected upon PKA-mediated platelet inhibition (Table 20), which usually activates this PP2A holoenzyme.[160] Maybe we observe a OA-mediated pS67 ENSA signal because the PP2A complex is inhibited, that is normally active during platelet inhibition and that therefore would dephosphorylate pS67 ENSA upon platelet inhibition. Alternatively, the S67 ENSA kinase in platelets is normally inhibited upon platelet inhibition but it stays active with a complete inhibition of PP2A (through OA incubation). Our phosphoproteomic analysis of inhibited platelets revealed a strong phosphorylation of ENSA at S109 and a reduced phosphorylation at S67. The S109 phosphorylation of ENSA needs to be analyzed upon PP2A inhibition with OA in human platelets. As PKA and PKG are active under OA treatment, one would expect a strong phosphorylation of S109 ENSA under the same conditions.

For the near future, it will be important to increase our knowledge about the functional heterogeneity of PP2A and the role of the various B subunits for specific inhibition by ENSA/ARPP19 proteins and for substrate specificity in platelets.

5.7. The cell cycle regulatory components (MASTL–ENSA/ARPP19-PP2A) in non-dividing cells

The eukaryotic cell cycle is an essential cellular process controlled by a complex regulatory system with cyclins, cyclin-dependent kinases (CDK), their substrates and counteracting protein phosphatases.[172] The cyclin-CDKs phosphorylate numerous substrates that initiate chromosome duplication in S phase, mitotic spindle assembly and functions for chromosome segregation in mitosis. Whereas the yeast cell cycle is controlled by a single CDK (CDK1), mammalian cell cycles are more elaborate and have multiple CDKs, with CDK1 and CDK2 being the key players. The mammalian PP2A is also more heterogeneous than that of lower species. As already mentioned the Gwl/MASTL-ARPP19/ENSA-PP2A B55 pathway has been recognized as the major regulatory system, which antagonizes the function of CDKs by dephosphorylating CDK substrates,[151] a pathway also conserved from yeast to man.
A very important finding of my work is that human platelets (and by analogy also murine platelets) contain the entire [Gwl/MASTL]–ENSA/ARPP19–PP2A (B55/B56) pathway, although

platelets are clearly non-dividing, post-mitotic cells. At present, it is not certain whether the clearly detectable S67 ENSA/S62 ARPP19 kinase activity is due to MASTL or a closely related kinase. In addition, we can only speculate, which protein kinase/protein phosphatase targets and activates/inhibits this MASTL-like kinase in platelets. These are important topics to clarify.
It is of interest that a similar machinery (MAST3-ARPP16-PP2A) was also found in non-dividing neurons of the striatum.[92] There, ARPP16 (a shorter but similar ARPP19 isoform) was shown to be phosphorylated at the MAST(L) site by a kinase different than MASTL kinase, but still very similar, MAST3. This converted ARPP16 to a strong inhibitor of PP2A B55α and B56δ, a process reciprocally regulated/inhibited by PKA-mediated phosphorylation of ARPP16 and MAST3.[94, 104] However, the functional effects and consequences of this pathway in neurons have not been elucidated so far.

It has been speculated by some groups that the Gwl/MASTL-ENSA/ARPP19/PP2A pathway has functions outside the classical cell cycle control, since they observed a Gwl/ENSA- and ubiquitin-proteasome dependent degradation of some proteins in cultured human cells.[173] The various PP2A holoenzymes are thought to control the phosphorylation status of many important structural and regulatory proteins, which are also present and regulated in human platelets such as p38, VASP, Akt, PLA_2, ENSA, ARPP19, but also the apoptotic proteins BAD and Bcl-2. To elucidate these regulatory processes in human platelets will be important not only to improve our understanding of platelets, but also of neurons and other cells.
Finally, one can never exclude that both ENSA and ARPP19 have functions in addition to PP2A inhibition. ENSA was first detected as peptide ligand of the sulfonylurea receptor, which generated its name.[174] Later, it was shown by NMR studies that ENSA interacts with the small protein α-synuclein which was inhibited by mutation of the PKA-phosphorylation site of ENSA, S109.[107, 175] However, these early data have not been followed up further.

5.8. Conclusions

The most important finding of my work is that human platelets (and by analogy also murine platelets) contain the entire [Gwl/MASTL]–ENSA/ARPP19–PP2A (B55/B56) pathway, as mentioned above. First, I established that ENSA/ARPP19 are phosphorylated at a specific C-terminal phosphorylation site (S109/S104) by both PKA and PKG in intact platelets and with recombinant proteins. Then, I discovered a MASTL-related kinase activity in both intact human platelets and platelet lysates, which phosphorylates ENSA/ARPP19 at their centrally localized phosphorylation site (S67 in ENSA, S62 in ARPP19) under conditions, which required PP2A inhibition by okadaic acid. I also showed that ENSA/ARPP19 and a broad spectrum of PP2A subunits, including the very relevant B55/B56 subunits, are well expressed in human and also in murine platelets. HisENSA and GST-ARPP19 phosphorylated by recombinant human MASTL at S67/S62 partially inhibited PP2A activity in a human platelet lysate, which obviously contains a large spectrum of platelet PP2A holoenzymes. With intact human platelets, inhibition of PP2A by low dose okadaic acid increased the phosphorylation of ENSA, p38 and VASP and reduced thrombin-induced platelet aggregation. Also with intact human platelets and HEK293 cells, PKA activation reduced ENSA S67 phosphorylation. This is expected to decrease PP2A inhibition, resulting in increased PP2A activity and subsequently decreased substrate phosphorylation. This may be partially mediated by direct PKA-mediated phosphorylation of PP2A B56δ that we also observed. Overall, MASTL and PKA/PKG phosphorylate ENSA/ARPP19 at different sites, which leads to inhibited/less-inhibited PP2A activity, resulting into increased/decreased phosphorylation of PP2A substrates as summarized in the final figures (Figure 60, Figure 61). Although there are still many questions

open, I conclude that human platelets have all components of the entire [Gwl/MASTL]–ENSA/ARPP19–PP2A (B55/B56) pathway which is of functional relevance.

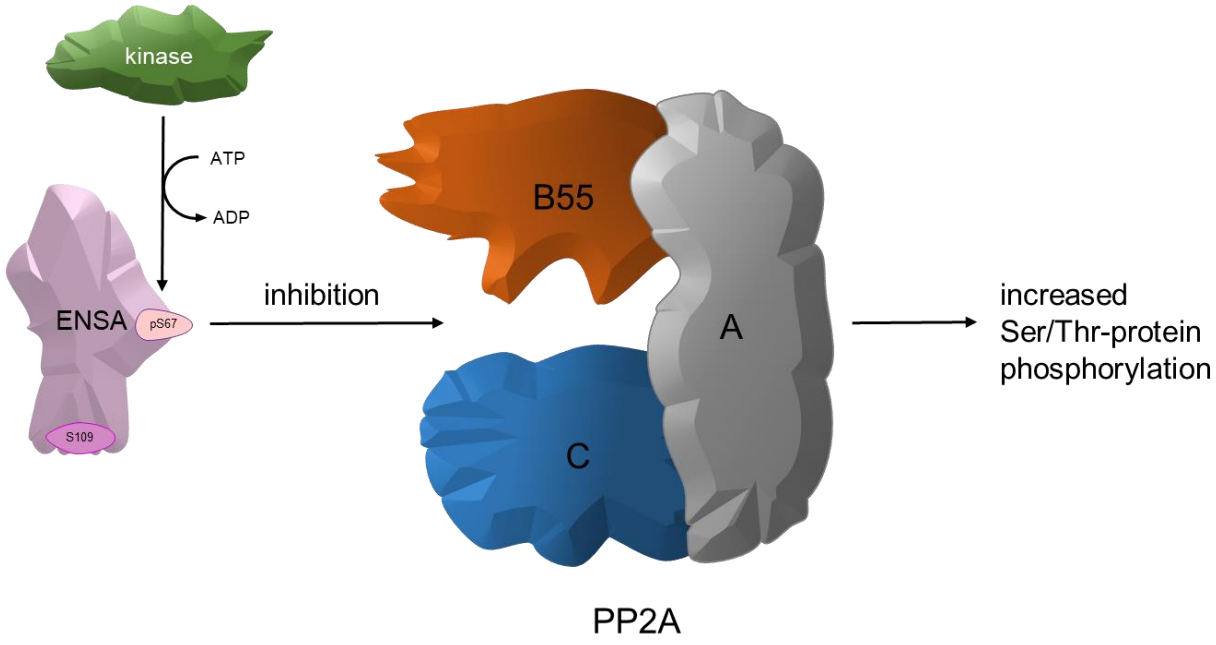

Figure 60: Regulation of PP2A inhibition by ENSA in human platelets.
The same is probably true for ARPP19.

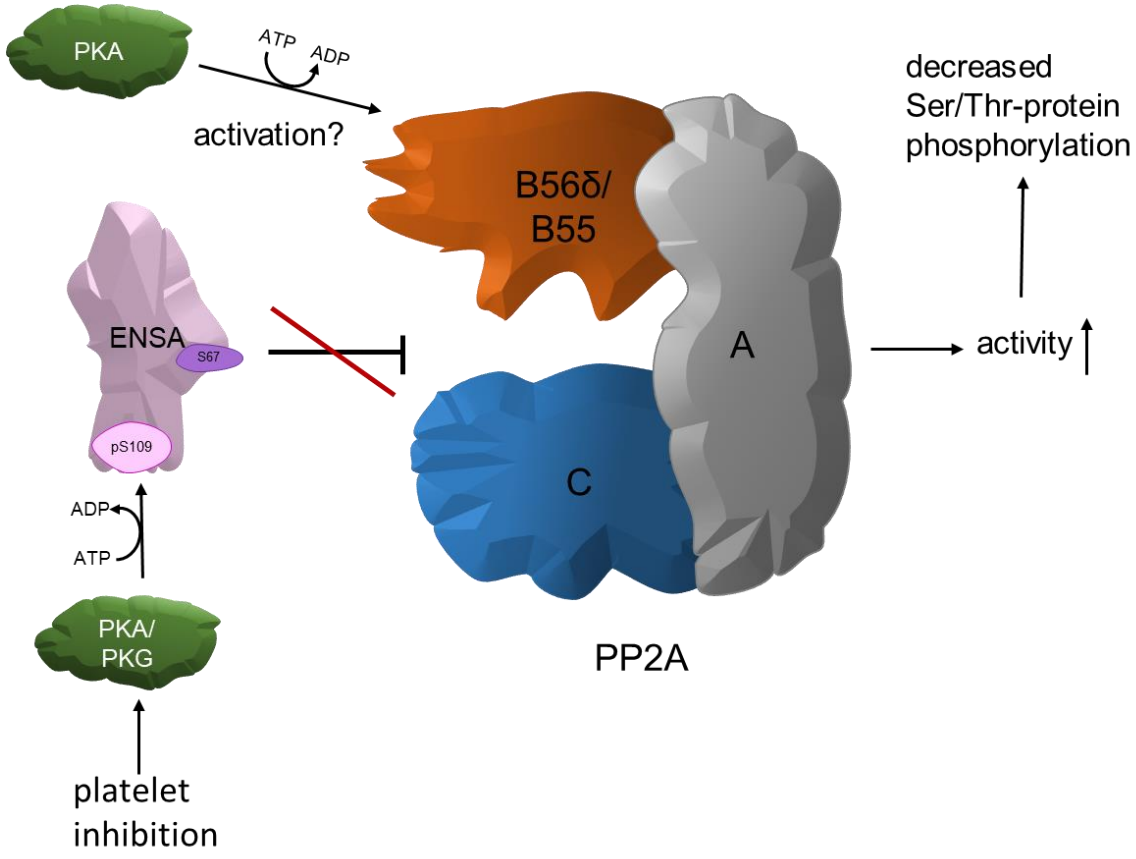

Figure 61: Possible mechanism of PP2A activation upon platelet inhibition via PKA/PKG.
The same is probably true for ARPP19.

5.9. Outlook

One important question to address is, which of the several platelet PP2A holoenzymes/isoforms are targeted and regulated/inhibited by S67/S62 phosphorylated ENSA/ARPP19 and if there are differences between the two proteins. This could be studied by analyzing the phosphatase activity, and ENSA/ARPP19 effects on this activity, in isoform-specific PP2A immunoprecipitates. Furthermore, ENSA/ARPP19 or PP2A pulldowns could be analyzed for their PP2A activity and proteins and by immunoblots and mass spectrometry. The identification of ENSA/ARPP19 PP2A targets in human platelets will be very valuable for future studies to search for PP2A subtype-specific substrates, since often PP2A and important substrates form complexes.

It would be also important to know, if the PP2A complexes that are inhibited by pS67 ENSA/pS62 ARPP19, dephosphorylate ENSA/ARPP19 and other proteins in human platelets.

I could document in my work that one can analyze the human platelet [Gwl/MASTL]–ENSA/ARPP19–PP2A (B55/B56) pathway with intact cells, cell lysates and recombinant proteins. For example, inhibition of PP2A by the general PP2A inhibitor okadaic acid in human platelet lysates could be monitored by several distinct phosphoprotein substrates. This could be extended to study the effect of thio-phosphorylated S67 HisENSA or thio-pS62 GST-ARPP19 in platelet lysates by analyzing a broader spectrum of phosphoproteins, perhaps using a MAPK phosphoprotein array.

Another important point is the precise identification of the S67/S62 ENSA/ARPP19 protein kinase in human platelets. Considering my top candidates, MASTL and/or NDR1/2 kinases, it should be possible to use a pull-down approach, remove the corresponding candidates from platelet lysates and then quantify the remaining kinase activity in the supernatant. In addition, kinase-ENSA interaction could be studied by a combined cross-linking/mass spectrometry approach. Finally, it may be possible to study the S67/S62 ENSA/ARPP19 protein kinase in platelets from KO mice lacking the suspected kinases only in platelets/megakaryocytes. A complete KO of these proteins including ARPP19 in mice is often lethal.

A last short statement for the overall relevance of PP2A and its regulation. PP2A has been known for a long time with only moderate attention (when compared to protein kinases). For many years protein phosphatases were only viewed as simple turn-off mechanisms for protein kinases/phosphoproteins. However, the enormous heterogeneity of PP2A, its regulation by many mechanisms including phosphorylation and inhibitors, and its broad role in the regulation of other intracellular pathways (via its effect on phosphoproteins) has been only recently appreciated.[167, 171, 176] Interestingly, there is increasing evidence that acquired and genetic defects in phosphatases lead to diseases, especially cancer and inflammation.[176] Platelets and the hemostatic system have not been explored with respect to PP2A, which opens a future research direction. I am sure that there is much more to be discovered about PP2A in platelets.

6. Appendix

List of abbreviations

AD	Alzheimer’s disease
ADP	adenosine 5’-diphosphate
AGC	protein kinase A, G, C families
Akt	PKB
Amp	ampicillin
APS	ammonium persulfate
ARPP16	cAMP-regulated phosphoprotein 16
ARPP19	cAMP-regulated phosphoprotein 19
ATP	adenosine 5‘-triphosphate
BAD	Bcl-2-associated agonist of cell death
Bcl-2	B-cell lymphoma 2
Bod1	Biorientation of chromosomes in cell division protein 1
bp	base pairs
BSA	bovine serum albumin
bzw.	beziehungsweise
CalDAG-GEFI	Ca^{2+}- and DAG-regulated guanine-nucleotide exchange factor I
CAMK	Ca^{2+}/Calmodulin-dependent protein kinase
cAMP	cyclic adenosine monophosphate
CDK	cyclin-dependent kinase
cGMP	cyclic guanosine monophosphate
CGS	citrate-glucose-sodium chloride (buffer)
CIN85	SH3 domain-containing kinase-binding protein 1
CK1	cell kinase 1
CMGC	CDK, MAPK, GSK3, CLK families
CLEC-2	C-type lectin-like receptor 2
DAG	diacylglycerole
dATP	2'-deoxyadenosine 5'-triphosphate

dCTP	2'-deoxycytidine 5'-triphosphate
dd	double distillated
DEA-NO	diethylamine NONOate
dGTP	2'-deoxyguanosine 5'-triphosphate
CMGC	CDK, MAPK, CSK3, CLK families
Dbf2	cell cycle protein kinase (related to NDR)
DMEM	Dulbecco's Modified Eagle Medium
DMSO	dimethyl sulfoxide
DNA	deoxyribonucleic acid
dNTP	nucleotide mix (contains dATP, dCTP, dGTP and dTTP)
DSK	dual-specificity kinase
DTS	dense tubular system
DTT	dithiotreitol
dTTP	2'-deoxythymidine 5'-triphosphate
E.coli	*Escherichia coli*
EDTA	ethylenediaminetetraacetic acid
e.g.	for example (exempli gratia)
EGTA	ethylene glycol-bis(β-aminoethyl ether)-*N*,*N*,*N*′,*N*′-tetraacetic acid
ENSA	α-endosulfine
Erk1	MAPK4
Erk2	MAPK1
EtOH	ethanol
FA	formaldehyde
FACS	fluorescence-activated cell sorter
FBS	fetal bovine serum
Frk	forskolin
g	gram
GP	glycoprotein
Gi	G-protein subunit iα

Gs	G-protein αs
GST	glutathione S-transferase
Gwl	Greatwall kinase
His	histidine/6xhistidine-tag
HP	high pressure
HRP	horseradish peroxidase
IC_{50}	half maximal inhibitory concentration
IgG	immunoglobulin G
Ilo	iloprost
IP	immunoprecipitation
IP_3	inositol-1,4,5-triphosphate
IP_3R1	inositol-1,4,5-triphosphate receptor 1
IPTG	isopropyl β-D-1-thiogalactopyranoside (inductor of lactose operon in *E.coli*)
IRAG	inositol trisphosphate receptor-associated cGMP-kinase substrate
ITAM	immunoreceptor tyrosine-based activation motif
kb	kilo base pairs
K_D	dissociation equilibrium constant of the enzyme-inhibitor complex
kDa	kilo Dalton
KO	knock-out
L	liter
LATS	large tumor suppressor kinase
LCMT1	leucine carboxyl-methyl transferase 1
LTA	light transmission aggregometry
M	mol/L
MAPK	mitogen-activated protein kinase
MAPKAPK	MAP kinase activated protein kinases
MAST	microtubule-associated serine/threonine protein kinase
MASTL	microtubule-associated serine/threonine protein kinase-like
MeOH	methanol

min.	minute(s)
MLCK	myosin light-chain kinase
MLCP	myosin-light chain phosphatase
MOB	Mps1-one binder
mRNA	messenger RNA
µM	µmol/L
n.d.	not detected
NDR	nuclear Dbf2-related protein kinase
nM	nmol/L
NO	nitric oxide
NP-40	nonyl phenoxypolyethoxylethanol
n.s.	not significant
OA	okadaic acid
OD	optical density
$P2X_1$	ATP-gated ion channel
$P2Y_1$	ADP-gated ion channel
$P2Y_{12}$	ADP-gated ion channel
p38 MAPK	mitogen-activated protein kinase p38
PAR(1/4)	protease-activated receptor
PBS	phosphate buffered saline
PCR	polymerase chain reaction
PDE	phosphodiesterase
PF4	platelet factor 4
PGI_2	prostaglandin I_2 or prostacyclin
pH	potential of Hydrogen
PI3	Phosphatidylinositol-4,5-bisphosphate 3
PI3K	Phosphatidylinositol-4,5-bisphosphate 3-kinase
PKA	protein kinase A
PKB	protein kinase B

PKC	protein kinase C
PKG	protein kinase G
PLA_2	phospholipase A_2
PLC	phospholipase C
PME-1	PP2A-specific methyl esterase 1
PP1	protein phosphatase 1
PP1cγ	catalytic γ subunit of PP1
PP2A	protein phosphatase 2A
PP2B	protein phosphatase 2B
PP2C	protein phosphatase 2C
PP4	protein phosphatase 4
PP7	protein phosphatase 7
PPM	metallo-dependent protein phosphatase
PPP	phosphoprotein phosphatase
PPP	platelet-poor plasma
PRP	platelet-rich plasma
PS	phosphatidyl serine
PTP	protein tyrosine phosphatases
PTP-1B	protein tyrosine phosphatase 1B
PTPA	protein phosphatase 2A phosphatase activator
PVDF	polyvinylidene difluoride
Rap1	Ras-related protein 1
RBC	reaction biology corporation
RIAM	Rap1-GTP-interacting adaptor molecule
RNA	ribonucleic acid
ROCK	Rho-associated protein kinase
Rp-8-Br-PET-cGMPS	8-Bromo-β-phenyl-1,N^2-ethenoguanosine-3’,5’-cyclic monophosphorothioate, RP-isomer
rpm	revolutions per minute
RT	room temperature

S/Ser	serine
sAC	soluble adenylyl cyclase
SDS	sodium dodecyl sulfate
SDS-PAGE	sodium dodecyl sulfate – polyacrylamide gel electrophoresis
sec.	seconds
SFK	Src family kinase
sGC	soluble guanylyl cyclase
SNC	S-nitrosocysteine
SNP	sodium-nitroprusside
S.O.C.	super optimal broth with catabolite repression
Src	sarcoma
STE	sterile kinase
STK	serine/threonine kinase
T/Thr	threonine
TAE	tris/acetate
TBS	tris-buffered saline
TBST	tris-buffered saline with Tween20
TEMED	N, N, N', N' tetramethyl-ethyldiamine
TGS	tris-glycine-SDS
Thr	thrombin
TK	tyrosine kinase
TKL	tyrosine kinase-like
TP	thromboxane-prostanoid receptor
Tris	tris(hydroxymethyl)aminomethane
TSP-1	thrombospondin-1
TXA_2	thromboxane A_2
U	Units
VASP	vasodilator-stimulated phosphoprotein
VEGF	vascular endothelia growth factor

vWF	von Willebrand factor
WB	western blot
xg	relative centrifugal force
Y/Tyr	tyrosine

List of figures

List of tables

References

1. Jurk, K. and B.E. Kehrel, *Platelets: physiology and biochemistry.* Semin Thromb Hemost, 2005. **31**(4): p. 381-92.
2. Kaushansky, K., *The molecular mechanisms that control thrombopoiesis.* J Clin Invest, 2005. **115**(12): p. 3339-47.
3. Leytin, V., *Apoptosis in the anucleate platelet.* Blood Rev, 2012. **26**(2): p. 51-63.
4. Jurk, K. and B.E. Kehrel, *Pathophysiologie und Biochemie der Thrombozyten.* Der Internist, 2010. **51**(9): p. 1086-1094.
5. Yadav, S. and B. Storrie, *The cellular basis of platelet secretion: Emerging structure/function relationships.* Platelets, 2017. **28**(2): p. 108-118.
6. Richardson, J.L., et al., *Mechanisms of organelle transport and capture along proplatelets during platelet production.* Blood, 2005. **106**(13): p. 4066.
7. Rowley, J.W. and A.S. Weyrich, *Ribosomes in platelets protect the messenger.* Blood, 2017. **129**(17): p. 2343.
8. Blair, P. and R. Flaumenhaft, *Platelet alpha-granules: basic biology and clinical correlates.* Blood Rev, 2009. **23**(4): p. 177-89.
9. Pagel, O., et al., *Taking the stock of granule cargo: Platelet releasate proteomics.* Platelets, 2017. **28**(2): p. 119-128.
10. Golebiewska, E.M. and A.W. Poole, *Platelet secretion: From haemostasis to wound healing and beyond.* Blood Rev, 2015. **29**(3): p. 153-62.
11. McArthur, K., S. Chappaz, and B.T. Kile, *Apoptosis in megakaryocytes and platelets: the life and death of a lineage.* Blood, 2018. **131**(6): p. 605-610.
12. Bleeker, J.S. and W.J. Hogan, *Thrombocytosis: diagnostic evaluation, thrombotic risk stratification, and risk-based management strategies.* Thrombosis, 2011. **2011**: p. 536062-536062.
13. Erkurt, M.A., et al., *Thrombocytopenia in Adults: Review Article.* Journal of Hematology; Vol. 1, No. 2-3, Jun 2012, 2012.
14. Jurk, K., *Analysis of platelet function and dysfunction.* Hamostaseologie, 2015. **35**(1): p. 60-72.
15. Bye, A.P., A.J. Unsworth, and J.M. Gibbins, *Platelet signaling: a complex interplay between inhibitory and activatory networks.* J Thromb Haemost, 2016. **14**(5): p. 918-30.
16. Butt, E., et al., *cAMP- and cGMP-dependent protein kinase phosphorylation sites of the focal adhesion vasodilator-stimulated phosphoprotein (VASP) in vitro and in intact human platelets.* J Biol Chem, 1994. **269**(20): p. 14509-17.
17. Wentworth, J.K., G. Pula, and A.W. Poole, *Vasodilator-stimulated phosphoprotein (VASP) is phosphorylated on Ser157 by protein kinase C-dependent and -independent mechanisms in thrombin-stimulated human platelets.* Biochem J, 2006. **393**(Pt 2): p. 555-64.
18. Gawaz, M., H. Langer, and A.E. May, *Platelets in inflammation and atherogenesis.* J Clin Invest, 2005. **115**(12): p. 3378-84.
19. Versteeg, H.H., et al., *New fundamentals in hemostasis.* Physiol Rev, 2013. **93**(1): p. 327-58.
20. Stalker, T.J., et al., *Platelet signaling.* Handb Exp Pharmacol, 2012(210): p. 59-85.
21. Wolberg, A.S. and R.A. Campbell, *Thrombin generation, fibrin clot formation and hemostasis.* Transfusion and apheresis science : official journal of the World Apheresis Association : official journal of the European Society for Haemapheresis, 2008. **38**(1): p. 15-23.
22. Wood, J.P., et al., *Prothrombin activation on the activated platelet surface optimizes expression of procoagulant activity.* Blood, 2011. **117**(5): p. 1710-1718.
23. Swieringa, F., et al., *Targeting platelet receptor function in thrombus formation: the risk of bleeding.* Blood Rev, 2014. **28**(1): p. 9-21.
24. Li, Z., et al., *Signaling during platelet adhesion and activation.* Arteriosclerosis, thrombosis, and vascular biology, 2010. **30**(12): p. 2341-2349.
25. Brass, L.F., et al., *Regulating thrombus growth and stability to achieve an optimal response to injury.* J Thromb Haemost, 2011. **9 Suppl 1**: p. 66-75.

26. Schoenwaelder, S.M., et al., *Identification of a unique co-operative phosphoinositide 3-kinase signaling mechanism regulating integrin alpha IIb beta 3 adhesive function in platelets.* J Biol Chem, 2007. **282**(39): p. 28648-58.
27. Rivera, J., et al., *Platelet receptors and signaling in the dynamics of thrombus formation.* Haematologica, 2009. **94**(5): p. 700-711.
28. Smolenski, A., *Novel roles of cAMP/cGMP-dependent signaling in platelets.* Journal of Thrombosis and Haemostasis, 2012. **10**(2): p. 167-176.
29. Makhoul, S., et al., *Effects of the NO/soluble guanylate cyclase/cGMP system on the functions of human platelets.* Nitric Oxide, 2018. **76**: p. 71-80.
30. Manning, G., et al., *The protein kinase complement of the human genome.* Science, 2002. **298**(5600): p. 1912-34.
31. Chen, M.J., J.E. Dixon, and G. Manning, *Genomics and evolution of protein phosphatases.* Science Signaling, 2017. **10**(474).
32. Olsen, J.V., et al., *Global, in vivo, and site-specific phosphorylation dynamics in signaling networks.* Cell, 2006. **127**(3): p. 635-48.
33. Capra, M., et al., *Frequent alterations in the expression of serine/threonine kinases in human cancers.* Cancer Res, 2006. **66**(16): p. 8147-54.
34. Ardito, F., et al., *The crucial role of protein phosphorylation in cell signaling and its use as targeted therapy (Review).* Int J Mol Med, 2017. **40**(2): p. 271-280.
35. Senis, Y.A., A. Mazharian, and J. Mori, *Src family kinases: at the forefront of platelet activation.* Blood, 2014. **124**(13): p. 2013-2024.
36. Jin, J. and T. Pawson, *Modular evolution of phosphorylation-based signalling systems.* Philos Trans R Soc Lond B Biol Sci, 2012. **367**(1602): p. 2540-55.
37. Senis, Y.A., *Protein-tyrosine phosphatases: a new frontier in platelet signal transduction.* Journal of Thrombosis and Haemostasis, 2013. **11**(10): p. 1800-1813.
38. Eto, M. and D.L. Brautigan, *Endogenous inhibitor proteins that connect Ser/Thr kinases and phosphatases in cell signaling.* IUBMB Life, 2012. **64**(9): p. 732-9.
39. Janssens, V. and J. Goris, *Protein phosphatase 2A: a highly regulated family of serine/threonine phosphatases implicated in cell growth and signalling.* Biochem J, 2001. **353**(Pt 3): p. 417-39.
40. Price, N.E. and M.C. Mumby, *Effects of regulatory subunits on the kinetics of protein phosphatase 2A.* Biochemistry, 2000. **39**(37): p. 11312-8.
41. Hemmings, B.A., et al., *alpha- and beta-forms of the 65-kDa subunit of protein phosphatase 2A have a similar 39 amino acid repeating structure.* Biochemistry, 1990. **29**(13): p. 3166-73.
42. Zhou, J., et al., *Characterization of the Aalpha and Abeta subunit isoforms of protein phosphatase 2A: differences in expression, subunit interaction, and evolution.* Biochemical Journal, 2003. **369**(2): p. 387.
43. Khew-Goodall, Y. and B.A. Hemmings, *Tissue-specific expression of mRNAs encoding alpha- and beta-catalytic subunits of protein phosphatase 2A.* FEBS Lett, 1988. **238**(2): p. 265-8.
44. Shi, Y., *Serine/threonine phosphatases: mechanism through structure.* Cell, 2009. **139**(3): p. 468-84.
45. Seshacharyulu, P., et al., *Phosphatase: PP2A structural importance, regulation and its aberrant expression in cancer.* Cancer Lett, 2013. **335**(1): p. 9-18.
46. Jiang, L., et al., *Structural basis of protein phosphatase 2A stable latency.* Nat Commun, 2013. **4**: p. 1699.
47. Schmitz, M.H., et al., *Live-cell imaging RNAi screen identifies PP2A-B55alpha and importin-beta1 as key mitotic exit regulators in human cells.* Nat Cell Biol, 2010. **12**(9): p. 886-93.
48. Kuo, Y.C., et al., *Regulation of phosphorylation of Thr-308 of Akt, cell proliferation, and survival by the B55alpha regulatory subunit targeting of the protein phosphatase 2A holoenzyme to Akt.* J Biol Chem, 2008. **283**(4): p. 1882-92.
49. Eichhorn, P.J., M.P. Creyghton, and R. Bernards, *Protein phosphatase 2A regulatory subunits and cancer.* Biochim Biophys Acta, 2009. **1795**(1): p. 1-15.

50. Chiang, C.W., et al., *Protein phosphatase 2A activates the proapoptotic function of BAD in interleukin- 3-dependent lymphoid cells by a mechanism requiring 14-3-3 dissociation.* Blood, 2001. **97**(5): p. 1289-97.
51. Santoro, M.F., et al., *Regulation of protein phosphatase 2A activity by caspase-3 during apoptosis.* J Biol Chem, 1998. **273**(21): p. 13119-28.
52. Jin, Z., et al., *PP2A:B56{epsilon}, a substrate of caspase-3, regulates p53-dependent and p53-independent apoptosis during development.* J Biol Chem, 2010. **285**(45): p. 34493-502.
53. Lambrecht, C., et al., *Loss of protein phosphatase 2A regulatory subunit B56delta promotes spontaneous tumorigenesis in vivo.* Oncogene, 2017. **37**(4): p. 544-552.
54. Janssens, V., J. Goris, and C. Van Hoof, *PP2A: the expected tumor suppressor.* Curr Opin Genet Dev, 2005. **15**(1): p. 34-41.
55. Sontag, E., et al., *Protein phosphatase 2A methyltransferase links homocysteine metabolism with tau and amyloid precursor protein regulation.* J Neurosci, 2007. **27**(11): p. 2751-9.
56. Mochida, S., et al., *Greatwall phosphorylates an inhibitor of protein phosphatase 2A that is essential for mitosis.* Science, 2010. **330**(6011): p. 1670-3.
57. Gharbi-Ayachi, A., et al., *The substrate of Greatwall kinase, Arpp19, controls mitosis by inhibiting protein phosphatase 2A.* Science, 2010. **330**(6011): p. 1673-7.
58. Porter, I.M., et al., *Bod1 regulates protein phosphatase 2A at mitotic kinetochores.* Nat Commun, 2013. **4**: p. 2677.
59. Reguera, B., et al., *Dinophysis Toxins: Causative Organisms, Distribution and Fate in Shellfish.* Marine Drugs, 2014. **12**(1): p. 394.
60. Kato, Y., et al., *Bioactive marine metabolites. Part 16. Calyculin A. A novel antitumor metabolite from the marine sponge Discodermia calyx.* Journal of the American Chemical Society, 1986. **108**(10): p. 2780-2781.
61. Kong, R., et al., *Elucidation of the Biosynthetic Gene Cluster and the Post-PKS Modification Mechanism for Fostriecin in Streptomyces pulveraceus.* Chemistry & Biology, 2013. **20**(1): p. 45-54.
62. Xing, Y., et al., *Structure of Protein Phosphatase 2A Core Enzyme Bound to Tumor-Inducing Toxins.* Cell, 2006. **127**(2): p. 341-353.
63. Hunt, T., *On the regulation of protein phosphatase 2A and its role in controlling entry into and exit from mitosis.* Adv Biol Regul, 2013. **53**(2): p. 173-8.
64. Lee, J. and J. Stock, *Protein phosphatase 2A catalytic subunit is methyl-esterified at its carboxyl terminus by a novel methyltransferase.* J Biol Chem, 1993. **268**(26): p. 19192-5.
65. De Baere, I., et al., *Purification of porcine brain protein phosphatase 2A leucine carboxyl methyltransferase and cloning of the human homologue.* Biochemistry, 1999. **38**(50): p. 16539-47.
66. Xing, Y., et al., *Structural mechanism of demethylation and inactivation of protein phosphatase 2A.* Cell, 2008. **133**(1): p. 154-63.
67. Kong, M., et al., *The PP2A-associated protein alpha4 is an essential inhibitor of apoptosis.* Science, 2004. **306**(5696): p. 695-8.
68. Jordens, J., et al., *The protein phosphatase 2A phosphatase activator is a novel peptidyl-prolyl cis/trans-isomerase.* J Biol Chem, 2006. **281**(10): p. 6349-57.
69. Longin, S., et al., *Selection of protein phosphatase 2A regulatory subunits is mediated by the C terminus of the catalytic Subunit.* J Biol Chem, 2007. **282**(37): p. 26971-80.
70. Luo, Y., et al., *PTPA activates protein phosphatase-2A through reducing its phosphorylation at tyrosine-307 with upregulation of protein tyrosine phosphatase 1B.* Biochim Biophys Acta, 2013. **1833**(5): p. 1235-43.
71. Hombauer, H., et al., *Generation of active protein phosphatase 2A is coupled to holoenzyme assembly.* PLoS Biol, 2007. **5**(6): p. e155.
72. Khosravi-Far, R., et al., *Programmed Cell Death*. Methods in Enzymology. 2008: Elsevier Science.
73. Zhang, X., et al., *Protein phosphatase 2A regulates central sensitization in the spinal cord of rats following intradermal injection of capsaicin.* Molecular pain, 2006. **2**: p. 9-9.

74. Sundaresan, P. and R.W. Farndale, *P38 mitogen-activated protein kinase dephosphorylation is regulated by protein phosphatase 2A in human platelets activated by collagen.* FEBS Lett, 2002. **528**(1-3): p. 139-44.
75. Moscardo, A., et al., *Regulation of cytosolic PlA2 activity by PP1/PP2A serine/threonine phosphatases in human platelets.* Platelets, 2006. **17**(6): p. 405-15.
76. Murányi, A., et al., *Identification and localization of myosin phosphatase in human platelets.* The Biochemical journal, 1998. **330 (Pt 1)**(Pt 1): p. 225-231.
77. Moscardo, A., et al., *Serine/threonine phosphatases regulate platelet alphaIIbbeta3 integrin receptor outside-in signaling mechanisms and clot retraction.* Life Sci, 2013. **93**(20): p. 707-13.
78. Gushiken, F.C., et al., *The catalytic subunit of protein phosphatase 1 gamma regulates thrombin-induced murine platelet alpha(IIb)beta(3) function.* PloS one, 2009. **4**(12): p. e8304-e8304.
79. Khatlani, T., et al., *A Novel Interaction of the Catalytic Subunit of Protein Phosphatase 2A with the Adaptor Protein CIN85 Suppresses Phosphatase Activity and Facilitates Platelet Outside-in alphaIIbbeta3 Integrin Signaling.* J Biol Chem, 2016. **291**(33): p. 17360-8.
80. Abel, K., G. Mieskes, and U. Walter, *Dephosphorylation of the focal adhesion protein VASP in vitro and in intact human platelets.* FEBS Lett, 1995. **370**(3): p. 184-8.
81. Heron, L., et al., *Human alpha-endosulfine, a possible regulator of sulfonylurea-sensitive KATP channel: molecular cloning, expression and biological properties.* Proc Natl Acad Sci U S A, 1998. **95**(14): p. 8387-91.
82. Von Stetina, J.R., et al., *alpha-Endosulfine is a conserved protein required for oocyte meiotic maturation in Drosophila.* Development, 2008. **135**(22): p. 3697-706.
83. Bontron, S., et al., *Yeast endosulfines control entry into quiescence and chronological life span by inhibiting protein phosphatase 2A.* Cell Rep, 2013. **3**(1): p. 16-22.
84. Dulubova, I., et al., *ARPP-16/ARPP-19: a highly conserved family of cAMP-regulated phosphoproteins.* J Neurochem, 2001. **77**(1): p. 229-38.
85. Girault, J.A., et al., *Differential expression of ARPP-16 and ARPP-19, two highly related cAMP- regulated phosphoproteins, one of which is specifically associated with dopamine-innervated brain regions.* The Journal of Neuroscience, 1990. **10**(4): p. 1124.
86. Horiuchi, A., et al., *Purification and cDNA cloning of ARPP-16, a cAMP-regulated phosphoprotein enriched in basal ganglia, and of a related phosphoprotein, ARPP-19.* J Biol Chem, 1990. **265**(16): p. 9476-84.
87. Peyrollier, K., et al., *Alpha endosulfine is a novel molecule, structurally related to a family of phosphoproteins.* Biochem Biophys Res Commun, 1996. **223**(3): p. 583-6.
88. Voets, E. and R.M. Wolthuis, *MASTL is the human orthologue of Greatwall kinase that facilitates mitotic entry, anaphase and cytokinesis.* Cell Cycle, 2010. **9**(17): p. 3591-601.
89. Juanes, M.A., et al., *Budding yeast greatwall and endosulfines control activity and spatial regulation of PP2A(Cdc55) for timely mitotic progression.* PLoS Genet, 2013. **9**(7): p. e1003575.
90. Yu, J., et al., *Greatwall kinase participates in the Cdc2 autoregulatory loop in Xenopus egg extracts.* Mol Cell, 2006. **22**(1): p. 83-91.
91. Lorca, T. and A. Castro, *The Greatwall kinase: a new pathway in the control of the cell cycle.* Oncogene, 2013. **32**(5): p. 537-43.
92. Andrade, E.C., et al., *ARPP-16 Is a Striatal-Enriched Inhibitor of Protein Phosphatase 2A Regulated by Microtubule-Associated Serine/Threonine Kinase 3 (Mast 3 Kinase).* J Neurosci, 2017. **37**(10): p. 2709-2722.
93. Mochida, S., *Regulation of alpha-endosulfine, an inhibitor of protein phosphatase 2A, by multisite phosphorylation.* FEBS J, 2014. **281**(4): p. 1159-69.
94. Andrade, E.C., et al., *ARPP-16 Is a Striatal-Enriched Inhibitor of Protein Phosphatase 2A Regulated by Microtubule-Associated Serine/Threonine Kinase 3 (Mast 3 Kinase).* Journal of Neuroscience, 2017. **37**(10): p. 2709-2722.
95. Ammarah, U., et al., *Identification of new inhibitors against human Great wall kinase using in silico approaches.* Scientific Reports, 2018. **8**(1): p. 4894.

96. Pearce, L.R., D. Komander, and D.R. Alessi, *The nuts and bolts of AGC protein kinases.* Nature Reviews Molecular Cell Biology, 2010. **11**: p. 9.
97. Johnson, H.J., et al., *In vivo inactivation of MASTL kinase results in thrombocytopenia.* Exp Hematol, 2009. **37**(8): p. 901-8.
98. Bettencourt-Dias, M., et al., *Genome-wide survey of protein kinases required for cell cycle progression.* Nature, 2004. **432**(7020): p. 980-7.
99. Wang, L., et al., *Mastl kinase, a promising therapeutic target, promotes cancer recurrence.* Oncotarget, 2014. **5**(22): p. 11479-89.
100. Yu, J., et al., *Greatwall Kinase Participates in the Cdc2 Autoregulatory Loop in Xenopus Egg Extracts.* Molecular Cell, 2006. **22**(1): p. 83-91.
101. Medema, R.H. and A. Lindqvist, *Boosting and suppressing mitotic phosphorylation.* Trends Biochem Sci, 2011. **36**(11): p. 578-84.
102. Labandera, A.M., et al., *The mitotic PP2A regulator ENSA/ARPP-19 is remarkably conserved across plants and most eukaryotes.* Biochem Biophys Res Commun, 2015. **458**(4): p. 739-44.
103. Williams, B.C., et al., *Greatwall-phosphorylated Endosulfine is both an inhibitor and a substrate of PP2A-B55 heterotrimers.* Elife, 2014. **3**: p. e01695.
104. Musante, V., et al., *Reciprocal regulation of ARPP-16 by PKA and MAST3 kinases provides a cAMP-regulated switch in protein phosphatase 2A inhibition.* Elife, 2017. **6**.
105. Ahn, J.H., et al., *Protein kinase A activates protein phosphatase 2A by phosphorylation of the B56delta subunit.* Proc Natl Acad Sci U S A, 2007. **104**(8): p. 2979-84.
106. Woods, W.S., et al., *Conformation-specific binding of alpha-synuclein to novel protein partners detected by phage display and NMR spectroscopy.* J Biol Chem, 2007. **282**(47): p. 34555-67.
107. Boettcher, J.M., et al., *Membrane-induced folding of the cAMP-regulated phosphoprotein endosulfine-alpha.* Biochemistry, 2008. **47**(47): p. 12357-64.
108. Kim, S.H. and G. Lubec, *Brain α-endosulfine is manifold decreased in brains from patients with Alzheimer's disease: a tentative marker and drug target?* Neuroscience Letters, 2001. **310**(2): p. 77-80.
109. Kim, S.H., et al., *Decreased levels of ARPP-19 and PKA in brains of Down syndrome and Alzheimer's disease.* J Neural Transm Suppl, 2001(61): p. 263-72.
110. Vigneron, S., et al., *The master Greatwall kinase, a critical regulator of mitosis and meiosis.* International Journal of Developmental Biology, 2016. **60**(7-9): p. 245-254.
111. Burkhart, J.M., et al., *The first comprehensive and quantitative analysis of human platelet protein composition allows the comparative analysis of structural and functional pathways.* Blood, 2012. **120**(15): p. e73-82.
112. Zeiler, M., M. Moser, and M. Mann, *Copy Number Analysis of the Murine Platelet Proteome Spanning the Complete Abundance Range.* Molecular & Cellular Proteomics, 2014. **13**(12): p. 3435-3445.
113. Beck, F., et al., *Time-resolved characterization of cAMP/PKA-dependent signaling reveals that platelet inhibition is a concerted process involving multiple signaling pathways.* Blood, 2014. **123**(5): p. e1-e10.
114. Smolenski, A., *Novel roles of cAMP/cGMP-dependent signaling in platelets.* J Thromb Haemost, 2012. **10**(2): p. 167-76.
115. Graham, F.L., et al., *Characteristics of a human cell line transformed by DNA from human adenovirus type 5.* J Gen Virol, 1977. **36**(1): p. 59-74.
116. Addgene. *Vector map pCMV-3Tag-1A*. Available from: addgene.org/browse/sequence_vdb/2202/.
117. adgene. *Map of pCMV-3Tag-1A*. Available from: https://www.addgene.org/browse/sequence_vdb/2202/.
118. *BioRad molecular weight standard*. Available from: http://www.bio-rad.com/de-de/sku/1610374-precision-plus-protein-dual-color-standards-500-ul?ID=1610374.
119. Walsh, A.H., A. Cheng, and R.E. Honkanen, *Fostriecin, an antitumor antibiotic with inhibitory activity against serine/threonine protein phosphatases types 1 (PP1) and 2A (PP2A), is highly selective for PP2A.* FEBS Lett, 1997. **416**(3): p. 230-4.
120. *staurosporine - abcam*. Available from: https://www.abcam.com/staurosporine-ab120056.html#top-547.

121. Mitsuhashi, S., et al., *Tautomycetin is a novel and specific inhibitor of serine/threonine protein phosphatase type 1, PP1.* Biochem Biophys Res Commun, 2001. **287**(2): p. 328-31.
122. Lee, P.Y., et al., *Agarose gel electrophoresis for the separation of DNA fragments.* J Vis Exp, 2012(62).
123. Born, G.V.R., *Aggregation of Blood Platelets by Adenosine Diphosphate and its Reversal.* Nature, 1962. **194**: p. 927.
124. Paniccia, R., et al., *Platelet function tests: a comparative review.* Vascular health and risk management, 2015. **11**: p. 133-148.
125. Koltai, K., et al., *Platelet Aggregometry Testing: Molecular Mechanisms, Techniques and Clinical Implications.* Int J Mol Sci, 2017. **18**(8).
126. Laemmli, U.K., *Cleavage of Structural Proteins during the Assembly of the Head of Bacteriophage T4.* Nature, 1970. **227**: p. 680.
127. Zhang, W., et al., *Titanium Dioxide Photocatalytic Polymerization of Acrylamide for Gel Electrophoresis (TIPPAGE) of Proteins and Structural Identification by Mass Spectrometry.* Sci Rep, 2016. **6**: p. 20981.
128. Blum, H., H. Beier, and H.J. Gross, *Improved silver staining of plant proteins, RNA and DNA in polyacrylamide gels.* ELECTROPHORESIS, 1987. **8**(2): p. 93-99.
129. Kerényi, L. and F. Gallyas, *Über probleme der quantitativen auswertung der mit physikalischer entwicklung versilberten agarelektrophoretogramme.* Clinica Chimica Acta, 1973. **47**(3): p. 425-436.
130. Merril, C.R., et al., *Ultrasensitive stain for proteins in polyacrylamide gels shows regional variation in cerebrospinal fluid proteins.* Science, 1981. **211**(4489): p. 1437-8.
131. Chevallet, M., S. Luche, and T. Rabilloud, *Silver staining of proteins in polyacrylamide gels.* Nat Protoc, 2006. **1**(4): p. 1852-8.
132. Block, H., et al., *Chapter 27 Immobilized-Metal Affinity Chromatography (IMAC)*, in *Guide to Protein Purification, 2nd Edition*. 2009. p. 439-473.
133. Promega. *Protein purification*. Available from: https://www.promega.de/resources/product-guides-and-selectors/protocols-and-applications-guide/protein-purification-and-analysis/.
134. Bradford, M.M., *A rapid and sensitive method for the quantitation of microgram quantities of protein utilizing the principle of protein-dye binding.* Analytical Biochemistry, 1976. **72**(1): p. 248-254.
135. Beck, F., et al., *Temporal quantitative phosphoproteomics of ADP stimulation reveals novel central nodes in platelet activation and inhibition.* Blood, 2017. **129**(2): p. E1-E12.
136. Reiss, C., et al., *The sGC stimulator riociguat inhibits platelet function in washed platelets but not in whole blood.* Br J Pharmacol, 2015. **172**(21): p. 5199-210.
137. Butt, E., et al., *Inhibition of cGMP-dependent protein-kinase by (Rp)-guanosine 3',5'-monophosphorothioates.* Febs Letters, 1990. **263**(1): p. 47-50.
138. Zeiler, M., M. Moser, and M. Mann, *Copy number analysis of the murine platelet proteome spanning the complete abundance range.* Mol Cell Proteomics, 2014. **13**(12): p. 3435-45.
139. *Bethyl Laboratories, data about MASTL antibody*. Available from: https://www.bethyl.com/product/A302-190A?referrer=pca_a-z&target=MASTL.
140. Yu, J., et al., *Greatwall kinase.* The Journal of Cell Biology, 2004. **164**(4): p. 487.
141. Ocasio, C.A., et al., *A first generation inhibitor of human Greatwall kinase, enabled by structural and functional characterisation of a minimal kinase domain construct.* Oncotarget, 2016. **7**(44): p. 71182-71197.
142. *UniProt*. Available from: uniprot.org.
143. *Staurosporine - Guide to pharmacology*. Available from: http://www.guidetopharmacology.org/GRAC/LigandScreenDisplayForward?ligandId=346&screenId=3.
144. *Kinexus BioInformatics Corporation*. Available from: kinasenet.ca.
145. Ma, H., S. Deacon, and K. Horiuchi, *The challenge of selecting protein kinase assays for lead discovery optimization.* Expert opinion on drug discovery, 2008. **3**(6): p. 607-621.

146. Junttila, M.R., S.P. Li, and J. Westermarck, *Phosphatase-mediated crosstalk between MAPK signalling pathways in the regulation of cell survival.* Faseb Journal, 2008. **22**(4): p. 954-965.
147. Benz, P.M., et al., *Differential VASP phosphorylation controls remodeling of the actin cytoskeleton.* Journal of Cell Science, 2009. **122**(21): p. 3954.
148. Sakon, M., J.I. Kambayashi, and K.H. Murata, *The involvement of protein phosphatases in platelet activation.* Platelets, 1994. **5**(3): p. 130-4.
149. Higashihara, M., et al., *The inhibitory effects of okadaic acid on platelet function.* FEBS Letters, 1992. **307**(2): p. 206-210.
150. Labandera, A.M., et al., *The mitotic PP2A regulator ENSA/ARPP-19 is remarkably conserved across plants and most eukaryotes.* Biochemical and Biophysical Research Communications, 2015. **458**(4): p. 739-744.
151. Castro, A. and T. Lorca, *Greatwall kinase at a glance.* J Cell Sci, 2018. **131**(20).
152. Burgess, A., et al., *Loss of human Greatwall results in G2 arrest and multiple mitotic defects due to deregulation of the cyclin B-Cdc2/PP2A balance.* Proc Natl Acad Sci U S A, 2010. **107**(28): p. 12564-9.
153. Hergovich, A., et al., *NDR kinases regulate essential cell processes from yeast to humans.* Nat Rev Mol Cell Biol, 2006. **7**(4): p. 253-64.
154. Stegert, M.R., et al., *Regulation of NDR2 protein kinase by multi-site phosphorylation and the S100B calcium-binding protein.* J Biol Chem, 2004. **279**(22): p. 23806-12.
155. Millward, T.A., D. Hess, and B.A. Hemmings, *Ndr Protein Kinase Is Regulated by Phosphorylation on Two Conserved Sequence Motifs.* Journal of Biological Chemistry, 1999. **274**(48): p. 33847-33850.
156. Hergovich, A., *The Roles of NDR Protein Kinases in Hippo Signalling.* Genes (Basel), 2016. **7**(5).
157. Rehberg, K., et al., *The serine/threonine kinase Ndr2 controls integrin trafficking and integrin-dependent neurite growth.* J Neurosci, 2014. **34**(15): p. 5342-54.
158. Gandhi, M.J., C.L. Cummings, and J.G. Drachman, *FLJ14813 Missense mutation: A candidate for autosomal dominant thrombocytopenia on human chromosome 10.* Human Heredity, 2003. **55**(1): p. 66-70.
159. Hurtado, B., et al., *Thrombocytopenia-associated mutations in Ser/Thr kinase MASTL deregulate actin cytoskeletal dynamics in platelets.* J Clin Invest, 2018.
160. Ahn, J.H., et al., *Protein kinase A activates protein phosphatase 2A by phosphorylation of the B56 delta subunit.* Proceedings of the National Academy of Sciences of the United States of America, 2007. **104**(8): p. 2979-2984.
161. Leslie, S.N. and A.C. Nairn, *cAMP regulation of protein phosphatases PP1 and PP2A in brain.* Biochim Biophys Acta Mol Cell Res, 2019. **1866**(1): p. 64-73.
162. Dupre, A.I., O. Haccard, and C. Jessus, *The greatwall kinase is dominant over PKA in controlling the antagonistic function of ARPP19 in Xenopus oocytes.* Cell Cycle, 2017. **16**(15): p. 1440-1452.
163. Mochida, S., *PP1 inactivates Greatwall to release PP2A-B55 from mitotic confinement.* EMBO Rep, 2015. **16**(11): p. 1411-2.
164. Muranyi, A., et al., *Identification and localization of myosin phosphatase in human platelets.* Biochem J, 1998. **330 (Pt 1)**: p. 225-31.
165. Jurk, K. and U. Walter, *New Insights into Platelet Signalling Pathways by Functional and Proteomic Approaches.* Hamostaseologie, 2018.
166. Pedruzzi, I., et al., *TOR and PKA Signaling Pathways Converge on the Protein Kinase Rim15 to Control Entry into G_0.* Molecular Cell, 2003. **12**(6): p. 1607-1613.
167. Sangodkar, J., et al., *All roads lead to PP2A: exploiting the therapeutic potential of this phosphatase.* Febs j, 2016. **283**(6): p. 1004-24.
168. Haesen, D., et al., *The Basic Biology of PP2A in Hematologic Cells and Malignancies.* Front Oncol, 2014. **4**: p. 347.
169. Beck, F., et al., *Temporal quantitative phosphoproteomics of ADP stimulation reveals novel central nodes in platelet activation and inhibition.* 2017. **129**(2): p. e1-e12.
170. Silverstein, A.M., et al., *Actions of PP2A on the MAP kinase pathway and apoptosis are mediated by distinct regulatory subunits.* Proceedings of the National Academy of Sciences of the United States of America, 2002. **99**(7): p. 4221-4226.

171. Meeusen, B. and V. Janssens, *Tumor suppressive protein phosphatases in human cancer: Emerging targets for therapeutic intervention and tumor stratification.* Int J Biochem Cell Biol, 2018. **96**: p. 98-134.
172. Harashima, H., N. Dissmeyer, and A. Schnittger, *Cell cycle control across the eukaryotic kingdom.* Trends in Cell Biology, 2013. **23**(7): p. 345-356.
173. Charrasse, S., et al., *Ensa controls S-phase length by modulating Treslin levels.* Nature Communications, 2017. **8**.
174. Virsolvyvergine, A., et al., *Endosulfine, an Endogenous Peptidic Ligand for the Sulfonylurea Receptor - Purification and Partial Characterization from Ovine Brain.* Proceedings of the National Academy of Sciences of the United States of America, 1992. **89**(14): p. 6629-6633.
175. Woods, W.S., et al., *Conformation-specific binding of alpha-synuclein to novel protein partners detected by phage display and NMR spectroscopy.* Journal of Biological Chemistry, 2007. **282**(47): p. 34555-34567.
176. Reynhout, S. and V. Janssens, *Physiologic functions of PP2A: Lessons from genetically modified mice.* Biochim Biophys Acta Mol Cell Res, 2019. **1866**(1): p. 31-50.

VERSICHERUNG

für das Gesuch um Zulassung zur Promotion in dem Fachbereich 09

Hiermit versichere ich gemäß § 10 Abs. 3d der Promotionsordnung vom 24.07.2007:

Ich habe die jetzt als Dissertation vorgelegte Arbeit selbst angefertigt und alle benutzten Hilfsmittel (Literatur, Apparaturen, Material) in der Arbeit angegeben.

Datum	Elena Johanna Kumm